POLITECNICO
MILANO 1863

Scuola di Ingegneria Industriale e dell'Informazione
Master of Science Degree in Energy Engineering– Renewables and Environmental Sustainability

DIRECT AIR CAPTURE BY LARGE SCALE REFORESTATION OF SAHARA DESERT

Supervisor: Prof. Stefano Consonni

Co-Supervisor: Prof. Lorenzo Mari

Master Thesis of:

Ana Blanco Hernández, 916891

Academic Year 2019-2020

Acknowledgments.

To all the people that did my stay in Italy unforgettable and contribute to my personal, academic and professional growth, particularly those who inspired, took care and believed in me. Especial mention to my family, that made all of it possible.

Contents

List of figures

List of tables

Nomenclature and Abreviations

AD: Adsorption Desalination.
A. senegal: Acacia senegal.
A. tortilis: Acacia tortilis.
Avg: Average
BWRO: Brackish Water Reverse Osmosis.
CAPEX: Capital cost.
CCGT: Combined Cycle Gas Turbine.
CCS: Carbon Capture and Storage.
CGLS: Copernicus Global Land Service.
COP21: Conference of the Parties 2021/Paris Agreement.
CR: Concentration Ratio.
CSP: Concentrated Solar Power.
CTG: Combustion Turbine Generator.
DBH: Diameter at Breast Height.
DWEER: Dual Work Exchanger Energy Recovery.
ED: Electrodialysis.
ERD: Energy Recovery Device.
FAO: Food and Agriculture Organization for the United Nations.
FO: Forward Osmosis.
FT: Francis Turbine.
GCC: Gulf Cooperation Council.
GGW: Great Green Wall.
GHG: Greenhouse Gas.
GOR: Gained Output Ratio.
GW: Groundwater.
HPP: High-Pressure Pumps.
HRSG: Heat Recovery Steam Generator.
IEA: International Energy Agency.
IGCC: Integrated Gasification Combined Cycle.
LC: Levelized Cost.
LCC: Levelized Capital Cost.
LCCS: Land Cover Classification System.
LHV: Lower Heating Value
LMCS: Land Monitoring Core Service.
LOC: Levelized Operational Cost.
MD: Membrane Distillation.
MED: Multi-Effect Distillation.
MENA: Middle East and North Africa.
MIGD: Million Imperial Gallons per Day.
MSF: Multi-Stage Flash.
NG: Natural Gas.
NGCC: Natural Gas Combined Cycle
OPEX: Operating cost.
O&M: Operation and maintenance.
PC: Pulverized Coal.
PT: Pelton Turbine.
PVC: Polyvinyl Chloride.
PX: Pressure Exchanger.
RES: Renewable Energy Source.
RGS: Renewable Groundwater Stress.
RO: Reverse Osmosis.
SCOW: Simplified Cost of Water
SEC: Specific Energy Consumption.
SEEC: Specific Electrical Energy Consumption.
STEC: Specific Thermal Energy Consumption.
STG: Steam Turbine Generator.
SWRO: Seawater Reverse Osmosis.
TBT: Top Brine Temperature.
TDS: Total Dissolved Solids.
UNESCO: United Nations Educational, Scientific and Cultural Organization.
VC: Vapor Compression.
WHYMAP: World-wide Hydrogeological Mapping and Assessment Program.
WWF: World Wide Fund.

Sommario

La tesi verte sullo studio dell'effetto della riforestazione come contributo per limitare i cambiamenti climatici tramite assorbimento di CO_2. In particolare, la suddetta è stata simulata nel deserto del Sahara che, a causa del suo clima prevalentemente arido e della scarsità di acqua, rappresenta un buon candidato come scenario di riforestazione su larga scala.

La tesi si compone nel seguente modo:

- Nei primi tre capitoli è stato stabilito un quadro descrittivo degli aspetti ecologici dell'area di studio. In questo senso, è stata effettuata un'analisi dei tipi di suolo, del clima e delle risorse idriche. Infine, l'area di studio è stata classificata in base alle sue ecoregioni.
- Nel quarto capitolo è stata eseguita una simulazione della riforestazione selezionando gli alberi più adatti per le varie aree. A questo fine, per le tipologie di albero individuate, sono state stimate, attraverso le equazioni allometriche, la biomassa media e il contenuto di carbonio, ovvero la CO_2 che potrebbe essere assorbita, nonché le esigenze di irrigazione e il fabbisogno idrico del progetto. Inoltre, sono state selezionate tre regioni specifiche con una superficie di 10.000 km^2 al fine di analizzare situazioni diverse e contrastanti; in particolare, sono state prese in esame: la costa del deserto, l'interno del deserto e le terre coltivate, quest'ultime sofferenti di deforestazione a causa dei recenti cambiamenti climatici.
- Nel quinto capitolo sono state studiate due delle tecnologie di dissalazione più comunemente utilizzate, al fine di ovviare al problema della scarsità di risorse idriche: la prima, basata su membrane, come negli impianti di desalinizzazione ad osmosi inversa; la seconda, basata su processi termici, come negli impianti di desalinizzazione Multi-stage Flash (MSF). Si è approfondita la descrizione di entrambe le tecnologie e i processi, comprese le analisi termodinamiche dei suddetti, i parametri operativi e la loro efficienza. Inoltre, sono stati analizzati fabbisogni energetici di entrambe le tecnologie di dissalazione, le emissioni di CO_2, le loro possibili fonti di alimentazione e le tendenze future per ridurre il consumo di energia.
- Nel sesto capitolo è stata fatta una valutazione finale del progetto, legando insieme ciò che è stato discusso nei capitoli precedenti in maniera organica. È stato adottato un approccio tecnologico alla progettazione degli impianti di desalinizzazione, delle centrali elettriche e delle reti di distribuzione idrica più idonee.
- Nel setimo capitolo, i bilanci di CO_2, tra sequestro ed emissioni, sono stati analizzati con un approccio ambientale.
- Nell'ottavo e ultimo capitolo è stata sviluppata l'analisi dei costi del progetto. Il costo complessivo del progetto è stato computato includendo i costi di dissalazione, i costi della rete di distribuzione idrica e i costi di gestione forestale. In ultima analisi, è stato calcolato un costo conclusivo per chilogrammo di CO_2 sequestrato.

Parole chiave.

Riforestazione, Acacia, Assorbimento di CO_2, Desalinizzazione, Osmosi Inversa, Multi-stage Flash (MSF).

Abstract

The scope of this project is the study of how reforestation can contribute to limiting the climate change by capturing CO_2. In this case, a reforestation has been simulated in the Sahara Desert, since it is a good representative of large-scale but challenging and complicated reforestation scenario, because of its mainly arid desert climate and its water scarcity. The following topics have been developed along the project in the same order:

- In the first three chapters, a descriptive framework of the ecological aspects of the study area is established. Therefore, an analysis of the soil types, climate and water resources is carried out. The study area is also classified according to its ecoregions.
- In the fourth chapter, a simulation of the reforestation is made by selecting the most suitable trees for the areas in question, their allometric equations for estimating biomass and their carbon content, calculating the CO_2 that could capture, as well as the irrigation needs and hence, the water needs of the project. Moreover, three specific regions of 10.000 km^2 surface are selected as a representative of three very different and contrasted scenarios of the study area, such as: desert coastal, desert interior and cropland currently suffering deforestation due to climate change.
- In the fifth chapter, since it is an area with scarcity of water resources, two of the most commonly used desalination technologies have been studied: one using membranes, such as desalination plants based on Reverse Osmosis technology; and another through thermal system processes, such as desalination plants based on Multi Stage Flash (MSF). Reference is made to the description of both components and processes, including thermodynamic analyzes of said processes, operational and efficiency parameters. In addition, the energy needs of both desalination technologies, their CO_2 emission, their possible energy sources and the future trends for reducing energy consumption have been analyzed.
- In the sixth chapter, a technical approach of the project is developed to design and calculate the most suitable desalination plants and infrastructure, such as power plants and water distribution networks.
- In the seventh chapter, an environmental approach has been considered to calculate the CO_2 balances, between sequestration and emissions.
- In the eighth and last chapter, the cost analysis of the project has been developed. The overall cost of the project includes desalination costs, water distribution network costs as well as the forestry running costs. With all, a price per kilogram of CO_2 sequestered has been achieved.

Key words.

Reforestation, Acacia, CO_2 capture, Desalination, Reverse Osmosis, Multi-stage Flash (MSF).

Executive summary

1. Introduction.

Anthropogenic greenhouse gas (GHG) emissions have increased since the pre-industrial era, driven largely by economic and population growth, and are now higher than ever. Continued GHG emission will cause further warming and long-lasting changes in all components of the climate system, increasing the likelihood of severe, pervasive and irreversible impacts for people and ecosystems (IPCC, 2014b). GHG can be reduced by supply-side mitigations options, i.e. by reducing GHG emissions per unit of land. The IPCC summary of supply-side mitigations options in the Agriculture, Forestry and Other Land Use (AFOLU) sector (IPCC, 2014a) considered reforestation as one of the categories, defining reforestation as an increase in biomass stocks achieved by planting trees on non-forested agricultural lands. This can include either monocultures or mixed species plantings.

The scope of this project is to understand whether a reforestation in Sahara Desert has any chance of success and how reforestation can contribute to limiting climate change by capturing CO_2. For the success of the project, the final net CO_2 sequestration balance must result in positive values and, at the same time, the reforestation and the derived infrastructures must be feasible and economically competitive. For that, three different areas of the Sahara Desert have been selected and studied by doing soil, climate, water resources and flora analysis. Reforestation and the necessary derived infrastructures have been designed and calculated for each of the three regions. Considering that Sahara Desert presents mainly arid desert climate and water scarcity, also a desalination plant project design has been carried out.

2. Methods and assumptions.

2.1. Soil, climate and water resources analysis.

Soil analysis.

Satellite data provided by Copernicus Global Land Service (Copernicus, 2020) has been used for the description of the land uses in Sahara Desert. The products are used to monitor the vegetation, the water cycle, the energy budget and the terrestrial cryosphere. Thanks to this tool, it has been possible to differentiate the major land cover types present in the countries within the study area. Total bare land covering the Sahara Desert has been identified. According to the Land Cover Classification System (LCCS), bare land or sparse vegetation is defined as Lands with vegetation cover lower than 10%, including desert, sandy fields, Gobi, bare rocks, saline and alkaline lands.

The second step is to study the composition, the development profiles and the agricultural value of the different soils occurring in the bare lands of Sahara and Sahel deserts. The information has been extracted from (D'Hoore, 1964) whose aim was to map the different type of soils present in Africa. The most common types of soil present in the countries within the study region result in: raw mineral soils, weakly developed soils, hydromorphic soils, vertisols and similar soils of depressions and halomorphic soils.

Climate analysis.

Köppen climate classification has been used. The Köppen climate classification system is by far the most widely used in modern climate classification system. It uses only the average annual and monthly values of temperature and precipitation and divides climates into five main groups (+1), each having several types and subtypes.

On the other hand, Climate dataset (Climate-Data.org, 2020) has been used as a source for the data recollection for the climate study. Temperature and precipitation data have been collected for each region of each country belonging to the studied area. Finally, climates present in the regions result in: Hot Arid Desert (BWh), Cold Arid Desert (BWk), Hot Arid Steppe (BSh), Tropical Savanna Dry Winter (Aw).

Water resources analysis.

Surface water bodies present throughout the study area include rivers, lakes, chotts, dams, oasis, wadis and the surrounding seas (Red Sea and Mediterranean Sea) and oceans (Atlantic Ocean). However, some of the surface water bodies are classified as Ramsar sites, sites recognized as wetlands with high ecological, economic, cultural, scientific and recreational value and collected in the List of Ramsar wetlands of international importance (Ramsar Convention, 2020), which are not suitable sources since they are

protected because of their high ecological value. Moreover, chotts, oasis, wadis, sabhkas and some small lakes are not trustable sources since their water reserve volumes present big fluctuations (can be full because of flood but also dry in some seasons). Finally, the permanent lakes, rivers, seas and oceans are trustable sources. Existing dams can be used for hosting new water quantities for desert irrigation.

Regarding the groundwater bodies as a source of irrigation, it has a number of essential advantages when compared with surface water: as a rule, it is of higher quality, better protected from possible pollution, less subject to seasonal and perennial fluctuations, and much more uniformly spread over large regions than surface water. Very often groundwater is available in places where there is no surface water. Groundwater is also a trustable source. However, as analyzed in the paper by (Voss et al., 2015), there are different levels of stress status in water bodies (Overstressed, Variable Stress, Human-dominated Stress, and Unstressed). Use and Groundwater availability are the two factors defining the Renewable Groundwater Stress ratio and their signs define the level of stress. Basins present in Northern Africa have a high level of stress resulting from a combination of large withdrawals and negative recharge, except for the basins in the South-Sahelian part (Niger Basin and Senegalo – Mauritanian Basin) that are considered unstressed basin systems (Voss et al., 2015). In conclusion, the Overstressed basins systems will not be suitable as water sources for the present project since they can be considered as nonrenewable sources. On the other hand, South-Sahelian basins will be considered as suitable water irrigation sources for the project.

2.2. Reforestation.

The reforestation of the present project consists of the monoculture of two endemic acacia species: Acacia tortilis in the Eastern Desert (Egypt) and the Ténére Desert (Niger) and Acacia senegal in the Sylvo-Pastorale des Six Forages Reserve (Sahel region, in the border between Mauritania and Senegal). The selection of these specific tree species is based on a research of the ecoregions in the Sahara Desert. The Ecoregions analysis shows that

- A. tortilis is one of the characteristic species that can be found in the Red Sea coastal plain. It grows naturally along the wadis, thanks to the soil moisture conditions (Indian Council of Forestry Research and Education, 1958). A. tortilis is the most important species for sand dune stabilization and it is suitable for deep sandy soils of arid regions. It is widely distributed in Africa.
- A. senegal is the characteristic species in the drier parts of Anglo-Egyptian Sudan and the northern Sahara and is found throughout the vast area from Senegal to the Red Sea

On the other hand, the specific study regions have been selected because they represent three totally different ecosystems: desert coastal, desert interior and cropland currently suffering deforestation due to climate change.

Finally, the estimation of the carbon capture ability by the tree communities is based on the use of allometric equations reported in several scientific papers. The allometric equations calculate the growth ratio and the biomass of the selected tree species with input parameters such as: trunk height (H), diameter at breast height (DBH) and wood density (ρ). Once the biomass of a tree is known, it must be consider that the total dry weight of the tree will be 72,5% average (Toochi, 2018) and the carbon content of the tree is the 50% of the total dry weight. Finally, to obtain the total CO_2 sequestration per tree, carbon content is multiplied times 3,67 (Toochi, 2018).

It should be mentioned that several other ways can be used to simulate a reforestation scenario: mixed species communities instead of monoculture, software to calculate biomass instead of specific allometric equations or equations relating growth rate-water availability instead of H-DHB-ρ.

A. tortilis.

Regarding the *A. tortilis* growth and longevity study, the paper by Andersen & Krzywinski, 2007 has been used. It analyses several samples of A. tortilis in different sites of the Eastern Desert of Egypt. It is shown that, in *A. tortilis*, a narrow marginal parenchymatic band associated with crystalliferous calcium oxalate chains is present in the wood, and according to some studies they are formed coincidentally with a temporary pause in growth. Such bands are also found in *A. tortilis* wood from the Eastern Desert. If these bands are formed regularly, they are internal time markers that can facilitate age determination. The radial growth rate is represented by a bell-shaped curve; i.e. the growth rate increases at the beginning and decreases later in the lifetime of the tree. This behavior can be modeled with a Gompertz equation.

Regarding the A. tortilis biomass study, the use of allometric regression models is widely used. Model 7 (Djomo et al., 2016) is used, since it offers the best accuracy and represents "Dry forest" (below 1500 mm/year, over 5 months dry season), closests conditions to the study area of the project. the final step is to consider that the belowground biomass is around 26% of the aboveground biomass (Cairns et al., 1997).

A. senegal.

Regarding the *A. senegal* growth and longevity study, it is used a paper by Diallo et al., 2014 reporting the results of research done in a silvo-pastoral zone of Senegal, where A. senegal is a common species. The study aims to deepen the knowledge of A. Senegal dendrometric parameters. For this project, only the measurements of total height of the tree and diameter and the DBH have been used. Some models for height and diameter development of the tree have been simulated for a life span of 14 years.

Regarding the A. senegal biomass study, the use of allometric regression models (Djomo et al., 2016) such as Model 8 offers the best accuracy when three parameters are known (height, DBH and wood density). Most accurate forest type for this project is, again, "Dry forest" (below 1500 mm/year of precipitation, over 5 months dry season). Again, the final step is to consider that the belowground biomass is around 26% of the aboveground biomass (Cairns et al., 1997).

2.3. Irrigation analysis.

The paper by Green et al., 2019 has been used to analyze the water need of Eastern and Ténéré Desert. The method applied by (Green et al., 2019) is in the hyper-arid deserts of Abu Dhabi for A. tortilis species, sharing climate and soil characteristics with the regions studied in the present project. Green et al., 2019, measures A. tortilis water-use, ETc, in L/d, using sapflow monitoring of groundwater (GW) irrigated trees, and trees irrigated with treated sewage effluent (TSE). In addition, (Green et al., 2019) also measures the seasonal pattern of evapotanspiration, ETo, in mm/d. For the present project, groundwater irrigation and tree water-use (ETc) stream flow are considered.

For the Sahel region, the methodology is based on a climate comparison between the mentioned region and the "Gum Arabic Belt" region in Sudan, where A. senegal is one of the most widespread acacia species (Awouda, 1990). The method for the watering calculation takes into consideration the temperature and precipitation data of some different regions of the "Gum Arabic Belt" to summarize and calculate the average precipitations of each month of the year and the total precipitations. Also, the temperature and the precipitations of the Sylvo-Pastorale des Six Forages Reserve region are taken into consideration.

2.4. State-of-art of desalination technology.

Among different desalination commercial technologies available, Multi-Stage Flash (MSF) distillation and Reverse Osmosis (RO) dominate the existing plants.

MSF desalination technology.

The MSF desalination system (with brine recirculation system flow) includes three main sections: the heat input section (brine heater), the heat recovery section and the heat rejection section. The recovery and rejection sections both have a series of stages. Each stage has a flash chamber and a condenser where the vapor is flashed off in the chamber and later condensed. The flash chamber is separated from the condenser by a demister, where entrained brine droplets are removed from the flashing vapor. Along Chapter 5, the reader can find general process description, thermodynamic analysis (study case) of the most relevant parameters (temperature, pressure, brine salinity and latent heat of vaporization water) along the stages of the MSF plant.

Regarding the performance indicators of MSF plants, typical Concentration Ratio (CR) is about 1,5, not higher to avoid scale formation on the heat transfer surfaces (A.M.K. El-Ghonemy, 2018). In addition, regarding energy consumption indicators, the STEC and the SEEC have been reported in a wide range. Some studies mentioned that the STEC generally ranged from 190 to 300 MJ/m^3 of products, while a typical SEEC is ranges between 2,5-5,0 $kWhelec/m^3$. Finally, regarding the GHGs emissions of MSF plants, In general terms, the GHG footprint made by MSF desalination technologies is about 10-20 kg CO_{2eq}/m^3, but mainly depends on the energy providing plant that is coupled with.

RO desalination technology.

The typical processes of a RO desalination plant start with pre-treatment units, employed to remove large-size particles and solids before the RO system because they can cause fouling and/or scaling on the surface of the membrane. TDS should also be removed to produce freshwater. Semi-permeable membranes, which allows water molecules to permeate while blocking solids molecules, are employed for that separation. However, the osmotic pressure across the semi-permeable membrane becomes an obstacle to desalination. Therefore, the RO process requires high pressure to overcome the osmotic pressure of seawater, for which a high-pressure pump is utilized. Desalted fresh water is obtained while concentrate is discharged from the RO train. In the concentrate, a considerable amount of pressure still remains. To improve the energy efficiency, the pressure in the concentrate should be recovered, for example, by energy recovery devices (ERDs). The recovered pressure is utilized to increase the pressure of the feed stream. However, this pressure increase is not enough, and the feed stream pressure is supplemented by a booster pump (Kim et al., 2019). Depending on the intake water of the RO system, the process will require a higher level of pretreatment. Influent TDS levels for seawater desalination (SWRO) are on the order of 35.000 mg/L compared to 1000–15.000 mg/L for brackish water (BWRO) such as groundwater (Cornejo et al., 2014).

Regarding the energy consumption indicators of the RO plants, the typical values of SEC are studied for both cases, SWRO and BWRO. SEC of a real-scale SWRO plant is between 3,5-4,5 kWh_{elec}/m^3, including pre-treatment and post-treatment processes. While today's BWRO processes required from 1,5-2,5 kWh_{elec}/m^3 of SEEC for brackish water from large to medium size of plants (Wakil et al., 2017). Moreover, for both plants the STEC remains in 0 MJ/m^3. Finally, GHG footprint has been widely reported and says that its value varies from 1.4-3.6 kg CO_{2eq}/m^3 of produced water for SWRO plants and 0,4-2,5 $kgCO_{2eq}/m^3$ of produced water (Cornejo et al., 2014), depending on the fuel used to produce the electricity.

Even if RO has greater advantages over MSF, such as reduced energy consumption and, therefore, reduced GHG emissions and reduced costs (Wakil et al., 2017), MSF desalination is still needed for high salinity and/or high total dissolved solids (TDS) intake waters (Saeed et al., 2019; Wali, 2014). As a result, this project assess the use of Brackish Water RO (BWRO) desalination for the plants along the Sahel region that are fed with groundwater and MSF desalination for the plants along the coast, specifically Red Sea coast, because of its high salinity and TDS (well above average).

2.5. CO_2 balances.

Here the CO_2 fluxes (sequestration and emissions) involved in the project are presented. Regarding the sequestration, there is the total CO_2 sequestration by region from Chapter 4. Regarding the emissions, there are emissions due to electricity production for desalination and emissions due to water distribution (pumping work). The total CO_2 emissions by region can be obtained multiplying the number of desalination plants needed per region times the CO_2 emissions per plant. At the same time, the total number of plants needed can be calculated dividing the total watering needs per region over total freshwater output per plant.

To complete the CO_2 balance, the only missing term is the avoided or displaced emissions. Estimating displaced emissions in electric generation results from the consideration that the power produced by the desalination power plants (so, MSF plants only) of the project will be displaced from the regional grid of each country where the power plants are. In this way, the value of the avoided emissions can be obtained by multiplying the average CO_2 emissions of the grid of each country times the power produced by all the desalination power plants of the project (in MWh). The avoided emissions will contribute positively to the CO_2 balance, in the same way as sequestration does.

2.6. Cost evaluation.

Cost evaluation is performed to finally obtain the cost per ton of CO_2 sequestered of each of the study regions. The procedure to calculate the overall cost will is divided into two sections: first section refers to the reforestation costs, including the inputs and consumables, as well as the labor (manual and machinery work). Through some calculations, a cost per area and time rotation is obtained and, then, an estimation of the cost per year. Second section refers to the desalination costs and the water distribution costs. It will be developed for the 3 different scenarios: MSF plants and short-distance pipeline (in the Red Sea coast for the Eastern Desert), MSF plants and long-distance pipeline (in the Libya coast for the Ténéré Desert) and BWRO plant and short-distance pipeline (in the Senegalo-Mauritanian Basin for the Sylvo-Pastorale des Six Foreges Reserve). Once the components and the system definition diagram are clear and the boundary conditions defined, the final step is to choose a calculation methodology. The amortization method is used.

However, since each of the three study scenarios are designed in a general way and based on hypothesis (not real plant design and calculations), performing the amortization method accurately will be difficult. Therefore, the performance of the method is based on using average values found in the assessed bibliography (Papapetrou et al., 2017; Shahabi et al., 2015) of the main components of the method, such as CAPEX and OPEX.

In addition, total investment cost of the desalination plant of the most suitable scenario (MSF plant in the Easter Desert) has been performed and reasonable values are obtained, concluding that the previous assumptions about the amortization method were correct.

3. Results.

3.1. Reforestation.

The following results are derived from applying the methodologies described before:

- The total surface where the reforestation has been simulated: 10.000 km^2 in the Eastern Desert (Egypt), 10.000 km^2 in the Ténéré Desert (Niger) and 10.000 km^2 in the Sylvo-Pastorale des Six Forages Reserve (Mauritania-Senegal).
- Best practices for sand dunes planting techniques assess 5x5m spacing blocks. So, the total number of trees that can be grown per region are 400.000.000. In other words, the trees density for the three regions is around 40.000 trees/km^2.
- Estimated CO_2 sequestration per tree species is: 6,822 $kgCO_{2eq}$/year for *A. Tortilis* and 3,174 $kgCO_{2eq}$/year for *A. Senegal*. The sequestration per tree is more than double for *A. Tortilis* than *A. Senegal*, which makes it more suitable for a reforestation. With all, the total CO_2 sequestration by region is: 68,627 $MtCO_{2eq}$/year in Eastern Desert and Ténéré Desert, then, 6,825 $MtCO_{2eq}$/year in the Sylvo-Pastorale des Six Forages Reserve.
- Estimated water needs are 2,31 m^3 of water/year for *A. Tortilis* and 7,395 m^3 of water/year for a *A. Senegal*. The water needs are more than double for *A. Senegal* than *A. Tortilis*, which again demonstrates the suitability of *A. Tortilis* for the reforestation. Total water needs for irrigation per area are: 924.000.000 m^3/year in Eastern Desert and the same amount for Ténéré Desert, then, 2.958.000.000 m^3/year in the Sylvo-Pastorale des Six Forages Reserve.

3.2. Desalination plants and infrastructures.

The following decisions are taken by reviewing the previous bibliography:

- According to the reviewed state-of-art in Chapter 5 of the specific energy consumption values for MSF and RO desalination, RO technology is the most suitable for desalination, due to its reduced energy consumption.
- Research and developments are being done in order to improve RO membranes efficiency. However, nowadays SWRO technology is still not recommendable for desalination of the Red Coast seawater because the membranes used for RO process have yet to be fully customized for the high salinity of Red Sea and Gulf seawater. Normal seawater salinity of the Red Sea and the Arabian Gulf is around 35% and average TDS values recorded in the study by Saeed et al., 2019 were stable at 45.000 mg/l. Therefore, MSF will be the technology used for the desalination plants of the project in the Red Sea Coast and Libya cost. The project includes MSF desalination plants distributed along the Red Sea coast to provide freshwater to the reforestation in Egypt, then MSF desalination plants in Libya that will provide freshwater to the Niger reforesting region.
- On the other hand, BWRO and MSF technologies can be used for water desalination in the silvo-pastoral reserve of south Senegal since the salinity and turbidity are low. Preferably, SWRO will be used for the underground water of the unstressed Senegalo-Mauritanian basin, because of the advantages in energy consumption mentioned before and more described along Chapter 5.
- Regarding the selection of the type of power plant feeding the MSF plants, single purpose plants are less efficient and hence they have high environmental impact; in multi-purposed plants, combined cycle gas turbine (CCGT) power and desalination plant can achieve 80% overall efficiency and 25% environmental impact as compared to 57% efficiency and 35% environmental impact of single purpose CCGT power plant (Wakil et al., 2017). Therefore, desalination plant together with a CCGT is chosen for the project, since it is the most efficient option, and so, it has the lowest environmental impact.

Design of desalination plants of the project.

After the calculations performed in Chapter 6, the following tables describe the characteristics of the MSF and BWRO plants to install in the study regions of Eastern and Ténéré Desert, since these designs meet all the energy and water requirements. On the left side, Table 25 and Table 26 on the right side.

Table 25: Description of the MSF plant type to install at Eastern and Ténéré Deserts, according to the energy and water requirements.

Table 26: Description of the BWRO plant type to install at Sylvo-Pastorale des Six Foreges Reserve, according to the energy and water requirements.

MSF DESALINATION PLANTS		
Power plant performance		
Net plant power	1000	MW_{elec}
	1	GW_{elec}
LHV Net heat rate (NG)	8047	$kJ/kW_{elec}h$
Fuel LHV input (NG - CHP)	8.047.000	MJ/h
	2235	MW
Net electrical efficiency	44,74	%
Electricity generation process		
CO_2 emissions per electricity production		
Equivalent operating hours per plant	8000	h
Power produced per year per plant	8.000.000	$MW_{elec}h$/year
Avg CO_2 emissions (Egypt) per kWh	0,4213	$kgCO_{2eq}/kW_{elec}h$
Total CO_2 emissions (in time) per plant per year	107	$kgCO_{2eq}$/s
	3,3702	$MtCO_{2eq}$/year
Avg CO_2 emissions (Libya) per kWh	0,5693	$kgCO_{2eq}/kW_{elec}h$
Total CO_2 emissions (in time) per plant per year	4.554.400.000	$kgCO_{2eq}$/year
	144	$kgCO_{2eq}$/s
	4,5544	$MtCO_{2eq}$/year
Desalination process		
Energy consumption		
Avg SEEC	3,75	$kW_{elec}h/m^3$
STEC	190-300	MJ_{therm}/m^3
	15-25	$kW_{elec}h/m^3$
Avg STEC	20	$kW_{elec}h/m^3$
SEC = SEEC + STEC	23,75	$kW_{elec}h/m^3$
Freshwater production		
Total water output per plant	11,7	m^3/s
	1.010.526	m^3/day
	368.842.105	m^3/year
CO_2 emissions per desalination		
Avg CO_2 emissions per m3	10	$kgCO_{2eq}/m^3$
Total CO_2 emissions (in time) per plant	117	$kgCO_{2eq}$/s
	3.688.421.053	$kgCO_{2eq}$/year
	3,6884	$MtCO_{2eq}$/year

BWRO DESALINATION PLANTS		
Desalination process		
Energy consumption		
Avg SEEC	0,48	$kW_{elec}h/m^3$
Avg STEC	0	MJ_{therm}/m^3
SEC = SEEC + STEC	0,48	$kW_{elec}h/m^3$
Freshwater production		
Total water output per plant	350.000.000	m^3/year
	958.904	m^3/day
	11	m^3/s
CO_2 emissions per desalination		
Avg CO_2 emissions per m3	1,5	$kgCO_{2eq}/m^3$
Total CO_2 emissions (in time) per plant per year	17	$kgCO_{2eq}$/s
	525.000.000	$kgCO_{2eq}$/year
	0,0005	$MtCO_{2eq}$/year
Power taken from the grid		
Power consumption per plant	0,0192	GW_{elec}
	19,2	MW_{elec}
Electricity generation process		
CO_2 emissions per electricity production		
Equivalent operating hours per plant	8000	h
Avg CO_2 emissions (Mauritania) per kWh	0,5693	$kgCO_{2eq}/kW_{elec}h$
Total CO_2 emissions (in time) per plant	87.344.658	$kgCO_{2eq}$/year
	3	$kgCO_{2eq}$/s
	0,0873	$MtCO_{2eq}$/year

Design of the derived infrastructures of the project.

Freshwater produced must be delivered to the reforested areas, so that, water distribution network must be considered in the project. Two scenarios will be studied: short-distance pipeline and long-distance pipeline. Short-distance pipeline is for water distribution from Red Sea cost desalination plants to the Eastern Desert and for water distribution from the Senegalo-Mauritanian Basin groundwater to the Sylvo-Pastorale des Six Foreges Reserve. On the other hand, long-distance pipeline scenario will be used for the water distribution from the Libya cost desalination plants to the Ténéré Desert. Both scenarios include the same water parameters and pipe parameters, but different pipe dimensions (diameter and length). Table 28 collects long-distance pipeline results. It is shown as representative of the calculations performed in both scenarios.

From Table 28, by considering the average CO_2 equivalent emissions per kWh produced in each of the countries and the short or long-distance scenario, it is possible to obtain the total CO_2 equivalent emissions by pumping. They result in 0,065 $MtCO_{2eq}$/year in Easter Desert, 1,749 $MtCO_{2eq}$/year in Ténéré Desert and 0,280 $MtCO_{2eq}$/year in the Sylvo-Pastorale des Six Forages Reserve.

Table 1: Description of the long-distance pipeline to install at Ténéré Desert, according to the energy and water requirements.

LONG-DISTANCE PIPELINE SCENARIO		
0. Water parameters		
Density	997	kg/m^3
Dynamic viscosity	0,00089	Pa·s
1. Pipes' dimensions		
Diameter	3	m
Nominal Diameter (DN)	3000	mm
Length	1000	km
Area	7,07	m^2
2. Pipes' parameters		
Max velocity per pipe	2,5	m/s
Max flow rate per pipe	17,67	m^3/s
Reynolds number per pipe	8.401.685	-
3. Friction factor calculation		
ε/D (for steel pipe)	0,00005	-
f (turbulent flow)	0,01098	-
4. Total losses calculation		
l distributed per pipe	11.432,64	J/kg
l concentrated per pipe	571,63	J/kg
Total losses per pipe	12,00	kJ/kg
5. Energy needed per pipe		
Pumping power consumption	3,325	$kW_{elec}h/m^3$
Equivalent operating hours per plant	8000	hours/year
Total pumping energy consumption per year	2.805.346	$MW_{elec}h$
6. Number of pipes needed		
Water transport needs (Ténéré Desert)	924.000.000	m^3/year
Nº pipes needed (Ténéré Desert)	2	pipes
7. Total power needed for pumping		
Total pumping power consumption	350.668	kW_{elec}
8. Total CO2 emissions per pumping		
Avg CO2 emissions (Niger) per kWh	0,5693	$kgCO_{2eq}/kW_{elec}h$
Total pumping CO2 emissions (Ténéré Desert)	1,749	$MtCO_{2eq}$/year

3.3. CO_2 sequestration potential: balances.

As mentioned before in the methodology, overall CO_2 balance is composed by subtracting CO_2 emissions (desalination and pumping) to CO_2 sequestrations (reforestation and avoided/displaced emissions), obtaining a final number of 'Net CO_2 sequestration'. Moreover, the sequestration/emissions (S/E) ratio has been performed for each region. After all, S/E ratio is equal to 8.4 for Eastern Desert, 7,4 for Ténéré Desert and 6,27 for the Sylvo-Pastorale des Six Forages Reserve. While the Net CO_2 sequestration is 68,567 $MtCO_{2eq}$/year in Easter Desert, 70,131 $MtCO_{2eq}$/year in Ténéré Desert and 5,737 $MtCO_{2eq}$/year in the Sylvo-Pastorale des Six Forages Reserve. The next conclusions can be extracted:

- Total CO_2 balance is positive for the three regions considered. Moreover, the ratio Sequestration/Emissions has big and acceptable values in all the areas considered.
- However, the CO_2 sequestration by the region is relatively lower in the Sahel region than in Sahara ones, as well as the net CO_2 sequestration. Moreover, even if the CO_2 sequestration in the Sahel region is the lowest, the water needs are the highest, with a huge difference from the Sahara regions. Due to that, the number of desalination plants needed is large and not convenient.
- It must be said that, in the case of Sahel region, the tree species is *A. senegal*. *A. senegal* sequestrates considerably much less kg of CO_2 per tree that *A. tortilis* (estimated CO_2 sequestration per tree species is: 6,822 $kgCO_{2eq}$/year for *A. Tortilis* and 3,174 $kgCO_{2eq}$/year for *A. Senegal)*. Moreover, *A. senegal* consumes considerably much less water per tree that *A. tortilis* (estimated water needs are 2,31 m^3 of water/year for *A. Tortilis* and 7,395 m^3 of water/year for a *A. Senegal*).

Therefore, the reforestation seems suitable for the Eastern Desert and for the Ténéré Desert, but not for the Reserve. In this case, while the S/E ratio is higher, the Net CO_2 sequestration is markedly less than the other two and does not give enough worth to that large number of desalination plants construction. The reader can find the calculation performance (full version available in Chapter 7) and the final CO_2 balance results for each of the study regions in Tables 30 (on the left), 31 (center) and 32 (on the right).

Table 30: Final CO2 balance description of Eastern Desert due to the reforestation, desalination and water distribution design.

Table 312: Final CO2 balance description of Ténéré Desert due to the reforestation, desalination and water distribution design.

Table 3: Final CO2 balance description of Sylvo-Pastorale des Six Forages Reserve due to the reforestation, desalination and water distribution design.

EASTERN DESERT		
General characteristics of the region		
Total reforested surface	10.000	km^2
Total watering needs	924.000.000	m^3/year
	29,30	m^3/s
CO_2 seq. by the region	68.626.930.155	$kgCO_{2eq}$/year
	68,627	$MtCO_{2eq}$/year
Desalination characteristics		
Type of desalination plant	MSF	-
Power needed / Plant size	1	GW_{elec}
Nº of desalination plants needed	3	plants
Net electric energy produced by each plant	7.315.000.000	kW_{elech}/year
Total CO_2 emissions by desalination	9.240.000.000	$kgCO_{2eq}$/year
	9,240	$MtCO_{2eq}$/year
Displaced/avoided emissions		
Avg CO_2 emissions per kWh production (Egypt)	0,42127	$kgCO_{2eq}/kW_{elec}H$
Total avoided CO_2 emissions per electricity production	9.244.770.150	$kgCO_{2eq}$/year
	9,245	$MtCO_{2eq}$/year
Pumping characteristics		
Pipeline length	50	km
Number of pipes	2	pipes
Total pumping power needed	17.533	kW_{elec}
Total CO_2 emissions by pumping	0,065	$MtCO_{2eq}$/year
CO_2 balance		
Total CO_2 seq. by the region	77,872	$MtCO_{2eq}$/year
Total gross CO_2 emissions for the reforestation	9,305	$MtCO_{2eq}$/year
Net CO_2 sequestration	68,567	$MtCO_{2eq}$/year
Sequestration/Emission	8,4	-

TÉNÉRÉ DESERT		
General characteristics of the region		
Total reforested surface	10.000	km^2
Total watering needs	924.000.000	m^3/year
	29,30	m^3/s
CO_2 seq. by the region	68.626.930.155	$kgCO_{2eq}$/year
	68,627	$MtCO_{2eq}$/year
Desalination characteristics		
Type of desalination plant	MSF	-
Power needed / Plant size	1	GW_{elec}
Nº of desalination plants needed	3	plants
Net electric energy produced by each plant	7.315.000.000	kW_{elec}h/year
Total CO_2 emissions by desalination	9.240.000.000	$kgCO_{2eq}$/year
	9,240	$MtCO_{2eq}$/year
Displaced/avoided emissions		
Avg CO_2 emissions per kWh production (Mauritania)	0,5693	$kgCO_{2eq}$/ kW_{elec}h
Total avoided CO_2 emissions per electricity production	12.493.288.500	$kgCO_{2eq}$/year
	12,493	$MtCO_{2eq}$/year
Pumping characteristics		
Pipeline length	1000	km
Number of pipes	2	pipes
Total pumping power needed	350.668	kW_{elec}
Total CO_2 emissions by pumping	1,749	$MtCO_{2eq}$/year
CO_2 balance		
Total CO_2 seq. by the region	81,120	$MtCO_{2eq}$/year
Total gross CO_2 emissions for the reforestation	10,989	$MtCO_{2eq}$/year
Net CO_2 sequestration	70,131	$MtCO_{2eq}$/year
Sequestration/Emission	7,4	-

SYLVO-PASTORALE DES SIX FORAGES RESERVE		
General characteristics of the region		
Total reforested surface	10.000	km^2
Total watering needs	2.958.000.000	m^3/year
	93,80	m^3/s
CO_2 sequestration by the region	6.825.442.835	$kgCO_{2eq}$/year
	6,825	$MtCO_{2eq}$/year
Desalination characteristics		
Type of desalination plant	BWRO	-
Power needed / Plant size	0,019	GW_{elec}
Nº of desalination plants needed	8	Plants
Net electric energy produced by each plant	177.480.000	kW_{elec}h/year
Total CO_2 emissions by desalination	4.437.000.000	$kgCO_{2eq}$/year
	4,437	$MtCO_{2eq}$/year
Electricity production		
Avg CO_2 emissions per kWh production (Mauritania)	0,5693	$kgCO_{2eq}$/ kW_{elec}h
Total CO_2 emissions per electricity production	808.314.912	$kgCO_{2eq}$/year
	0,808	$MtCO_{2eq}$/year
Pumping characteristics		
Pipeline length	50	Km
Number of pipes	5	Pipes
Total power needed for pumping	56.130	kW_{elec}
CO_2 emissions per pumping	0,280	$MtCO_{2eq}$/year
CO_2 balance		
Total CO_2 seq. by the region	6,825	$MtCO_{2eq}$/year
Total CO_2 emissions for the reforestation	1,088	$MtCO_{2eq}$/year
Net CO_2 sequestration	5,737	$MtCO_{2eq}$/year
Sequestration/Emission	6,27	-

3.4. Cost evaluation.

As mentioned in the methodology, cost evaluation includes forestry running costs, desalination plants and operation costs and water distribution networks (short and long-distance pipeline scenarios). Table 35 shows, for Easter Desert, the cost breakdown of desalination (plants and operation costs) and water distribution network and the average values of the amortization factor used. Same procedure has been followed for the other two regions and can be found in Chapter 8. Also the forestry running costs have been performed for the three regions.

Table 4: Levelized cost breakdown for functional m3 of desalinated water by an MSF plant (with short distance pipeline).

Levelized cost breakdown for functional m³ of desalinated water by an MSF plant (with short distance pipeline)			
Desalination process costs			
Type of expenditure	Measurement	%	euros/m³
Capex	Building and facilities construction (equipment & material, engineering, construction & project management)	33	0,564
	Cost of land	2	0,034
Opex	Energy	20	0,342
	Chemicals & other consumables	2,5	0,043
	O&M (fixed costs)	2,5	0,043
	O&M (variable costs)	1,5	0,026
	Brine disposal & other externalities (brine, waste &sewer disposal, waste transport)	1	0,017
Water distribution network costs (short distance pipeline)			
Type of expenditure	Measurement	%	euros/m³
Capex	Transfer main pipeline construction	37	0,633
Opex	Distribution network electricity use	0,5	0,009
Total costs			
Type of expenditure	Measurement	%	euros/m³
Capex (total)	Levelized Capital Cost (LCC)	72	1,231
Opex (total)	Levelized Operational Cost (LOC)	28	0,479
Final cost	Levelized Cost (LC = LCC + LOC)	100	1,71

After all, the total cost per kilogram of CO_2 sequestered for each study scenario is: 26,544 euros/tCO_{2eq} for Eastern Desert, 185,093 euros/tCO_{2eq} for Ténéré Desert and 655,375 euros/tCO_{2eq} for the Sylvo-Pastorale des Six Forages Reserve. The difference between the costs of Eastern and Ténéré Desert is due to the water distribution network: the first one needs short-distance pipeline (around 50 km long) while the second one needs long-distance pipeline (around 1000 km long), which it increases highly the costs.

At last, some assumptions are made in order to estimate the investment cost of an MSF desalination plant of the Eastern Desert study case, since this case seems by far the most suitable scenario. Again, the reader should notice that it is a preliminary estimation, so the calculations are made only using the data provided before in Table 35:

Total CAPEX = Desalination plant CAPEX (0,564 euros/m^3) + Water distribution pipeline CAPEX (0,633 euros/m^3) = 1,197 euros/m^3. For 308.000.000 m3/year of freshwater production, it results in around 369.000.000 euros/year. Assuming that the ratio between Levelized Carrying Charge and Investment is 0,14, which is a reasonable number for the mix of average-life desalination plant and long-life pipeline (National Renewable Energy Laboratory, 2020), investment cost for 1 plant and its pipeline turns out to be:

(369 M€/year)/(0,14/year) = 2636 M€ = 2,6 billion Euro.

Finally, the cost attributable to the desalination plant will be:

2,6 billion Euro * (0,564/1,197) = 1,225 billion Euro for a 1 GW plant (which is about 1000 €/kW).

4. Conclusion and perspective.

It has been demonstrated that the most suitable scenario is the one proposed for the Eastern Desert, which includes 10.000 km^2 of A. tortilis reforestation, 3 MSF desalination plants along the Red Sea Coast and a water distribution network with short-distance pipeline. Therefore, this project shows that there are favorable locations where reforestation is feasible. Now, to understand if reforestation can be also economically competitive, it needs to be compared with other current technologies. The state-of-art of the CO_2 Capture and Storage (CSS) (Dadhich et al., 2005) shows that the major cost components of these technologies include capture (separation plus compression), transport, and storage (including measurement, monitoring and verification). The cost of capturing CO_2 is the largest component of overall CCS costs.

Capture costs include the cost of compressing the CO_2 to a pressure suitable for pipeline transport (typically about 14 MPa). Reported costs of CO_2 capture vary widely, even for similar applications. The CO_2 capture costs reported in the literature for baseload operations of new fossil fuel power plants (in the size range of 300–800 MW) employing current commercial technology is between 33-57 US$/tCO2 captured for new Natural Gas Combined Cycle (NGCC) plants, 23-35 US$/$tCO_2$ captured for new Pulverized Coal (PC) plants, 11-32 US$/tCO2 captured for new Integrated Gasification Combined Cycle (IGCC) plants and 2-39 US$/$tCO_2$ captured for new Hydrogen plants (see Annex C. Cost of CCS technologies).

Regarding transport costs, the most common and usually the most economical method to transport large amounts of CO_2 is through pipelines. While a cost competitive transport option for longer distances at sea might be the use of large tankers. The Annex C. Cost of CCS technologies includes a figure that shows the CO_2 transport costs range for onshore and offshore pipelines per 250 km, 'normal' terrain conditions. Note that economies of scale dramatically reduce the cost, but that transportation in mountainous or densely populated areas could increase cost.

At last, storage costs estimates range widely for individual options. Estimates of the storage cost in saline formations and disused oil and gas fields (geological storage) are typically between 0.5–8.0 US$/$tCO_2$ stored (see the related table in the Annex C. Cost of CCS technologies). Also ocean storage and storage via mineral carbonation are possible. In addition, monitoring is estimated to add 0.1–0.3 US$/$tCO_2$ stored.

Finally, it has been demonstrated by all the research and work developed in this project that reforestation is economically competitive with other CCS technologies, since the final cost per ton of CO_2 captured in the Eastern Desert is comprised between the ranged costs of other CCS technologies, so reforestation is economically competitive and it is a potential CO_2 capture method for some favorable locations.

The hey take-home messages of this project are:

- The project demonstrates that reforestation should be considered as a future potential tool for CO_2 capturing because of its feasibility and because it is economically competitive.
- Here, the reforestation has been simulated in specific areas of Sahara Desert, where there are several constrictions (such as severe climate conditions and water scarcity). However, the same process can be replicated in other different regions and ecosystems in a relatively easy way.
- Reforestation in the next decades may have a strong potential to mitigate climate change and meet the requirements of the current climate policies.

Finally, some future work and research can be derived from the project:

- It would be interesting to investigate how to expand the reforestation both in Sahara Desert and in other types of ecosystems, by studying the favorability and the feasibility of other large areas of the Sahara and around the world.
- New results could be obtained if other ways are used to simulate a reforestation scenario such as considering mixed species communities instead of monoculture
- Also, new results can be derived by using software to calculate forest biomass instead of specific allometric equations or equations relating growth rate-water availability instead of H-DHB-ρ.
- Geographic Information Systems (GIS) Software encompasses a broad range of applications which involve the use of a combination of digital maps and georeferenced data. It can be used to create more accurate descriptions about several environmental factors involved in this project, such as: hydrological resources, land cover and uses, soil types, solar radiation, air and soil humidity, precipitations, temperatures and biomass.

Chapter 1: Analysis of the Soil

This part of the project contains the analysis of the soil characteristics of the Sahara Desert and Sahel region (Figure 2). In the first part, the satellite data provided by Copernicus Global Land Service (Copernicus, 2020) has been used for the description of the land uses. Thanks to this tool, it has been possible to differentiate the major land cover types present in the countries composing the region studied. And so, the total bare land covering the Sahara Desert has been identified. In the second part, there is a description of the soil characteristics. With that, it has been possible to know the composition, the development profiles and the agricultural value of the different soils occurring in the bare lands of Sahara and Sahel deserts.

1.1. Copernicus Global Land Service.

Copernicus is the European flagship program for monitoring the Earth, using a combination of satellite and ground (in-situ) sensors. The Copernicus Global Land Service (CGLS) is a component of the Land Monitoring Core Service (LMCS) of Copernicus. The Global Land Service systematically produces a series of qualified bio-geophysical products on the status and evolution of the land surface, at global scale and at mid to low spatial resolution, complemented by the constitution of long-term time series. The products are used to monitor the vegetation, the water cycle, the energy budget and the terrestrial cryosphere.

1.1.1 The Global Land Cover Viewer.

The Global Land Cover Viewer (Copernicus, 2020) is one of the viewing services of Copernicus. The land cover classes follow the Land Cover Classification System (LCCS) developed by the Food and Agriculture Organization for the United Nations (UN FAO) to provide a consistent framework for the classification and mapping of land cover. The major land cover types and their domains are:

- **Forest**: Lands covered with trees, with vegetation cover over 30%, including deciduous and coniferous forests and sparse woodland with cover 10 - 30%.
- **Shrubland**: Lands covered with shrubs with cover over 30%, including deciduous and evergreen shrubs and desert steppe with cover over 10%.
- **Herbaceous Vegetation**: Lands covered by natural grass with cover over 10%.
- **Herbaceous Wetland**: Lands covered with wetland plants and water bodies, including inland marsh, lake marsh, river floodplain wetland, forest/shrub wetland, peat bogs, mangrove and salt marsh.
- **Bare land / sparse vegetation**: Lands with vegetation cover lower than 10%, including desert, sandy fields, Gobi, bare rocks, saline and alkaline lands.
- **Cropland**: Lands used for agriculture, horticulture and gardens, including paddy fields, irrigated and dry farmland, vegetation and fruit gardens.
- **Built-up**: Lands modified by human activities, including all kinds of habitation, industrial and mining area, transportation facilities, and interior urban green zones and water bodies.
- **Permanent water bodies**: Water bodies in the land area, including river, lake, reservoir, fish pond.

1.1.2. Global Land Cover: Sahara and Sahel region.

According to the previous land classification, the administrative areas (Figure 1) of the Sahara Desert and Sahel Desert which are Algeria, Chad, Egypt, Eritrea, Libya, Mali, Mauritania, Morocco, Niger, Nigeria, Senegal, Sudan, Tunisia, Western Sahara, have been classified (Tables 1 and 2). Maps and detailed visual data can be found in *Annex A: Global Land Cover by country*.

Figure 1: Map of the administrative areas of the Sahara and Sahel Deserts.

Source: (United Nations, 2020)

Figure 2: Map of the limiting borders of Sahara and Sahel Deserts.

Source: (Digital Journey, 2018)

Table 5: Land cover composition in km2 of the administrative areas of Sahara and Sahel Deserts.

	Land Cover composition (km^2)							
	Forest	Shrubland	Herbaceous vegetation	Herbaceous wetland	Bare / sparse vegetation	Cropland	Built-up	Permanent water bodies
Algeria	36.301,10	45.780,91	47.168,21	0,00	2.109.158,74	68.902,58	3.005,82	1.387,30
Chad	119.179,19	147.863,43	267.169,55	8.122,97	675.221,85	49.499,35	380,76	1.523,60
Egypt	3.051,25	1.968,55	2.755,97	885,85	925.612,21	39.075,72	4.133,96	6.299,36
Eritrea	811,98	25.244,90	21.935,57	12,12	65.697,64	7.319,94	60,6	48,48
Libya	2.272,94	4.221,17	5.682,34	0,00	1.589.918,30	20.131,71	974,12	162,35
Mali	76.083,78	170.874,64	192.846,64	5.022,30	723.298,16	83.993,49	2.134,36	1.381,60
Mauritania	833,20	9.373,50	168.723,00	520,75	859.341,65	2.187,15	208,30	104,15
Morocco	36.089,54	59.672,58	59.168,61	41,43	185.585,57	74.250,80	1.574,51	621,52
Niger	2.372,85	32.745,27	200.742,77	1.423,71	860.275,32	88.151,23	355,93	237,28
Nigeria	314.335,26	120.111,85	65.988,50	10.769,91	456,35	382.422,98	14.238,18	3,377
Senegal	41.628,89	65.357,75	45.980,82	2.678,11	610,45	38.005,56	728,6	354,46
Sudan	71.576,30	171.819,48	295.366,75	554,85	1.121.912,77	183.656,34	1.664,56	2.589,31
Tunisia	9.374,74	11.211,76	16.685,18	31,40	90.612,18	24.538,86	1.909,10	729,49
Western Sahara	0,00	619,15	2.449,67	0,00	265.992,57	0,00	0,00	107,68

Source: (Copernicus, 2020)

Table 6: Land cover composition in % of the administrative areas of Sahara and Sahel Deserts.

		Land Cover composition (km^2)							
	Total area (km^2)	% Forest	% Shrubland	% Herbaceous vegetation	% Herbaceous wetland	% Bare / sparse vegetation	% Cropland	% Built-up	% Permanent water bodies
Algeria	2.312.167	1,57	1,98	2,04	0,00	91,22	2,98	0,13	0,06
Chad	1.269.214	9,39	11,65	21,05	0,64	53,20	3,90	0,03	0,12
Egypt	984.275	0,31	0,20	0,28	0,09	94,04	3,97	0,42	0,64
Eritrea	121.191	0,67	20,83	18,1	0,01	54,21	6,04	0,05	0,04
Libya	1.623.525	0,14	0,26	0,35	0,00	97,93	1,24	0,06	0,01
Mali	1.255.508	6,06	13,61	15,36	0,40	57,61	6,69	0,17	0,11
Mauritania	1.041.500	0,08	0,90	16,20	0,05	82,51	0,21	0,02	0,01
Morocco	414.346	8,71	13,75	14,28	0,01	44,79	17,92	0,38	0,15
Niger	1.186.423	0,20	2,76	16,92	0,12	72,51	7,43	0,03	0,02
Nigeria	912.704	34,44	13,16	7,23	1,18	0,05	41,9	1,56	0,37
Senegal	169.920	21,14	33,19	23,35	1,36	0,31	19,3	0,37	0,18
Sudan	1.849.510	3,87	9,29	15,97	0,03	60,66	9,93	0,09	0,14
Tunisia	155.211	6,04	7,23	10,75	0,02	58,38	15,81	1,23	0,47
Western Sahara	269.196	0,00	0,23	0,91	0,00	98,81	0,00	0,00	0,04

Source: (Copernicus, 2020)

1.2. Soil development profiles.

The objective here is to describe the desert soil characteristics. The information has been extracted from (D'Hoore, 1964) whose aim was to map the different type of soils present in Africa. The general legend of the map comprises 63 elements of mapping units, recorded by a symbol. Each element of the map has its symbol, made up of a capital and a lower-case letter. The capital letter indicates the higher categories of the legend, the lower-case letter the under-categories.

The type of soil present in the countries within the desert region are listed in Table 3. The most repeated symbols are highlighted since they are the most common types of soil in these countries, meaning that they describe the main characteristics of the soil in the Sahara and Sahel deserts.

Table 7: Types of soil classification of the administrative areas of the Sahara and Sahel Desert.

		Algeria	Chad	Egypt	Libya	Mali	Mauritania	Morocco	Niger	Sudan	Tunisia	Western Sahara	**TOT**	
A – RAW MINERAL SOILS	Aa	X	x			x	x			x			5	
	Ab					x			x				2	
	Ab’	X						x					2	
	Ac	X	x	x	X	x	x	x	x	x	x	x	11	Not differentiated rocks
	An	X	x	x	X	x	x		x	x	x	x	10	Sands (ergs)
	Ao		x				x		x				3	
	Ap	X	x		X	x	x	x			x	x	8	Desert pavements, residual
	Ap’	X			X				x			x	4	
	Ar	X		x	X		x	x		x		x	7	Not differentiated desert
B – WEAKLY DEVELOPED SOILS	Bb					x			x				2	
	Bc					x	x			x			3	
	Bc’	X						x			x		3	
	Bd	X	x			x		x	x	x	x		7	Lithosols (skeletal soils) and lithic soils, Not differentiated
	Bf	X		x	X	x	x	x	x	x	x		9	Sub-desert soils, Not differentiated
	Bh	X								x	x		3	
	Bo	X	x	x		x	x	x	x	x	x		9	Juvenile soils on recent deposits on riverine and lacustrine alluvium
	Bq							x					1	
	Br	X	x	x	X						x		5	
C – CALCIMORPHIC SOILS	Ca	X						x	x		x		4	
	Cc	X									x		2	
D – VERTISOLS AND SIMILAR SOILS	Da		x				x						2	
	Db	X				x					x		3	
	Dj	X	x			x		x	x	x	x		7	Of topographic depressions, not differentiated
F – HIGHVELD PSEUDO-PODSOLIC SOILS	Fa	X						x			x		3	

G – BROWN AND REDDISH-BROWN SOILS OF ARID AND SEMI-ARID REGIONS	Ga		x			x	x		x	x			5	
	Gb		x			x	x		x	x			5	
	Gn	X			X			x			x		4	
H – EUTROPHIC BROWN SOILS OF TROPICAL REGIONS	Hb					x			x	x			3	
	Hc									x			1	
I – RED AND BROWN MEDITERRANEAN SOILS	Ia	X			X			x			x		4	
	In	X						x					2	
J – FERRUGINOUS TROPICAL SOILS (fersiallitic soils)	Ja		x			x			x	x			4	
	Jc		x			x	x		x				4	
	Jd		x			x	x		x	x			5	
K – FERRISOLS	Ka												0	
	Kb					x				x			2	
	Kc					x							1	
L – FERRALLITIC SOILS (sensu stricto)	Ll					x							1	
	Ln									x			1	
M – HALOMORPHIC SOILS	Mb	X			X		x		x		x		5	
	Mc	X				x	x				x	x	5	
	Md	X											1	
	Me	X	x	x			x	x	x		x		7	Not differentiated
N – HYDROMORPHIC SOILS	Na	X	x	x		x	x		x	x	x		8	Mineral hydromorphic soils
	Nb		x						x	x			3	

Source: (D'Hoore, 1964)

From highest to lowest, the main symbols and their descriptions for the desert area are:

1.2.1.1. A – Raw mineral soils.

Soil conditions of this type are so unfavorable to biological activities that living processes and the pedogenesis they promote are lacking almost completely. They are "pre-soils" or soils near zero time in soil formation.

- Ac: Rock and rock debris, not differentiated rocks.

Granite and gneiss of the basement complex are the main elements. The agricultural value is null to very low.

- An: Desert detritus, sands (ergs).

Loose materials of diverse particle size, bare of vegetation, subject to wind, situated in hot climates with very low and erratic rainfall or with none. The agricultural value is null, but presence of water permits the installation of gardens (oases).

- Ap: Desert pavements, residual.

Poor quality residual material produced mainly by physical erosion. The agricultural value is null.

- Ar: Not differentiated desert.

All loose materials submitted to desert conditions which, for lack of data, have not been separated. The agricultural value is null.

1.2.1.2. B – Weakly developed soils.

The soils have in common a low level of profile development, reflected in a very weak differentiation of horizons.

- Bf: Sub-desert soils, Not differentiated.

Sub-desert soils are transitional between the desert detritus that is practically abiotic and the brown soils of arid and semi-arid regions. They are soils very low in organic matter with slightly differentiated genetic horizons, sometimes with accumulation of carbonates or soluble salts slightly hardened at the surface and/or at some depth. They occur in hot climates with very low rainfall.

Regarding to the agricultural value, the nutrient potential of these soils is generally high. Under irrigation they may yield good crops, but their soluble salt content demands certain precautions. In their natural state they produce only poor pastures and certain products which may be collected such as resins, incense, and gum Arabic.

- Bo: Juvenile soils on recent deposits on riverine and lacustrine alluvium.

They are soils without clear differentiation of genetic horizons mainly due to the shortness of the soil forming period and having profiles developed from various recently deposited materials.

The agricultural potential is influenced largely by the composition of the sediments, which, in turn, are highly variable as affected by origin, transportation distance, and the speed of the transporting currents. Moreover, the sediments are found under very different climates that induce different types of appropriate agriculture. In a given region, alluvial plains often comprise the soils with the highest agricultural potential

- Bd: Lithosols (skeletal soils) and lithic soils, not differentiated.

Soils with very weak differentiation of genetic horizons, containing grainy elements and having solid rock within 30 centimeters depth. This element is characteristic of regions where erosion is important. On the map its presence may indicate excessive relief, climates with intense precipitation, or vegetative covers that afford only small protection. The agricultural value is generally low but can be afforested when the climate allows it. In another place, poor pastures and game reserves.

1.2.1.3. N – Hydromorphic soils.

- Na: Mineral hydromorphic soils.

Soils whose development and characteristics are influenced by permanent or seasonal waterlogging. Some of these soils have a relatively high level of cation saturation.

Several of these soils have relatively high agricultural value, especially those that are waterlogged either temporarily or seasonally. Their reclamation may necessitate control of the water level. They are much used for rice and sugar cane, and when well drained they are suitable also for intensive cultivation of bananas.

1.2.1.4. D – Vertisols and similar soils.

- Dj: Of topographic depressions, not differentiated.

These soils are found in topographic depressions where poor external drainage aggravates the effects of inherently poor internal drainage. They seem to develop only under climates where potential evaporation is high during part of the year. So, they present slow permeability and poor internal drainage, even though external drainage may be favorable. Profiles show the effect of mechanical reworkings such as dry season cracks. Moreover, the reserve of weatherable minerals is often high.

These soils deserve particular attention in view of the possibilities they offer to agriculture, and the relatively small use that has been made of them thus far. However, their topographic situation frequently associates them with calcimorphic or halomorphic formations and impedes their drainage and their desalinization. Several are developed under subtropical climates that are very favorable to agriculture

1.2.1.5. M – Halomorphic soils.

- Me: Not differentiated.

These soils barely cover 1% of the total surface of Africa. Soils whose morphology is mainly due to the presence in the profile of soluble salts and of exchangeable cations notably sodium, probably modified for the growth of most crop plants.

In the natural state many of these soils are unfit for use. In order to make them suitable to agriculture, the process may require important investments since a preliminary leaching of soluble salts and/or exchangeable cations is often necessary. Reclaimed soils are frequently used for cotton or sugar cane.

1.3. Summary.

Along this first part of the project, some conclusions can be summarized. On the one hand, since the aim of the project is about reforestation, the bare land of the Sahara Desert and Sahel Desert countries has been illustrated, localized and quantified thanks to Copernicus Global Land Service. With all, the total bare land existing is summarized in Table 4:

Table 8: Summary of the land cover composition of Sahara and Sahel Deserts per administrative area.

	Bare / sparse vegetation (km²)	%
Algeria	2.109.158,74	22,263
Chad	675.221,85	7,127
Egypt	925.612,21	9,770
Eritrea	65.697,64	0,693
Libya	1.589.918,30	16,782
Mali	723.298,16	7,635
Mauritania	859.341,65	9,071
Morocco	185.585,57	1,959
Niger	860.275,32	9,081
Nigeria	456,35	0,005
Senegal	610,45	0,006
Sudan	1.121.912,77	11,842
Tunisia	90.612,18	0,956
Western Sahara	265.992,57	2,808
TOTAL	9.473.693,76	100

Source: (Copernicus, 2020)

On the other hand, the main soil types (D'Hoore, 1964) present in the region have been collected. They are:

RAW MINERAL SOILS: "pre-soils" or soils near zero time in soil formation. They are so unfavorable to biological activities and their agricultural value is very low. Can be classified as: rock and rock debris (granite and gneiss); ergs (sands, which have bare of vegetation and are subject to wind, situated in hot climates with very low rainfall) and desert residual pavements (poor quality residual material produced mainly by physical erosion).

WEAKLY DEVELOPED SOILS: low level of profile development, reflected in a very weak differentiation of horizons. Can be classified as: sub-desert soils (very low in organic matter, but generally high nutrient potential, so under irrigation they may yield good crops producing certain products such as resins, incense, and gum Arabic); juvenile soils on recent deposits on riverine and lacustrine alluvium (clear differentiation of genetic horizons, agricultural potential influenced by the composition of the sediments); lithosols (skeletal soils) and lithic soils (very weak differentiation of genetic horizons, containing grainy elements and having solid rock within 30 cm depth, low agricultural value but can be afforested when the climate allows it).

HYDROMORPHIC SOILS: such as mineral hydromorphic soils (development and characteristics influenced by permanent or seasonal waterlogging, relatively high agricultural value).

VERTISOLS AND SIMILAR SOILS OF DEPRESSIONS: soils with poor external drainage and slow permeability, so they seem to develop only under climates where potential evaporation is high during part of the year, they deserve particular attention in view of the agriculture possibilities but some of them are very favorable to agriculture).

HALOMORPHIC SOILS: soils barely covering 1% of the total surface of Africa. In the natural state many of these soils are unfit for use. In order to make them suitable to agriculture, the process may require important investments since a preliminary leaching of soluble salts and/or exchangeable cations is often necessary.

Chapter 2: Analysis of the Ecoregions

This part of the project aims to describe the ecoregions present in the Sahara and Sahel deserts in order to understand the biodiversity of flora, fauna and ecosystems shared between the different territories.

2.1. Description of the ecoregions.

An ecoregion is an area defined by its ecology, meaning the unique characteristics of its climate, geomorphology, soils, hydrology, flora and fauna. In the following points, the ecoregions of the Sahara and Sahel deserts will be described according to the information given in the World Wide Fund for Nature (WWF Panda) (WWWF Panda, 2020).

2.1.1. Atlantic Coastal Desert.

Location and General Description.

The Atlantic Coastal Desert is a narrow strip of land fringing the Atlantic Coast of Western Sahara and Mauritania. This ecoregion covers the vast majority of Western Sahara's 1110 km coastline, from La'ayoune southwards, and roughly two-thirds of Mauritania's 754 km of coastline (Figure 3).

The ecoregion lies between sea level and a maximum of 200 m in elevation. Much of the coast is formed of cliffs 20 to 50 meters high and a sandy or gravelly hamada plateau stretches inland. The climate is extremely hot and arid, with only low amounts of episodic rainfall. Despite this, mists blown in from the Atlantic are common. Condensation of these mists permits the growth of lichens on shrubs and on the bare ground between vascular plants. The ecoregion has a much denser vegetation cover than that of other parts of the Sahara and is also relatively rich in plant species.

Justification of Ecoregion Delineation.

The boundaries of this ecoregion, extending from the coast to 40 km inland, are taken directly from the 'Atlantic coastal desert' vegetation unit of the reference (White, 1983). Its uniqueness derives from the mist it receives from the Atlantic making it relatively rich in endemic plants.

2.1.2. North Saharan steppe and woodlands.

Location and General Description.

This ecoregion extends across northern Africa and covers parts of Western Sahara, Mauritania, Morocco, Algeria, Tunisia, Libya, and Egypt. It is generally found inland of the coast but stretches to the shore in areas where there is low rainfall. In Morocco, Algeria and Tunisia, this ecoregion forms a transition between the Mediterranean domain towards the north and the true desert in the south.

Water is a serious constraint in this ecoregion. In the northern Sahara, the climate is hot and dry in the summer and cooler with rain in the winter. Rains come from the Mediterranean and these occur mostly from October to April. Average annual rainfall varies from 50 mm in the south to 100 mm in the North. The highest temperature ranges between 40 and 45°C, creating evaporation that far exceeds the amount that falls as rain.

Figure 3: Map of the limiting borders of North Saharan steppe and woodlands ecoregion.

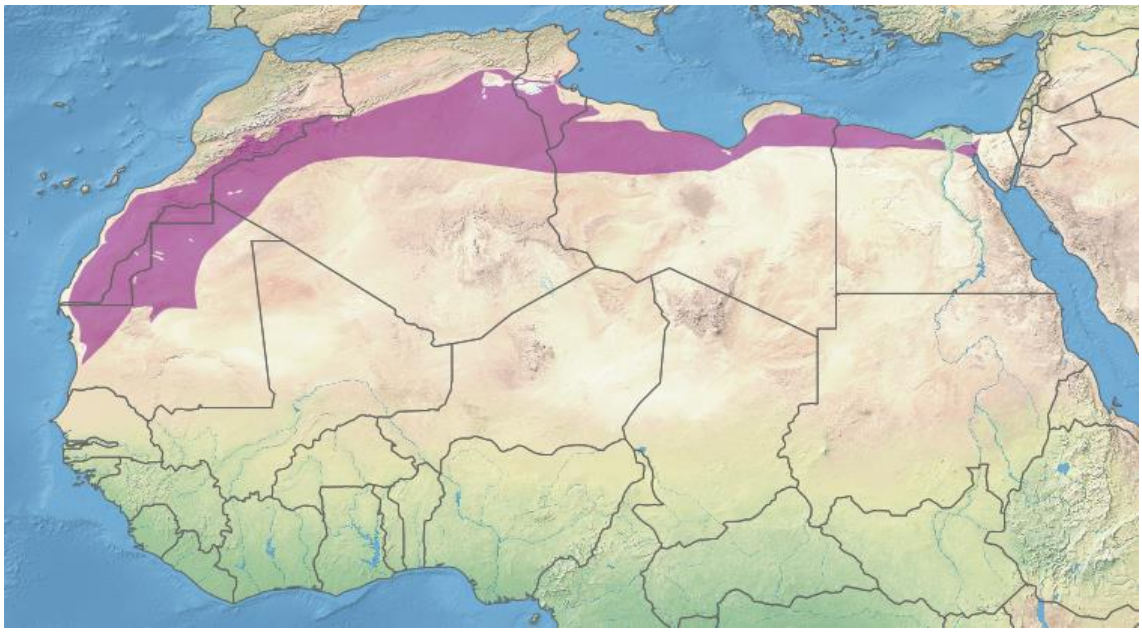

Source: (Wikipedia, 2013)

The ecoregion contains several geomorphologic features with different origins:

- Ergs: sandy systems such as dunes, "placages", "nebkhas", "barkanes" whose heights vary annually.
- Regs: mixture of sand and gravel often described as a desert pavement of loose stone.
- Hamadas: wide and elevated rocky plateaus where vegetation is relatively rare.
- Wadis: wide river beds, indicating a rainy past (as Oued Saoura, Oued M'Zi, Oued Mya) hosting "woodlands" of Acacia.
- Dayas: depressions which are not salty and are favorable to the development of vegetation, with high number of Leguminosea, good for grazing.
- Mountains i.e. "Ougarta Mountains in Algeria": that dominate Beni Abbès plateaus covered by Acacia raddiana vegetation.

Biodiversity Features.

On sandy habitats there are several endemic plants, including *Retama retam*, *Genista saharae*, *Rhanterium suaveolens*, *Calligonum comosum*, *Tamarix sp.* and *Zilla spinosa*. On dayas and bed wadis are woodlands of *Acacia raddiana* and *Acacia seyal* which support several endemic plant species including *Panicum turgidum*, *Pithuranthos sp.*, *Neurada procumbens*, *Anastatica hyrochuntina*, and *Astragalus gombo*. On the hammadas habitats also there are some endemics, such as *Pithuranthos chloranrhus*, *Helianthemum lippii*, *Gymnocarpos decander* and *Helianthemum kahirikum* (Quézel, 1965).

Justification of Ecoregion Delineation.

This ecoregion is delineated from (White, 1983) 'regs, hamadas and wadis' and 'desert dunes with perennial vegetation' units north and west of the Sahara Desert.

2.1.3. Central Sahara Desert.

Figure 4: Map of the limiting borders of Central Sahara Desert ecoregion.

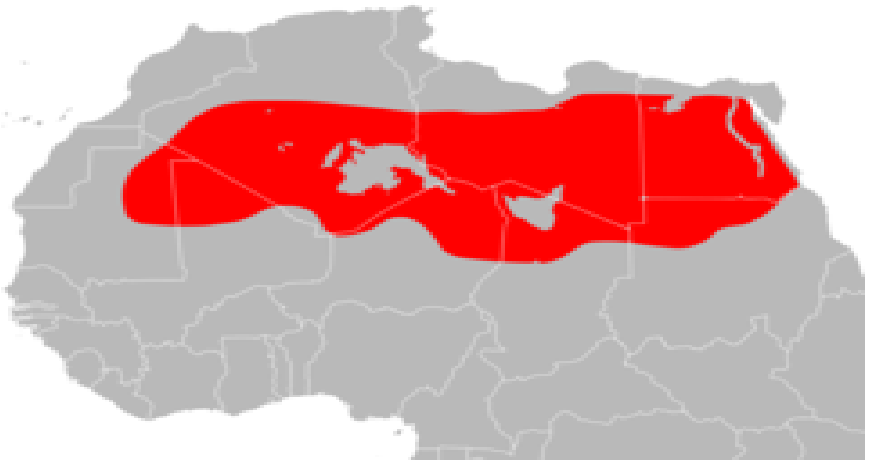

Source: (Wikipedia, 2008c)

Location and General Description.

The ecoregion includes the hyper-arid central portion of the Sahara where rainfall is minimal and sporadic. Now only rock, sand and sparse vegetation exist over huge areas. This ecoregion covers the central Sahara Desert, between 18º and 30º N, and has an area of 4.619.260 km^2 (Figure 4).

The surface of the desert ranges from large areas of sand dunes (erg Chech, Raoui), to stone plateaus (hamadas), gravel plains (reg), dry valleys (wadis), and salt flats (Cloudsley-Thompson, 1984; Williams & Faure, 1980). Vast underground aquifers that underlie much of the region sometimes penetrate the surface, resulting in oases.

The annual rainfall is below 25 mm, and in the eastern part of the desert it is less than 5 mm per year. In the hottest months, temperatures can rise over 50°C, and temperatures can fall below the freezing point in the winter. A single daily variation of -0.5°C to 37.5°C has been recorded. The Central Sahara is also extremely windy. Hot, dust-filled winds create dust devils which can make the temperatures seem even hotter.

Shifting sands and bare rocks cover only about one-fifth of the greater Central Sahara. More than half of the area comprises soils known as yermosols, with shallow profiles over gravel or pebble beds. These soils have been developing over the past 50 million years. Large expanses of ergs and regs will be devoid of any visible plant life for years, but following rainfall, vegetation cover may reach more than 50 percent on sand dunes and 20 percent on the gravel plains (WWWF Panda, 2020).

Biodiversity Features.

The flora of the central Sahara Desert is very poor and estimated to include only 500 species (Le Houérou, 1990). This is extremely low considering the huge extent of the area. It mainly consists of xerophytes and ephemeral plants (called also locally *Acheb*), with halophytes in moister areas. Vegetation is very contracted along the wadis and the dayas with *Acacia sp.*, *Tamarix sp.* and *Calotropis procera.* Where there is enough groundwater, hammadas are covered by *Anrthirrnum ramosissimuma* and *Ononis angustissima* (Quézel, 1965).

Justification of Ecoregion Delineation.

The borders for this ecoregion follow ‘desert dunes with perennial vegetation’ and ‘absolute desert’ (White, 1983) and correspond approximately to the region with less than 25 mm of mean annual rainfall.

2.1.4. South Saharan Steppe and Woodlands (Sahelian region).

Figure 5: Map of the limiting borders of South Saharan steppe and woodlands ecoregion.

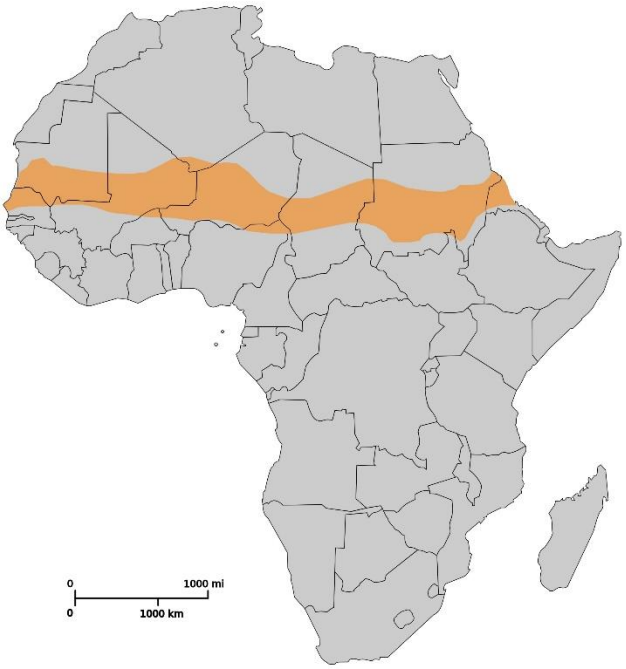

Source: (Wikipedia, 2008b)

Location and General Description.

The South Saharan Steppe and Woodlands ecoregion extends in a narrow band from central Mauritania, through Mali, southwestern Algeria, Niger, Chad, and across Sudan to the Red Sea, covering the southern fringes of the Sahara Desert (Figure 5).

Rainfall occurs mainly during the summer months of July and August but is unreliable and varies greatly from year to year. On average, annual rainfall is between 100 and 200 mm, declining along a gradient from south to north. Mean annual temperature throughout the Sahelian portion of the ecoregion is between 26ºC and 30ºC. Rainfall in this ecoregion is insufficient for rain-fed agriculture, but some irrigated agriculture is practiced near water points and along wadis (seasonally dry watercourses).

Biodiversity features.

It serves as a transition from the Sahara to the Sahel. Delineated by 'regs, hamadas and wadis' vegetation type (White, 1983). Woody species include *Acacia tortilis*, *Acacia ehrenbergiana*, *Balanites aegyptiaca*, and *Maerua crassifolia*, which mainly grow along wadis. In the south, the vegetation of the ecoregion grades into the Sahelian Acacia Savanna ecoregion and includes steppes of *Panicum turgidum* perennial tussock grass.

Justification of Ecoregion Delineation.

This ecoregion is delineated from 'regs, hamadas and wadis' and 'desert dunes with perennial vegetation' (White, 1983) units south of the Sahara Desert.

2.1.5. West Saharan Montane Xeric.

Figure 6: Map of the limiting borders of West Saharan Montane Xeric ecoregion.

Source: (Wikipedia, 2008d)

Location and General Description.

Tassili-n-Ajjer, found largely in southeastern Algeria, comprises a majority of the ecoregion, the Ahaggar massif. Also the three smaller outliers occur including the Air ou Azbine in northern Niger (with Monts Bagouezane reaching over 2000 m), Dhar Adrar in Mauritania (reaching almost 700 m) and Adrar des Iforas in Mali and Algeria (reaching 900 m). Previous locations are shown in Figure 6.

Climatically, this ecoregion is cold and dry in the winter and hot and dry in the summer. Rainfall is variable, but averages less than 100 mm per year, with most falling at higher elevations. Even during the summer the ecoregion may receive precipitation at elevations above 2400 m. The mean maximum temperature reaches 30°C at the lower elevations and 18° to12°C at the highest elevations. The mean minimum temperatures are as low as 3°C at the highest elevations and as high as 15°C at the lowest elevations in the ecoregion. Frosts are common, and snow can be found on the higher peaks in the winter.

The largest part of the ecoregion, the Tassili-n-Ajjer area, is comprised of volcanic lava. The soils that developed over these deposits are mapped as a mixture of bare rock and lithosols at higher elevations and yermosols at lower elevations. Forests of wind-eroded rocks cover much of the ground (Cloudsley-Thompson, 1984). The historical alternation between wetter and drier periods, and their accompanying geomorphologic processes have led to the unique morphologic structure and steep sided valleys of the Tassili-n-Ajjer. The past wet periods also produced large lakes in the region that are today the great ergs, or vast areas of shifting sand dunes.

Biodiversity features.

At lower elevations, the vegetation is mapped as regs, hamadas and wadis, but at the highest altitudes there is a transition to saharomontane vegetation (White, 1983).

Vegetation within this ecoregion varies according to elevation and landscape features and contains a number of endemic and rare species. The most notable of these is *Duprey cypress*, or "tarout" (*Cupressus depreziana*), wild olive (*Olea lapperrini*) and myrtle (*Myrtus nivellei*), all of which are relict Saharan-Mediterranean species.

2.1.6. Tibesti-Jebel Uweinat montane xeric woodlands.

Figure 7: Map of the limiting borders of Tibesti-Jebel Uweinat montane xeric woodlands ecoregion.

Source: (Wikipedia, 2008d)

Location and General Description.

This ecoregion is made up of two isolated montane areas in the central part of the Sahara Desert. The larger Tibesti Mountains area is found in the northern portion of Chad and extends marginally into southern Libya. The Tibesti Mountains consist of seven inactive volcanoes, with the highest peak reaching 3415 m. The second, smaller area is the Jebel Uweinat, located further to the east along the intersection of eastern Libya, southwestern Egypt, and northwestern Sudan. The Jebel Uweinat includes peaks reaching elevations just under 2000 m (Figure 7).

Annual average rainfall in the surrounding Sahara Desert is under 100 mm, and extremely unreliable. Lowland wadis areas receive their water from the mountains down storm channels. This water remains for a considerable period, as these areas have natural impermeable layers and shield-like sand covers that slow evaporation (Cloudsley-Thompson, 1984). The mean maximum temperature is approximately 30°C in the lowlands and falls to 20°C in the highest elevations. Mean minimum temperatures are 12°C in the lowlands but fall to 9°C over most of the ecoregion and are as low as 0°C at the highest elevations during winter months.

The geology of this ecoregion is volcanic in origin, with a large area of Tertiary basalt within an expanse of Nubian sandstones. The soils developed over the basalts are typically thin, with lithosols being predominant. Bare rock and regosols also occupy large areas of the ecoregion.

Biodiversity features.

The vegetation is mapped at the lower elevations as regs, hamadas, and wadis, and at the highest elevations as Saharomontane. The Tibesti mountain vegetation varies according to elevation and slope. Large wadis areas radiate from the southwestern slopes supporting tree species such as the doum palm (*Hyphaene thebaica*), *Salvadora persica*, *Tamarix articulata*, *Acacia nilotica adstringens* and *Acacia albida* (White, 1983). The Saharomontane vegetation of the higher elevations supports the endemic *Ficus teloukat*, which grows on the south and southwestern slopes, *Myrtus nivellei* and *Nerium oleander* on the western slopes, and *Tamarix `gallica nilotica'* and *Nerium oleander* on the wetter northern slopes. The northern slopes also support wetland species such as *Juncus maritimus*, *Typha australis*, Scirpus holoschoenus, *Phragmites australis* and *Equisetum ramosissimum* (White, 1983).

The peak of the Jebel Uweinat is virtually devoid of vegetation with only some shrub species like Lavandula and Salvia (White, 1983). Dominant species include *Fagonia indica*, *Aerva javanica*, *Acacia tortilis*, and *Cleome chrysantha*. The Jebel Uweinat, however, is not highly vegetated. The wadis support the greatest

quantity of lower elevation desert vegetation, since they receive rainwater runoff from the mountain areas. In these Jebel Uweinat the wadis vegetation comprises open *Acacia tortilis-Panicum turgidum* plant communities of Mediterranean affinity (White, 1983).

Justification of Ecoregion Delineation.

These high elevation areas over 3400 m are unique geological formations with distinct biota within the Sahara Desert. The boundaries of the ecoregion are taken from 'Saharamontane vegetation' (White, 1983).

2.1.7. Saline areas of Sahara Desert.

Location and General Description.

Ecoregion of flooded grassland that occupies 54.000 km^2 spread over several chotts from the west and north of the Sahara. Chotts are salt depressions that flood sporadically. These areas are too saline areas to be cultivated.

In North Africa, there are salty lakes in semi-arid regions, mainly in Algeria and Morocco. These lakes have changing shores and are dry for much of the year. They are formed with the waters of the spring thaw of the summits of the Atlas mountain system, with occasional rainwater or coming from underground waters of the Sahara.

Biodiversity features.

The flora is low in height.

2.1.8. Red Sea coastal desert.

Figure 8: Map of the limiting borders of Red Sea Coastal Desert ecoregion.

Source: (Wikipedia, 2008a)

Location and General Description.

Rocky desert ecoregion of 56.300 km^2. It occupies almost the all Egyptian coast of the Red Sea and the northern half of the Sudanese. The Egyptian part is bordered to the west by the ecoregion of the Sahara Desert, while the Sudanese is done with the steppe and wooded savannah of the southern Sahara and contains small enclaves of Ethiopian mountain jungle. To the south, it borders the acacia savanna of the Sahel (Figure 8).

Biodiversity features.

In this ecoregion, only plant species resistant to salinity and drought survive. Along the interior wadis, acacia is one of the resistant species.

2.2. Analysis of climate.

This part of the project consists of a climate study. For that, Köppen climate classification has been used. The Köppen climate classification system is by far the most widely used in modern climate classification system. It uses only the average annual and monthly values of temperature and precipitation. The Köppen climate classification scheme divides climates into five main groups (+1), each having several types and subtypes.

Climate dataset (Climate-Data.org, 2020) has been used as a source for the data recollection for the climate study. Climate-Data.org is based on two data sources:

- *CLIMATE-MODEL BY CLIMATE-DATA.ORG: all the climate data comes from a climate model. The model has more than 220 million data points and a resolution of 30 arc seconds. The model uses weather data from thousands of weather stations from all over the world. This weather data was collected between 1982 and 2012. This data will also be refreshed from time to time.*
- *LOCATION DATA BY OPENSTREETMAP.ORG: all of the location data for the cities is based on data from the OpenStreetMap project. OpenStreetMap is an open-source platform, licensed under the Open Data Commons Open Database License. The OpenStreetMap data has not been modified. This data is refreshed regularly to quickly reflect any changes in the data of the OpenStreetMap project.*

The data recollected will be used in the next points of the project, e.g. for tree selection for reforestation, which requires to take into account the climate characteristics of a region.

2.2.1. Climate classification by country.

Temperature and precipitation data have been collected for each region of each country belonging to the studied area (Table 5 and 6). Specifically, the data extracted from the source refers to:

- the regions of the Sahara Desert classified as bare land
- the regions of the Sahel Desert comprised in the "Great Green Wall Project" (GGW, 2020). The Great Green Wall (GGW) Project consists on the reforestation of the areas affected by the desertification of the Sahel region due to the climate change. The aim of the project is to create a "green wall" that reduces the propagation of the desertification.

Table 9: Köppen-Geiger classification by regions of the Sahara Desert.

SAHARA: BARE LAND		
Country	**Regions**	**Köppen-Geiger classification**
Algeria	Tindouf	BWh
	Adrar	BWh
	Tamanrasset	BWh
	Illizi	BWh
	Ouargla	BWh
	Ghardaïa	BWh
	Bechar	BWh
	El Oued	BWh
Chad	Tibesti (Bouro)	BWh
	Borkou (Faya-Largeau)	BWh
	Ennedi (Fada)	BWh
Egypt	Matrouh (Marsa Matruh)	BWh
	Giza	BWh
	New Valley (Al Ghirizat)	BWh
	Red Sea (Hurghada)	BWh

	Minya (Al-Minya)	BWh
	Cairo	BWh
	Suez	BWh
	North Sinai (Al Arish)	BWh
	South Sinai (Nueiba)	BWh
Libya	Al Wahat (Awjilah)	BWh
	Butnan (Tobruk)	BWh
	Kufra	BWh
	Nalut	BWh
	Jabal al Gharbi (Gharyan)	BSh
	Misrata	BSh
	Sirte (Ras Lanuf)	BWh
	Jufra (Waddan)	BWh
	Wadi al Shatii (Addisha)	BWh
	Wadi al Hayaa (Awbari)	BWh
	Murzuq (Waw al Kabir)	BWh
	Sabha	BWh
Mali	Tombouctou (Timbuktu)	BWh
	Kidal	BWh
	Gao	BWh
Mauritania	Tiris Zemmur (Bir Moghrein)	BWh
	Adrar (Ouadane)	BWh
	Tagant (Tidjikja)	BWh
	Inchiri	BWh
	Dakhlet Nouadhibou	BWh
	Hodh el Charqui	BWh
Morocco	Guelmim	BWh
	Bouarfa	BWk
	Taourirte	BWk
	Er Rachidia	BWh
Niger	Agadez	BWh
	Zinder	BWh
	Diffa	BWh
Sudan	North Darfur (Kutum)	BWh
	Ash-Shamaliyah (Northern State)	BWh
	Shamal Kurdufan	BWh
	Khartoum	BWh
	Nahr an Nil (Nile River state)	BWh
	Al-Bahr Al-Ahmar (Red Sea State)	BWh
Tunisia	Tataouine	BWh
	Kebili	BWh
	Medenine	BWh
	Gabes	BWh
	Tozeur	BWh
Western Sahara	Dakhla	BWh

	Laayoune	BWh
	Guelmim	BWh

Source: (Climate-Data.org, 2020)

Table 10: Köppen-Geiger classification by regions of the Sahel Desert.

SAHEL: GREAT GREEN WALL		
Country	**Regions**	**Köppen-Geiger classification**
Burkina Faso	Ouahigouya	BSh
Chad	Borkou (Faya-Largeau)	BWh
Eritrea	Keren	BSh
Ethiopia	Mekele	BSh
Djibouti	Djibouti	BWh
Mali	Mopti	BSh
Mauritania	Tagant (Tidjikja)	BWh
Niger	Tounga Aoudou	Aw
	Dolé	Aw
Nigeria	Sokoto	BSh
	Katsina	BSh
Senegal	Kébémer	BWh
Sudan	North Darfur (Kutum)	BWh

Source: (Climate-Data.org, 2020)

From the Tables 5 and 6, it is easy to see that the climates present in the regions result to be:

- BWh - Hot desert climate (Hot Arid Desert): defined by little precipitation, hot-month average temperatures normally between 29 and 35 °C and midday readings of 43–46 °C.
- BWk - Cold desert climate (Cold Arid Desert): defined by little precipitation with hot, dry and though summers but not typically as hot as hot desert climates. BWh tend to feature cold, dry winters. Snow tends to be rare in regions with this climate.
- BSh - Hot semi-arid climate (Hot Arid Steppe): characterized by hot, sometimes extremely hot, summers and warm to cool winters, with some to minimal precipitation.
- Aw - Tropical savanna climate (Dry winter): this type of climate has every month of the year with an average temperature of 18 °C or higher, with significant precipitation and with the driest month having precipitation less than 60 mm.

All the data of temperature and precipitation of each country and each region can be found in the *Annex B: Minimum, maximum and average temperatures and precipitations by country.*

Chapter 3: Analysis of Water Resources

This part of the project focuses on the identification and description of the main water sources of the Sahara Desert and Sahel Desert. First, the permanent surface water bodies are listed and characterized. They include rivers, lakes, chotts, dams, oasis, wadis and the surrounding seas (Red Sea and Mediterranean Sea) and oceans (Atlantic Ocean). Second, the groundwater sources and their related basins are explained. Finally, some conclusions are made in reference to the possible use of the sources, summarizing the total water resources available for irrigation in the project.

3.1. Surface water bodies.

The main surface water bodies are described below. The locations with an *(*)* are Ramsar sites. Ramsar sites are recognized as wetlands with high ecological, economic, cultural, scientific and recreational value and are collected in the *List of Ramsar wetlands of international importance* (Ramsar Convention, 2020). There are *Guidelines for reviewing laws and institutions to promote the conservation and wise use of wetlands.* The descriptions of the non-Ramsar sites are based on information extracted from general encyclopedia (Encyclopedia Britannica, 2020).

3.1.1. Algeria.

Inside the bare land.

- Chott Melghir *(*).*

Chott Melghir has a surface of 6700 km^2 and a watershed of 68.751 km^2. It is the largest lake in Algeria. It lies almost entirely below the sea level and contains the lowest point in Algeria, −40 meters. During the rainy season in winter, the lake is filled by numerous wadi (periodically drying rivers), mostly from north and north-west. The largest of them are the Djedi and Arab. In summer, the lake and most the rivers feeding it dry out, and Chott Melghir turns into a salt pan. The annual water evaporation varies between 9,6 and 20 km^3 and evaporation from soil nearby the lake can reach 14 km^3.

- Chott El Hodna *(*).*

It is located within an endorheic basin in the Hodna region. Its size is about 80 km long and 16 km wide and has a surface of 76.000 ha. It is located 394 meters above the sea level. Owing to the extreme rate of evaporation, Chott el-Hodna is of varying size and is often dry.

- Djorf Torba Dam.

Djorf Torba is a dam used for the purposes of irrigation and water supply. The impounds are Oued Guir and Oued Saoura. Its height is 38 meters. The dam volume is 1.900.000 m^3 (built-up) and the reservoir total capacity is 360.000.000 m^3. However, the reservoir active capacity is about 190.000.000 m^3.

- Sebkhel el Melah *(*).*

It is an endorheic salt-lake formed in a basin. The lake is fed by the seasonal river Oued Saoura but most of the year the volume of water evaporated from the surface exceeds the volume of water flowing in, and a salt crust is formed. Periodically, heavy rains cause the Saoura to flood and water flows into the sabkha. Some water infiltrates the clayey ground forming an impervious layer under which is an aquifer. Evaporation of the water in the lake occurs and, after a few months, the sabkha dries up, and a new crust is formed.

3.1.2. Chad.

Out of the bare land.

- Lake Chad *(*).*

Lake Chad is a historically large, shallow, endorheic lake. Lake provides water to more than 30 million people living in Chad, Cameroon, Niger and Nigeria. It is the largest lake in the Chad Basin. The primary inflow is Chari River and the primary outflows are Soro and Bodelé depressions. The surface area is 1350

km^2 with an average depth of 1,5 m. The water volume is 72 km^3. The surface elevation is 278 to 286 meters and the shore length is 650 km.

- Lake Fitri *(*).*

The normal size of the lake is about 500 km^2. The size of this lake can triple in wetter years. This freshwater lake is shallow and is fed by seasonal rainfall and run-off from a catchment area estimated at 70.000 km^2. The principal river feed is the seasonal Batha River which carries water from the Ouaddai massif to the west. The catchment area is 70.000 km^2.

3.1.3. Egypt.
Inside the bare land.

- Red Sea.
- Mediterranean Sea.
- Nile River.

It is the longest river in Africa about 6650 km long. Its mouth is the Mediterranean Sea (sea level elevation). The basin size 3.400.000 km^2. Its maximum width is 2,8 km and its average depth is between 8 and 11 meters. The discharge locations are Aswan with 2830 m^3/s and Cairo with 1400 m^3/s.

- Siwa Oasis.

The Siwa oasis is in a deep depression that reaches below sea level, to about −19 metres. It is an urban oasis in Egypt. About 80 km in length and 20 km wide, Siwa Oasis is one of Egypt's most isolated settlements with about 33.000 people (berbers).

- Qara Oasis.

It is one of the inhabited oases of Egypt, with a population of 363 Berbers. This oasis is often disregarded when it comes to counting the number of Egyptian oases as it is very small compared to the others.

- Qarun Lake (Faiyum Oasis) *(*).*

It is a depression in the desert immediately to the west of the Nile south of Cairo in Egypt. The extent of the basin area is estimated at between 1270 km^2 and 1700 km^2. The basin floor comprises fields watered by a channel of the Nile, the Bahr Yussef, as it drains into a desert depression to the west of the Nile Valley.

- Wadi El Rayan *(*).*

The valley of Wadi El-Rayan has an area of 1759 km^2, 113 km^2 of which are the dominating water body of the Wadi El Rayan lakes. The Wadi has been used for man-made lakes from agricultural drainage which has made a reserve of the two separate Wadi El Rayan Lakes. The reserve is composed of a 50,90 km^2 upper lake and a 62 km^2 lower lake, with waterfalls between the two. Wadi El Rayan Waterfalls are the largest waterfalls in Egypt.

- Nasser Lake.

It is a vast reservoir in southern Egypt and northern Sudan. It is one of the largest man-made lakes in the world. Strictly, "Lake Nasser" refers only to the much larger portion of the lake that is in Egyptian territory (83% of the total), with the Sudanese preferring to call their smaller body of water Lake Nubia. The primary inflows are the Nile River and Wadi Allaqi. The primary outflows are Nile River and Toshka Spillway. The basin countries are Egypt and Sudan. The maximum length is 550 km, the average depth is 25,2 m. The maximum width is 35 km. The surface area the 5250 km^2. The maximum depth is 180 m. The water volume is 132 km^3. Shore length: 7844 km. Surface elevation: 183 m. Nasser lake, together with the Nile River, creates the Toshka Lakes, a new lake system that is endorheic, so the waters can never flow on to the sea. It also helps to recharge the underlying aquifer; but desert temperatures cause very high levels of evaporation.

- Aswan High Dam.

It is an embankment dam built across the Nile in Aswan (Egypt) providing increased water storage for irrigation and generating hydroelectricity. About the dam and spillways: type of dam is embankment, the impound is River Nile, the height is 111 m, the length is 3830 m, the width (base) is 980 m and the spillway capacity is 11000 m^3/s. About the reservoir: the total capacity is 132 km^3, the surface area is 5250 km^2, the maximum length is 550 km, the maximum width is 35 km, the maximum water depth is 180 m and the normal elevation is 183 m.

3.1.4. Eritrea.
Inside the bare land.

- Red Sea.
- Barka River.

Barka River flows from the Eritrean Highlands to the plains of Sudan. With a length of over 640 km, it rises just outside Asmara and flows in a northwestern direction through Agordat. The river merges with the Anseba River near the border with Sudan.

- Seasonal rivers: Anseba River, Damas River, Wokiro River and Haddas River.

3.1.5. Libya.
- Mediterranean Sea.

3.1.6. Mali.
Inside the bare land.

- Niger River.

Principal river of West Africa, extending about 4180 km. Its drainage basin is 2.117.700 km^2 in area. Its source is in the Guinea Highlands in southeastern Guinea. It runs in a crescent through Mali, Niger, on the border with Benin and then through Nigeria, discharging through a massive delta, known as the Niger Delta in the Atlantic Ocean. The discharge average is 5589 m^3/s.

Outside the bare land.

- Débo Lake.

It is a lake in the central part of Mali, formed by the seasonal flooding of the Niger River basin. It is in the Inner Niger Delta of the Niger River. During high water stages of the river, the delta formed by lakes, creeks, and backwaters form part of Lake Débo. The inner delta has many wide channels, which are shallow and flooded marshes. Its size is largely reduced during the dry season of September to March. Surface area: 160 km^2.

- Faguibine Lake.

Lake Faguibine is a lake in Mali on the southern edge of the Sahara Desert situated 80 km west of Timbuktu and 75 km north of the Niger River to which it is connected by a system of smaller lakes and channels. In years when the height of the annual flood of the river is enough, water flows from the river into the lake. Primary inflows: Niger River. The lake forms part of a system of five interconnected low-lying depressions that fill to variable depths depending on the extent of the annual flood of the Niger River. Lake Faguibine is by far the largest of these depressions with an area of 590 km^2.

3.1.7. Mauritania.
- Atlantic Ocean.

3.1.8. Morocco.
Inside the bare land.

- Al Massaira Dam *(*)*.

The Al Massira Dam is a gravity dam providing water for the irrigation of over 100.000 hectares of farmland in the Doukkala region. The dam's hydroelectric power plant also generates 221 GWh on average annually. The dam's reservoir and wetlands were designated as a Ramsar site in 2005. About the dam and spillways:

the type of dam is gravity, the impounds is Oum Er-Rbia River, the height is 82 m and the length is 390 m. The reservoir total capacity: 2,76 km^3, the catchment area is 28 500 km^2 and the surface area is 80 km^2.

- Bin El-Ouidane Dam.

It is an arch dam. The purpose of the dam is hydroelectric power production and irrigation. Its 135 MW power station produces an average of 287 GWh annually and water from the reservoir helps irrigate 69.500 hectares in the Beni Moussa and Tadla plains. About the dam and spillways: the impound is El Abid River, the height is 133 m, the length is 290 m and the dam volume is 365.000 m^3 (built-up). About the reservoir: the total capacity is 1,5 km^3. The catchment area is 6400 km^2.

Outside the bare land.

- El Wahda Dam.

It is an embankment dam on the Ouergha River. It was constructed for flood control, irrigation, water supply and hydroelectric power production. It is the second largest dam in Africa and the largest in Morocco. About the dam and spillways: the impound is Ouergha River, the height is 88 m and the length is 2600 m. About the reservoir: the total capacity is 3,8 km^3, the catchment area is 6200 km^2 and the surface area is 123 km^2.

- Idriss I Dam.

It is a gravity dam on the Inaouen River. The dam serves to provide irrigation for 72.300 hectares of land and its power plant generates 66 GWh of electricity annually. About the dam and spillways: the height is 72 m, the length is 447 m and the dam volume is 450.000 m^3. About the reservoir: the total capacity is 1186 km^3 and the catchment area is 3300 km^2.

3.1.9. Niger.
Out of the bare land.

- Niger River.

3.1.10. Nigeria.
Out of the bare land.

- Dadin Kowa Dam.

The reservoir has a capacity of 800 million m^3 of water and a surface area of 300 km^2. Around 26.000 people were displaced by the reservoir.

- Challawa Gorge Dam.

The dam is 42 m high and 7,8 km in length. The dam has a full storage capacity of 904.000.000 m^3. The direct catchment area is 3857 km^2.

- Kainji Dam.

Kainji Dam extends for about 10 km, including its saddle dam, which closes off a tributary valley. The primary section across the outflow to the Niger is 550 m. Most of the structure is made from earth, but the center section, housing the hydroelectric turbines, was built from concrete. This section is 65 m high. Kanji Dam is one of the longest dams in the world.

- Kaduna River.

The Kaduna River is a tributary of the Niger River which flows for 550 km through Nigeria. It starts in Plateau State on the Jos Plateau 29 km southwest of Jos town, flows through its namesake Kaduna State and through its capital Kaduna, and meets the Niger River in Niger State.

- Hadejia River.

It is a river in northern Nigeria and is a tributary of the Yobe River (Komadugu Yobe). Damming of the river for the purposes of irrigation has led to a decrease in the amount of water in the Hadejia-Nguru

wetlands, which the river forms along with Nguru Lake. The Hadejia river is now 80% controlled by the Tiga and Challawa Gorge dams in Kano State.

- Golgola River.

It is in northeastern Nigeria, the principal tributary of the Benue River. The upper course of the river as well as most of its tributaries are seasonal streams but fill rapidly in August and September. The Gongola rises on the eastern slopes of the Jos Plateau and falls to the Gongola Basin, running northeasterly until Nafada. After the Kiri dam was constructed, downstream flood peaks dropped from 1420-1256 m^3/s, while flows in dryer seasons increased from 5,7-21 m^3/s. The river downstream from the dam also narrowed and became less winding, with fewer separate channels.

3.1.11. Senegal.
Inside the bare land.

- Senegal River.

It is a 1,086 km long river in West Africa that forms the border between Senegal and Mauritania. It has a drainage basin of 270.000 km^2, a mean flow of 680 m^3/s, and an annual discharge of 21,5 km3. Important tributaries are the Falémé River, Karakoro River, and the Gorgol River.

Outside the bare land.

- Atlantic Ocean.
- Lac de Guiers.

It is a chief source of fresh water for the city of Dakar, hundreds of kilometers to the south-west, through underground pipes. It is about 35 km long and 8 km wide and is supplied by the Ferlo or Bounoum River. Lac de Guiers is designated an Important Bird Area by BirdLife International.

3.1.12. Sudan.
Inside the bare land.

- Red Sea.
- Nile River.
- Lake Nubia.

See Nasser Lake.

Strictly, "Lake Nasser" refers only to the much larger portion of the lake that is in Egyptian territory (83% of the total), with the Sudanese preferring to call their smaller body of water Lake Nubia.

Outside the bare land.

- White Nile River.

It is one of the tributaries of the Nile River. The basin size is about 1.800.000 km^2, the length is 3700 km and the discharge point has its location in Rwanda, with a discharge average of 878 m^3/s.

- Blue Nile River.

It is one of the tributaries of the Nile River. The basin size is about 325.000 km^2, the length is 1450 km and the discharge point has its location in Tana Lake, with a discharge average of 1548 m^3/s.

- Roseires Dam.

It is a dam on the Blue Nile at Ad Damazin, in Sudan. It consists of a concrete buttress dam 1 km wide with a maximum height of 68 m, and an earth dam on either side. The earth dam on the eastern bank is 4 km long, and that on the western bank is 8,5 km long. The reservoir is about 290 km^2. The dam was completed in 1966, initially for irrigation purposes. A power generation plant, with a maximum capacity of 280 MW, was added in 1971. About the dam and spillways: the height is 78 m and the length is 24.410 km. About the reservoir: the total capacity is 7,4 km^3 and the surface area is 29.000 ha.

3.1.13. Tunisia.
Inside the bare land.

- Mediterranean Sea.
- Chott el Djerid *(*)*.

It is a large endorheic salt-lake in southern Tunisia. The bottom of Chott el Djerid is located between 10 and 25 meters below sea level. Width varies widely; at its narrowest point, it is only 20 km across, compared to its overall length of 250 km. The narrow eastward inlet of the chott is also known as Chott el Fejej. It is the largest salt pan of the Sahara Desert, with a surface area of over 7000 km^2. During winter, a small tributary of water can be seen discharging into the lake. Currently, freshwater irrigation schemes are being applied in the region to help eliminate salt from soils and increase the productive area.

Outside the bare land.

- Cherita Sabhka.

Sabkha is a coastal, supratidal mudflat or sandflat in which evaporite-saline minerals accumulate as the result of semiarid to arid climate. It is a salt-lake wetland. It covers an area of 11.600 hectares and is 17 by 9 km wide. Fueled by several wadis, such as the Oued Merguellil, Oued Nebhana and Oued Zeroud.

- Sidi El Hani Sabkha *(*)*.

Is a salt-lake in the Sousse Governorate of Tunisia. It covers an area of 36.000 hectares and consists of three depressions: the Sidi El Hani Sebkha stricto sensu, the Sebkha Souassi and the Sekha Dkhila. Fueled by several wadis, such as the Wadi Chrita, the Wadi Mansoura and the Wadi Oum El Mellah, it retains water all year round only occasionally. The catchment area is 360 km^2 and the system empties into the Mediterranean Sea. It is a UNESCO World Heritage Site.

3.1.14. Western Sahara.

- Atlantic Ocean.

3.2. Groundwater bodies.

Groundwater has a growing role in the economic and social development of Africa. The development of irrigated agriculture by groundwater is possible in areas underlain by extensive regional aquifer systems or local aquifers with adequate replenishment. Because of their interest for the project, the major aquifer systems will be described in this paragraph. Bibliography (IAEA, 2017; Zektser, 2004) has been checked to obtain information about the major groundwater basins of North Africa: the Nubian Basin, the Northwestern Sahara Basin, the Niger Basin, the Chad Basin, Taoudeni Basin and Senegalo – Mauritanian Basin.

Favorable conditions exist in alluvial, lacustrine, basaltic and wadi aquifers. However, the sustainable use of nonrenewable water resources, occurring mainly in large sedimentary basin underlying the Sahara, needs a special approach. Variation of precipitation through time and limited availability of groundwater, which characterize the semi-arid belts of Africa, presents the greatest challenges to the management of water resources of these parts of Africa.

3.2.1. Major groundwater basins of North Africa.

The extensive arid belt of the northern part of Africa are underlain by large sedimentary basins (shown in Figure 9), characterized by large reserves and very low recharge.

Figure 9: Major Groundwater basins in North Africa: 1. Nubian Basin; 2. Northwestern Sahara Basin; 3. Niger Basin; 4. Chad Basin; 5. Taoudeni Basin; 6. Senegalo – Mauritanian Basin.

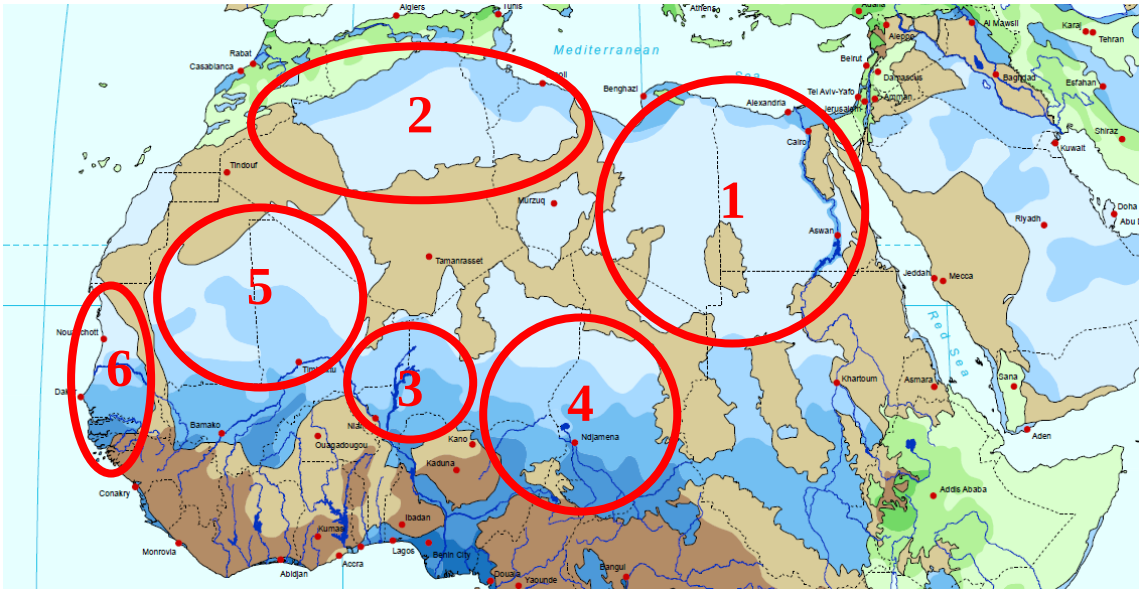

Source: (WHYMAP, 2020)

3.2.1.1. The Nubian basin.

The Nubian groundwater reservoir contains huge reserves estimated at about 150.000 km^3 (Thorweihe, 2002). The rate of recharge, however, is so low that the water of the aquifer system is considered to represent, to a large extent, a nonrenewable resource at the human timescale. Several sub-basins and uplifts have been recognized in the area underlain by the Nubian, including the Dakhla Basin, the Kufra Basin and the North-western Basin (Egypt). Based on the estimates of the regional hydraulic, the groundwater flow velocity was estimated at 1 m/year. Thus, the groundwater needs about one million years to pass through the system from recharge areas at the southern boundary to the Qattara discharge area. The groundwater of the Nubian Basin is generally characterized by its high quality. The total dissolved solids range from 100 to 1000 mg/l. Salinity increases northward.

3.2.1.2. The Northwestern Sahara basin.

The Sahara basin covers an area of about 780.000 km^2. It is underlain by two major aquifers: the Lower aquifer, the 'Continental Intercalaire' composed of continental sediments and the Upper aquifer and the

'Complex Terminal', a multilayered aquifer consisting of sand stones and limestones. They are separated by the M'zab high. The western Timimoune basin occupies about 280.000 km^2 and is covered by the sand dunes of the Great Western Erg. The Eastern Mya basin extends over an area of about 500.000 km^2 and is covered by the Great Oriental Erg (Khouri, 1989). Towards the Mediterranean coast they are interconnected or merge to form one aquifer system. The Sahara aquifer system is generally considered a nonrenewable aquifer system. The groundwater reserve is estimated to be around 60.000 km^3 in volume.

3.2.1.3. The Niger basin.

The Niger basin extends for about 1000 km from the Hoggar Precambrian massif, in the North, to the Nigerian Shield, in the south, and extends over 800 km from east to west. In the east it communicates with the Chad basin through Damergou shelf, a subsurface extension of the Air massif, and to the west it communicates with the Taoudenni basin through the Sudan graben. The Niger basin is a relatively deep basin filled with a thick sequence of sedimentary rocks ranging in age from Paleozoic to Quaternary.

This complex range of detrital and carbonate sediments can be classified into four hydrogeological units or major aquifers (Khouri, 1989):

I) The Lower continental sandstone aquifer system: consists of two major aquifers, the Izeguandane aquifer and the Agades-dabla aquifer. Both aquifers are composed primarily of sandstone and overlain by clayey confining layer (the Irhazer clays). The aquifer system covers an area of about 50.000 km^2 and is recharged from wadi runoff in the large outcrop areas of the air. Recharge is however small compared to the large reserves estimated at 1500–3000 mln m^3. Groundwater is slightly mineralized ranging from 700 to 3000 mg/l.

II) The Tegama 'Continental Intercalaire' aquifer system: consists of continental sediments, mainly sandstones, the Tegama sandstone and Farak series. It underlies some 488.000 km^2. It is a water table aquifer in the eastern part of the basin and confined in the central and southern parts. The average thickness of the aquifer is 500 m in the greater part of Niger and ranges from 240 to 500 m in Nigeria. It reaches about 1000 m in the western areas.

III) The Upper Cretaceous carbonate aquifer system: formations with predominantly low-permeability marine deposits. The sandy formations of the Maestrichtian are moderately productive and their waters have relatively low concentration of dissolved solids between 600–3000 mg/l.

IV) The Upper Continental aquifer system: a water-table aquifer consisting of sands and alluvium. The thickness of the aquifer varies from featheredge to 60 m. Recharge occurs in the periphery of the Doutchi syncline, leakage from the lower aquifers is probable.

3.2.1.4. The Chad basin.

The Chad basin is a huge depression extending for about 260.000 km^2 between Tibesti and Hoggar Precambrian massifs in the north. It communicates with several large basins: the Niger basin in the west, the Murzuk basin in the north and the Benue basin in the southwest. The degree of interconnection with these basins is not, however, clearly defined.

Chad can be divided into two big aquifer systems:

I) The Pliocene aquifer system (130.000 km^2) in Chad and which could be tapped at a depth of about 300 m in the center of the basin. In the lake Chad basin occurs under confined conditions and constitutes an important source of freshwater. Groundwater is slightly mineralized; the concentration of dissolved solids ranges between 500 and 1500 mg/l.

II) The continental Terminal aquifer system consisting of sandstone and argillaceous sands. The aquifer occupies in Chad two separate areas: one in the north (130.000 km^2) at a depth of 80–100 m. It is exploited by traditional wells whose depth may reach 100 m. The aquifer is only slightly developed**.**

2.1.5. The Taoudeni basin.

The Taoudeni basin is one of the largest basins in the world. It covers an area of about 1,8 mln. km^2. The major aquifer systems in the Taoudeni basin include:

- Fissured aquifer systems:

I) The Precambrian basement form generally poor aquifers. Groundwater could be tapped however in fracture zones. The depth of groundwater varies from few meters to 100 m. Water is, however, acidic with pH values between 5,5 and 7,7. The concentration of dissolved solids is generally low, less than 500 mg/l.

II) The fractured infra-cambrian sandstones are aquiferous in their upper parts, down to a depth of some tens of meters. The water table lies at a depth of 10 to 25 m. The aquifers depth may reach 60 m. Mineralization is low, about 300 mg/l.

- Intergranular aquifer systems:

I) The Continental Intercalaire aquifer system consists on confined groundwater that could be tapped at a depth of about 100 m. The depth of the potentiometric surface, ranges between 35 and 60 m. Productivity is generally low, even in wells drilled into depth of 150–200m.

II) The Continental Terminal aquifer system consists of sands and sandstones. In the interior delta of the Niger river, the Continental Terminal aquifer is recharged from surface water. The concentration of dissolved solids is low (80–100 mg/l) in the Niger Delta areas, where recharge is relatively high. It increases northwards to about 3500 mg/l.

To conclude, recharge in the Taoudeni basin is very low, or negligible, in the northern part, but relatively high in the south. The Niger river plays an important role in this respect. Recharge of the Paleozoic sandstone occurs mainly in the southern part of the basin, whereas replenishment of the Continental Intercalaire aquifer system occurs mainly in the central delta of the Niger River. Concentration of dissolved solids in groundwater increases, generally, from the peripheral zones towards the center of the basins and, in the alluvial aquifer, from the upper reaches to the lower reaches of the Niger river.

3.2.1.6. The Senegalo – Mauritanian Basin.

The Senegalo-Mauritanian Basin, which includes parts of Mauritania, Senegal, Gambia and Guinea Bissau, is the largest of the northwest African Atlantic margin basins and covers roughly more than 300.000 km^2 (Bellion, 1897).

Three main aquifer systems providing exploited ground water resources can be distinguished:

I) The Shallow aquifer system: covers the whole sedimentary SMB. It is dominantly made of sand and sandy clay. The aquifers are intergranular, and the best groundwater potential occurs in sand layers. It comprises the Boulanouar (3000 km^2), the Bennichab (1200 km^2) and the Trarza (20 000 km^2) aquifers. The Shallow aquifer system ranges between 0 to 150 m thick, with a water table depth between a few meters to a depth of 72.5 m.

II) The Intermediate aquifer system: includes Eocene and Paleocene formations, and mainly comprises limestone, often karstic or affected by faults. Ranges between 40 to 120 m thick, with a water table depth between a few meters to 102,5 meters depth. The Eocene aquifer is exploited in the central western part of Senegal and along the Senegal River. The Paleocene aquifer occurs mainly in western Senegal. These aquifers constitute one of the main sources of drinking water for Dakar.

III) The deeper aquifer system: mainly of Maastrichtian age, extends across the whole of the Senegal Mauritanian Basin and generally consists of sand, sandy-clay and calcareous sandstone. Groundwater storage and flow are largely intergranular. This aquifer constitutes the main source of groundwater supply in Senegal. It is a transboundary system but is not exploited in Mauritania due to low hydraulic conductivity and high salinity. The deeper aquifer system is about 250 m thick, with a water table depth between a few meters to 140 meters. Recharge occurs from direct rainfall and indirectly from rivers and is estimated at about 103 x 10^6 m^3/a to the Maastrichtian deeper aquifer system.

In Mauritania, the renewable surface water resources are estimated to be about 11 km^3/year, mainly provided by the Senegal River. At the beginning of 1920, the extracted water volume was estimated at about 1700 mm^3 (88% irrigation, 9% for domestic use and 3% for industrial activities).

3.2.2. Renewable groundwater stress: definition and cases.

It is important to talk about the different stress status in which a water body can be classified, and it is necessary to evaluate the current status of the major basins of North Africa. These two topics are covered

in a recent bibliography (Voss et al., 2015). Understanding the amount of groundwater used versus the volume available is crucial to evaluate future water availability. Following the traditional water stress approach (Alcamo et al., 1997; UN; et al., 1997) Renewable Groundwater Stress (RGS) is defined as the ratio of groundwater use to renewable groundwater availability as shown in (Eq. 1). This dimensionless ratio represents the percent of renewable water being used to meet human water demand.

$$RGS = \frac{use}{availability} \qquad \text{(Eq. 1)}$$

Previous studies defined water use as water withdrawals and quantified use with national withdrawal statistics in which a single value represents per-capita water use for an entire country (Vorosmarty et al., 2000), thus assuming water is used homogenously within a country.

Additionally, the definition of availability has focused on the renewable fluxes of the dynamic water cycle (United Nations, 2003), including river runoff and groundwater recharge (Postel et al., 1996; Shiklomanov, 2000; United Nations, 2003).

Four characteristic stress regimes are defined: Overstressed, Variable Stress, Human-dominated Stress, and Unstressed. The regimes are a function of the sign of use (positive or negative) and the sign of groundwater availability, defined as mean annual recharge. These end members encompass the spectrum of out comes given positive (gaining) or negative (depleting) estimates of use and positive (recharging) or negative (discharging) estimates of annual recharge. Thus, quite simply, the ratio represents the percent of recharge that is used to meet water demands. Stress will occur in the systems where withdrawals exceed capture such that storage loss occurs.

3.2.2.1. Overstressed case.

The RGS ratio is positive since both recharge and use are negative. This case, resulting from a combination of large withdrawals and negative recharge, implies groundwater mining or active depletion (Figure 10). In shallow aquifers, negative or negligible recharge is largely driven by groundwater supported evapotranspiration, especially in summer months and during dry periods (Koirala et al., 2014; Yeh, 2005) observed this kind of dynamics in semiarid to arid regions.

Figure 10: Diagram of groundwater Use-Availability. Overstressed case.

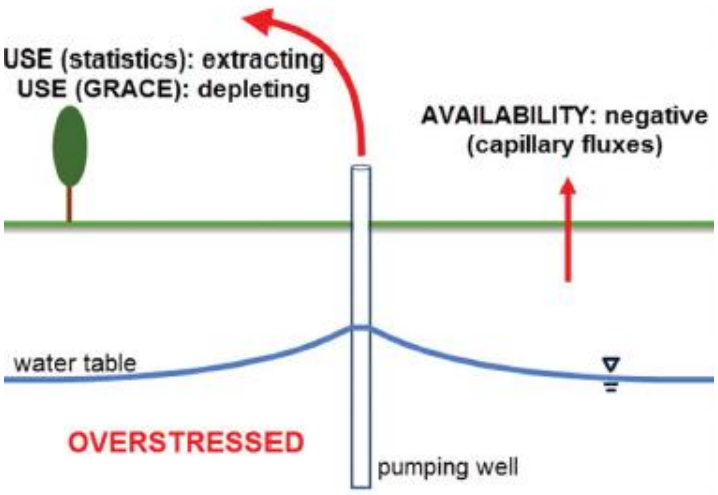

Source: (Voss et al., 2015)

3.2.2.2. Variable Stress case.

Use is negative (withdrawals) and recharge is entering the system (positive, so it is recharging), resulting in a negative RGS ratio (Figure 11).

Figure 11: Diagram of groundwater Use-Availability. Variable stress case.

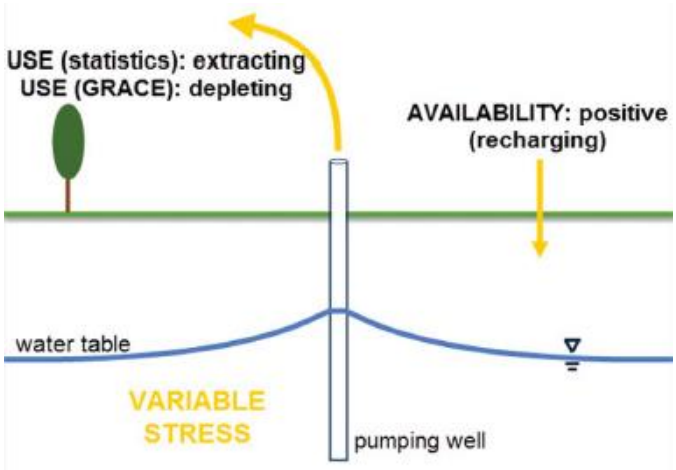

Source: (Voss et al., 2015)

There are four levels of Variable Stress, according to the Table 7. The reader should notice that the RGS ratios in the table are in absolute value:

Table 11: United Nations Renewable Stress Scale.

Stress Ratio	Stress Level
0–0.1	Low
0.1–0.2	Moderate
0.2–0.4	High
> 0.4	Extreme

[a]The stress ratio represents the dimensionless Renewable Groundwater Stress Ratio used in this study.

Source: (Voss et al., 2015)

3.2.2.3. Human-dominated case.

Human-Dominated case is the result of a positive trend from GRACE and negative recharge (Figure 12). Natural behavior of these systems would be a loss of groundwater through capillary flux to the root zone (De Vries, 2002; Lo et al., 2008; Walvoord, 2004) by direct evapotranspiration.

Figure 12: Diagram of groundwater Use-Availability. Human-dominated case.

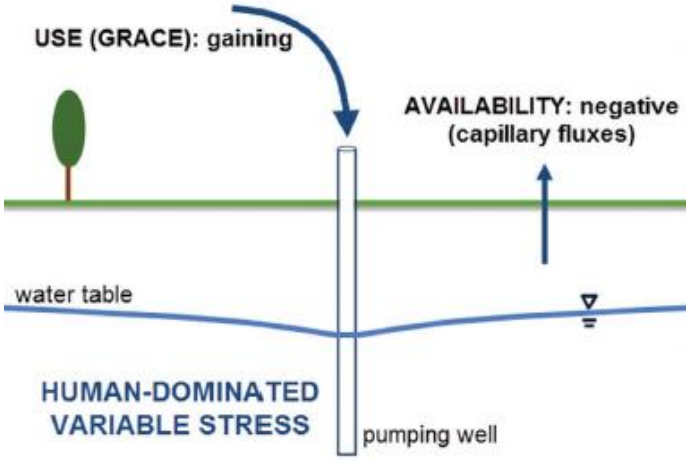

Source: (Voss et al., 2015)

3.2.2.4. Unstressed case.

The Unstressed case has a positive trend in groundwater storage anomalies and positive recharge (Figure 13). This case is only considered unstressed from a water quantity perspective.

Figure 13: Diagram of groundwater Use-Availability. Unstressed case.

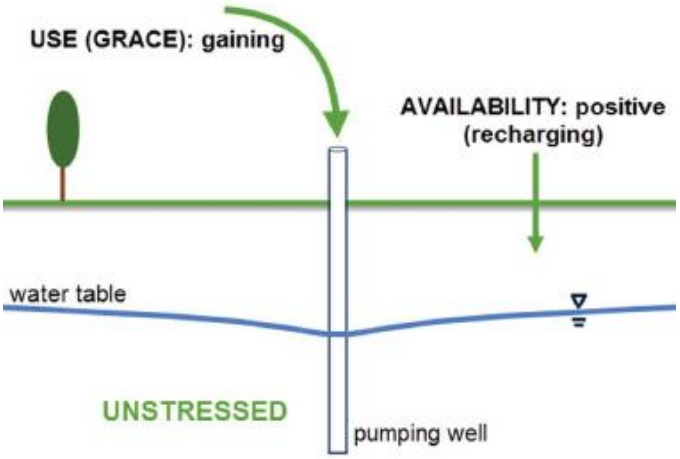

Source: (Voss et al., 2015)

3.2.3. Renewable groundwater stress of the major basins of North Africa.

The studied basins with their identification number are shown in the Figure 14 and Table 8:

Figure 14: Map of the major groundwater basins in Africa with their identification number.

Source: (Voss et al., 2015)

Table 12: Study Aquifers with the Aquifer identification number.

Aquifer ID	Aquifer Name
1	Nubian Aquifer System (NAS)
2	Northwestern Sahara Aquifer System (NWSAS)
3	Murzuk-Djado Basin
4	Taoudeni-Tanezrouft Basin
5	Senegalo-Mauritanian Basin
6	Iullemeden-Irhazer Aquifer System
7	Lake Chad Basin

Source: (Voss et al., 2015)

The parameters described are shown in Table 9 for the major basins of the Sahara Desert region:

Table 13: Study aquifers with Basin Average Groundwater Withdrawal statistics (Qstat) (mm/yr), Mean Annual Recharge (R) (mm/yr) and the dimensionless statistics-based Renewable Groundwater Stress ratio (RGSstat).

Aquifer ID	**Q_{stat}**	**R**	**RGS_{stat}**
1	-0,46	-0,27	1,69
2	-0,34	-0,26	1,33
3	-0,46	-0,23	2,04
4	-0,01	1,04	-0,01
5	-0,38	34,38	-0,01
6	-0,15	11,18	-0,01
7	-0,23	5,99	-0,04

Source: (Voss et al., 2015).

where groundwater use is quantified by groundwater withdrawal statistics, Qstat, and mean annual recharge, R_0, is used to calculate renewable groundwater availability, as shown in Eq. 2.

$$RGS_{stat} = \frac{Q_{stat}}{R_0} \quad \text{(Eq. 2)}$$

Finally, according to the parameters shown, it is possible to classify the major basins of the Sahara Desert as shown in Figures 15, 16 and 17:

Figure 15: Overstressed conditions present in basins 1, 2 and 3, assuming non available recharge (mm/year).

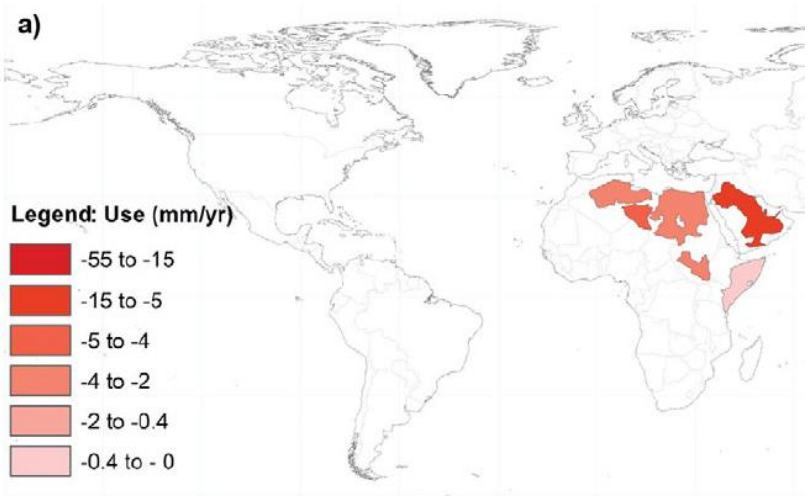

Source: (Voss et al., 2015)

Figure 16: Variable stressed conditions present in basins 4 and 7.

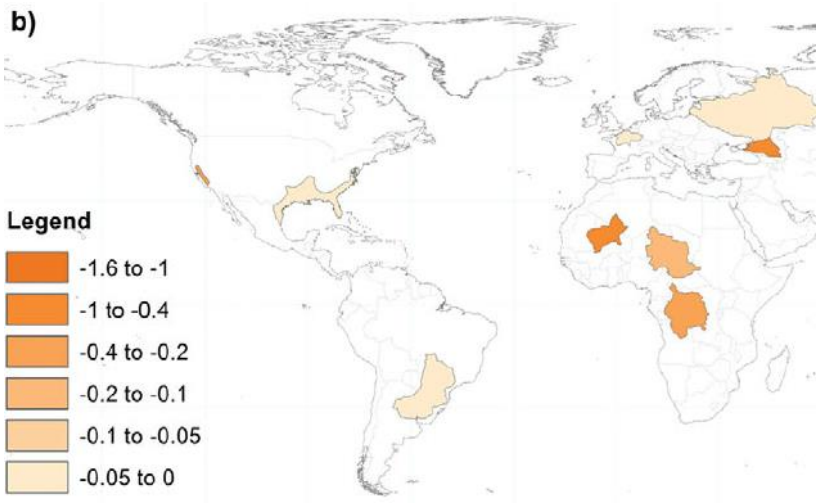

Source: (Voss et al., 2015)

Figure 17: Unstressed systems present in basins 5 and 6.

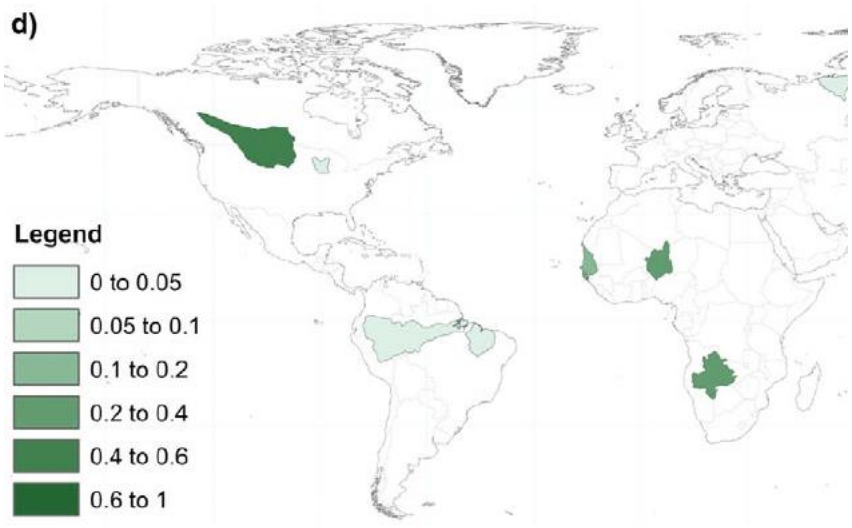

Source: (Voss et al., 2015)

3.2.4. WHYMAP: Groundwater Resources of the World Map.

According to all the previous information, the water resources of the studied region can be illustrated and mapped through web map applications and services, such as WHYMAP (World-wide Hydrogeological Mapping and Assessment Program) (WHYMAP, 2020).

WHYMAP was launched in 2000 to provide data and information about the major groundwater resources of the world and thus contribute to their rational management and protection. The program compiles data on groundwater from national, regional and global sources, and visualizes them in maps, web map applications and services. The generated products provide information on quantity, quality and vulnerability of the groundwater resources on earth and help communicating groundwater related issues to water experts as well as decision makers and the general public.

The Water Resources Map of the World (Figure 18) at the scale of 1: 25.000.000 and 1: 40.000.000 combines the related data known or published so far. It shows various characteristic groundwater environments in their areal extent:

- Blue color is used for large and rather uniform groundwater basins (aquifers and aquifer systems usually in large sedimentary basins that may offer good conditions for groundwater exploitation).
- Green color symbolizes hydrogeological environments of complex geological structure. These are areas in heterogeneous folded or faulted regions where productive aquifers (including karst aquifers) may occur in close vicinity to non-aquiferous strata. In these areas remote sensing techniques as well as detailed ground surveys coupled with spring and stream flow analysis may help identify zones of high yielding aquifers.
- Brown color outlines areas with local and shallow aquifers in which relatively dense bedrock is exposed to the surface. In these areas, groundwater is comprised to the alteration zone of the bedrock and overlying shallow layers of weathered bedrock.

Figure 18: Water Resources Map of North Africa.

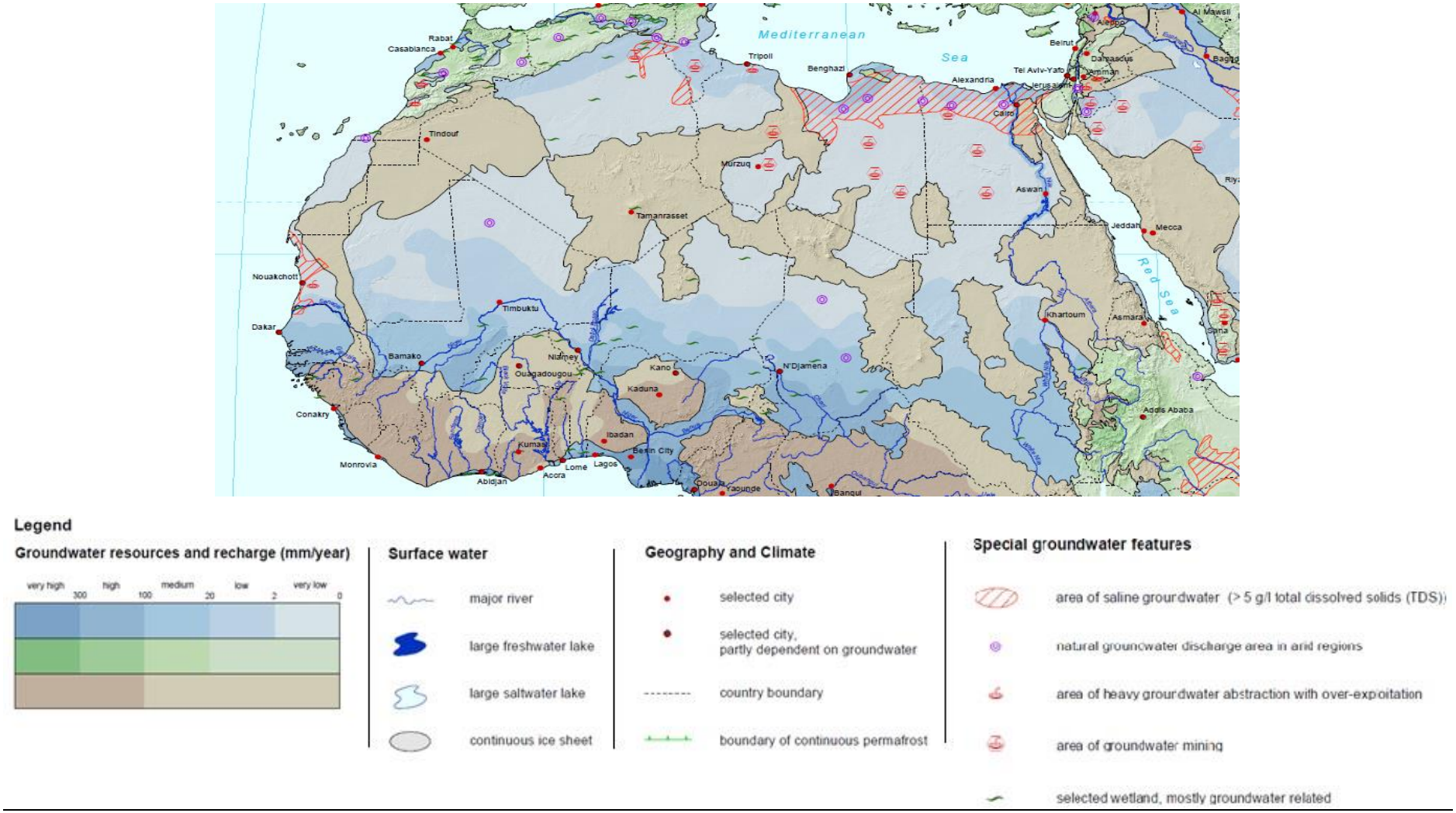

Source: (WHYMAP, 2020)

3.3. Keys of the water resources analysis.

Surface water and groundwater resources are present throughout the study region. As shown in Table 10, the quantity (in billion m^3 -bcm-) of surface and groundwater resources in North Africa are:

Table 14: Classification of surface and groundwater resources in North Africa in billions of cubic meters.

Country	Surface water	Ground water	Overlap	Total	Inflow	Total water resources
Algeria	13,20	1,70	1	13,90	0,43	14,33
Egypt	0,50	1,30	0	1,80	66,70	68,50
Libya	0,10	0,50	0	0,60	0	0,6
Morocco	22,50	7,50	0	30	0	30
Tunisia	2,31	1,21	0	3,52	0,42	3,94
Chad	13,50	11,50	10	15	28	43
Mali	50	20	10	60	40	100
Mauritania	0,10	0,30	0	0,40	11	11,40
Niger	1	2,50	0	3,50	29	32,50
Sudan	28	7	0	35	119	154

Source: (FAO, 1997)

where: Total = Surface water + Ground water – Overlap [bcm] and Global water resources = Total + Inflow [bcm].

Regarding the surface water bodies: Ramsar sites (highlighted with *(*)*) are not suitable sources since they are protected because of their high ecological value. Moreover, chotts, oasis, wadis, sabhkas and some small lakes are not trustable sources since their water reserve volumes have big fluctuations (can be full because of flood but also dry in some seasons). Finally, the permanent lakes, rivers, seas and oceans are trustable sources. Existing dams can be used for hosting new water quantities for desert irrigation.

Regarding the groundwater bodies as a source of irrigation, it has a number of essential advantages when compared with surface water: as a rule, it is of higher quality, better protected from possible pollution, less subject to seasonal and perennial fluctuations, and much more uniformly spread over large regions than surface water. Very often groundwater is available in places where there is no surface water. With all, groundwater is also a trustable source. However, as shown in figures 16 and 17, basins present in Northern Africa have a high level of stress resulting from a combination of large withdrawals and negative recharge, except for the basins in the South-Sahelian part (Niger Basin and Senegalo – Mauritanian Basin) that are considered unstressed basin systems. In conclusion, the Overstressed basins systems will not be suitable as water sources for the present project since they can be considered as nonrenewable sources. On the other hand, South-Sahelian basins will be considered as suitable water irrigation sources for the project.

Chapter 4: Reforestation. Methods and results

The aim of this part of the project is to choose some different areas of the Sahara and Sahel where to simulate the reforestation. Specific regions will be selected to represent three totally different ecosystems. In this case, they will be desert coastal, desert interior and cropland currently suffering deforestation due to climate change. Moreover, the best trees for the selected areas will be chosen and described. Once the areas and the trees are chosen, it will be possible to calculate the water needed for irrigation as well as their CO_2 capture.

4.1. Selection of areas.

Three areas have been chosen for the reforestation (Figure 19). The first region is in the Sahel, with a semi-arid and dry sub-humid climate. This area has been selected to combat the desertification caused by the climate change. The second and third areas have been selected inside the Sahara Desert, with a dry arid climate: one area close to the Red Sea coast, the other in the interior of the Sahara Desert. The purpose of this selection is to work on the reforestation of three different and very contrasted areas, with their respective challenges.

Figure 19: Location map of the selected areas for the reforestation.

Source: (Google Maps, 2020)

4.1.1. Sahel region – Sylvo-Pastorale des Six Forages Reserve (Senegal-Mauritania).

The Sahel region is located on the southern fringes of the Sahara Desert. The fragile ecosystems in this zone are constantly being deteriorated by the effects of human pressure and strong climate variation (floods and droughts) aggravated by climate change. Climate change creates major rainfall variation that is causing a southward movement of the isohyets and alteration of dry and wet seasons in the Sahel and more extreme phenomena such as temperature peaks and flooding (FAO et al., 2012). The objective of the selection and reforestation of this area is to face the effects of the deterioration due to the climate change.

The Great Green Wall Project is already working on the reforestation of the Sahel region (Figure 20). The idea of a barrier to reverse desertification is motivated by this project. The total distance from extreme to extreme, from Senegal to Djibouti, is 7775 km and the total area to be converted is around 116.625 km^2. The main natural vegetation ranges from herbaceous steppe in areas with 100-200 mm annual rainfall to the wooded savannah with 1000 mm.

The reforestation will be simulated in the *Sylvo-Pastorale des Six Forages* Reserve, on the border between Senegal and Mauritania. Only a surface of 10.000 km^2 will be considered for the study of reforestation.

Figure 20: Spatial evolution of the GGW path. The original (light green) and the updated (dark green) approximate paths for the 11 founding countries. The GGW path was progressively expanded to include 21 countries across the African continent (in light gray).

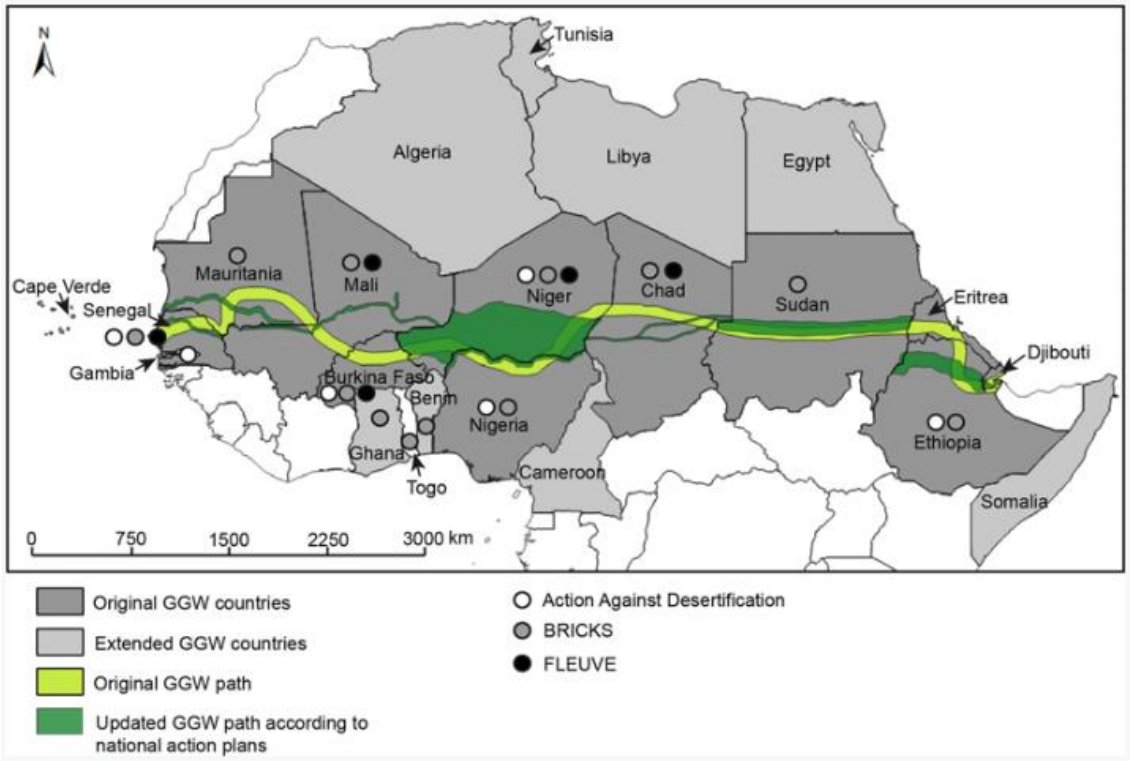

Source: (Goffner et al., 2019)

4.1.2. Red Sea coastal desert region – Eastern Desert (Egypt).

The Red Sea coastal plain is 15-20 km wide and receives very little rainfall. Apart from halophytic communities on the littoral itself, the plain is devoid of vegetation except in the wadis. Inland from the coastal plain a chain of rugged mountains, with peaks up to 2184 m high, runs the entire length of the Red Sea. Their summits intercept cloud moisture in the form of orographic rain or condensation that feeds permanent springs or 'nakkat' and contributes to the water revenue of tunnels and wadis associated with the mountains. Elsewhere in the wadis, *Acacia tortilis, Zilla spinosa, Capparis decidua, Calligonum comosum, Lasiurus hirsutus, Panicum turgidum* and *Retama retam* are characteristic species. (White, 1983)

The reforestation will be simulated in part of the Eastern Desert of Egypt, that has a surface of 222.000 km^2. Only a surface of 10.000 km^2 will be considered for the study of reforestation.

4.1.3. Interior desert region – Ténéré Desert (Niger).

Along the Sahara Desert there are two principal sandy habitats: desert dunes and sandy regs. Sandy regs are frequent throughout the Sahara, especially in the hyper-arid zone. Their vegetation is extremely homogeneous and consists almost exclusively of therophytes. Wind erosion of the sand is greatly reduced because of a superficial covering of somewhat larger rock fragments. In the driest parts of the western Sahara, episodic rainfall of 10-20 mm, which occurs in certain years, is sufficient for the development of ephemeral vegetation on sandy regs. The plants, which grow very quickly, cover 8-20% of the surface. (White, 1983)

The selected area is Ténéré, a desert region comprising a vast plain of sand stretching from northeastern Niger into western Chad, occupying an area of over 400.000 km^2. The Ténéré's boundaries are said to be the Aïr Mountains in the west, the Hoggar Mountains in the north, the Djado Plateau in the northeast, the Tibesti Mountains in the east, and the basin of Lake Chad in the south. The central part of the desert, the

Erg du Bilma. The location is shown in the figure below. Only a surface of 10.000 km^2 will be considered for the study of reforestation.

4.2. Selection of trees.

4.2.1. Approach and general considerations.

Regarding the natural dynamics expected and the growth of an ecological system, time and space are needed to grow and expand big and successful communities of trees. Reforestation can be attempted with two different approaches: monoculture or association of cultures. The first one consists of growing only one type of trees in a region, while the other consists of growing different species simultaneously to benefit from possible inter-specific facilitation effects.

Taking into consideration that the boundary conditions are hard in Sahara and Sahel deserts, it is challenging to have high trees diversity since the growth conditions are tough. That is the reason why, in the reforestation of the three regions described below, monoculture has been selected as a first approach for this project. Furthermore, the selection of the tree species is based on the observation that these species are abundant in each region considered, and so, they grow and develop nowadays there.

4.2.2. *Acacia tortilis*.

As already mentioned, *Acacia tortilis* (*A. tortilis*) (Figure 21) is one of the characteristic species that can be found in the Red Sea coastal plain together with other vegetation species. It grows naturally along the wadis, thanks to the soil moisture conditions (Indian Council of Forestry Research and Education, 1958).

Figure 21: Image of Acacia tortilis species.

Source: (Kaukora, 2020)

A. tortilis is the most important species for sand dune stabilization and it is suitable for deep sandy soils of arid regions. It is widely distributed in Africa, from South Africa to the north, to Algiers and Egypt, extending in Asia to Israel and southern Arabia. It is well adapted to disturbances such as drought, fire, browsing and pollarding. It was particularly found a suitable species for sand dunes and sandy plains. It is also being planted on degraded sites such as shallow soils with low fertility, low hills, ravines etc. It thrives well in extremely arid climates with less than 200 mm rainfall and extreme temperatures as high as 50ºC and as low as 0ºC. *A. Tortilis* grows on poor sites and has low maintenance requirement.

Because of its characteristics, *A. tortilis* has been selected as the tree for the reforestation of the Eastern Desert (Egypt) and for the Ténéré Desert (Niger).

Planting techniques.

A. tortilis plantations are raised as block plantations as well as row plantations in the form of shelter belts along roads, canals, farms etc. In block plantations the space needed between trees is 3m x 3m on sandy plains and 5m x 5m on sand dunes.

To raise *A. tortilis* on sand dunes, the site is to be prepared as follows. Protect the planting site by erecting suitable barbed wire fencing before planting. Erect micro-wind breaks (about 2 m height) of locally available shrubs or other plant material at 5 m spacing across the prevailing wind direction in parallel strips or in checker boards design at 5 m x 5 m spacing. The material used for micro-wind breaks is usually the shrubs *Aerva psuedotomentosa* or *Crotolaria burhia*.

Fertilizer application is not advised in *A. tortilis* plantations in arid regions. Fertilizer application under moisture stress conditions has detrimental effect on tree growth.

4.2.3. *Acacia senegal*.

Drought-tolerant, *Acacia senegal* (*A. senegal*) (Figure 22) is the characteristic species in the drier parts of Anglo-Egyptian Sudan and the northern Sahara and is found throughout the vast area from Senegal to the Red Sea and to eastern India. It extends southwards to northern Nigeria, Uganda, Kenya, Tanzania and southern Africa. In India it is found chiefly in Sind and Ajmere. In Sudan, the tree both exists in the wild and is cultivated - mainly on sandy hills, but it also grows well in cotton soil.

A. senegal is a deciduous shrub, growing to 15 m tall and usually branched from the ground. Branches fork repeatedly and in mature trees commonly form a rounded growth, flat-topped crown. The trunk may vary in diameter up to about 30 cm. *A. senegal* has optimum ecological conditions occurring on sandy soils and with a mean annual rainfall of 300-500 mm. However it may occur on clayey low-lying areas with vertisols, particularly in the Sudan.

Inside its biophysical limits, the altitude is around 100-1700 m, the mean annual temperature is about 4 to 48 ºC and the mean annual rainfall is about 300-1200 mm. The suitable soil types where it develops vary from coarse-textured, deep sandy soils to dry, rocky soils, slightly acidic to moderately alkaline. It is intolerant to waterlogging.

Finally, it is a species native from: Angola, Botswana, Burkina Faso, Eritrea, Ethiopia, Gambia, Kenya, Mali, Mozambique, Namibia, Niger, Nigeria, Senegal, Sudan, Tanzania, Uganda, Zambia, Zimbabwe. For all these reasons, *Acacia senegal* has been chosen as the tree for the reforestation of the *Sylvo-Pastorale des Six Forages* Reserve (Senegal-Mauritania).

Figure 22: Image of Acacia senegal species.

Source: (Yinyangperu, 2020)

4.3. CO_2 capture analysis.

4.3.1. Approach and general considerations.

There are different approaches that can be followed to understand the ability of a tree community to capture CO_2. One of them is the use of a software to calculate local CO_2 fluxes, and so, local carbon budget. However, in this project the selected approach consists in the use of allometric equations for each tree species to estimate the growth rate and the total amount of carbon contained aboveground (in trunk, and leaves) and belowground (in roots). Then, with the total biomass is possible to calculate the estimated CO_2 captured by each tree, as explained in the following parts.

On the other hand, there is also a relationship between the growth rate of a tree and water availability. The growth rate provided by allometric equations typically depends on different variables such as trunk diameter, height of the tree and specific weight or wood density, but does not consider water availability. That is because, until today, there is not enough data in literature that can be used to build a proper and complete model. All in all, allometric models are built under the assumptions of local growth scenarios. Therefore, it is true that different growth rates can be expected depending on actual availability of water. So, some variations on the calculated growth can exist depending on water availability.

4.3.2. CO_2 sequestration by *Acacia tortilis*.

4.3.2.1. Longevity and growth: Diameter at Breast Height (DBH) calculation.

The paper by Andersen & Krzywinski, 2007 analyses several samples of *A. tortilis* in different sites of the Eastern Desert of Egypt. It is shown that, in *A. Tortilis*, a narrow marginal parenchymatic band associated with crystalliferous calcium oxalate chains is present in the wood, and according to these studies they are formed coincidentally with a temporary pause in growth. Such bands are also found in *A. tortilis* wood from the Eastern Desert. If these bands are formed regularly, they are internal time markers that can facilitate age determination. Moreover, correlations between individual band patterns are of interest because they mark times when conditions did not permit growth. As such, band patterns may provide insight into the spatial variability of growth conditions and consequently into the factors affecting the growth of trees.

According to the research method and the results obtained by Andersen & Krzywinski, 2007, the calculations for *A. tortilis* in Hulus Upper site will be done. The radial growth rate is represented by a bell-shaped curve; i.e. the growth rate increases at the beginning and decreases later in the lifetime of the tree. This behavior can be modeled with a Gompertz equation. Considering the data of the study and the age scenarios, the Gompertz model that fits to the data by a non-linear least square's regression is shown in (Eq. 3) and (Eq. 4):

$$y = a \cdot \exp[-b \cdot \exp[-c \cdot t]] \quad \text{(Eq. 3)}$$

$$y' = a \cdot b \cdot c \cdot \exp[-c \cdot t] \cdot \exp[-b \cdot \exp[-c \cdot t]] \quad \text{(Eq. 4)}$$

where (Eq. 3) is the integral form and (Eq. 4) the differential form; y=tree radial size (in mm/year), y'=size increment (in mm/year), t=age (in years) and a, b and c are the Gompertz parameters. The Gompertz parameter 'a' indicates the maximum possible trunk radius of the tree in question.

For the Hulus Upper, the parameters of the Gompertz equation are: a = 249,9; b = 1,623 and c = 0,094. Applying Gompertz equation in a harvesting time of 40 years, the bell-shaped curve shpwn in Figure 23 is obtained:

Figure 23: Trunk radial growth increment of Acacia tortilis (40 years harvesting).

Source: Own elaboration based on (Andersen & Krzywinski, 2007).

Then, considering all the trunk radial size increments year by year, we can obtain the total radial dimension, which is the diameter of the trunk. It is shown in Figure 24:

Figure 24: Trunk radial growth of Acacia Tortilis (40 years harvesting).

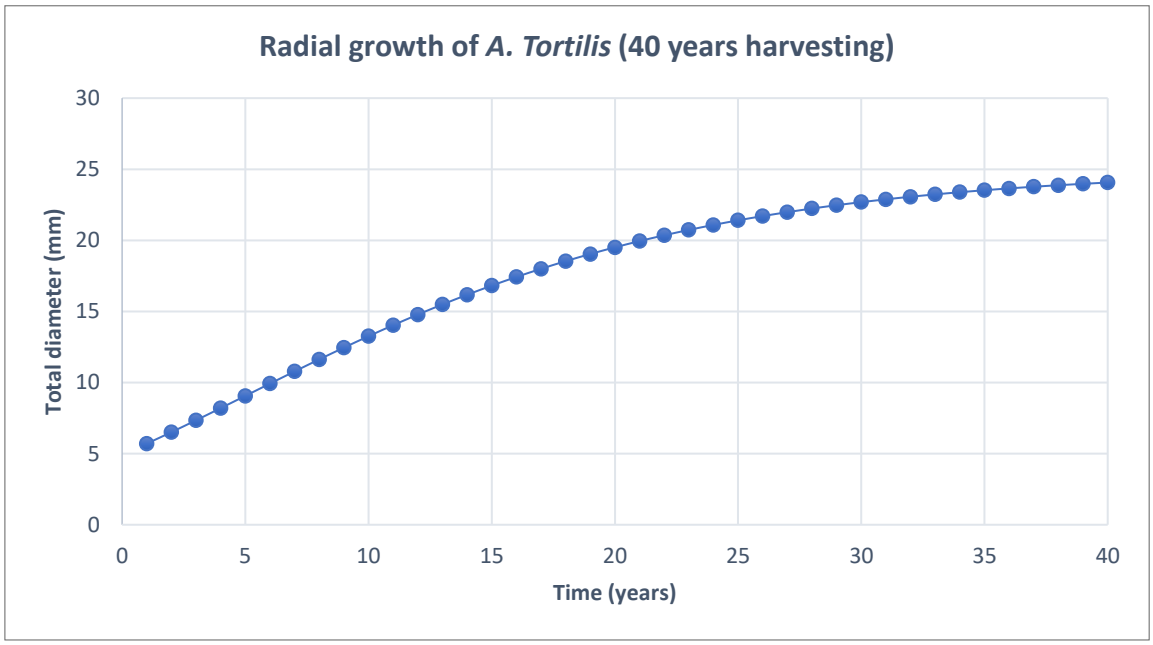

Source: Own elaboration based on (Andersen & Krzywinski, 2007).

4.3.2.2. Tree biomass calculation.

Another necessary step to perform before the CO_2 sequestration calculations is the estimation of the total biomass of the tree. For that, the use of allometric regression models is widely used. Model 7 will be used, since it offers the best accuracy and because the closest forest type for this project is the "Dry forest" (below 1500 mm/year, over 5 months dry season). The model (Djomo et al., 2016) is described by the following (Eq. 5):

$$\ln(M) = a + b \cdot \ln(D) + c \cdot \ln(\rho) \qquad \text{(Eq. 5)}$$

where M= aboveground biomass (in kg), D= trunk diameter (in cm), ρ= specific weight or wood density (g/cm^3) and a, b and c are the parameters of the model. The values for this model are: a= -0,841; b= 2,082; c= 1,248. Moreover, the wood density for *A. tortilis* is 0,6 g/cm^3.

Next step is to consider that the belowground biomass is around 26% of the aboveground biomass (Cairns et al., 1997). With all, the results obtained for the total biomass of the tree are shown in the Figure 25:

Figure 25: Total biomass of Acacia tortilis (40 years harvesting).

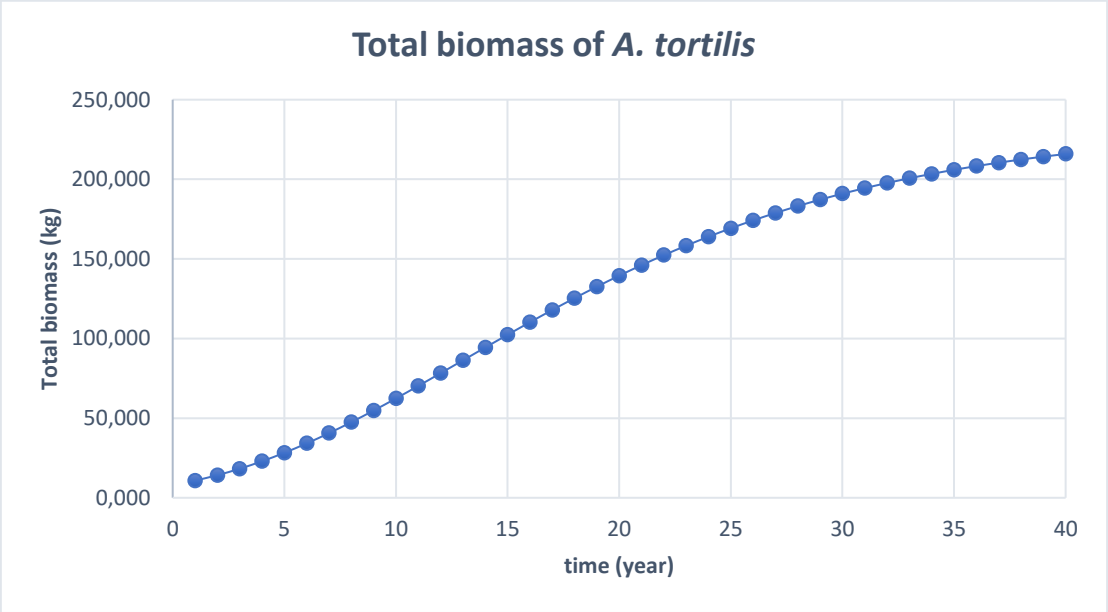

Source: Own elaboration based on (Djomo et al., 2016).

where:

$$\text{Total Biomass (kg/tree)} = (1+0{,}26)*\text{Aboveground Biomass (kg/tree)}. \qquad \text{(Eq. 6)}$$

4.3.2.3. CO_2 sequestration per tree.

Once the total biomass of the tree has been estimated, it is possible to calculate the CO_2 sequestrated by it. For that, the following steps will be used. First it is assumed that the total dry weight of the tree will be 72,5% average (Toochi, 2018). Second consideration is that the carbon content of the tree is 50% of the total dry weight. Then, for obtaining total CO_2 sequestration per tree, it is needed to multiply the carbon content times 3,67.

The next values for *A. tortilis* are shown in the Figure 26 and Figure 27:

Figure 26: CO_2 sequestration increment of Acacia tortilis per year (40 years harvesting).

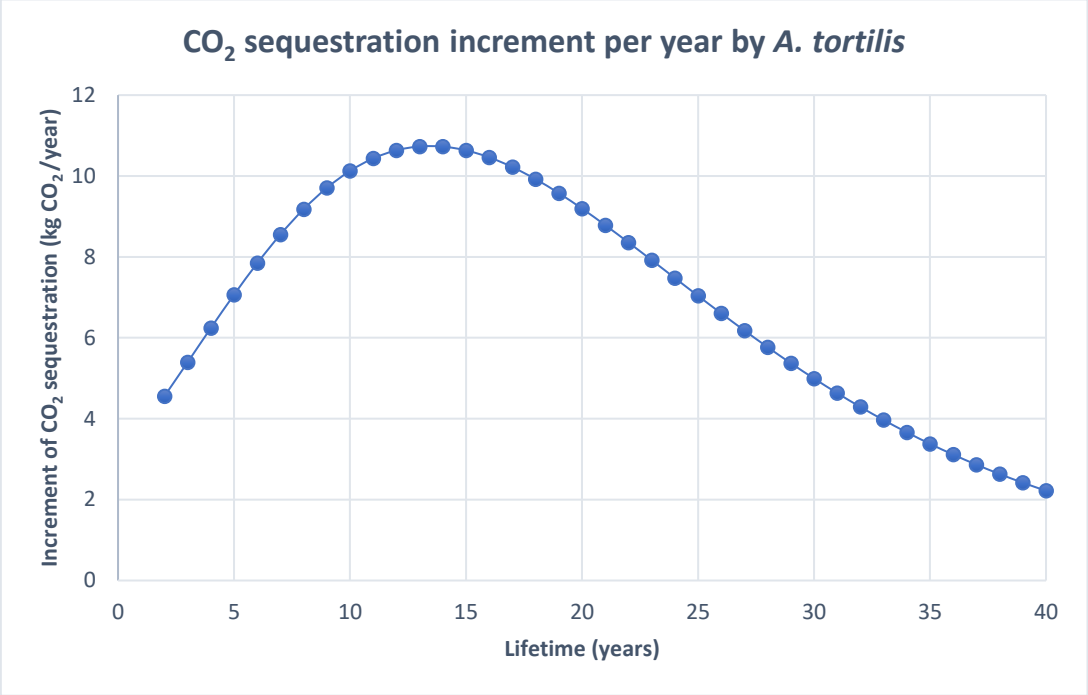

Figure 27: Total CO_2 sequestration of Acacia tortilis per year (40 years harvesting).

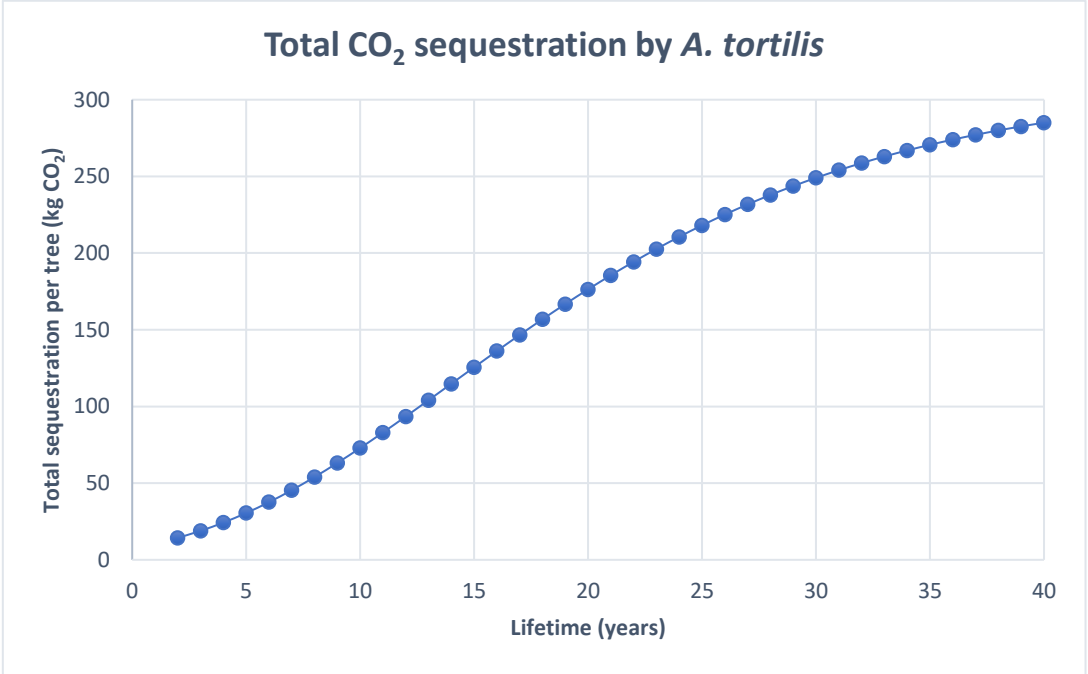

Being this project a preliminary estimation of the CO_2 capture potential of Sahara Desert, it is assumed that all the trees will be planted at the same time and the harvesting of *A. tortilis* will be 40 years. The reader should notice that this is just an assumption that is made to simplify the calculations, since this scenario is not feasible in real life.

Finally, according the previous assumption, over lifetime of an *A. tortilis* tree grown in the Eastern Desert of Egypt, the average CO_2 sequestrated by a tree and the average increment of CO_2 sequestration per year is:

Average CO_2 seq per tree	171,5673	Kg · tree^{-1}
Average CO_2 seq per year	6,822	kg CO_2 tree^{-1} year^{-1}

4.3.2.4. Total CO_2 sequestration on the Eastern Desert (Egypt).

The area will be considered as deep sand dunes with a total surface of 10.000 km^2. Following the planting practices described before, it is assumed that trees will be planted on a regular grid with 5 meters spacing. With all, 400.000.000 trees can be grown and it means that the total CO_2 capture by all the trees in the region is as shown in Figure 28:

Figure 28: Total CO_2 sequestration of Eastern Desert per year (40 years harvesting).

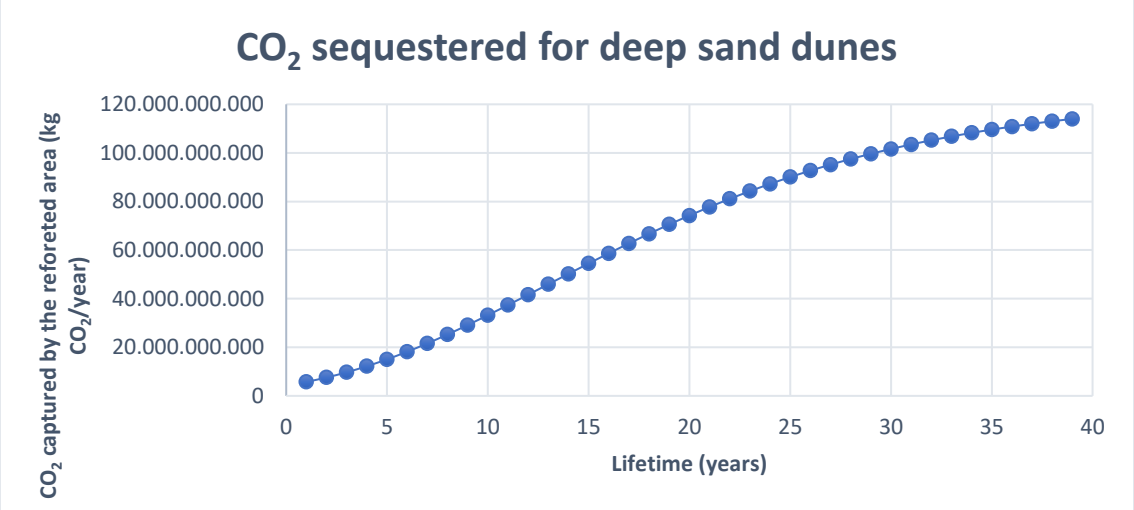

Finally, it can be summarized that the total average of CO_2 sequestration per total surface of Eastern Desert is:

Average CO_2 seq per area	68.626.930.155	kg CO_2/year

4.3.2.5. Total CO_2 sequestration on the Ténéré Desert (Niger).

Following the same procedure as in the Eastern Desert, we can evaluate CO_2 sequestration caused by reforestation for the Ténéré Desert. The area will be considered as deep sand dunes with a total surface of 10.000 km^2. Following the planting practices described before, it is assumed that trees will be planted on a regular grid with 5 meters spacing. Therefore, also in this casa, 400.000.000 trees can be grown and it means that the total CO2 capture by all the region would be as shown in Figure 29:

Figure 29: Total CO_2 sequestration of Ténéré Desert per year (40 years harvesting).

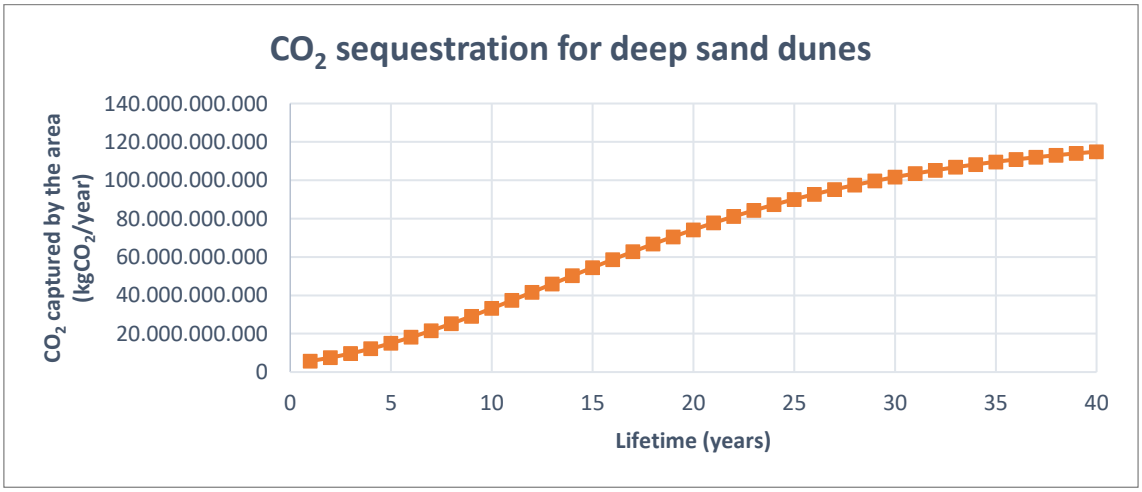

Finally, it can be summarized that the total average of CO_2 sequestration per total surface of Ténéré Desert is:

Average CO_2 seq per area	68.626.930.155	kg CO_2/year

4.3.3. CO_2 sequestration by *Acacia senegal*.

4.3.3.1. Longevity and growth: Diameter at Breast Height (DBH) and height calculation.

A paper by Diallo et al., 2014, reporting the results of research done in a silvo-pastoral zone of Senegal, where *A. senegal* is common. The study aims to deepen the knowledge of *A. Senegal* dendrometric parameters. The following parameters were reported: diameter of the base, DBH (1.3 m), breast height circumference, total height of the tree, length of the trunk and width of the crown. The sample consists of a population of 76 feet locust trees in Senegal.

For this project, only the measurements of total height of the tree and diameter and the DBH have been used. They have been plotted on Excel and adjusted to a model that gave the best R^2 value, as shown in Figures 30 and 31:

Figure 30: Height growth of Acacia senegal per year (14 years harvesting).

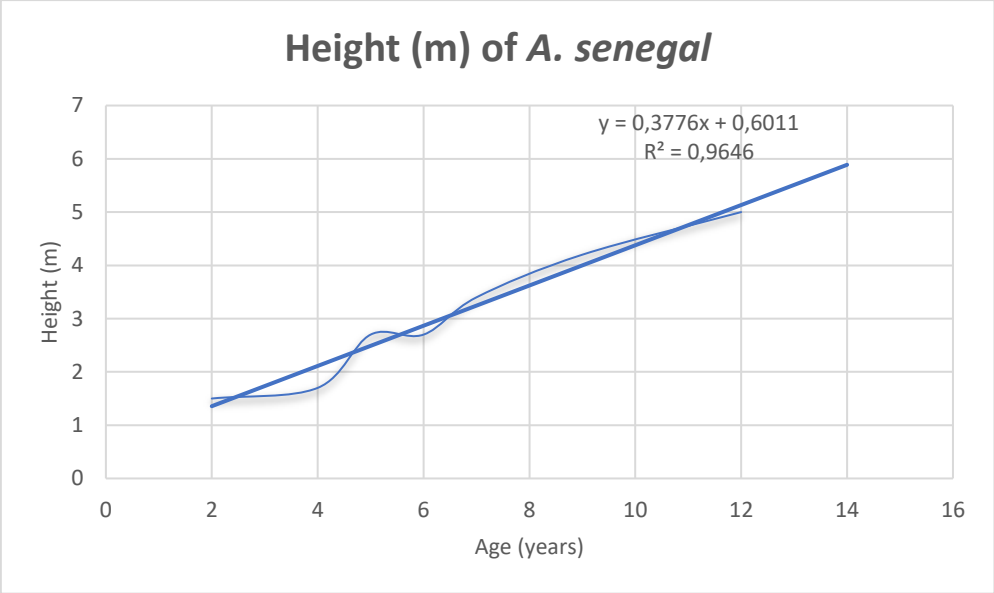

Source: Own elaboration based on data by Diallo et al., 2014.

Figure 31: DHB growth of Acacia senegal per year (14 years harvesting).

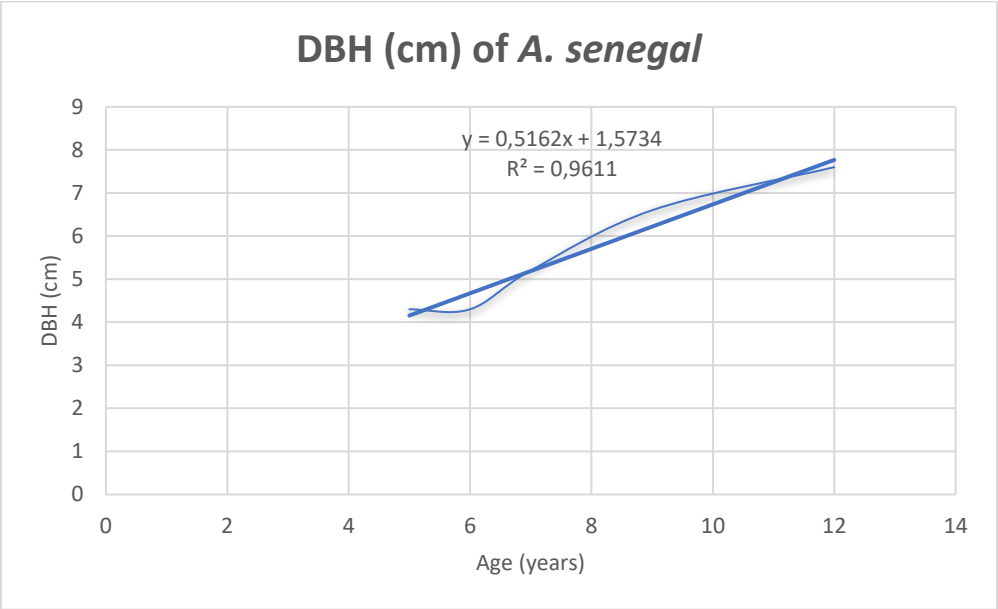

Source: Own elaboration based on data by Diallo et al., 2014.

With these models for height and diameter, the growth of the tree has been simulated for a life span of 14 years. For height of the tree, a linear approximation gives satisfactory results, shown in the following (Eq. 7):

$$H(y)=0,3776*y+0,6011 \quad \text{(Eq. 7)}$$

where H(y) is the height by y (in years) and the R^2=0.9646. The simulation of height for a cropping of 14 years is shown in Table 11:

Table 15: Simulation of height for a cropping of 14 years of Acacia senegal species.

y (years)	H (m)
0	0,601
1	0,979
2	1,356
3	1,734
4	2,112
5	2,489
6	2,867
7	3,244
8	3,622
9	4,000
10	4,377
11	4,755
12	5,132
13	5,510
14	5,888

Source: Own elaboration based on data by Diallo et al., 2014.

Using the same procedure for DBH, it is found the linear approximation (Eq. 8):

$$DBH(y)=0,5162*y+1,5734 \quad \text{(Eq. 8)}$$

where DBH(y) is the diameter at breast height for y in (years) and the R^2=0,9611. The simulation of DBH for a cropping of 14 years is shown in Table 12:

Table 16: Simulation of DBH for a cropping of 14 years of Acacia senegal species.

y (years)	DBH (cm)
0	1,573
1	2,090
2	2,606
3	3,122
4	3,638
5	4,154
6	4,671
7	5,187
8	5,703
9	6,219
10	6,735
11	7,252
12	7,768
13	8,284
14	8,800

Source: Own elaboration based on data by Diallo et al., 2014.

4.3.3.2. Tree biomass calculation.

Following the same procedure as for the *A. tortilis*, previous step before the CO_2 sequestration calculations is the calculation of the total biomass of the tree. For that, the use of allometric regression models (Djomo et al., 2016) is widely used. Model 8 of the paper is used this time for *A. senegal*, since it offers the best accuracy if the three parameters are known (height, DBH and wood density) and because the most accurate forest type for this project is the "Dry forest" (below 1500 mm/year of precipitation, over 5 months dry season). The model is described by the following (Eq.9):

$$\ln (M) = a + b \cdot \ln(D) + c \cdot \ln(H) + d \cdot \ln(\rho) \qquad \text{(Eq. 9)}$$

where M= aboveground biomass (in kg), D= trunk diameter (in cm), H= height of the tree (in m), ρ=specific weight or wood density (g/cm^3) and a, b, c and d are the parameters of the model. The values for this model are: a= -1,134; b= 1,969; c= 0,295, d= 1,185. Moreover, the wood density for *A. tortilis* is 0.728 g/cm^3.

The next step is to consider that the belowground biomass is around 26% of the aboveground biomass (Cairns et al., 1997), as already said in (Eq. 6). With all, the results obtained for the total biomass of the tree are shown in Figure 32:

Figure 32: Total biomass of Acacia senegal (14 years harvesting).

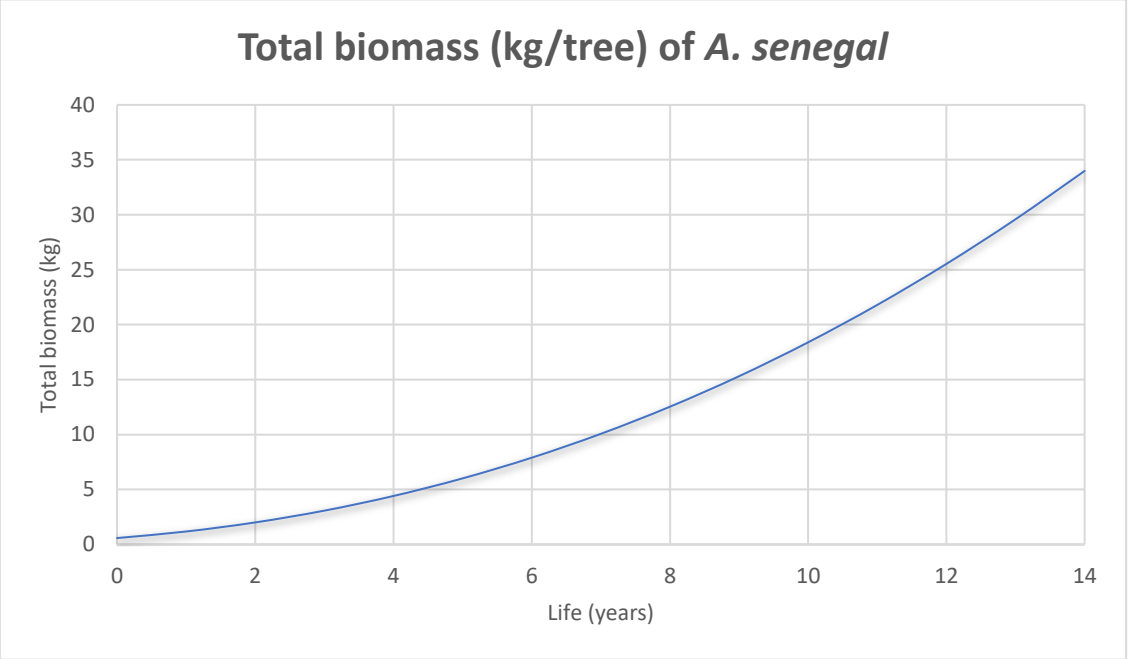

Source: Own elaboration based on data by Djomo et al., 2016.

4.3.3.3. CO_2 sequestration per tree.

As in the case of *A. tortilis*, once the total biomass of the tree has been estimated, it is possible to calculate the CO_2 sequestrated by each tree. First, considering that the total dry weight of the tree will be 72,5% average (Toochi, 2018). Second, assuming that the carbon content of the tree is the 50% of the total dry weight. Then, for obtaining the total CO_2 sequestration per tree, it is needed to multiply the carbon content times 3,67.

The next values for the *A. senegal* are shown in Figures 33 and 34:

Figure 33: Total CO_2 sequestration increment of Acacia senegal per year (14 years harvesting).

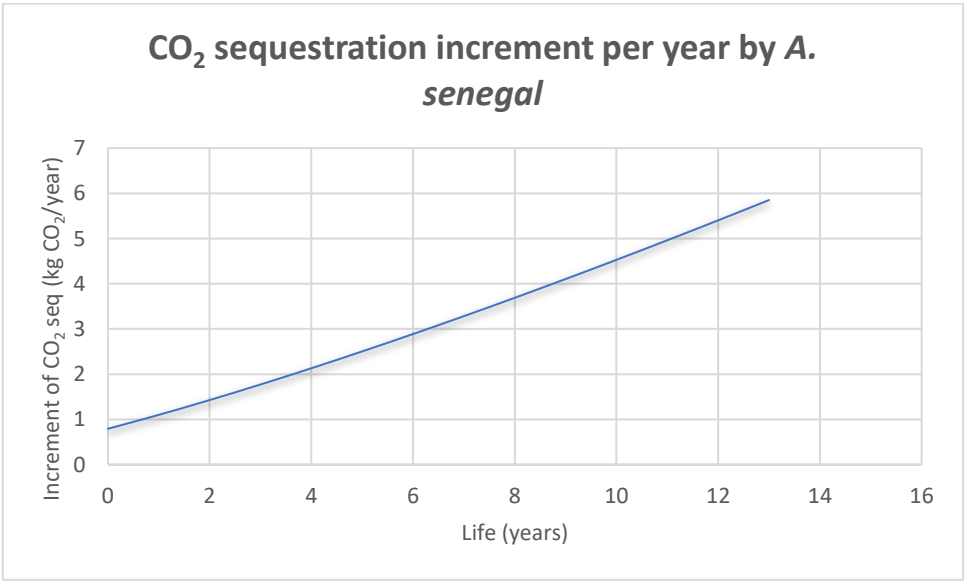

Figure 34: Total CO2 sequestration of Acacia senegal per year (14 years harvesting).

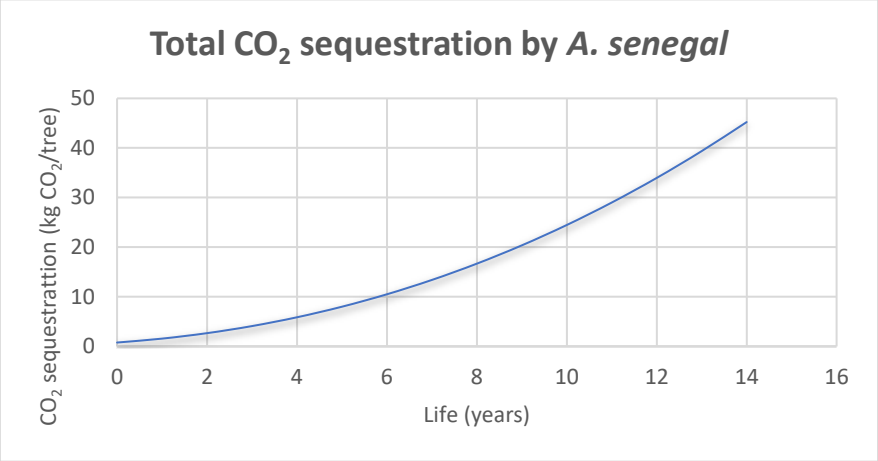

Being this project a preliminary estimation of the CO_2 capture potential of Sahara Desert, it is assumed that all the trees will be planted at the same time and the harvesting of *A. tortilis* will be 14 years. The reader should notice that this is just an assumption that is made to simplify the calculations, since this scenario is not feasible in real life.

Finally, over the lifetime of an *A. senegal* tree, the average amount of CO_2 sequestrated by a tree and the average increment of CO_2 sequestration per year is:

Average CO_2 seq per tree	18,282	Kg · tree^{-1}
Average CO_2 seq per year	3,174	kg CO_2 tree^{-1} year^{-1}

4.3.3.4. Total CO_2 sequestration in Sylvo-Pastorale des Six Forages Reserve (Senegal-Mauritania).
Following the planting practices described before for deep sand dunes, it is assumed that trees will be planted on a regular grid with 5 meters spacing. Therefore, 400.000.000 trees can be grown and it means that the total CO2 capture by all trees in the region is shown in Figure 35:

Figure 35: Total CO_2 sequestration of Sylvo-Pastorale des Six Forages Reserve per year (14 years harvesting).

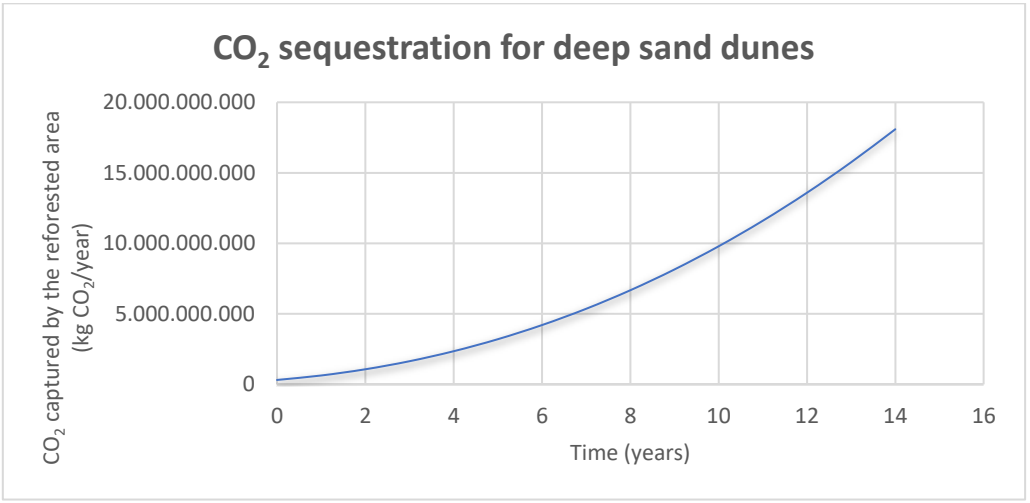

Finally, the total average of CO2 sequestration per total surface of Sahel region is:

Average CO_2 seq per area	6 825 442 835	kg CO_2/year

4.4. Irrigation analysis.

4.4.1. Watering of the Easter Desert and Ténére Desert.

The final step is to calculate the water needed for irrigation of the tree plantation of Eastern Desert and Ténéré Desert. For that, the paper by Green et al., 2019 has been used, because the method is applied in the hyper-arid deserts of Abu Dhabi for *A. tortilis* species, sharing climate and soil characteristics with the regions studied in this project. In the paper of Green et al., 2019, they have measured *A. tortilis* water-use, ETc, in (L/d), using sapflow monitoring of groundwater (GW) irrigated trees, and trees irrigated with treated sewage effluent (TSE). In addition, they also measure the seasonal pattern of evapotanspiration, ETo (mm/d). For the present project, only the cases of groundwater as the irrigation source and the tree water-use as the stream flow are considered.

Figure 36: Seasonal pattern in the reference evapotranspiration, ETo (mm d^{-1}), the red line, and the measured average tree water-use, ETc (L d^{-1}) of the three instrumented Acacia tortilis irrigated with groundwater (GW) is shown as the blue line.

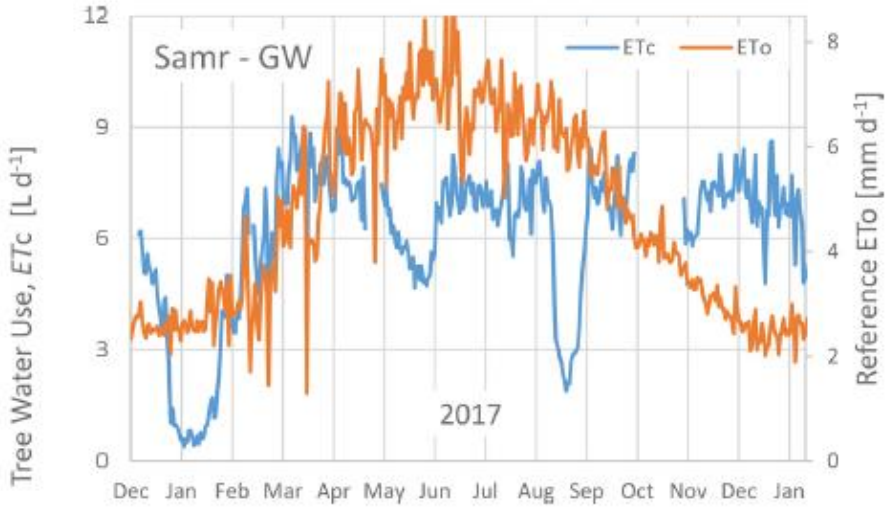

Source: (Green et al., 2019)

Extracting the data from Figure 36 and considering the total trees to be grown in the two surfaces, the water needs are shown in Table 13:

Table 17: Total water needs for irrigation of Eastern Desert and Ténéré Desert selected areas.

			EASTERN DESERT (EGYPT)		TÉNÉRÉ DESERT (NIGER)	
	Average water-use per tree (L/day)		Total water use - Deep Sand dunes plantation (m^3)		Total water use - Deep Sand dunes plantation (m^3)	
Month	First half (15 days)	Second half (15 days)	First half (15 days)	Second half (15 days)	First half (15 days)	Second half (15 days)
Jan	1	4	6.000.000	24.000.000	6.000.000	24.000.000
Feb	6	6	36.000.000	36.000.000	36.000.000	36.000.000
March	8	8	48.000.000	48.000.000	48.000.000	48.000.000
April	8	7	48.000.000	42.000.000	48.000.000	42.000.000
May	6	5	36.000.000	30.000.000	36.000.000	30.000.000
June	7	7	42.000.000	42.000.000	42.000.000	42.000.000
July	7	7	42.000.000	42.000.000	42.000.000	42.000.000
Aug	7	3	42.000.000	18.000.000	42.000.000	18.000.000
Sept	7,5	7	45.000.000	42.000.000	45.000.000	42.000.000
Oct	7	6	42.000.000	36.000.000	42.000.000	36.000.000
Nov	7	8	42.000.000	48.000.000	42.000.000	48.000.000
Dec	7,5	7	45.000.000	42.000.000	45.000.000	42.000.000
			TOTAL WATER (m^3/year)	924.000.000	TOTAL WATER (m^3/year)	924.000.000

Source: Own elaboration based on (Green et al., 2019).

Furthermore, the water need of each tree can also be calculated. The value for *Acacia tortilis* in Sahara Desert regions considered is:

Total water per tree	2,310	m^3 of water/tree/year

4.4.2. Watering of the Sylvo-Pastorale des Six Forages Reserve.

The calculations of the water use in the irrigation of this area of the Sahel region are based on the comparison with the "Gum Arabic Belt" region. The "Gum Arabic Belt" is a region located in the south of Sudan. In Sudan, *A. senegal* is one of the most widespread acacia species and extends over a wide ecological range that is known as the "Gum Arabic Belt" (Awouda, 1990), where this tree grows as a native species despite the harsh environmental conditions such as low and erratic rainfall, intense solar radiation and high wind velocity.

The method for the watering calculation takes into consideration the temperature and precipitation data of some different regions of the "Gum Arabic Belt" to summarize and calculate the average precipitations of each month of the year and the total precipitations. Also, the temperature and the precipitations of the Sylvo-Pastorale des Six Forages Reserve region are taken into consideration.

Tables 14 and 15 show the data and the method described about:

If the total precipitation of the region is smaller than the total average precipitations of the “Gum Arabic Belt”, the value is in red. Otherwise, the value is in green. For the red case, the comparison between the precipitation values of the hottest months of each region and the “Gum Arabic Belt” region needs to be done.

Table 18: Watering needs per region of Sylvo-Pastorale des Six Forages Reserve with respect to the Gum Arabic Belt region in South Sudan.:

GUM ARABIC BELT	January	February	March	April	May	June	July	August	September	October	November	December	TOTAL
Precipitation range (mm)	0	0	0-1	2-12	14-41	49-122	118-170	126-189	71-128	18-38	0-2	0	
Precipitation average (mm)	0	0	0,4	4,2	18,6	62	115	129	71,6	19,6	0,8	0	**421,2**

SENEGAL (Kébémer)	January	February	March	April	May	June	July	August	September	October	November	December	TOTAL
Precipitation (mm)	1	0	0	0	0	11	66	137	120	28	2	1	366

MAURITANIA (Tagant)	January	February	March	April	May	June	July	August	September	October	November	December	TOTAL
Precipitation (mm)	2	2	0	1	3	9	21	48	31	8	2	1	128
Precipitation differences (mm) with GUM ARABIC BELT					15,6	53	94	81	40,6	11,6			

Source: Own elaboration based on data by Awouda, 1990.

Finally, recalling that the units of the precipitation (mm/year) are equivalent to L/m^2/year and knowing the surface to be reforested, it is possible to evaluate the irrigation needs has been developed as shown in Figure 15:

Table 19: Total water needs for irrigation of Sylvo-Pastorale of Six Forages Reserve selected area.

	Average water-use per area (L/m^2)/month	Average water-use (m^3/month)
Month	MAURITANIA	MAURITANIA
May	15,6	156.000.000
June	53	530.000.000
July	94	940.000.000
Aug	81	810.000.000
Sept	40,6	406.000.000
Oct	11,6	116.000.000

TOTAL WATER	2.958.000.000	m^3/year

Source: Own elaboration based on data by Awouda, 1990.

Furthermore, for each tree can also be calculated the water need. The value for *A. senegal* in Sahel region considered is:

Total water per tree	7,395	m^3 of water/tree/year

Chapter 5: Desalination Plants analysis

5.1. State-of-art of desalination technologies.

Seawater desalination has been regularly practiced over the past 50 years. Around half of the world's desalination plant capacity is installed in Gulf Cooperation Council (GCC) countries: Saudi Arabia, Kuwait, Qatar, Bahrain, UAE, and Oman. The commercial desalination technologies can be divided into two main categories: thermally driven (MSF, MED and AD) and membrane separation (RO) processes. Among different technologies available, Multi-Stage Flash (MSF) distillation and Reverse Osmosis (RO) dominate the existing plants. Other technologies include Multi-Effect Distillation (MED), Vapor Compression (VC), and Electro-Dialysis (ED).

The share of the main categories of the existing desalination technologies is shown in the Figure 37 for the GCC and the World (Wakil et al., 2017):

Figure 37: Total desalination installed capacities and share of different technologies in the World and in GCC countries.

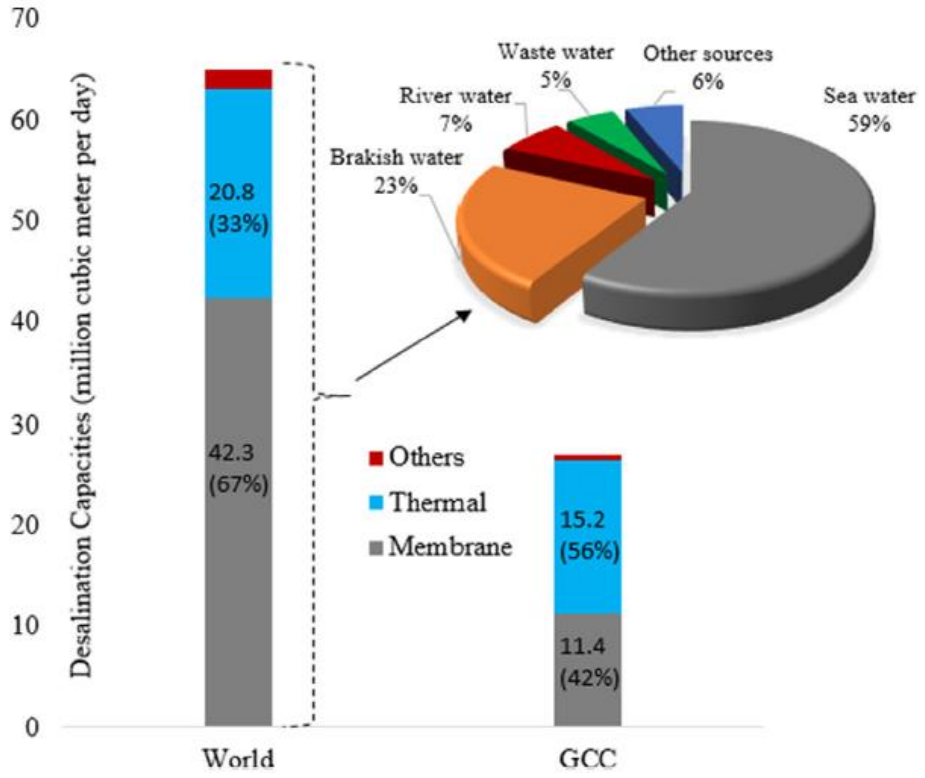

Source: (Wakil et al., 2017)

Therefore, the GCC plants are dominated by thermal processes (specifically MSF) and the rest of the world by membrane processes (specifically RO). The main reasons for the domination of the MSF process in the GCC are (Mehdizadeh, 2006):

- operational limitations of RO at high turbidity of seawater (high concentrations above 45.000 ppm of TDS -Total Dissolved Solids- in the Persian Gulf) and no pretreatment needed for the MSF process,
- the low cost of energy in the GCC countries,
- the maturity and reliability of MSF technology,
- the problems faced by membranes dealing with fouling and scaling problems.

On the other hand, RO processes are dominating in the World. They showed and increasing trend for seawater desalination from 2,0 Mm^3/day to 3,5 Mm^3/day from 2005 to 2008. This trend is expected to further increase in the future due to graphene membrane development. In the last decades, RO processes

highly improved in efficiency due to pressure recovery devices and NF integrated pre-treatment processes. RO processes only required electricity for desalination and the energy consumption depends on recovery ratio and TDS in the feed since the osmotic pressure is related to TDS. For severe feedwater conditions such as high turbidity, high algae concentration, high temperature and high TDS, the RO cost will be higher than thermally driven processes because of extensive pre-treatment process requirement (Wakil et al., 2017). Six of the largest desalination plants nowadays in the world are:

1) Ras Al Khair, Saudi Arabia – 1.036.000 m^3/day. Hybrid project that uses both thermal MSF and RO technologies. The site also has a substantial power generation component, with a capacity of 2400 MW.
2) Taweelah, UAE – Reverse Osmosis project with a production capacity of 909.200 m^3/day.
3) Shuaiba 3, Saudi Arabia – World's third largest integrated water desalination and power plant, consisting of 14 units with a total capacity of 5,600 MW and water production of 880.000 m3/day.
4) Sorek, Israel – 624.000 m^3/day. Considered the heavyweight membrane plant of the world in operation. The project was and continues to be unique in the use of 16-inch seawater RO membranes but in a vertical formation.
5) Rabigh 3 IWP, Saudi Arabia – It is a Seawater Reverse Osmosis plant producing 600.000 m^3/day.
6) Fujairah 2, United Arab Emirates – 591.000 m^3/day. It includes multiple components: a 450.000 m^3/day thermal plant, a 136.500 m^3/day RO facility and a 2000 MW power plant.

5.2. Multistage Flash (MSF) desalination.

5.2.1. General process description.

The MSF desalination system (with brine recirculation system flow) in Figure 28 includes three main sections: the heat input section (brine heater), the heat recovery section and the heat rejection section. The recovery and rejection sections both have a series of stages. Each stage has a flash chamber and a condenser where the vapor is flashed off in the chamber and later condensed. The flash chamber is separated from the condenser by a demister, where entrained brine droplets are removed from the flashing vapor.

The main principles of this type of desalination system operation can be summarized as follows: the intake seawater flows through the condenser tubes of the heat rejection section where its temperature increases by gaining the latent heat of the condensing fresh water vapor. At the output of the first rejection stage, the warm stream of intake seawater splits into two parts: cooling seawater stream, which discharged back to the sea and feed seawater stream, which is mixed in the brine pool of the last flashing stage in the heat rejection section. The function of the cooling seawater is to remove the excess heat added to the system by the saturated driving steam in the brine heater.

In the last stage of the heat rejection section, two flows are extracted from the brine pool, which includes the blow-down brine and the recycle brine. The blow-down flow is discharged to the sea, which controls the salt concentration of the cycle. The recycle brine stream then enters the condenser tubes of the last stage of the heat recovery section where its temperature increases as it flows in the condenser tubes across the stages by absorbing the latent heat of the condensing fresh water vapor in each stage.

In general, it can be revealed that increasing the number of flashing stages in an MSF plant helps to raise the temperature of the brine inside the condenser tubes, because of the latent heat of the condensing vapor given to it. In this way, the temperature step needed in the brine heater is smaller and it supposes less thermal energy consumption in the process, and so, a better plant efficiency.

Subsequently, the recycle brine stream passes through the brine heater tubes where motive saturated steam is condensed on the outside surface of the tubes. This step increases the temperature of the recycle brine to the desired value known as the Top Brine Temperature (TBT) above 100ºC. The hot brine enters the flashing stages where a small amount of fresh water vapor is formed by brine flashing in each stage. This vapor passes through the demister and is condensed onto the heat exchanger where the cold recycle brine flow passes through and recovers the latent heat of the fresh water vapor. Finally, the condensed vapor drips onto a distillate tray and is accumulated across the stages as the desired distillate product (Najafi et al., 2014).

Figure 38: Diagram of Multistage Flash (MSF) desalination plant process.

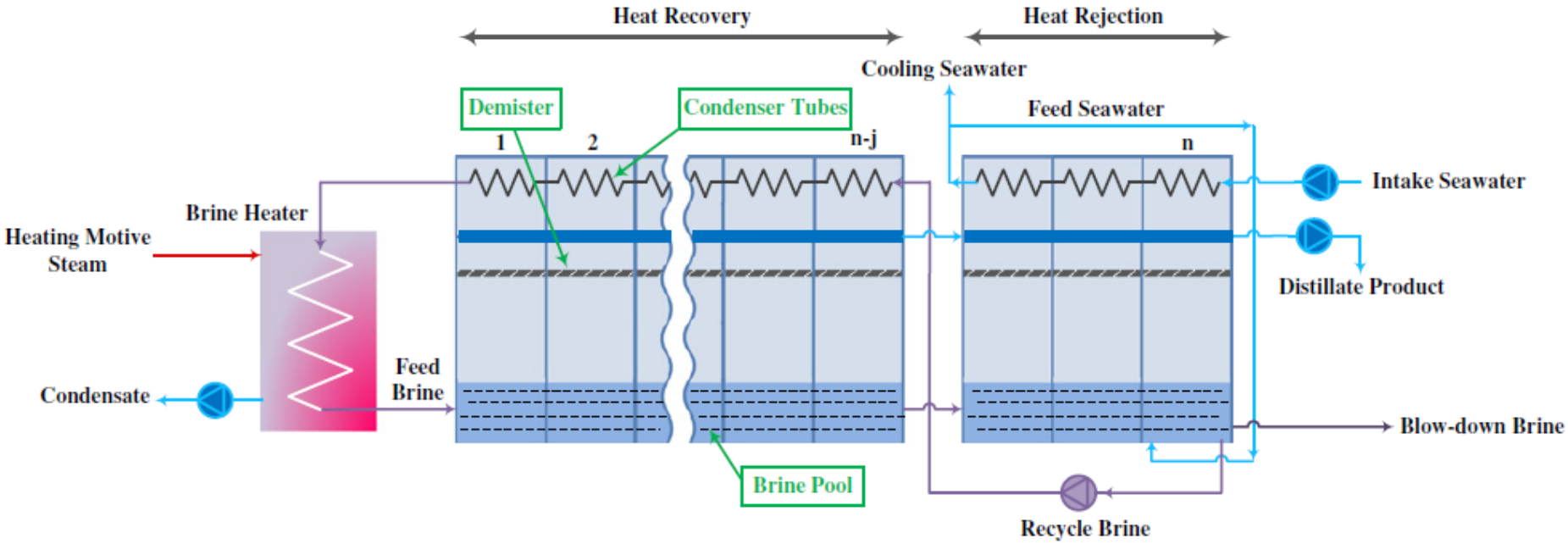

Source: (Najafi et al., 2014)

5.2.2. Plant description by parts.

Description extracted from the scientific paper (El-Ghonemy, 2018).

5.2.2.1. Seawater feed.

Seawater is screened and pumped through the condenser tubes located in the upper part of the heat rejection stages. Some chemicals are added to the feed water (anti-scale, chlorine and anti-foaming).

5.2.2.2. Cooling water and makeup water.

After heating the sea water feed in the condenser tubes of the heat rejection section, part of this feed water is discharged to the sea (known as cooling water) and the rest of feed water is supplied to the deaerator (known as makeup water).

5.2.2.3. Deaerator.

The feed water stream is pumped to a deaerator tower to decompose bicarbonates for separation of dissolved gases such as oxygen and nitrogen and carbon dioxide. Such gases have a negative effect on the heat transfer due to their low thermal conductivity. In addition, the chemical corrosion in various locations of the plant is caused by carbon dioxide and oxygen. In summary, inside the deaerator, oxygen is removed from the seawater to avoid tube corrosion in the heat recovery stages.

5.2.2.4. Heat recovery section and brine heater.

After the deaerator, the treated feedwater (makeup) is mixed with concentrated brine from the last stage. Then, the mixture is pumped to the heat recovery section and passes through until it reaches a brine heater. There it is heated to its maximum temperature, the TBT above 100 ºC, by a steam coming from a boiler. After that, from the heater, the brine passes through a flow control valve into the first and hottest stage of the MSF plant.

Inside this stage, a small amount of the water in the brine flashes into vapor which condenses on tubes located in the upper part and collected in a tray as distillate water. This process is repeated in the several stages until the brine leaves the last and coldest heat rejection stage at about 32 ºC. At the same time, the distillate is pumped to storage tanks where it is chemically treated by chlorination and adjustment of its pH value. In the last stage evaporator, some of the brine is discharged back to the sea as blowdown to prevent buildup of salts.

5.2.2.5. Vacuum system.

It is essential to use a vacuum system for removing the non-condensable gases from the plant and to maintain the required reduced pressures. A typical system is a two-stage steam jet ejector with a barometric vent condenser, an inter condenser and a final condenser.

5.2.2.6. Heat rejection system.

The heat rejection section is designed to control the temperature of the intake seawater and reject the excess heat added by the brine heater. A part of the rejected cooling seawater is returned and mixed with the feed seawater. This is useful to prevent the temperature reduction in the last stage during winter operation.

5.2.3. Thermodynamic analysis of MSF plants: a study case.

A thermodynamic analysis of an MSF desalination plant has been performed by Kotb, 2015. In this study, an MSF desalination system is designed and the feasibility of using the MSF desalination process in proximity of a 650 MW power plant is investigated. This power plant can provide 385,03 kg/s superheated steam from low pressure section of Heat Recovery Steam Generator (HRSG) for thermal desalting system. Three modules were tested with different numbers of heat rejection sections. The optimum design was 25 stages in the heat recovery section and 3 stages in heat rejection section. The designed MSF system with Gained Output Ratio (GOR) of 8,76 has 28 flashing stages and can produce 2229 kg/s of freshwater (it should be taken as insightful and general information because there are infinite cases of MSF plants design).

The scheme of the plant is shown in Figure 39, where some of the most important parts and elements are identified. Also some of the relevant physical and thermodynamic parameters are represented and quantified, such as mass flow rates, temperature and salinity concentration:

Figure 39: Diagram of Multistage Flash (MSF) desalination with brine recirculation. Example of the process and relevant physic and thermodynamic parameters.

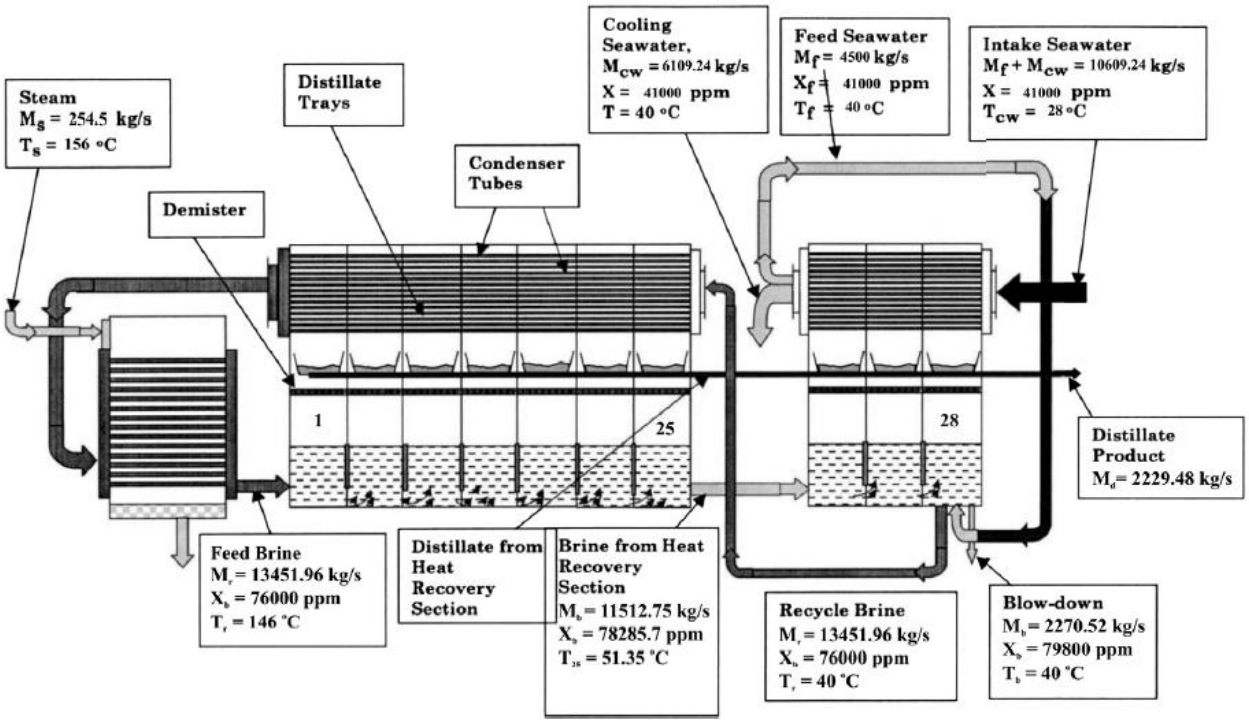

Source: (Kotb, 2015)

In addition, Table 16 shows the most relevant thermodynamic parameters is given for each of the stages:

Table 20: Most relevant thermodynamic parameters given for each of the stages of an MSF desalination process.

Stage nº	Temp. of the intake recycle brine (ºC)	Temp. of effluent recycle brine (ºC)	Temp. of intake brine (ºC)	Temp. of effluent brine (ºC)	Pressure (bar)	Brine salinity (ppm)	Latent heat of vaporization water (kJ/kg)
1	130,864	134,650	146,000	142,214	3,637	67 000	2144
2	127	130,864	142,214	138,428	3,250	67 445	2156
3	123	127,078	138,428	134,642	2,923	67 892	2166
4	120	123,292	134,642	130,856	2,609	68 340	2177
5	115,72	119,506	130,856	127,070	2,324	68 791	2188
6	112	115,72	127,070	123,284	2,066	69 243	2200
7	108	111,934	123,284	119,498	1,834	69 697	2210
8	104	108,148	119,498	115,712	1,625	70 154	2221
9	101	104,362	115,712	111,926	1,433	70 613	2229
10	96,79	100,576	111,926	108,140	1,260	71 074	2241
11	93	96,790	108,140	104,354	1,108	71 537	2250
12	89	93,004	104,354	100,568	0,969	72 003	2261
13	85	89,218	100,568	96,782	0,844	72 471	2271
14	82	85,432	96,782	92,996	0,732	72 941	2274
15	77,86	81,646	92,996	89,210	0,644	73 414	2289
16	74	77,860	89,210	85,424	0,548	73 889	2300
17	70	74,074	85,424	81,638	0,469	74 367	2310
18	67	70,288	81,638	77,852	0,400	74 848	2319
19	63	66,502	77,852	74,066	0,344	75 331	2329
20	58,93	62,716	74,066	70,280	0,290	75 817	2338
21	55	58,930	70,280	66,494	0,250	76 305	2346

22	51	55,440	66,494	62,708	0,200	76 796	2358
23	48	51,358	62,708	58,922	0,174	77 290	2366
24	44	47,572	58,922	55,136	0,150	77 786	2373
25	40	43,786	55,136	51,350	0,122	78 286	2385
26	36	40	51,350	47,564	0,100	78 788	2392
27	32	36	47,564	43,778	0,082	79 293	2402
28	28	32	43,778	40	0,067	79 800	2411

Source: (Kotb, 2015)

5.2.3.1. Temperature variation.

Figure 40 represents the temperature variation through the stages of the MSF plant study case:

Figure 40: Temperature variation along the stages of a MSF desalination plant.

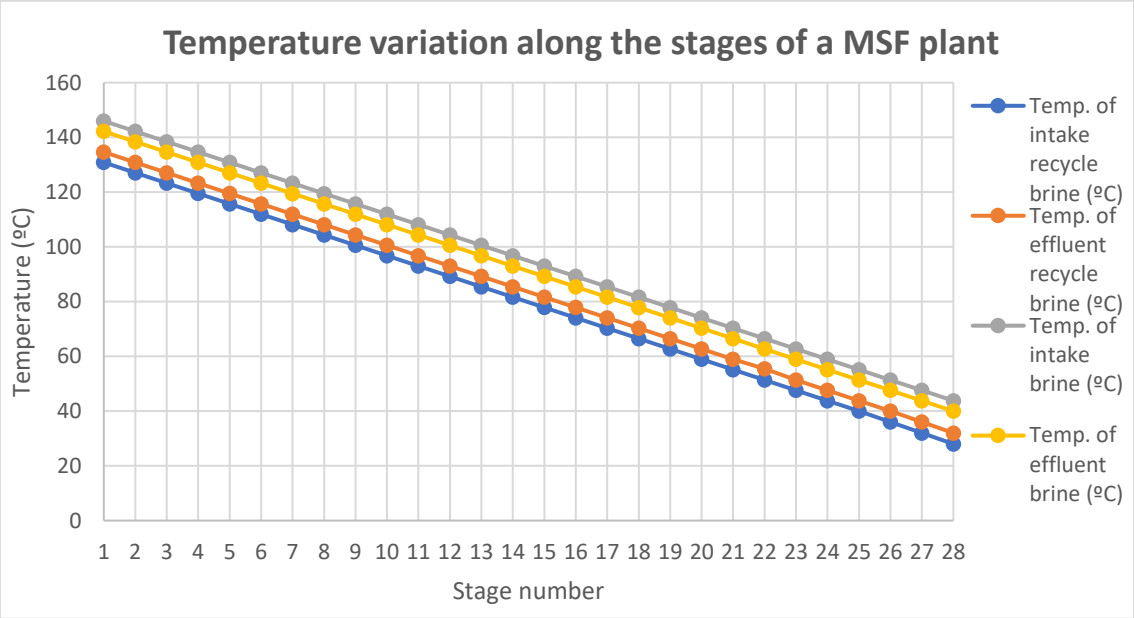

Source: Own elaboration based on data by (Kotb, 2015)

The information that can be extracted and extrapolated to the general functioning of temperature variation through the stages of an MSF plant is:

- There are four different temperatures studied: the temperature of the intake recycle brine and the temperature of the effluent recycle brine, which are the brines going up in the top of the stage through the condenser tubes and, then, the temperature of the intake brine and the effluent brine, which are the brines going down in the stages contained in the brine pools.
- The four temperatures have a strong linear variation, meaning that all the streams are heated up almost in the same proportion in each stage until the last one (from stage nº 28 until stage nº1). Temperature variation for all streams between two consecutive stages is assumed to be 3,786 ºC.
- The intake and effluent recycle brine streams is the coldest because they play the role of cooling down the vapor to condensate and obtaining the distillate. The hottest are the intake and effluent brines because they come directly from the brine heater and then they flashes into vapor.
- The temperatures of all the streams described vary around 28-45ºC in the last stage and are heated up during the way to the brine heater, thanks to the flash, helping to reach the suitable temperature to enter the brine heater, around 135ºC and the brine is heated up until 146ºC.

5.2.3.2. Pressure variation.

Figure 41 represents the pressure variation through the stages of the MSF plant study case:

Figure 41: Pressure variation along the stages of a MSF desalination plant.

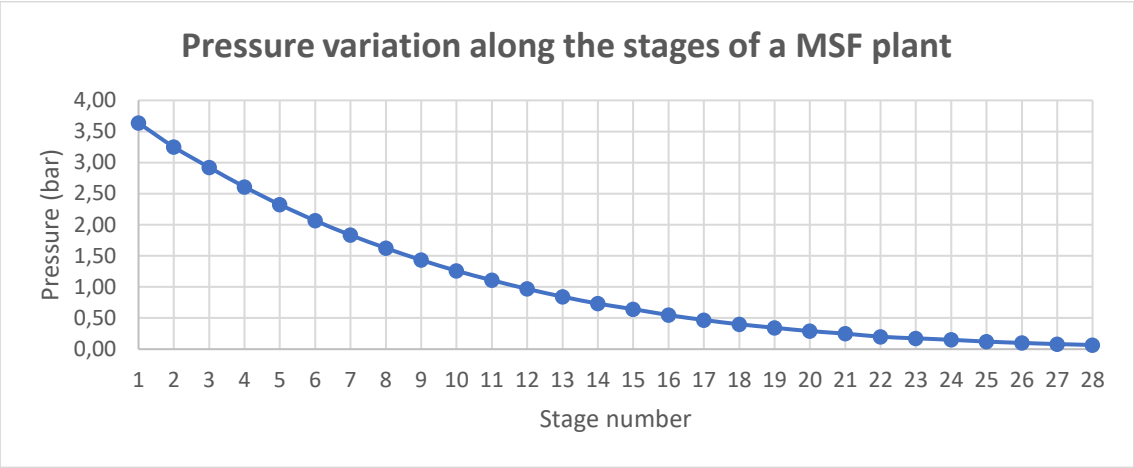

Source: Own elaboration based on data by (Kotb, 2015)

The information that can be extracted and extrapolated to the general functioning of pressure variation through the stages of an MSF plant is that:

- Pressure decays exponentially from the first stage until the last one.
- The design pressure of the shell as a function of saturation temperature is processed and maintained by the vacuum system along the stages. The first and the last stages have maximum and minimum shell pressures with values of about 3,6367 and 0,067 bar abs., respectively.
- Pressure can be described similarly to temperature variation, since it increases from the heat rejection stages to the recovery section stages at the same time with the temperature, in order to reach the suitable thermodynamic conditions for the flash and for the brine heater inlet.

5.2.3.3. Brine salinity variation.

Figure 42 represents the brine salinity variation through the stages of the MSF plant study case:

Figure 42: Brine salinity variation along the stages of a MSF desalination plant.

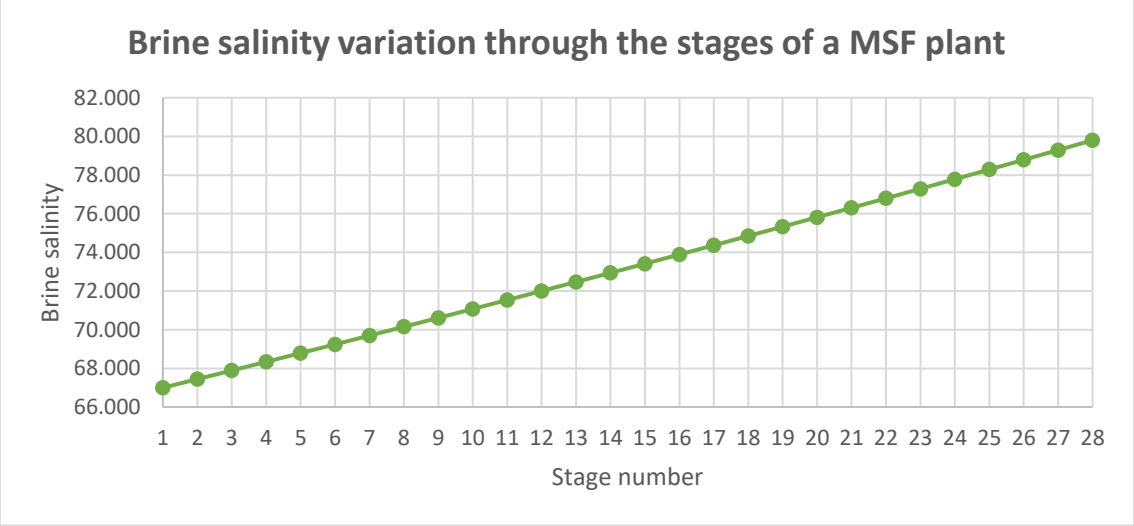

Source: Own elaboration based on data by (Kotb, 2015)

The information that can be extracted and extrapolated to the general functioning of the brine salinity variation through the stages of an MSF plant is:

- Since the pressure decreases, part of the brine water will evaporate and the water salt concentration will increase consequently, so the maximum brine salinity is obtained in the last stage (79.800 ppm).

5.2.3.4. Latent heat of vaporization water variation.

Figure 43 represents the latent heat of vaporization water variation through the stages of the MSF plant study case:

Figure 43: Latent heat of vaporization through the stages of a MSF desalination plant.

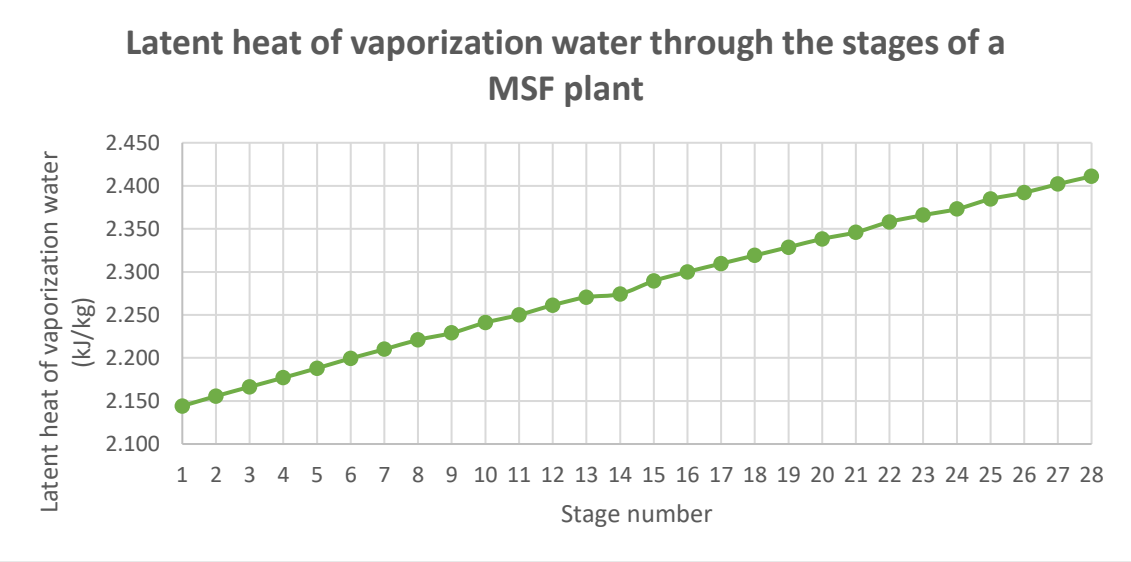

Source: Own elaboration based on data by (Kotb, 2015)

The information that can be extracted and extrapolated to the general functioning is:

- The latent heat of vaporization is gradually decreased from last stage (nº28) to first stage (nº1). That can be explained because, in a MSF plant, the recycle brine flows through the condenser tubes (from stage nº25 to stage nº1) of the heat rejection section where its temperature increases by gaining the latent heat of the condensing fresh water vapor. So that, latent heat is decreased each time.

In general, it can be revealed that increasing the number of flashing stages in an MSF plant helps to raise up the temperature of the recycle brine, because of the latent heat of the condensing water vapor given to it. Temperature step needed in the brine heater is smaller and it supposes less thermal energy consumption of the process, and so, a better plant efficiency.

5.2.4. Performance indicators.

5.2.4.1. Gained Output Ratio.

Generally, thermal desalination systems are steam consumers. So, how much steam required for heating section, to achieve the plant capacity of distillate is expressed as GOR and calculated as follows in (Eq. 10):

$$\text{GOR} = \frac{\text{mass flow rate of product water}}{\text{mass flow rate of steam}} \quad \left(\text{in } \frac{\text{kg distillate product}}{\text{kg steam}}\right) \qquad \text{(Eq. 10)}$$

For MSF plants, a typical GOR is between 6 and 12, normally about 8 (El-Ghonemy, 2018).

5.2.4.2. Concentration ratio.

Measuring the salt concentration in both sea water and circulation water (as TDS), the Concentration Ratio (CR) is obtained as follows in (Eq. 11):

$$CR = \frac{\text{Circulation brine water TDS}}{\text{Seawater TDS}} \quad \text{(Eq. 11)}$$

For MSF plants, a typical CR is about 1,5, not higher to avoid scale formation on the heat transfer surfaces (El-Ghonemy, 2018).

5.2.5. Energy consumption.

5.2.5.1. Indicators.

The specific energy consumption (SEC) (kWh/m^3) is defined in (Eq. 12) as the amount of total energy supplied (heat and electrical energy) to produce a unit mass of the product, freshwater. In other words:

$$SEC = SEEC + STEC \quad \text{(Eq. 12)}$$

where SEEC is the specific electrical energy consumption and STEC is the specific thermal energy consumption.

Specific electrical energy consumption (SEEC).

SEEC is defined as the amount of electrical energy consumed to produce a unit mass of pure water. In fact, this performance indicator is used to compare results with processes which consume electrical energy. In MSF plants, electrical energy is consumed by the flow pumps of the system, such as the intake, recirculation, drain and ejector pumps.

Specific thermal energy consumption (STEC).

STEC, or specific heat consumption is a measure of the amount of thermal energy needed to generate a unit of freshwater. In MSF plants, thermal energy is consumed in the brine heater.

5.2.5.2. Typical values of SEC in MSF.

Typical values of SEC of MSF plants have been reported in several scientific papers. A summary is made by (Wakil et al., 2017).

For MSF plants, STEC and SEEC have been reported in a wide range. Some studies mentioned that the STEC generally ranges from 190 to 300 MJ/m^3 of products, while a typical SEEC is ranges between 2,5-5,0 kWh$_{elec}$/m^3.

Summarizing the typical values in Table 17:

Table 21: Typical values of STEC and SEEC of MSF desalination plants.

	MSF plants	
STEC	190 - 300	MJ/m^3 produced water
SEEC	2,5 – 5,0	kWh$_{elec}$/m^3 produced water

5.2.5.3. Factors affecting the SEC of MSF plants.

The values of STEC, hence the values of SEC, are strongly dependent on the TBTs, the steam temperature supplied to a brine heater and the seasonal temperature variation of feeding seawater. Furthermore, STEC will be significantly vary depending on whether the thermal energy of the freshwater condensed in a brine heater is included or not.

In addition, the freshwater production rate is increased and the STEC is decreased by adopting the brine re-utilization method.

5.2.6. Power Plant energy providing.

As described before, MSF desalination plants need thermal and electrical energy supply. Therefore, they are tipically associated with a power plant able to produce electricity by means of a generator connected to a turbine. Conventionally, the power plants able to supply both electrical and thermal energy are called cogeneration plants and are based on steam turbine cycles (also known as Rankine cycle) or combined cycles, including steam and gas turbine cycles. These kind on power plants are conventionally fed by fossil fuels (coal, oil, natural gas, etc).

In addition, MSF and RO can also be combined together in the same plant. In what follows, the most widely used power plants for energy providing and the most typical plant configurations will be described.

5.2.6.1. Steam cycle power plant.

A steam cycle power plant is composed by the elements shown in Figure 44:

Figure 44: Sketch of a steam power plant.

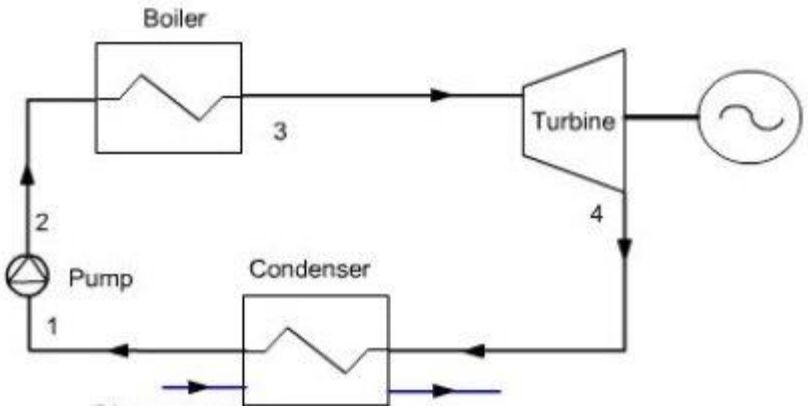

The process within a steam cycle power plant is: first, water enters the boiler or steam generator through a section in the convection pass called the economizer, then the process of adding the latent heat of vaporization begins. The boiler transfers energy to the water by the chemical reaction of burning some type of fuel. From the economizer, it passes to the steam drum, from where it goes down the down comers to the lower inlet water wall headers and finally rises through the water walls. Some of it is turned into steam due to the heat being generated by the burners located on the front and rear water walls (typically). The produced steam spins a steam turbine which drives an electrical generator. After it passes through the turbine, the steam is condensed in a condenser.

Figure 45 shows the scheme of a desalination plant powered by a steam cycle power plant:

Figure 45: Scheme of a desalination plant powered by a steam cycle power plant.

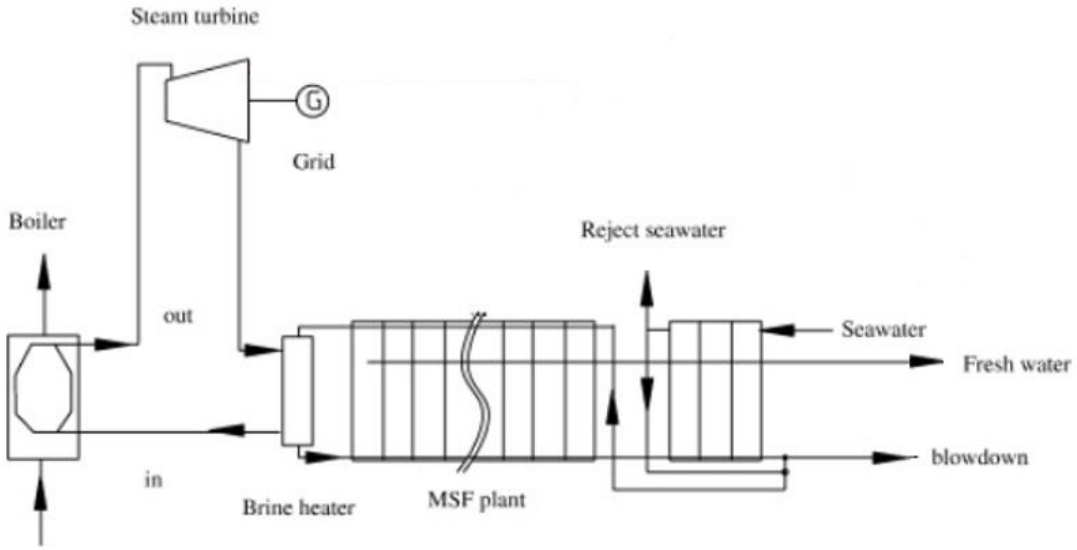

The fuel is combusted in the boiler to produce the superheated steam. The steam is sent to the steam turbine to generate the electric energy, which is used for MSF and the grid. The whole or part steam extracted from turbine is fed to the brine heater of MSF and condensed to recycle the boiler.

5.2.5.2. Combined cycle power plant.

A combined cycle is composed by the elements shown in Figure 46:

Figure 46: Sketch of a combined cycle.

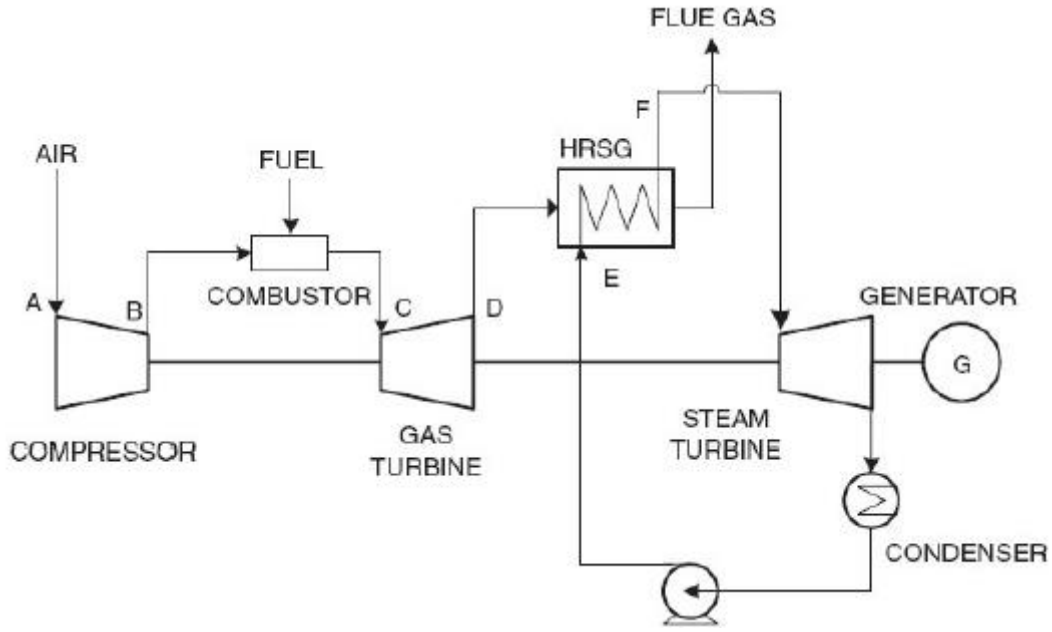

The process within a combined cycle power plant is: first, an air feed stream is compressed and sent to a combustor chamber. Inside, it is mixed with fuel and a combustion reaction takes place. The reactants of the combustion reaction go to the gas turbine. The hot air-fuel mixture moves through the gas turbine blades, making them spin. The fast-spinning turbine drives a generator that converts a portion of the spinning energy into electricity. Then, the exhaust heat from a gas turbine is routed to a conventional boiler or to a heat recovery steam generator. Subsequently, the exhaust heat is converted into electricity since the steam turbine sends its energy to the generator drive shaft, where it is converted into additional electricity. Figure 47 shows the scheme of a desalination plant powered by a combined cycle power plant:

Figure 47: Scheme of a desalination plant powered by a combined cycle power plant.

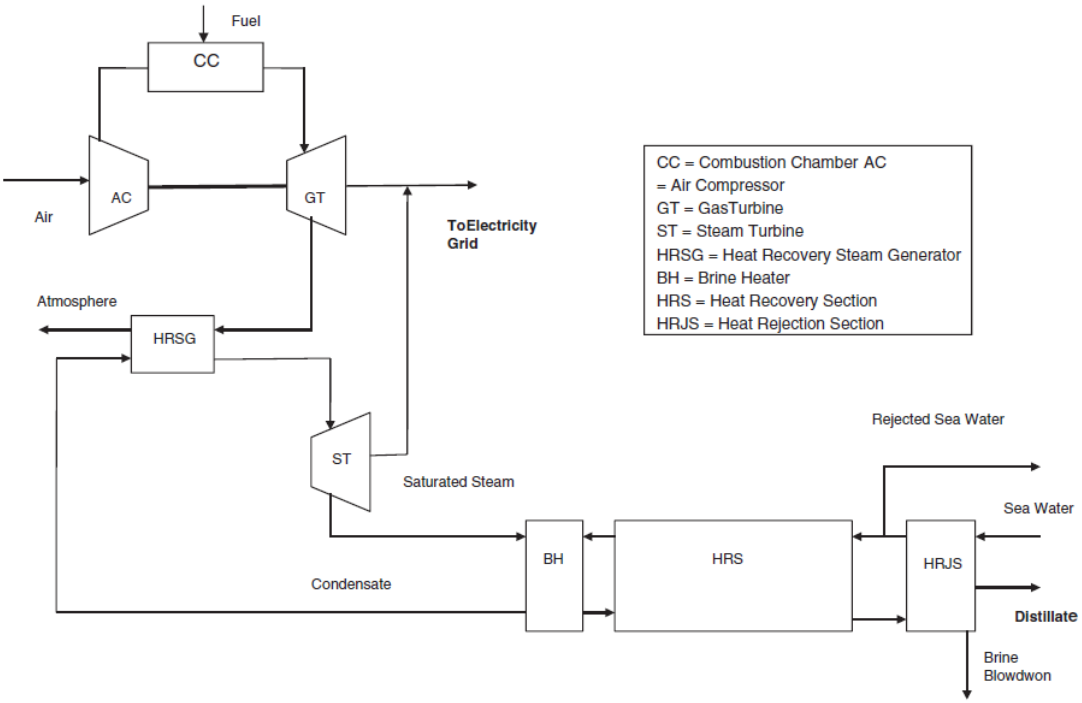

Source: (Ghamdi & Mustafa, 2016)

Here, the heat recovery steam generator is the responsible to supply the thermal energy needed for the brine heater of the desalination plant. Moreover, part of the electricity produced by generator is used to provide the plant with the electrical energy it needs.

5.2.6.3. Hybrid cycle: RO & steam cycle.

Figure 48 illustrates the schematic of the combined power–desalination system for simultaneous generation of electric power and fresh water. The power generation cycle includes the boiler and the steam turbine that produces the electric energy and the thermal energy. The desalination plant includes the MSF and RO.

The fuel is combusted in the boiler to produce the superheated steam. The steam is sent to the steam turbine to generate the electric energy, which is used for MSF, RO and the grid. The whole or part steam extracted from the turbine is fed to the brine heater of MSF and condensed to recycle the boiler (Lianying et al., 2013).

Figure 48: Scheme of a desalination plant powered by a hybrid cycle: RO & steam cycle.

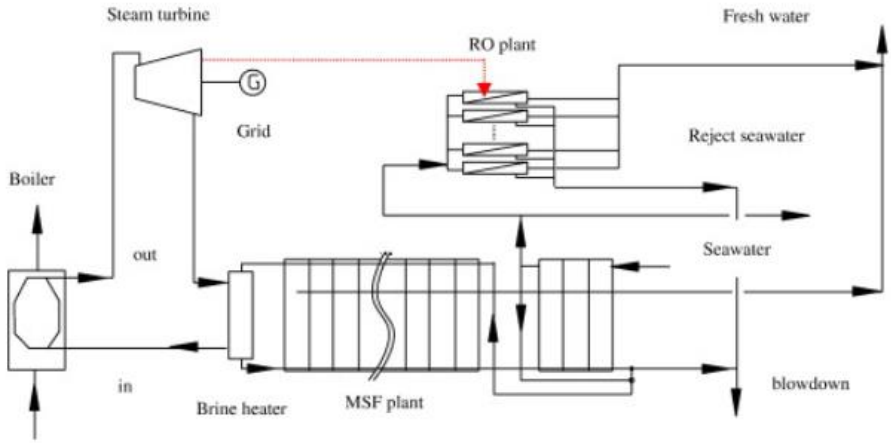

Source: (Lianying et al., 2013)

5.2.6.4. Hybrid cycle: RO & combined cycle.

Results from a mix of the combined cycle power plus a stream going out from the steam turbine and feeding electrically to a RO desalination plant, as in the scheme of the hybrid cycle: RO & steam cycle.

5.2.7. GHGs emissions.

5.2.7.1. GHGs emissions estimation model.

Desalination can cause considerable damage to the environment in several ways. For instance, desalination plants get thermal and electrical energy from an attached power plant. The energy used in the process amounts to a certain carbon dioxide emission, one of the greenhouse gas (GHG) emissions promoting climate change, which results in environmental pollution. Generally the lesser the energy requirement by the desalination technology the lesser the indirect environmental impact is going to be (Fath et al., 2011).

Focusing now on the GHG emissions of seawater desalination, it is possible to propose an estimation model for their calculation mainly considering the emissions from energy consumption. The estimation method is based on the calculation method as follows in (Eq. 13):

$$GHG = EM_e + EM_{in} + EM_{waste} \quad \text{(Eq. 13)}$$

where GHG is the GHG emissions of the desalination plants; EM_e is the emission of energy consumption; EM_{in} is the emission of material inputs and EM_{waste}, is the indirect emission from treating the waste generated from the desalination processes. Each of the elements composing the estimation model are contributing in $kgCO_{2eq}/m^3$, which means the kilograms of CO_2 equivalent emitted per each cubic meter of freshwater produced (Jia, 2019).

5.2.7.2. GHGs emissions of MSF plants powered by conventional fossil fuels.

The CO_{2eq} emissions from MSF plants coupled with different energy providing plants have been reported. Table 18 shows the carbon dioxide emissions per cubic meter of freshwater produced of different MSF configurations using natural gas (NG) as a fuel as well as their cost impact.

Table 22: CO2 equivalent emissions from MSF desalination plants coupled with different energy providing power plants.

Configuration (Fuel)	Kg CO_{2eq}/m3	abatement cost ($/$m_3$)
Cogeneration, steam cycle, NG	13,9-15.6	0,28-0,31
Cogeneration, combined cycle, NG	9,41	-
Cogeneration, hybrid RO, steam cycle, NG	9,45	-
Cogeneration, hybrid RO, combined cycle, NG	5,56	-

Source: (Fath et al., 2011)

Since MSF has relatively high specific energy consumption, more GHG emissions are expected. Combined cycle coupled with MSF desalination has a high thermal efficiency and, therefore, a low environmental impact. Anyway, the GHG footprint values vary due to the fuel used (the situation becomes worse if coal or oil is used as fuel), location of the plants, quality, technologies, life cycle stages, efficiency and parameters considered, price of energy, etc.

In general terms, the GHG footprint made by MSF desalination technologies is about 10-20 kg CO_{2eq}/m^3.

On the other hand, abatement cost refers to the cost of reducing environmental impacts such as pollution. Abatement cost is used by several organisms in several fields, such as: carbon traders use marginal abatement cost curves to derive the supply function for modelling carbon price fundamentals; power companies may employ marginal abatement cost curves to guide their decisions about long-term capital investment strategies to select among a variety of efficiency and generation options; economists have used marginal abatement cost curves to explain the economics of interregional carbon trading; policy-makers use marginal abatement cost curves as merit order curves, to analyze how much abatement can be done in an economy at what cost, and where policy should be directed to achieve the emission reductions (Fath et al., 2011).

5.3. Reverse Osmosis (RO) desalination.

5.3.1. General aspects.

The typical processes of a RO desalination plant are explained below. Pre-treatment units are employed to remove large-size particles and solids before the RO system because they can cause fouling and/or scaling on the surface of the membrane. TDS should also be removed to produce freshwater.

In RO, a semi-permeable membrane which allows water molecules to permeate while blocking solids molecules is employed for that separation. However, the osmotic pressure across the semi-permeable membrane becomes an obstacle to desalination. Therefore, the RO process requires high pressure to overcome the osmotic pressure of seawater, for which a high-pressure pump is used.

After the RO system, desalted fresh water is obtained while concentrate is discharged from the RO train. In the concentrate, a considerable amount of pressure still remains. To improve the energy efficiency, the pressure in the concentrate should be recovered, for example, by energy recovery devices (ERDs). The recovered pressure is used to increase the pressure of the feed stream. However, this pressure increase is tipically not enough, and the feed stream pressure is supplemented by a booster pump (Kim et al., 2019).

5.3.2. Plant description.

A general RO plant scheme is shown in Figure 49:

Figure 49: Diagram of a Reverse Osmosis (RO) desalination plant process.

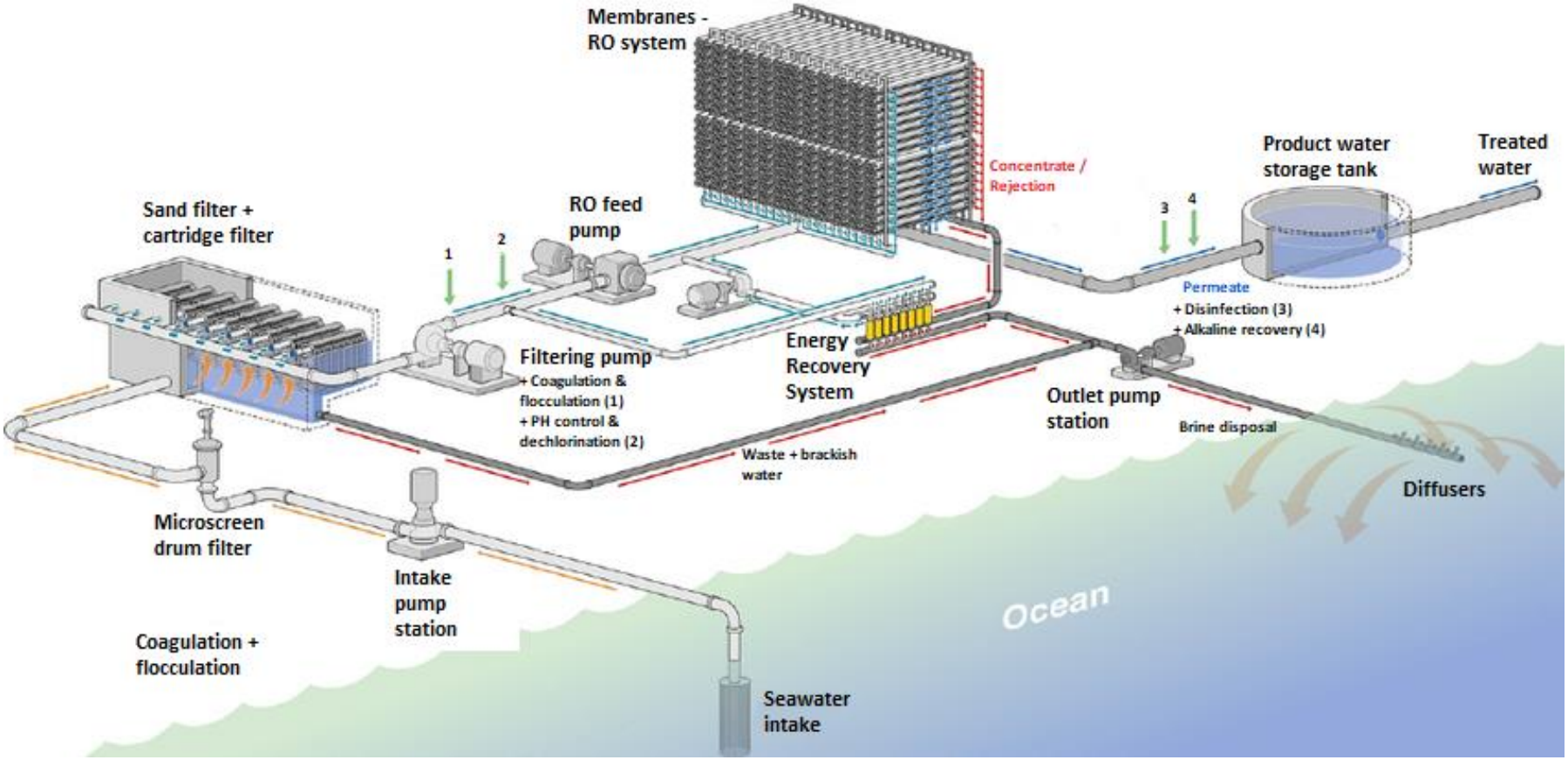

Source: (Voutchkov, 2017)

5.3.2.1. Water intake and physical pre-treatments.

Water is pumped through the intake pump station and sent to the filtration operations. These operations are carried out through micro screen drum filters and conventional sand filters to control the particles maximum size. A set of cartridge filters forms a second filtration stage as a final safety barrier before the membranes. All filters are periodically backwashed (Migliorini & Luzzo, 2004).

5.3.2.2. Feed water chemical pre-treatments.

Description extracted from the scientific paper (Migliorini & Luzzo, 2004).

Coagulation.

After the physical pre-treatments, the water is sent to the coagulation stage. Flocculation and coagulation agents are added to water to create nuclei onto which colloidal and suspended material in the water can adsorb, thus creating floe of larger dimensions and mass which can be removed by sedimentation.

The coagulants can be of two different types: polyelectrolytes and iron or aluminum salts. In general, however, the most common coagulant utilized is the ferric chloride with dosing rates between 0.3 and 3 ppm. But, in some installations, it is possible to use both types to improve the sand filters performances. The relevant reaction is:

$$2FeCI_3 + 3Ca(HCO_3)_2 <-> 2Fe(OH)_3 + 3CACl_2 + 6CO_2$$

During coagulation, some CO_2 is produced. According to the stoichiometric reaction it is possible to calculate the relevant CO_2 released after the injection as follows in (Eq 14):

$$CO_2 = X_{FeCl_3} * \frac{6 \text{ x } 44}{2 \text{ x } 162,5} \text{ ppm} \qquad \text{(Eq. 14)}$$

pH regulation.

In the case of seawater intake, under normal conditions, water is usually supersaturated with calcium carbonate. The pH of most natural waters is generally assumed to be controlled by the carbonic acid system.

The applicable equilibrium reactions are:

$$CO_2 + H_20 <-> (H_2CO_3) <-> H^+ + HCO^-_3$$

$$HCO^-_3 <-> H^+ + CO^{2-}_3$$

The CO_2/ HCO^-_3/ CO^{2-}_3 equilibrium in seawater can be calculated starting from alkalinity and pH values.

Limiting salt calculation: scaling control.

Scaling control is essential in RO membrane filtration. The amount of anti-scalant or acid addition is determined by the limiting salt. The limiting salt can be determined from the solubility products of potential limiting salts and the actual feed-stream water quality and from the ionic strength. Calcium carbonate scaling is commonly controlled by sulphuric acid addition; however, sulphate salts are often the limiting salt.

Dechlorination.

Before entering in the membrane trains the feed water residual chlorine content must be removed to avoid damages to the membrane. The stoichiometric weight ratios of the most common sulphite compounds needed per mg/1 of residual chlorine are given in Table 19:

Table 23: Dechlorination compounds needs for the RO desalination process.

Dechlorination compound			Quantity, mg/(mg/l) residual	
Name	Formula	Molecular weight	Stoichiometric amount	Range in use
Sulphur dioxide	SO_2	64.09	0.903	1.0–1.2
Sodium sulphite	Na_2SO_3	126.04	1.775	1.8–2.0
Sodium bisulphite	$NaHSO_3$	104.06	1.465	1.5–1.7
Sodium metabisulphite	$Na_2S_2O_5$	190.10	1.338	1.4–1.6

Source: (Ahuchaogu et al., 2018)

5.3.2.3. Membrane desalination.

RO is the process of forcing a solvent from a region of high solute concentration through a semi-permeable membrane to a region of low solute concentration by applying a pressure in excess of osmotic pressure (Figure 50). Water is pressurized against one surface of the membrane, causing transport of salt – depleted water across the membrane and emergence of portable drinking water from the low-pressure side.

Membranes are some of the most important parts of RO. The membranes used for RO have a dense layer in the polymer matrix (0,25 microns), either the skin of an asymmetric membrane or an interfacial polymerized layer within a thin-film composite membrane, where the separation occurs and 100 microns of support layer. Most of the membranes used in commercial RO plants are made from cellulose acetate, polyamide, polysulfonate and polyoxadiazole (Ahuchaogu et al., 2018).

Figure 50: Basic RO process sketch and typical RO membrane element structure.

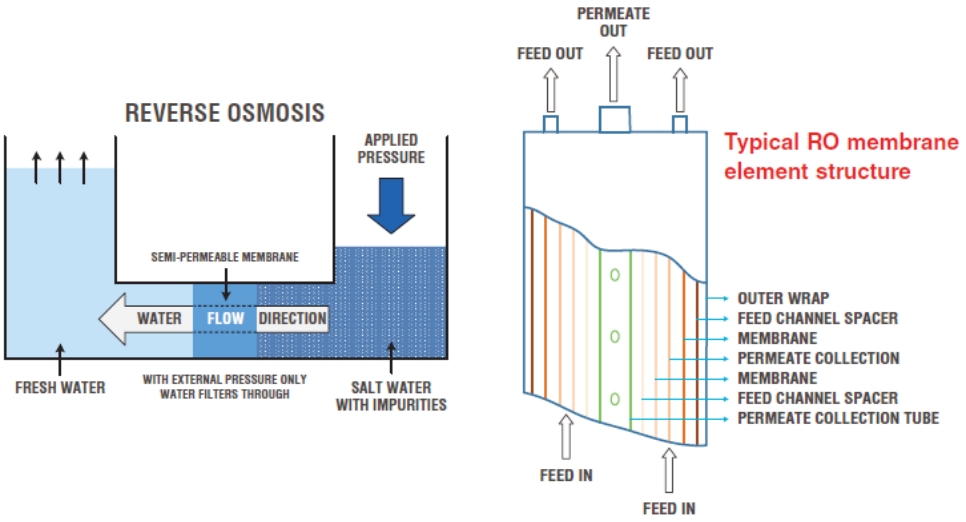

Source: (Diagrams, 2017)

5.3.2.4. Permeate chemical post-treatments.

Description extracted from the scientific paper (Migliorini & Luzzo, 2004).

Disinfection.

Chlorine converts some alkalinity that passes through the membranes to carbon dioxide. The pH after chlorination can be determined by summing the protons from the HCl added past the point of neutralization to the protons at neutralization.

Alkaline recovery.

Since acid addition is used for scaling control, all the alkalinity in the raw water will be destroyed but not lost. The membrane is a closed system and the carbon dioxide will remain under pressure until exposed to an open system. Since carbon dioxide will pass unhindered through the membrane, the desired amount of

alkalinity can be recovered in the permeate by acidifying the desired amount. In the case the base used is $Ca(OH)_2$ the reaction can be assumed as:

$$2CO_2 + H_2O + Ca(OH)_2 \rightarrow Ca^{2+} + 2HCO^-_3 + H_2O$$

5.3.2.5. Energy recovery system.

Figure 51: Scheme of the Energy recovery system of a RO plant.

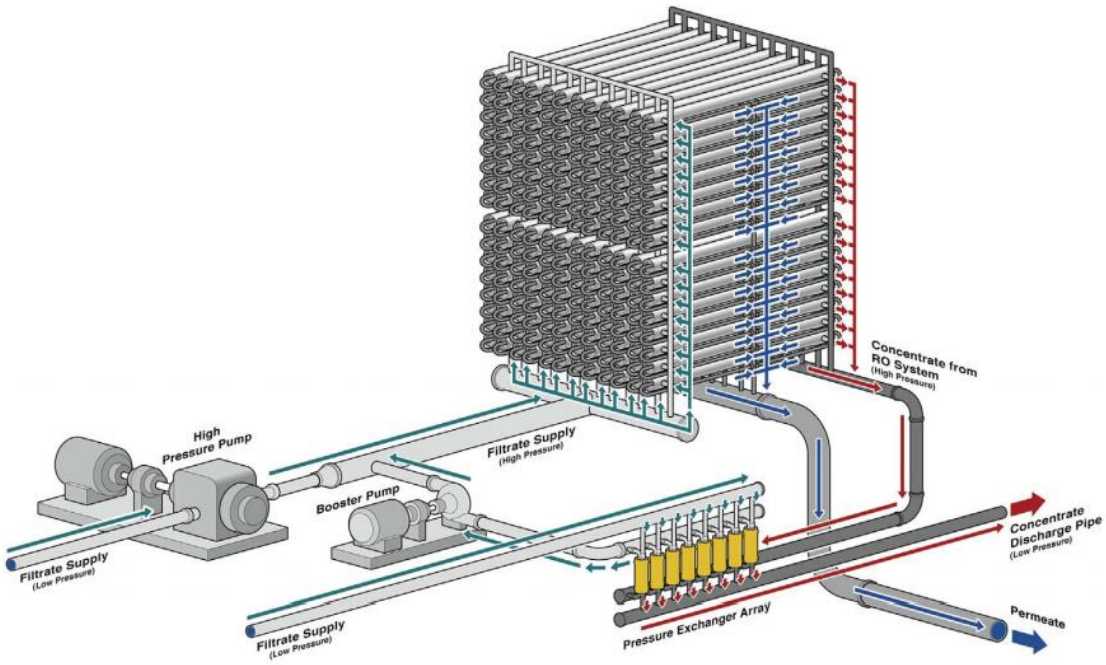

Source: (Voutchkov, 2017)

Since the RO process requires high pressure to overcome the osmotic pressure of water, the concentrate stream has a considerable amount of remaining pressure. To improve the energy efficiency of the plant, the pressure in the concentrate should be recovered by ERDs (Figure 51).

Turbines were used in the first ERD applications. Francis turbines (FTs) were the earliest, followed by Pelton turbines (PTs). In these systems, a turbine is attached to a shaft that is common to the high-pressure pumps (HPP) and the electric motor. The turbine-type ERD is not highly efficient due to the double energy conversion, where hydraulic energy in the concentrate is converted to mechanical energy to rotate the shaft and converted again to hydraulic energy in the feed. To further improve energy efficiency, isobaric ERDs, such as for dual work exchanger energy recovery (DWEER) devices or pressure exchanger (PXs) are adopted (Kim et al., 2019).

5.3.2.7. Brine disposal: rejection blowdown.

Finally, the rejection or concentrate goes out of the heat recovery stage by the outlet pump station. The brine exit velocity on the submarine emissary must be very high so that the brine can be diluted with the open water and no high concentrations of salt are created in the vicinity of the emissary. The velocity is controlled by the design of the diffusers located at the end of the emissary (Migliorini & Luzzo, 2004).

5.3.3. Performance indicators.

The performance indicator applicable to the RO plants is the CR, that is already explained in the MSF desalination plant chapter *(see "Performance indicators of MSF plants").*

5.3.4. Energy consumption.

5.3.4.1. Indicators.

Specific electrical energy consumption (SEEC).

SEEC is defined as the amount of electrical energy consumed to produce a unit mass of pure water. In fact, this performance indicator is used to compare results with processes which consume electrical energy. In RO, electrical energy is consumed by the flow pumps of the system.

Specific thermal energy consumption (STEC).

STEC or the specific heat consumption is a measure of the amount of thermal energy needed to generate a unit of freshwater. In RO, there is no thermal energy consumed (Miladi et al., 2019).

5.3.4.2. Typical values of SEC in RO.

Depending on the intake water of the RO system, the process will require a higher level of pretreatment. Influent TDS levels for seawater desalination are on the order of 35.000 mg/L compared to 1000–15.000 mg/L for brackish water (Cornejo et al., 2014) such as the water of the groundwater bodies, like the ones studied in the Sahel region). The typical values of SEC will be studied for both cases: seawater RO desalination plants (SWRO) and brackish water RO desalination plants (BWRO).

5.3.4.2.1. SWRO.

The lowest theoretical energy consumption for desalination of seawater of 33.500 mg/L and temperature of 25°C is 0,7 kWh_{elec}/m^3. This energy use corresponds to a condition of complete conversion of intake water into fresh water (100% recovery), which cannot be achieved in practical terms. For a more realistic 50% recovery, this minimum theoretical energy use would be 1,1 kWh_{elec}/m^3. However, this energy consumption assessment assumes that all desalination plant equipment has 100% energy efficiency and all energy contained in the desalination plant concentrate is reused in the desalination process. Therefore, this energy threshold is the ideal theoretical minimum for SWRO desalination (Voutchkov, 2017).

It has been reported that the SEC of the SWRO process is about 2,5–3,5 kWh_{elec}/m^3, which is significantly higher than its minimum specific energy. Moreover, the SEC of a real-scale SWRO plant is even higher, approximately 3,5-4,5 kWh_{elec}/m^3, including pre-treatment and post-treatment processes. It means that the SEC of the SWRO plant is approximately 1 kWh_{elec}/m^3 higher that of the SWRO system. Thus, it can be inferred that the energy consumption for pre- and post-treatment is close to 1 kWh_{elec}/m^3 regardless of feed conditions and other factors. In this scenario, it is important to understand the factors affecting the energy consumption of a SWRO system, which ultimately relates to the SEC of the plants.

Moreover, the SEC of SWRO desalination plants with different types of ERDs is presented. The plants with FTs obtain a high SEC over 6 kWh_{elec}/m^3, but those with PTs obtained SEC in the range of 3,5–5,9 kWh_{elec}/m^3. Then, isobaric ERDs show lower energy use than turbine ERDs. The plants with DWEER devices consume 3,5–4,6 kWh_{elec}/m^3, and those with PXs exhibit a wider range, with energy use of 3,0–5,3 kWh_{elec}/m^3 (Kim et al., 2019). Summarizing in Table 20:

Table 24: Typical values of STEC and SEEC of the SWRO desalination plants.

	SWRO plants	
STEC	0	MJ/m^3 produced water
SEEC	3,5 – 4,5	kWh_{elec}/m^3 produced water

5.3.4.2.2. BWRO.

Following the same road, it has been reported and assessed that today's BWRO processes required from 1,5-2,5 kWh_{elec}/m^3 of SEEC for brackish water from large to medium size of plants (Wakil et al., 2017), while the STEC of the plant remains in 0 MJ/m^3. Summarizing in Table 21:

Table 25: Typical values of STEC and SEEC of the BWRO desalination plants.

	BWRO plants	
STEC	0	MJ/m^3 produced water
SEEC	1,5 – 2,5	kWh_{elec}/m^3 produced water

5.3.4.3. Factors affecting SEC in RO.
Description extracted from scientific paper (Kim et al., 2019).

Salinity.

A feed with high salinity possesses high osmotic pressure. To produce fresh water from a high salinity feed, higher hydraulic pressure must be applied. Therefore, SEC increases with increased salinity.

Energy recovery device.

Low SEC can be explained by the highly efficient RO system, in which a single pass is configured, high-performance membranes are accommodated, and PXs are employed as ERDs. Although ERDs reduce the SEC of RO systems, the SEC of the plant also decreases with different ERD applications, because the SEC of plants has a linear relationship with the RO SEC.

High pressure and booster pump.

The efficiency of the HPP and BP is one of the factors that determine the SEC of a RO system. The pump efficiency can be improved by increasing its size. Thus, a RO plant with large capacity is advantageous in reducing RO SEC.

Permeate quality.

RO plants that produce high-quality permeate also exhibit high SEC. This is because the purer the obtained water, the higher the minimum energy required for separation.

Permeate quantity.

Recovery is a ratio that can be expressed as permeate flow rate per feed flow rate. A high recovery ratio can minimize the overall intake, pre-treatment, and brine disposal. Thus, a high-recovery operation can reduce the costs of intake and brine disposal. So, increasing permeate quantity can also increase the SEC but it is important to operate the RO system with a recovery that properly satisfies the optimal SEC and cost.

Figure 52 shows the summary of the factors affecting the SEC of a SWRO plant:

Figure 52: Summary of the factors affecting the SEC of a SWRO plant.

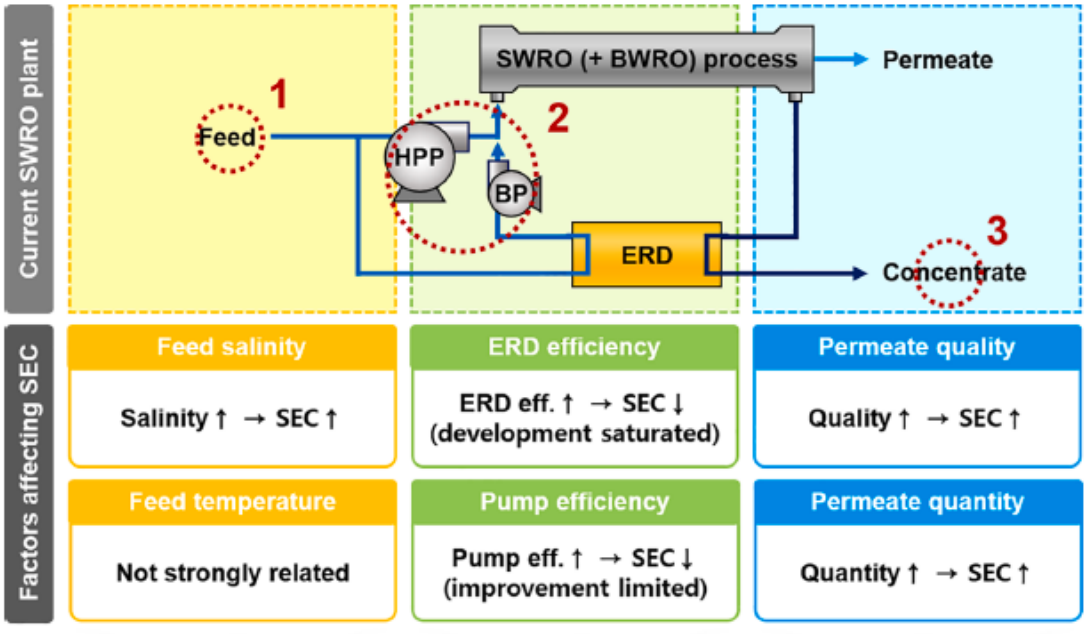

Source: (Kim et al., 2019)

5.3.6. Energy providing.

As explained before, the energy consumption of a RO desalination plant is due to the pumping stations. The use of the intake pumps, the filtering pumps, the high pressure pumps and the outlet pumps requires only electrical energy supply. Because of that, RO desalinations plants can be fed with any type of electric energy system.

5.3.7. GHGs emissions.

5.3.7.1. GHGs emissions of RO plants powered by conventional fossil fuels.

5.3.7.1.1. SWRO.

Several scientific papers report the GHG footprint of seawater RO desalination plants. Here, two of them are being selected as representative to give general values of CO_{2eq} emissions of RO.

Table 22 contains that information from paper (Fath et al., 2011) about SWRO plants powered by different energy systems:

Table 26: CO2 equivalent emissions from SWRO desalination plants coupled with different energy providing power plants.

Energy system	Kg CO_{2eq}/m^3
Steam cycle	2,79
Combined cycle	1,75

Moreover, from paper (Macedonio & Drioli, 2017) the GHG footprint has been reported in a more general way and says that its value varies from 1.4-3.6 kg CO_{2eq}/m^3 of produced water, depending on the fuel used to produce the electricity.

5.3.7.1.2. BWRO.

In general, brackish groundwater and brackish surface water desalination yields lower GHG emissions than seawater desalination due to lower levels of electricity needed to treat lower levels of TDS (Cornejo et al., 2014). The reported values of the GHGs emissions of BWRO plants range between 0,4-2,5 kgCO_{2eq}/m^3 of produced water (Cornejo et al., 2014).

5.4. Future trends.

5.4.1. General considerations.

Nowadays, desalination processes are still energy intensive consumers. Future trends on desalination call to reduce energy consumption of the processes as well as GHGs emissions. So, the researches and improvements must be done in the direction of energy and environmental sustainability. In other words, potential for energy consumption, GHG emission and cost reduction should be found and the future trend seems to call to the application of:

- Enhanced **energy recovery units**,
- the integration of desalination plants and **renewable energy** or low potential heat,
- the development of new technologies (Jia, 2019).

Regarding the renewable energy sources, such as solar, geothermal and wind, over the last few decades their utility to run desalination processes has been explored. Solar and possibly geothermal energy could be good alternatives to fossil fuels because they are abundantly available, especially in regions that face water shortages. However, the expansion of these technologies to larger scales is hampered by techno-economic and thermo-economic challenges (Esfahani et al., 2016).

Regarding the future and new technologies, there are several new desalination technologies being developed to reduce consumption and produce sustainable desalination processes based on renewable energies. Some of them are:

- Adsorption Desalination (AD). AD is considered as one of the most energy efficient processes available. AD can use direct solar energy or industrial waste-heat to desalinate high-salinity water, but there are still issues with its initial capital cost which need to be addressed through modeling and investigating its payback cycle.
- Membrane distillation (MD). MD is a thermally driven low-energy process that utilizes a hydrophobic, microporous membrane to separate fresh water by liquid-vapor equilibrium. The process is based on the combination of conventional distillation and membrane technologies involving heat and mass transfer. More research is needed to develop novel MD membranes with high throughput to increase the permeate flux and thermal efficiency by using industrial waste-heat or by incorporating the direct use of solar energy.
- Forward osmosis (FO). FO processes can be used directly or indirectly to make the desalination process more energy efficient. Indirect FO desalination processes use low salinity feed solution like wastewater to dilute higher salinity seawater and produces partially desalinated water, which can be used for irrigation. Ongoing research shows that the fouling on membrane surfaces is lower while a complete removal of contaminants, such as micropollutants, natural organic matter, trace metals and nutrients from the feed water is possible. However, there are still several aspects that need to be explored before the technology can be applied for commercial production in the Middle East. The development of high throughput FO membranes will be a breakthrough towards process scale-up and commercialization.

As the demand for fresh water grows in the Middle East, the future of desalination will depend on combining established and emerging technologies. Researchers need to focus on the hybridization of FO, MD and AD coupled with and without conventional desalination processes such as thermal desalination and reverse osmosis.

This combination will assist the development of energy efficient and renewable energy-driven desalination technologies. Besides, good planning and management of water resources is essential. There is a huge potential in reusable water techniques to improve utilization of treated domestic and industrial wastewater to produce ample fresh water supplies (Wali, 2014).

5.4.2. Future trends in energy consumption of MSF plants.

In the past twenty years the request for MSF desalination plants has been limited only to the Middle East Region due to the low fuel cost there and to the difficulties of proper treatment of the seawater for a trouble-free operation of RO plants.

The reasons why the MSF technology survived well against the emerging RO technology are manly the following:

- High reliability of installed plant and possible life span higher than that foreseen at the time of construction.
- Easy operation, similar to the power plant they are always coupled with. This means that operations and maintenance personnel can be easily found and do not represent a major problem for the owner.
- Low performance degradation during the years: It is recognized worldwide that an MSF plant properly operated and maintained has practically no performance degradation in terms of water production and energy consumption (Borsani & Rebagliati, 2005).

However, the International Desalination Association (IDA) predicted in 2016, only 7% of all new plants going online will incorporate thermal processes, while the majority will be based on membrane technology utilizing the RO process. Manoj Sharma, vice president and general manager at Aquatech International said: “Over the last 20 years, desalination on a large scale has always included thermal technology like MSF, particularly in the Middle East. However, in the last 10-20 years, RO has taken over from thermal on the large-scale projects because it is more energy efficient. We are seeing thermal technologies being phased out except for industrial applications where waste heat is available.” (Bennett, 2016)

5.4.3. Future trends in energy consumption of RO plants.

Lastly, the future reported trends in RO application are (Kim et al., 2019):

- The increasing scale RO plants.
- The development of ERDs. EDRs significantly reduce energy consumption of RO, so results necessary to develop and use ERDs with higher efficiency.
- The increasing demand for high-quality product. It results in RO plants adopting two-pass RO designs to reduce the TDS of the permeate from the first-pass RO by using a second-pass RO. However, extra energy is required to undertake an additional RO pass.

5.4.4. Future trends in GHGs emissions of MSF plants.

Since desalination is an energy-intensive process, more sustainable energy sources such as renewable energies should be used to develop sustainable and environmentally friendly desalination systems and reduce the GHG emissions.

On the other hand, the selection of the most suitable renewable energy powered desalination technology depends on factors such as location of operation, amount of water production, size of the site, type of technology, and production costs related to the salinity of the feed water, remoteness, access to an electrical grid and the availability of renewable energy sources.

5.4.5. Future trends in GHGs emissions of RO plants.

Following the same pattern as in MSF plants, a reduction in coal-fired energy coupled with an increase in the use of renewable energy sources has the potential to decrease the carbon footprint of water treatment plants that use alternative feed sources.

However, large RO plants usually need storage and backup and, therefore, practically cannot rely 100% on renewable energy.

5.5. Summary.

5.5.1. Performance and operational parameters of MSF and RO technologies.

Table 23 contains a summary of all the performance and operational indicators described along the chapter. The aim of the table is to summarize the general aspects of MSF and RO desalination plants. Also, the cost of water (Wakil et al., 2017) will be added to the rest of parameters because it helps to draw a complete scenario of the two most used technologies.

Table 27: Summary of the performance and operational indicators of MSF and RO desalination plants.

Parameters	MSF plant	RO plant
Operating temperature (ºC)	90-110	Ambient
Thermal energy – STEC (MJ/m^3)	190-300	N/A
Electric energy – SEEC (kWh_{elec}/m^3)	2,5-5	3,5-4,5 (SWRO), 1,5-2,5 (BWRO)
Gain output ratio – GOR	6-12	NA
Technology growth trend	Moderate	High
Environmental impact	Discharge is 10–15 °C hotter than ambient, TDS increase of 15–20%	Brine discharge at ambient temperature, TDS increase of 50–80%
CO2 emissions ($kgCO_{2eq}/m^3$)	10-20	1,4-3,6 (SWRO) 0,4-2,5 (BWRO)
CO2 abatement cost ($/m^3$)	0,28-0,31	-
Cost of water ($/m^3$)	0,56-1,75	0,26-0,54
Plant life (years)	25-40	10-15

5.5.2. Performance and operational parameters summary: a study case.

The objective of this point is to describe parameters and indicators of a study case (Kamal, 2008) of two hypothetical desalination plants (MSF and RO, specifically SWRO) to understand the energetic requirements of the processes and the performance of the two technologies.

For the mentioned study case, the energy requirement was evaluated for MSF and SWRO utilizing GTPRO®, a software obtained under license from Thermoflow, Inc. to simulate the design of power/seawater desalination plants. The power plant simulation is based on 12 natural-gas fueled combustion turbine generators (CTGs) associated with four steam turbine generators (STGs) arranged in a four-train, three-on-one configuration. The same fuel input was used for all the cases.

- Figure 53, is the scheme of the combined cycle plant with steam extraction for MSF plant, where P is the pressure in psia (1 psia= 0,0689476 bar), T is the temperature in Fahrenheit degrees and M is the mass flow rate in kpph (1 kpph = 453,592 kg/h).
- Figure 54, is the scheme of the MSF desalination circuit, each of 6 units, with a GOR of 7,853 kg distillate water/kg of steam, where h is enthalpy in BTU/lb (1 BTU/lb = 2,326 kJ/kg) and w is the moisture content in the air in %.

Figure 53: Scheme of the combined cycle plant with steam extraction for MSF plant: parameters and indicators of a study case.

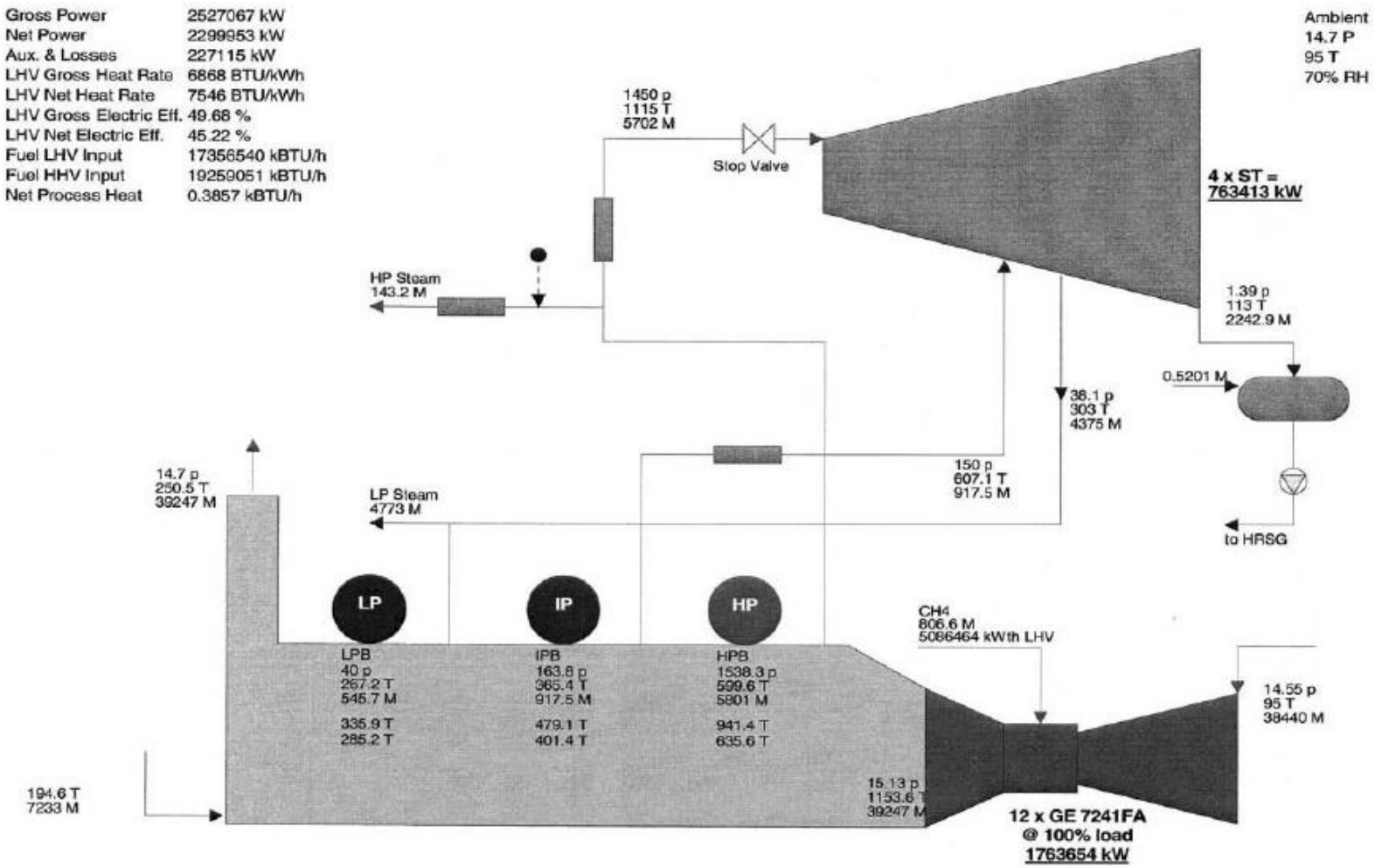

Source: (Kamal, 2008)

Figure 54: Scheme of the MSF desalination circuit: parameters and indicators of a study case.

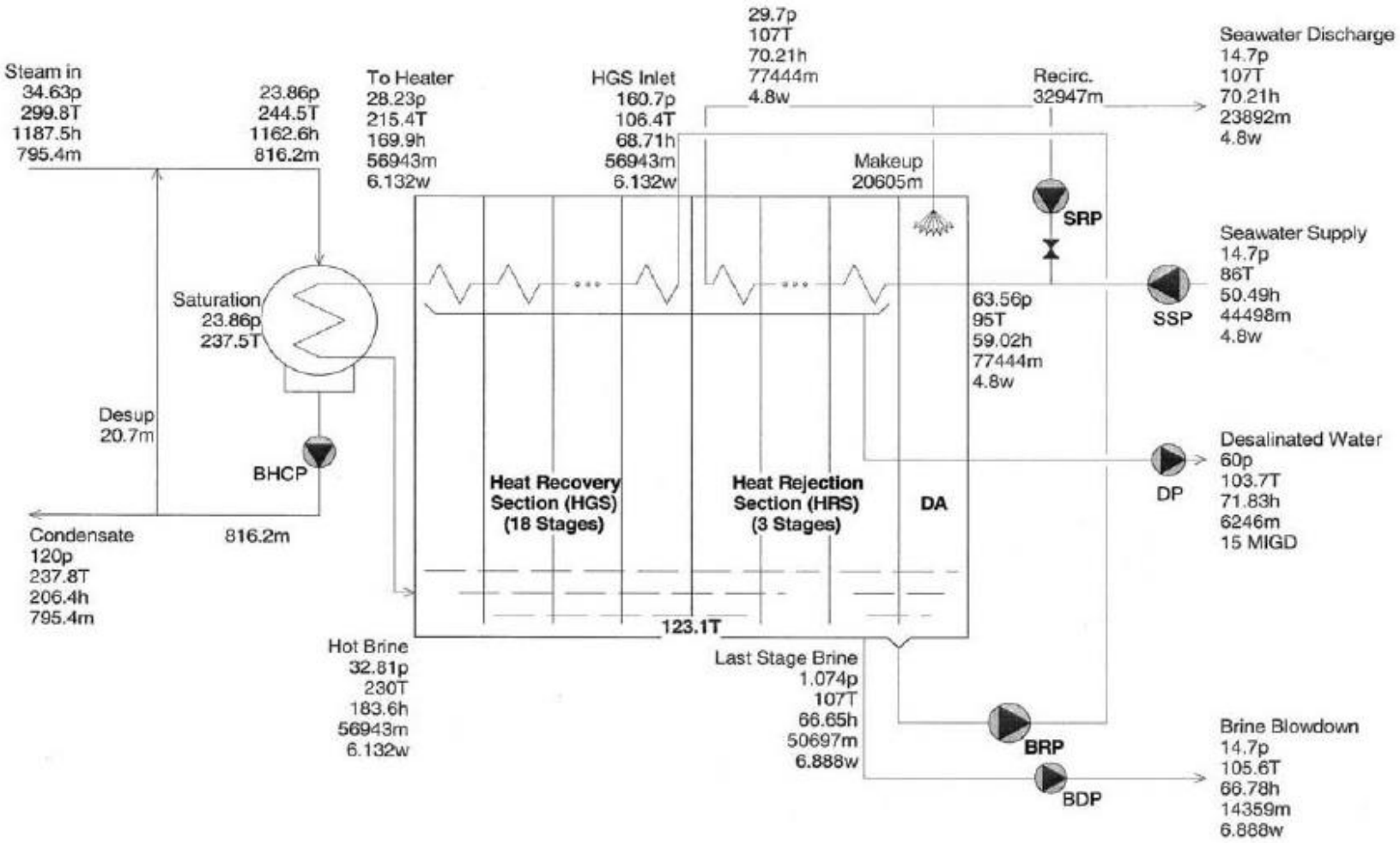

Source: (Kamal, 2008)

The data and indicators available of the two plants are shown in Table 24:

Table 28: Summary of the performance and operation indicators of MSF and RO plants: study case.

	MSF plant	SWRO plant
Number of CTGs	12	12
CTG output, each, in MW_{elec}	146,97	146,97
CTG output, total, in MW_{elec}	1763,65	1763,65
Number of STGs	4	4
STG output, each, in MW_{elec}	190,85	261,33
STG output, total, in MW_{elec}	763,41	1045,30
Gross power output, in MW_{elec}	2527,06	2808,96
Auxiliary power and losses, in MW_{elec}	227,12	135,24
Net plant power, in MW_{elec}	2299,95	2673,72
LHV Net heat rate, in $kJ/kW_{elec}h$	8047	8047
Fuel input LHV, total, in MJ/h	18 507 697,65	21 515 344,37
Fuel input, total, in MW_{elec}	5141	5976,48
Net electrical efficiency, in %	44,74	44,74
Total water output – fresh water output, in m^3/day	409 148,1 *(*)*	409 148,1 *(*)*
Energy consumption due to desalination plant, in MW_{elec}	441,27	67,50

Source: (Kamal, 2008)

(*) The total fresh water output production value is the product of a conversion units from MIGD (Million Imperial Gallons per Day) to m^3/day, where 1 MIGD=4546,1 m^3/day.

In this case, the total desalination plant output for both plants is designed to be around 409 148,1 m^3/day of produced water (90 MIGD). The plant considerations are the following:

- 12 combustion turbine generators (CTGs), with 146,97 MW of output power each. This makes a CTG total power output of 1763,65 MW_{elec} for both, MSF and SWRO desalination plants. They are natural gas fueled.
- 4 steam turbine generators (STGs), giving output power of 190,85 MW_{elec} each (so 763,41 MW_{elec} in total) for the MSF plant and 261,33 MW_{elec} (so 1045,30 MW MW_{elec} in total) for the SWRO plant. The power output of STGs in the RO plant is basically the maximum feasible power for the considered combined cycle. It means that, for a certain high pressure of the STGs inlet gas, the pressure of the outlet gases will be the lowest feasible in order to produce the highest amount of electric energy, since in the RO plant the electric power is preferred to the thermal energy. On the other hand, the pressure of the outlet gases in the MSF plant will be higher than the pressure in the RO, so more thermal energy will be extracted from the brine heater, since in the MSF plant the thermal energy is preferred.
- The gross power output of the MSF plant is around 2527,06 MW_{elec} and the gross power output of the SWRO is about 2808,96 MW_{elec}. In other words, the gross power output is higher in RO than in MSF plants.
- Moreover, regarding the power needs of the auxiliary component and the losses, in the MSF plant are considered around 9% of the gross power output while in the SWRO plants are considered around 5%. Again, helps to the net power output to be higher for the RO plant with respect to the MSF plant. All in all, for this specific example, it is possible to see that the net plant power is 2299,95 MW_{elec} for the MSF plant and 2673,72 MW_{elec} for the RO plant.
- Should be mentioned that the fuel input LHV for each CTG is the same for MSF and SWRO plant, what explains the same CTG power output in both plants. In this specific case, the LHV Net heat rate for NG is 8047 $kJ/kW_{elec}h$. So the fuel input LHV total can be calculated as:

$$\text{Fuel input LHV total} = \text{Net plant power} * \text{LHV Net heat rate}$$

- The net electrical efficiency can be calculated as shown in (Eq. 15):

$$\text{Net electrical efficiency} = \frac{\text{Net plant power}}{\text{Fuel input LHV total}} * 100 \text{ (in \%)} \qquad \text{(Eq. 15)}$$

- In addition, it is expressed the power consumed for the desalination part, which are 441,27 MW_{elec} for the MSF plant and 67,50 MW_{elec} for the RO plant. Again, **RO technology presents less power consumption** for the desalination processes involved.

From this data, it is possible to calculate an estimation of the SEC (also of SEEC and STEC) for each plant. In addition, it is possible to calculate an approximation of the GHGs emissions for each plant, so they can be compared with the reported values.

SEC estimation.

- SWRO plant:

$$\text{SEC} = \text{SEEC} = \frac{\text{required power}}{\text{mass flow rate of fresh water produced}} = \frac{67{,}5 \cdot 10^3\ \text{kW}_{\text{elec}}}{409\,148{,}1 \frac{\text{m}^3}{\text{day}} \cdot \frac{1\ \text{day}}{24\ \text{h}}} = 3{,}96\ \frac{\text{kW}_{\text{elec}}\text{h}}{\text{m}^3}$$

$$\approx 4\ \frac{\text{kW}_{\text{elec}}\text{h}}{\text{m}^3}$$

while $\text{STEC} = 0\ \frac{\text{MJ}}{\text{m}^3}$.

The obtained value is acceptable since the reported values of SEC (=SEEC) for RO desalination plants are between 3.5-4.5 $\frac{kWhelec}{\text{m}^3}$.

- MSF plant:

$$\text{SEC} = \frac{\text{required power}}{\text{mass flow rate of fresh water produced}} = \frac{441{,}27 \cdot 10^3\ \text{kW}_{\text{elec}}}{409\,148{,}1 \frac{\text{m}^3}{\text{day}} \cdot \frac{1\ \text{day}}{24\ \text{h}}} = 25{,}88\ \frac{\text{kW}_{\text{elec}}h}{\text{m}^3}$$

$$\approx 26 \frac{\text{kW}_{\text{elec}}\text{h}}{\text{m}^3}$$

For MSF plants, the reported values of STEC generally ranged from 190 to 300 MJ/m^3 of products (that is equivalent to 15–25 kWh_{elec}/m^3 at 30% power plant efficiency) while a typical SEEC ranges between 2,5-5 kWh_{elec}/m^3. Total SEC is approximately 20-30 kWh_{elec}/m^3 (Wakil et al., 2017). All in all, the obtained value of SEC is perfectly inside the range.

The data on electricity generation and CO_2 equivalent emissions from electric utility (EIA, 2020) shows that an approximated value of the emissions by fuel (natural gas in this case) in 2018 is around 0,92 pounds of CO_2/kWh=0,4173 kg CO_{2eq}/kWh.

CO2 emissions estimation.

- MSF plant:

$$\text{GHGs emissions } (\text{CO}_2 \text{ equivalent}) = \frac{0{,}4173 \frac{\text{kgCO}_{2\text{eq}}}{\text{kW}_{\text{elec}}\text{h}} * 441.27 \cdot 10^3\ \text{kW}_{\text{elec}}}{409\ 148.1 \frac{\text{m}^3}{\text{day}} * \frac{1}{24} \frac{\text{day}}{\text{h}}} = 10{,}80 \frac{\text{kgCO}_{2\text{eq}}}{\text{m}^3}.$$

- SWRO plant:

$$\text{GHGs emissions } (\text{CO}_2 \text{ equivalent}) = \frac{0{,}4173 \frac{\text{kgCO}_{2\text{eq}}}{\text{kW}_{\text{elec}}\text{h}} * 67.5 \cdot 10^3\ \text{kW}_{\text{elec}}}{409\ 148.1 \frac{\text{m}^3}{\text{day}} * \frac{1}{24} \frac{\text{day}}{\text{h}}} = 1{,}65 \frac{\text{kgCO}_{2\text{eq}}}{\text{m}^3}.$$

Both values are exactly inside the reported range.

Chapter 6: Plants and infrastructures.

6.1. Technical and environmental approach.

6.1.1. Desalination technology: suitable type selection.

The aim of this chapter section is the selection and the justification of the suitable desalination technology to be used for each of the regions studied.

According to the information and data provided in Chapter 5, it can be concluded that the RO process presents more advantages nowadays among other desalination technologies. The reasons are the following:

- Regarding the energy consumption, the RO technology requires less energy consumption and shows a higher plant efficiency than the MSF technology. In addition, energy requirement for RO can be further reduced with the pressure-exchanger and work-exchanger type of recovery devices, now increasing in popularity. All in all, SEC can be further reduced with the future and proper development of EDRs.
- Regarding GHGs emissions, the RO technology presents less environmental impact. CO_2 emissions are around 2,5 $kgCO_{2eq}/m^3$ of produced water for a SWRO combined cycle power desalination plant energy providing and 1,5 $kgCO_{2eq}/m^3$ of produced water in the BWRO case, while the emissions are around 9,5 $kgCO_{2eq}/m^3$ for an MSF plant with the same energy providing.
- Moreover, RO is the technology able to face the increasing demand for high-quality product. It results in RO plants adopting two-pass RO designs to reduce the TDS of the permeate from the first-pass RO by using a second-pass RO. However, extra energy is required.
- Finally, regarding the economic issue, the energy cost for thermal desalination processes is several times higher than the cost for RO, irrespective of the price of energy. Owing to dramatic improvements in technology and reductions in membrane costs, RO can currently produce water at about half the cost obtainable from the thermal processes. It has become the process of choice for seawater desalination plants being built in Europe, the Americas and the Far East. Desalination costs will be reviewed in the next chapter.

For all the reasons, around 70% of the thermal desalination plants have already moved over to RO. However, in the Middle East, only around 50% of desalinated water is treated in this way because the membranes used for RO process have yet to be fully customized for the high salinity of Red Sea and Gulf seawater. Another limitation is the high temperature of the region which impacts the operational capacity of RO plants (Wali, 2014). In general, seawater RO operational problems are site-specific. Localized procedures (pretreatment process design, operation techniques and troubleshooting responses), therefore, must be developed and practiced until they become established for a given location.

In this case, waters of the Red Sea and the Arabian Gulf are characterized by significantly higher salinities and TDS concentrations than in other open seas. Normal sea-salinity is around 35% and normal TDS concentrations are 25.000-35.000 mg/l. Average TDS values recorded in the study (Saeed et al., 2019) were stable at 45.000 mg/l. Carefully tested pilot pretreatment is essential in RO desalination plants along the Arabian Gulf shore, like the ones located in the Red Sea coast. The hot climate makes the water temperature conducive to biological growth and membrane fouling. The sea is very shallow, with abundant sunlight, which promotes biological productivity. Shallowness also allows the water column to become easily disturbed. Total suspended solids (TSS) vary greatly in their concentration due to this combination of high biological productivity and the easy disturbance of the water column. At times, high TSS values create filtration problems and plants may need to be totally shut down until values return to normal. This problem occurs in many plants along the Red Sea and Gulf coasts. (Saeed et al., 2019)

Regarding the groundwater of the unstressed basins located around the Senegal and Mauritania regions in the Sahel, which can be useful as water providing for irrigation (as mentioned in *Chapter 3*), they present low salinity and low TDS concentration, between 600-3000 mg/l. Therefore, both desalination technologies, RO (specifically BWRO) and MSF, can be used. Preferably, BWRO technology will be used because of the advantages presented before.

Most current research in RO desalination technology is focused on the development of new high throughput membranes which can operate at low pressure and high temperature and are resistant to fouling contaminants. But researchers also need to further focus on the development of pretreatment processes considering the high salinity of Persian Gulf and Arabian seawater (Wali, 2014).

Even if researches and developments are being done about improving RO membranes, nowadays SWRO technology is still not recommendable for desalination of the Red Coast seawater. Therefore, the MSF technology will be selected for the desalination plants of the project in the Red Sea Coast and Libya coast. The project includes some MSF desalination plants distributed along the Red Sea coast in order to provide freshwater to the reforestation in Egypt, then some MSF desalination plants in Libya that will provide freshwater to the Niger reforesting region.

On the other hand, BWRO and MSF technologies can be used for water desalination in the silvo-pastoral reserve of south Senegal since the salinity and turbidity are low. Preferably, SWRO will be used for the underground water of the unstressed Senegalo-Mauritanian basin, because of the several advantages already described. Numerical justifications will be carried out in the next points of this chapter.

6.1.2. Power plant: suitable type selection.

Turning now to the selection and justification of the power plant that will provide the electricity and heat to the desalination process. According to the information and data provided in Chapter 5, it can be concluded that the combined cycle presents more advantages nowadays as a power plant energy providing. This type of technology has the lowest environmental impact among the fossil fueled power plants, because its combination of components results in a higher plant efficiency. In Chapter 5, it has been mentioned that the CO_2 equivalent emissions for a SWRO desalination plant coupled with a combined cycle are 1,75 $kgCO_{2eq}/m^3$ of produced water in comparison with 2,79 $kgCO_{2eq}/m^3$ of produced water required for a steam cycle energy providing. While for the MSF plants, the GHGs emissions are 9,41 $kgCO_{2eq}/m^3$ of produced water in the combined cycle plant fueled with natural gas, whereas the emissions are around 14,5 $kgCO_{2eq}/m^3$ of produced water for the steam cycle plant fueled with natural gas. Figure 55 shows the overall system efficiency and environmental impact of different configuration of power and desalination systems:

Figure 55: Single purpose and cogeneration process impact on overall plant efficiency and environment.

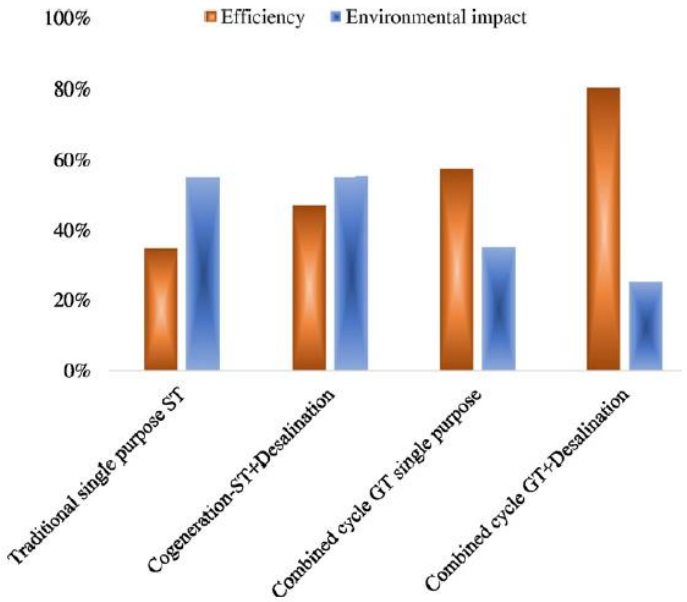

Source: (Wakil et al., 2017)

Single purpose plants are less efficient and hence they have higher environmental impact; in multi-purposed plants, combined cycle gas turbine (CCGT) power and desalination plant can achieve 80% overall efficiency and 25% environmental impact as compared to 57% efficiency and 35% environmental impact of single purpose CCGT power plant. This improvement in overall efficiency and reduction in environmental impact is due to the excellent thermodynamic synergy of the cascading arrangement of

thermally driven systems. A similarly improved trend has been observed with single purpose steam power plant combined with desalination cycle. This shows that the higher the overall system efficiency the lower the environmental impact (Wakil et al., 2017). All in all, desalination plant with a CCGT seems the most efficient option, and so, it has the lowest environmental impact. That is why it should be chosen in the design of this project.

6.1.3. Desalination power plants: performances and calculations.

The scope of this part of the project is to give a general description of the MSF and RO desalination plants designed for each of the candidate areas of the project to be reforested. The general description will contain information about power plant performances, electricity generation process and the desalination process.

6.1.3.1. MSF desalination power plants.

As it is already known, MSF desalination power plants are the technology selected for the study regions of the Sahara Desert: Eastern and Ténéré Desert. Table 25 describes the MSF plant that suits the energy and water requirements of both areas and provides the values of some of the total CO_2 emissions of the project.

Table 29: Description of the MSF plant type to install at Eastern and Ténéré Deserts, according to the energy and water requirements.

MSF DESALINATION PLANTS		
Power plant performance		
Net plant power	1000	MW_{elec}
	1	GW_{elec}
LHV Net heat rate (NG)	8047	$kJ/kW_{elec}h$
Fuel LHV input (NG - CHP)	8.047.000	MJ/h
	2235	MW
Net electrical efficiency	44,74	%
Electricity generation process		
CO_2 emissions per electricity production		
Equivalent operating hours per plant	8000	h
Power produced per year per plant	8.000.000	$MW_{elec}h/year$
Avg CO_2 emissions (Egypt) per kWh	0,4213	$kgCO_{2eq}/kW_{elec}h$
Total CO_2 emissions (in time) per plant per year	3.370.160.000	$kgCO_{2eq}/year$
	107	$kgCO_{2eq}/s$
	3,3702	$MtCO_{2eq}/year$
Avg CO_2 emissions (Libya) per kWh	0,5693	$kgCO_{2eq}/kW_{elec}h$
Total CO_2 emissions (in time) per plant per year	4.554.400.000	$kgCO_{2eq}/year$
	144	$kgCO_{2eq}/s$
	4,5544	$MtCO_{2eq}/year$
Desalination process		
Energy consumption		
Avg SEEC	3,75	$kW_{elec}h/m^3$
STEC	190-300	MJ_{therm}/m^3
	15-25	$kW_{elec}h/m^3$
Avg STEC	20	$kW_{elec}h/m^3$
SEC = SEEC + STEC	23,75	$kW_{elec}h/m^3$
Freshwater production		
Total water output per plant	11,7	m^3/s
	1.010.526	m^3/day
	368.842.105	$m^3/year$
CO_2 emissions per desalination		
Avg CO_2 emissions per m3	10	$kgCO_{2eq}/m^3$
Total CO_2 emissions (in time) per plant	117	$kgCO_{2eq}/s$
	3.688.421.053	$kgCO_{2eq}/year$
	3,6884	$MtCO_{2eq}/year$

First, the power plant performances has been calculated. The net plant power has been set in 1 GW_{elec}, as a limiting value. The limiting value can be estimated according to the actual state-of-art of the medium-large size MSF desalination plants. The cell is in blue because it refers to an input parameter. With all, knowing from Chapter 5, the value of the LHV heat rate for the natural gas, it is possible to calculate the fuel LHV input of the plant and its net electrical efficiency.

Regarding the electricity generation process, some CO_2 emissions by the electricity production will be produced. These emissions are calculated in the table by means of the average CO_2 emissions per kWh of electricity and heat production by gas in Egypt and in Libya, taken from the International Energy Agency (IEA) website (IEA, 2020).

Finally, regarding the desalination process, the average SEEC and STEC values have been taken from Chapter 5. With them, it is possible to calculate the total freshwater production per plant, and so, the total CO_2 emissions per unit of m^3 of freshwater produced.

6.1.3.2. BWRO desalination plants.

As it is already known, BRWO desalination plants are the technology selected for the region of the Sahel Desert studied: Sylvo-Pastorale des Six Forages Reserve. Table 26 describes the BWRO plant that suits the energy and water requirements of that area. Moreover, the table also provides the values of some of the total CO_2 emissions of the project.

Table 30: Description of the BWRO plant type to install at Sylvo-Pastorale des Six Forages Reserve, according to the energy and water requirements.

BWRO DESALINATION PLANTS		
Desalination process		
Energy consumption		
Avg SEEC	0,48	$kW_{elec}h/m^3$
Avg STEC	0	MJ_{therm}/m^3
SEC = SEEC + STEC	0,48	$kW_{elec}h/m^3$
Freshwater production		
Total water output per plant	350.000.000	m^3/year
	958.904	m^3/day
	11	m^3/s
CO_2 emissions per desalination		
Avg CO_2 emissions per m3	1,5	$kgCO_{2eq}/m^3$
Total CO_2 emissions (in time) per plant per year	17	$kgCO_{2eq}$/s
	525.000.000	$kgCO_{2eq}$/year
	0,0005	$MtCO_{2eq}$/year
Power taken from the grid		
Power consumption per plant	0,0192	GW_{elec}
	19,2	MW_{elec}
Electricity generation process		
CO_2 emissions per electricity production		
Equivalent operating hours per plant	8000	h
Avg CO_2 emissions (Mauritania) per kWh	0,5693	$kgCO_{2eq}/kW_{elec}h$
Total CO_2 emissions (in time) per plant	87.344.658	$kgCO_{2eq}$/year
	3	$kgCO_{2eq}$/s
	0,0873	$MtCO_{2eq}$/year

The procedure for the BWRO desalination plant calculations differs slightly from MSF. In this case, the main input parameter is the total freshwater output capacity, as the limiting value. The limiting value can be estimated according to the actual state-of-art of the medium size RO desalination plants. Considering the STEC of the BWRO plants and the freshwater output needed, the power consumption from the grid is 19,2 MW_{elec} and can be achieved in only one desalination plant. Then, knowing the CO_2 emissions by desalination, the total emissions per plant have been calculated.

Finally, regarding the electricity generation process, some CO_2 emissions by the electricity production per plant will exist. These emissions are calculated in the table by means of the average CO_2 emissions per kWh of electricity and heat production by gas taken from the International Energy Agency (IEA) website. Must be mentioned that there is no available data for Mauritania, so as an approximation the same value of average CO_2 emissions as Libya has been taken as an input parameter.

6.1.4. Pipelines: description and calculation.

After the desalination process, the freshwater produced must be delivered to the reforested areas. Due to that, a water distribution network must be considered in the project. Two scenarios will be studied: a short-distance pipeline scenario and a long-distance pipeline scenario. The short-distance pipeline scenario is for the water distribution from Red Sea cost desalination plants to the Eastern Desert, and also for the water distribution from the Senegalo-Mauritanian Basin groundwater to the Sylvo-Pastorale des Six Foreges Reserve. On the other hand, the long-distance pipeline scenario will be used for the water distribution from the Libya cost desalination plants to the Ténéré Desert.

Both scenarios include the same water parameters and pipe parameters, but different pipe dimensions. They are described in the following points, together with the total pumping energy consumption and the CO_2 emissions due to pumping.

6.1.4.1. Short-distance pipeline.

This scenario is characterized by the design of a pipeline of 50 kilometers of length (input parameter). This length is enough to distribute the water from the coast to the surrounding selected areas. The pipe chosen is one of the biggest ones, with a nominal diameter DN3000 (input parameter), since the water transportations needs are large. Moreover, the maximum velocity per pipe has been established with a value of 2,5 m/s (input parameter). The results are collected in Table 27 and the procedure is explained below.

Table 31: Description of the short-distance pipeline to install at Eastern Desert and Sylvo-Pastorale des Six Forages Reserve, according to the energy and water requirements.

EASTERN DESERT & SILVO-PASTORAL RESERVE (MAURITANIA)		
0. Water parameters		
Density	997	kg/m^3
Dynamic viscosity	0,00089	Pa·s
1. Pipes' dimensions		
Diameter	3	m
Nominal Diameter (DN)	3000	mm
Length	50	km
Area	7,07	m^2
2. Pipes' parameters		
Max velocity per pipe	2,5	m/s
Max flow rate per pipe	17,67	m^3/s
	557.288.424	m^3/year
Reynolds number per pipe	8.401.685	-
3. Friction factor calculation		
ε/D (for steel pipe)	0,00005	-
f (turbulent flow)	0,01098	-
4. Total losses calculation		
l distributed per pipe	571,63	J/kg
l concentrated per pipe	28,58	J/kg
Total losses per pipe	600,21	J/kg
	0,60	kJ/kg
5. Energy needed per pipe		
Pumping energy consumption	0,166	$kW_{elec}h/m^3$
6. Number of pipes needed		
Water transport needs (Eastern Desert)	924.000.000	m^3/year
Water transport needs (Mauritania-Sahel)	2.958.000.000	m^3/year
Nº pipes needed (Eastern Desert)	2,0	pipes
Nº pipes needed (Mauritania-Sahel)	5,0	pipes
7. Total energy needed for pumping		
Total pumping power consumption (Eastern Desert)	17.533	kW_{elec}
Total pumping power consumption (Mauritania-Sahel)	56.130	kW_{elec}
Equivalent operating hours per plant	8000	Hours/year
Total pumping energy consumption per year (Eastern Desert)	140.267	$MW_{elec}h$
Total pumping energy consumption per year (Mauritania-Sahel)	449.038	$MW_{elec}h$
8. Total CO2 emissions per pumping		
Avg CO2 emissions (Egypt) per kWh	0,4213	$kgCO_{2eq}/kW_{elec}h$
Total pumping CO2 emissions (Eastern Desert)	2,052	$kgCO_{2eq}/s$
	64.703.993	$kgCO_{2eq}$/year
	0,065	$MtCO_{2eq}$/year
Avg CO2 emissions (Mauritania) per kWh	0,5693	$kgCO_{2eq}/kW_{elec}h$
Total pumping CO2 emissions (Mauritania-Sahel)	8,876	$kgCO_{2eq}/s$
	279.922.581	$kgCO_{2eq}$/year
	0,280	$MtCO_{2eq}$/year

After setting the input parameters, Reynolds number and the relative roughness of the pipe must be calculated to obtain the friction factor and, then, the friction losses of the pipe. Friction losses will be separated between distributed and concentrated losses. The next expressions have been used:

- Reynolds number (Re):

$$\mathrm{Re} = \frac{\rho * v * D}{\mu} \quad \text{(Eq. 16)}$$

  where ρ is the water density (in kg/m^3), v is the water velocity inside the pipe (in m/s), D is the pipe diameter (in meters) and μ is the dynamic viscosity of the water (in Pa·s).
- Relative roughness:

$$\text{Relative roughness} = \frac{\varepsilon}{D} \quad \text{(Eq. 17)}$$

  where ε is the absolute roughness of the pipe material (in mm) and D is the diameter of the pipe (in mm).
- Friction factor (f) : is estimated through the Swamee-Jain equation for turbulent flow. The equation is (Eq. 18):

$$f = \frac{0{,}25}{\log_{10}\left(\left(\frac{1}{3{,}7} * \frac{\varepsilon}{D}\right) + \frac{5{,}74}{\mathrm{Re}^{0.9}}\right)} \quad \text{(Eq. 18)}$$

- Friction losses:

$$\begin{aligned}\text{Friction losses (l)} &= \text{Distributed losses } (l_{dist}) \\ &+ \text{Concentrated losses}(l_{conc})\end{aligned} \quad \text{(Eq. 19)}$$

  - Distributed losses (in J/kg) are calculated as follows in (Eq. 20):

$$l_{dist} = f * \frac{L}{D} * \frac{v^2}{2} \quad \text{(Eq. 20)}$$

    where f is the friction factor, L is the length of the pipe (in meters), D is the diameter of the pipe (in meters) and v is the velocity of the water inside the pipe (in m/s).
  - Concentrated losses (in J/kg) are calculated as follows in (Eq. 21):

$$l_{conc} = 0.05 * l_{dist} \quad \text{(Eq. 21)}$$

    Concentrated losses are estimated to be around 5% of the distributed losses, assuming that there will be some elbows along the pipelines when they go through the elevated areas. However, losses are mostly compensated with the gravity action in the slope down.

Thanks to the previous equations, the specific pumping energy consumption per m^3 of freshwater can be calculated. Now, the next step is the calculation of the number of pipes needed. This value is easy to obtain taking into consideration the total water needs per region (described in the Reforestation Chapter) and the maximum flow rate per pipe as considered in (Eq. 22) and (Eq. 23):

$$\text{Number of pipes} = \frac{\text{Total water transport needs (per region)}}{\text{Maximum flow rate per pipe}} \quad \text{(Eq. 22)}$$

$$\begin{aligned}\text{Maximum flow rate per pipe} &= \text{Maximum velocity per pipe} * \text{Area of the pipe} \\ &= v * \pi * \frac{D^2}{4}\end{aligned} \quad \text{(Eq. 23)}$$

where D is the diameter of the pipe (in meters).

In the last step, the total energy consumption by pumping can be calculated through the specific energy consumption per m^3 of freshwater times the total water transportation needs (in m^3). In this way, the CO_2 emissions by pumping can be obtained, again thanks to the average CO_2 emissions from the (IEA, 2020) for each country.

6.1.4.2. Long-distance pipeline.

This scenario is characterized by the design of a pipeline of 1000 kilometers of length (input parameter). That is the length required to distribute the water from the coast of Libya to the Ténéré Desert (Niger) selected areas. The pipe chosen is one of the biggest ones, with a nominal diameter DN3000 (input parameter), since the water transportations needs are large. Moreover, the maximum velocity per pipe has been established with a value of 2,5 m/s (input parameter). The results are collected in Table 28 and the procedure is the same explained for Table 27.

Table 32: Description of the long-distance pipeline to install at Ténéré Desert, according to the energy and water requirements.

TÉNÉRÉ DESERT		
0. Water parameters		
Density	997	kg/m^3
Dynamic viscosity	0,00089	Pa·s
1. Pipes' dimensions		
Diameter	3	m
Nominal Diameter (DN)	3000	mm
Length	1000	km
Area	7,07	m^2
2. Pipes' parameters		
Max velocity per pipe	2,5	m/s
Max flow rate per pipe	17,67	m^3/s
	557.288.424	m^3/year
Reynolds number per pipe	8.401.685	-
3. Friction factor calculation		
ε/D (for steel pipe)	0,00005	-
f (turbulent flow)	0,01098	-
4. Total losses calculation		
l distributed per pipe	11.432,64	J/kg
l concentrated per pipe	571,63	J/kg
Total losses per pipe	12.004,27	J/kg
	12,00	kJ/kg
5. Energy needed per pipe		
Pumping power consumption	3,325	$kW_{elec}h/m^3$
Equivalent operating hours per plant	8000	hours/year
Total pumping energy consumption per year	2.805.346	$MW_{elec}h$
6. Number of pipes needed		
Water transport needs (Ténéré Desert)	924.000.000	m^3/year
Nº pipes needed (Ténéré Desert)	2	pipes
7. Total energy needed for pumping		
Total pumping power consumption	350.668	kW_{elec}
8. Total CO2 emissions per pumping		
Avg CO2 emissions (Niger) per kWh	0,5693	$kgCO_{2eq}/kW_{elec}h$
Total pumping CO2 emissions (Ténéré Desert)	55,454	$kgCO_{2eq}/s$
	1.748.806.386	$kgCO_{2eq}$/year
	1,749	$MtCO_{2eq}$/year

6.1.5. Drilling design for Sahel region: general considerations.

As it has been mentioned along the project, the considerations taken for supplying the water needs in the Sahel region are based on SWRO desalination plants fed with water coming from the underground unstressed basins around. For that, the design of drilling wells may be studied.

In this part of the project, the approach and description of the drilling processes will be done, attending to classification of wells and drilling techniques, as well as the necessary equipment to operate the wells (Iglesias Martín, 2016).

6.1.5.1. Most relevant types of wells and how they work.

Some criteria must be considered to decide whether to dig or to drill the wells and which pumps to install on the wells. Table 29 proposes a classification (FAO, 1986) based on the following criteria:

- Depth to water bearing formation.
- The hardness of the formations to be penetrated to reach the aquifer which determines the difficulty of drilling wells.

Table 33: Classification of wells based on the depth and hardness of the formations to be penetrated.

Depth to water level	Depth to water bearing formation	Hardness of formations to be penetrated to reach the aquifer	Recommended well	Recommended water lifting method
From 0 to 70-80 m	From 10 to 70-80 meters	Soft to medium	Drilled wells	Wind/solar/motor pump
		Hard	Drilled wells	Motor pump driven
	More than 70-80 m	Soft to medium	Well cistern associated	Lifting device
		Hard	Drilled wells	Motor pump driven
More than 70-80 m	More than 70-80 m	Hard	Drilled wells	Motor pump driven

Source: (FAO, 1986)

According to Table 29, since the estimation of the requirements of the project is to deeper drill than 80 m, the last option of the table will be considered: drilled wells and motor driven pumps.

Drilling methods: types.

- Cable tool of percussion method. Based upon the principle of applying sufficient energy to pulverize the soil or rock by percussion. Three major operations are required: first, drilling of the hole by crushing the rock or clay or other material by the impact of the drill bit; second, removing the cuttings with a bailer as cuttings accumulate in the hole; and third, driving or forcing the well casing down into the hole as the drilling proceeds. Table cable tool is the simplest drilling method which is designed primarily for medium hard rock and cobbly or bouldery materials. Although the method can apply in many cases, the major constraint is the extreme slowness of the operation. On the other hand this method does not require large investment in purchase of rig and tools nor does it need lengthy training for operating the machine. Small private enterprises should be encouraged to use cable tools capable of drilling at low cost.
- Conventional mud-rotary drilling. Accomplished by rotating a drill pipe and bit by means of a power drive. The drill bit cuts and breaks up the rock material as it penetrates the formation. Drilling fluid, usually made of mixed water and special clay (bentonite), is pumped through the rotating drill pipes and holes in the bit. The fluid swirls into the bottom of the hole, picking up the drill cuttings, then flows upward in the well bore, carrying the cuttings to the surface. The cuttings settle out of the mud in puts before the mud is recirculated. The mud-rotary method is effective for drilling most rocks. Drilling is rapid in all except the hardest rocks. Difficulties may be encountered in penetrating loose, hard boulders. The rotary method is best suited for deep wells (deeper than 200 m), for wells aimed at developing artesian aquifers (aquifers under pressure) and for reconnaissance wells except in hardest rocks.
- Air-rotary and down-the-hole-hammer methods. They are usually associated in the drilling of the same well since air-rotary is applied in the soft and slightly consolidated part of the borehole

(usually the upper part, corresponding to the weathered formation) whereas the down-the-hole-hammer method is used in the hardest formation (usually corresponding to the basement). Air-rotary is like mud-rotary in principle, the main difference consisting of substituting mud with air and consequently mud pump with air compressor. Down-the-hole-hammer drilling consists of using air to drive a percussion hammer set at the lower end of the drilling string. Therefore air has two purposes: to drive the hammer and to carry the cuttings to the surface. Air consumption varies with the bit diameter and air pressure. To ensure the proper upward transportation of the cuttings it is usually considered that the vertical air velocity should be equal to 15 m/s minimum. Foam is sometimes added to the air to help carry up the cuttings and to limit the erosion of the wall of the borehole by the air flow. The main advantage of the method is rapidity of drilling in very hard formations. On the other hand the diameter of the hole is limited by the air velocity required to carry up the cuttings.

- Reverse circulation method. Used for drilling very large diameter boreholes in unconsolidated formations to obtain highly productive wells for irrigation purposes. This method does not suit the usual requirements of groundwater development in rangeland areas (limited discharge of the wells to avoid overgrazing around the water supply).

Casing materials.

Until recently drilled wells were cased with steel or wrought iron pipe casings using welded or threaded and coupled joints. For the last 10-15 years, polyvinyl chloride (PVC) plastic pipes have proved to be very convenient because they are lightweight and highly resistant against corrosion. PVC pipes can be used for wells up to 300 m depth, however the standard wall thickness allows a maximum setting depth of approximately 100 m. For deeper wells specially manufactured thicker pipes should be used.

Screens.

The most important part of any well is that area where the water flows from the aquifer into the well. The proper construction and development of this section of the well is essential for the efficient production of the optimum amount of groundwater.

In unconsolidated sand and gravel aquifer and more generally in all water bearing formations likely to cave or collapse when water flows, a screen or perforated casing is necessary to allow the water from the aquifer to enter the well and to stabilize the aquifer material.

Water lifting.

Many types of water lifting devices are in use in various parts of the world for irrigation, domestic supply or livestock watering. Those which may be envisaged in rangeland areas can be classified as: motor driven pumps, wind powered pumps and/or solar pumps.

Groundwater monitoring.

In principle a groundwater project designer should always be able to predict the long-term behavior of the aquifer in relation to the planned program of water abstraction and to the possible climatic fluctuations which may affect the recharge of the aquifer. Water wells should be designed in such a way that in no case the water level would drop down out of the reach of the designed water lifting devices. This means also, in the case of the drilled wells, usually much deeper than the water level, to design the pumping equipment in such a way that no risk would occur for the pumps to run dry and either to be damaged.

While the water resources of a continuous aquifer are relatively easy to estimate and in most cases they are, by an order of magnitude, bigger than the water demand for extensive stockbreeding, the problem may become serious in the case of discontinuous aquifers. Because hydraulic extrapolations are hazardous in discontinuous aquifers, the classical methods of groundwater resources evaluation do not apply and therefore the water project should be designed on a step by step basis in such a way that each new step of water development would be designed and implemented on the basis of a careful analysis of the effect of the previous step on the aquifer.

In a rangeland area, a rainfall observation network is usually planned to correlate precipitation and dry matter production and thus to predict the carrying capacity of the area during the next dry season. The same rainfall observations can be used for groundwater recharge monitoring

6.1.5.2. Wells operation and exploitation: equipment.

This part consists on the description of what is necessary to operate the wells, so the design of the well equipment is carried out. The electromechanical equipment project for the well must define the following facilities:

- Hydraulic installations: pumping group, drive pipe, auxiliary pipes and special parts, valves, flow meter, etc.
- Electrical installations: transformers, power cables, frequency variators, capacitors, etc.
- Control and protection facilities: control panel, network analyzer, programmable automaton, etc.
- Civil works and urbanization of the plot where the well is located: transformation centers and low-voltage centers, the well's well and the closure of the well's plot.

Going slightly into the hydraulic installations, the most important element is the pumping group, which extracts the water from inside the well to the delivery point. There are several types of pumps: horizontal axis, vertical axis and submersible electric pumps; the latter are the most used in equipping groundwater collection wells, since they allow water to be extracted from high depths.

– Drive pipe.

The drive pipe begins at the outlet of the pumping group and reaches the mouth of the well, ending at the water delivery point. This pipe must withstand a nominal pressure enough to withstand the possible pressure points expected in the installation, as well as the joints sandwiched between the flanges. These flanges have notches through which the feed cables of the pumping group and the piezometric pipe pass. The drive pipe must be of enough diameter to fit inside the casing of the wellbore, taking into account the maximum diameter of the flange, including the power supply cable of the pumps and the piezometric pipes (which are placed around it) and, in turn, must minimize pressure drops. The water velocity in this pipe must be less than 3.5 m/s for the flow to be laminar.

– Drain.

The well must be provided with a conduit that allows the water to be poured into a public channel in the event that it is necessary to carry out a cleaning pumping of the extracted water because the water does not have the adequate characteristics for the intended use. The drain pipe is derived from the discharge pipe, generally inside the manhole in which the wellhead is located and it ends in a manhole before going out into the public channel.

Chapter 7: CO_2 sequestration potential.

7.1. Final CO_2 balances.

It will be presented a summary of all the CO_2 fluxes (sequestration and emissions) involved in the project. The total CO_2 sequestration by region is already known from the Reforestation Chapter. Regarding the emissions, such as those due to electricity production for desalination plants and the emissions due to pumping for water distribution, they are already calculated per plant in the previous chapter. The total CO_2 emissions by a region can be obtained multiplying the number of desalination plants needed per region times the CO_2 emissions per plant. At the same time, the number of plants needed can be calculated dividing the total watering needs per region over the total freshwater output per plant.

To complete the CO_2 balance, the only missing term is the avoided or displaced emissions. Estimating displaced emissions in electric generation results from the consideration that, the power produced by the desalination power plants (so, MSF plants only) of the project will be displaced from the regional grid of each country where the power plants are. In this way, the value of the avoided emissions can be obtained by multiplication of the average CO_2 emissions of the grid of each country times the power produced by all the desalination power plants of the project (in MWh). The avoided emissions will contribute positively in the CO_2 balance, in the same way as sequestration does.

Figures 56 and 57 sketch the previous descriptions for both cases:

Figure 56: Sketch of CO_{2eq} fluxes for MSF desalination power plants.

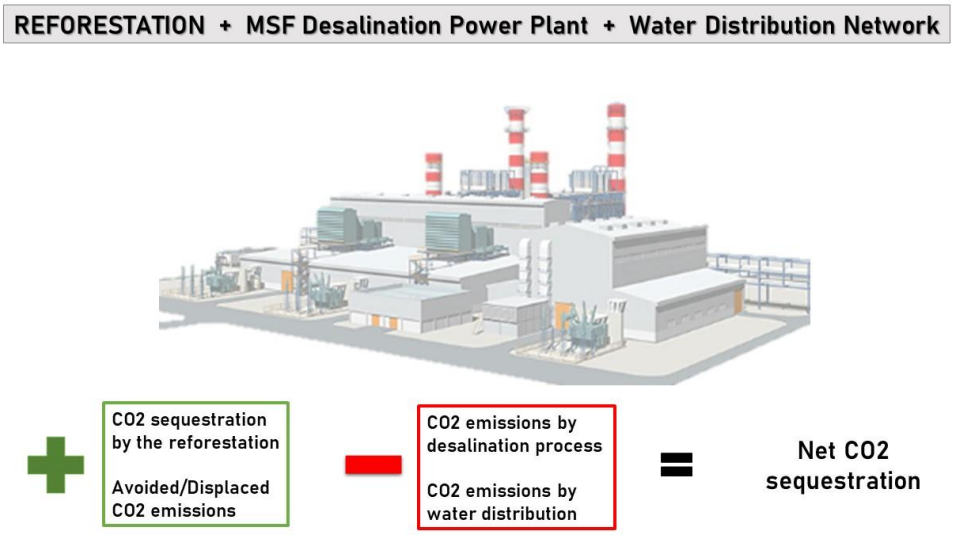

Figure 57: Sketch of CO2eq fluxes for BWRO desalination power plants.

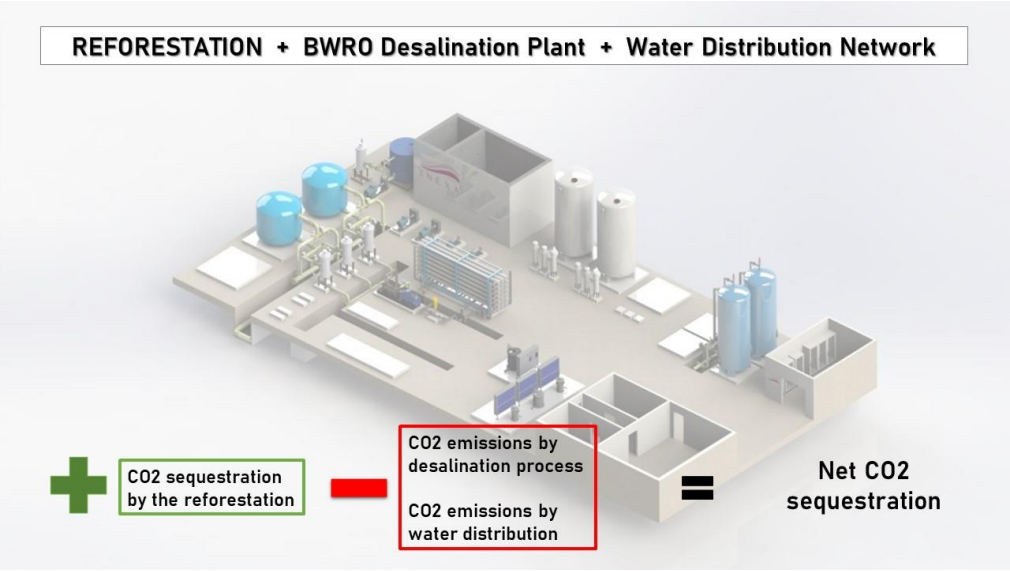

7.1.1. Eastern Desert.

Here it will be summed up the final CO_2 balance of the Eastern Desert. The general characteristics are taken and summarized from other chapters. The desalination characteristics announce that, finally, three MSF desalination power plants of 1 GW_{elec} will be needed for the irrigation of the region. Finally, the CO_2 balance for MSF desalination is done following the next expressions (Eq, 24), (Eq, 25), (Eq. 26) and (Eq. 27):

$$\text{Net } CO_2 \text{ seq.} = \text{Total } CO_2 \text{ seq. by the region} - \text{Total } CO_2 \text{ emissions for the reforestation} \quad \text{(Eq. 24)}$$

where:

$$\text{Total } CO_2 \text{ seq. by the region} = CO_2 \text{ Seq.} + \text{Avoided } CO_2 \text{ Emissions} \quad \text{(Eq. 25)}$$

$$\text{Total gross } CO_2 \text{ emissions for the reforestation} = \text{Electricity production } CO_2 \text{ Emission} + \text{Pumping } CO_2 \text{ Emissions} \quad \text{(Eq. 26)}$$

$$\frac{\text{Sequestration}}{\text{Emissions}} = \frac{\text{Total } CO_2 \text{ seq. by the region}}{\text{Total gross } CO_2 \text{ emissions for the reforestation}} \quad \text{(Eq. 27)}$$

For the Eastern Desert reforestation, the Sequestration/Emissions rate is the highest close to 8.5, while the net CO_2 sequestration by the region is around 68,5 $MtCO_{2eq}$/year.

Table 30 collects all the data described before:

Table 34: Final CO2 balance description of Eastern Desert due to the reforestation, desalination and water distribution design.

EASTERN DESERT		
General characteristics of the region		
Total reforested surface	10.000	km^2
Total watering needs	924.000.000	m^3/year
	29,30	m^3/s
CO_2 sequestration by the region	68.626.930.155	$kgCO_{2eq}$/year
	68,627	$MtCO_{2eq}$/year
Desalination characteristics		
Type of desalination plant used	MSF	-
Plant size	1	GW_{elec}
Nº of desalination plants needed	3	plants
Net electric energy produced by each plant	7.315.000.000	kW_{elech}/year
Total CO_2 emissions by desalination	9.240.000.000	$kgCO_{2eq}$/year
	9,240	$MtCO_{2eq}$/year
Displaced/avoided emissions		
Avg CO_2 emissions per kWh production (Egypt grid)	0,42127	$kgCO_{2eq}/kW_{elec}H$
Total avoided CO_2 emissions per electricity production	9.244.770.150	$kgCO_{2eq}$/year
	9,245	$MtCO_{2eq}$/year
Pumping characteristics		
Pipeline length	50	km
Number of pipes	2	pipes
Total power needed for pumping	17.533	kW_{elec}
Total CO_2 emissions by pumping	0,065	$MtCO_{2eq}$/year
CO_2 balance		
Total CO_2 sequestration by the region	77,872	$MtCO_{2eq}$/year
Total gross CO_2 emissions for the reforestation	9,305	$MtCO_{2eq}$/year
Net CO_2 sequestration	68,567	$MtCO_{2eq}$/year
Sequestration/Emission	8,4	-

7.1.2. Ténéré Desert.

Here it will be summed up the final CO_2 balance of the Ténéré Desert. The general characteristics are taken and summarized from the previous chapters. The desalination characteristics announce that three MSF desalination power plants of 1 GW_{elec} will be needed for the irrigation of the region. The avoided emissions are estimated following the same procedure as the Eastern Desert.

For the Ténéré Desert reforestation, the Sequestration/Emissions rate is around 7.5, lower than the Eastern Desert rate because here the water distribution network includes the long-distance pipe scenario, which increases the pumping energy needed, hence the pumping CO_2 emissions. Moreover, the net CO_2 sequestration by the region is around 70 $MtCO_{2eq}$/year, slightly lower than in the Eastern Desert.

Table 31 collects all the data described before:

Table 35: Final CO2 balance description of Ténéré Desert due to the reforestation, desalination and water distribution design.

TÉNÉRÉ DESERT		
General characteristics of the region		
Total reforested surface	10.000	km^2
Total watering needs	924.000.000	m^3/year
	29,30	m^3/s
CO_2 sequestration by the region	68.626.930.155	$kgCO_{2eq}$/year
	68,627	$MtCO_{2eq}$/year
Desalination characteristics		
Type of desalination plant used	MSF	-
Power needed / Plant size	1	GW_{elec}
Nº of desalination plants needed	3	plants
Net electric energy produced by each plant	7.315.000.000	$kW_{elec}h$/year
Total CO_2 emissions by desalination	9.240.000.000	$kgCO_{2eq}$/year
	9,240	$MtCO_{2eq}$/year
Displaced/avoided emissions		
Avg CO_2 emissions per kWh production (Mauritania grid)	0,5693	$kgCO_{2eq}$/ $kW_{elec}h$
Total avoided CO_2 emissions per electricity production	12.493.288.500	$kgCO_{2eq}$/year
	12,493	$MtCO_{2eq}$/year
Pumping characteristics		
Pipeline length	1000	km
Number of pipes	2	pipes
Total power needed for pumping	350.668	kW_{elec}
Total CO_2 emissions by pumping	1,749	$MtCO_{2eq}$/year
CO_2 balance		
Total CO_2 sequestration by the region	81,120	$MtCO_{2eq}$/year
Total gross CO_2 emissions for the reforestation	10,989	$MtCO_{2eq}$/year
Net CO_2 sequestration	70,131	$MtCO_{2eq}$/year
Sequestration/Emission	7,4	-

7.1.3. Sylvo-Pastorale des Six Forages Reserve.

Here it will be summed up the final CO_2 balance of the Sylvo-Pastorale des Six Forages Reserve. The general characteristics are taken and summarized from other chapters. The desalination characteristics announce that, finally, eight BWRO desalination plants of 19,2 MW_{elec} each would be needed to meet the irrigation needs of the region. It should be considered that there are not avoided emissions in the BWRO plants. Therefore, the CO_2 balance for BWRO desalination is done by following the previous equations (Eq. 24), (Eq. 26), (Eq. 27) and the new expressions for Total CO_2 sequestered by the region (Eq. 28):

$$\text{Total } CO_2 \text{ seq. by the region} = CO_2 \text{ Seq.} \quad \text{(Eq. 28)}$$

For the silvo-pastoral reserve reforestation, the Sequestration/Emissions rate is close to 6,3, while the net CO_2 sequestration by the region is around 5,4 $MtCO_{2eq}$/year.

Table 32 collects all the data described before:

Table 36: Final CO2 balance description of Sylvo-Pastorale des Six Forages Reserve due to the reforestation, desalination and water distribution design.

SYLVO-PASTORALE DES SIX FORAGES RESERVE		
General characteristics of the region		
Total reforested surface	10.000	km^2
Total watering needs	2.958.000.000	m^3/year
	93,80	m^3/s
CO_2 sequestration by the region	6.825.442.835	$kgCO_{2eq}$/year
	6,825	$MtCO_{2eq}$/year
Desalination characteristics		
Type of desalination plant used	BWRO	-
Power needed / Plant size	0,019	GW_{elec}
Nº of desalination plants needed	8	Plants
Net electric energy produced by each plant	177.480.000	$kW_{elec}h$/year
Total CO_2 emissions by desalination	4.437.000.000	$kgCO_{2eq}$/year
	4,437	$MtCO_{2eq}$/year
Electricity production		
Avg CO_2 emissions per kWh production (Mauritania grid)	0,5693	$kgCO_{2eq}$/ $kW_{elec}h$
Total CO_2 emissions per electricity production	808.314.912	$kgCO_{2eq}$/year
	0,808	$MtCO_{2eq}$/year
Pumping characteristics		
Pipeline length	50	Km
Number of pipes	5	Pipes
Total power needed for pumping	56.130	kW_{elec}
CO_2 emissions per pumping	0,280	$MtCO_{2eq}$/year
CO_2 balance		
Total CO_2 sequestration by the region	6,825	$MtCO_{2eq}$/year
Total CO_2 emissions for the reforestation	1,088	$MtCO_{2eq}$/year
Net CO_2 sequestration	5,737	$MtCO_{2eq}$/year
Sequestration/Emission	6,27	-

The reader can notice that the Net CO_2 sequestration in this region is more than ten times smaller than the other two study regions. This is because the lower CO_2 capture ability of *A. Senegal* and the higher water consumption with respect to *A. tortilis*. The whole explanation of this fact is explained below in point 7.1.4. Conclusions.

7.1.4. Conclusion.

From Tables 30, 31 and 32, the following conclusions can be extracted:

- The total CO_2 balance is positive for the three regions considered. Moreover, the ratio Sequestration/Emissions has big and acceptable values in all the areas considered.
- However, the CO_2 sequestration by the region is relatively lower in the Sahel region than in Sahara ones, as well as the net CO_2 sequestration. Moreover, even if the CO_2 sequestration in the Sahel region is the lowest, the water needs are the highest, with a huge difference from the Sahara regions. Due to that, the number of desalination plants needed is large and not convenient.
- It must be said that, in the case of Sahel region, the tree species is *A. senegal*. *A. senegal* sequestrates considerably much less kg of CO_2 per tree that *A. tortilis*. From *Chapter 4* it was known that, for *A. tortilis*:

Average CO_2 seq per tree	171,567	Kg · $tree^{-1}$
Average CO_2 seq per year	6,822	kg CO_2 $tree^{-1}$ $year^{-1}$

while for *A. senegal*:

Average CO_2 seq per tree	18,282	Kg · $tree^{-1}$
Average CO_2 seq per year	3,174	kg CO_2 $tree^{-1}$ $year^{-1}$

Moreover, *A. senegal* consumes considerably much less water per tree that *A. tortilis*. From *Chapter 4* it was known that, for *A. tortilis*:

Total water per tree	2,310	m^3 of water $tree^{-1}$ $year^{-1}$

while for *Acacia Senegal*:

Total water per tree	7,395	m^3 of water $tree^{-1}$ $year^{-1}$

- All in all, the reforestation seems suitable for the Eastern Desert and for the Ténéré Desert. However, seems not to be convenient for the Sylvo-Pastorale des Six Forages Reserve, since the net CO_2 sequestration is not worth that large number of desalination plants construction.

Chapter 8: Cost evaluation

The chapter consists of the cost's analysis of the overall project, namely to obtain the cost per ton of CO_2 sequestered of each of the scenarios studied. The procedure to calculate the overall cost will be divided into the following sections (Figure 58).

The first section refers to the reforestation costs, including the inputs and consumables, as well as labor. Through some calculations, a cost per area and time rotation is obtained and, then, an estimation of the cost per year.

The second section refers to the desalination costs and the water distribution costs. It will be developed for the 3 different scenarios: MSF plants and short-distance pipeline (in the Red Sea coast for the Eastern Desert), MSF plants and long-distance pipeline (in the Libya coast for the Ténéré Desert) and BWRO plant and short-distance pipeline (in the Senegalo-Mauritanian Basin for the Sylvo-Pastorale des Six Foreges Reserve).

Figure 58: Diagram of sequence to evaluate the overall costs of the project.

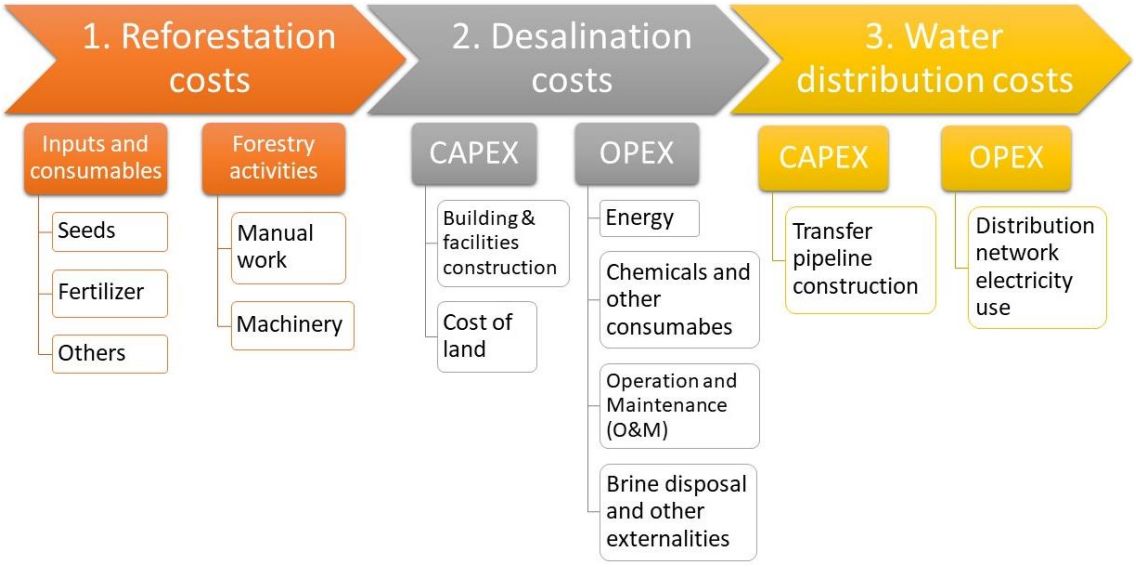

Source: Own elaboration.

It must be mentioned that, although the reforestation proposed in the Sahel region is not really convenient (as it was demonstrated in Chapter 7, because of the large number of desalination plants needed and the low net CO_2 sequestration), the costs analysis is also developed for this scenario to have a complete evaluation about the economic aspects of the membrane desalination.

8.1. Reforestation costs.

Reforestation costs can be obtained, in a general way, by considering the cost of the inputs and consumables and also the cost of forestry activities (Romero, 2016). The inputs and consumables are typically classified into:

- Seeds, fertilizers and Others.

Forestry activities normally are made manually or by means of machines. Inside the large group of activities, the following ones can be highlighted:

- Establishment activities:
  - Preparation of land (removal of vegetation or other elements).
  - Adaptation of land (plowing, subsoiling, raking, ridging, amendment, layout and drilling).
  - Establishment (production of the material, sowing, irrigation, reseeding)

  - Others.
- Maintenance activities:
  - Weed control (manual control, mechanical control and chemical control).
  - Fertilization.
  - Pruning (pruning of formation, pruning of branches).
  - Forest protection (phytosanitary control, fire control).
  - Others.

Although the cost per hectare for a forest of A. tortilis and A. senegal was not available in the literature, the costs per hectare for a forest of Acacia mangium (a similar tree species) have been reported (FAO, 2014). Table 33 shows the costs values per hectare of A. mangium forest for 5 years rotation:

Table 37: Forestry running cost breakdown per hectare.

Reforestation costs breakdown per hectare			
Type of expenditure	Measurement	Value	Unit
Inputs	Seeds & other consumables	400	euros/ha
Labor	Manual work and machinery (cleaning and adaptation of the land, planting, harvesting, etc)	800	euros/ha
Final cost	Total running costs	1200	euros/ha

Source: Own elaboration based on (FAO, 2014).

It should be mentioned that in order to estimate the costs of labor (salary per worker and per day - manual work), the average salaries of the countries of the project have been taken into consideration and have been contrasted with the values used to create the previous table.

In our case, a similar estimation of the overall forestry running costs can be obtained using the previous information, assuming similar costs for similar tree species as a first approach. Previous values need to be multiplied times the overall surface of each forest of the project and 5-year rotation. All in all, the costs per year for 10.000 km^2 of forest are shown in Table 34:

Table 38: Forestry running cost breakdown per year.

Reforestation costs breakdown per year			
Type of expenditure	Measurement	Value	Unit
Inputs	Seeds & other consumables	80.000.000	euros/year
Labor	Manual work and machinery (cleaning and adaptation of the land, planting, harvesting, etc)	160.000.000	euros/year
Final cost	Total running costs	240.000.000	euros/year

Source: Own elaboration based on (FAO, 2014)

8.2. Desalination and water distribution costs.

Based on (Papapetrou et al., 2017; Shahabi et al., 2015) to analyze desalination costs and the methodologies commonly used to calculate them.

Components and system definition diagram

First, it is necessary to present a system definition diagram of the desalination process to understand the inputs, the processes and the material flows that will be added in the costs due to desalination.

Figure 59 represents a general centralized system diagram of a desalination process:

Figure 59: General centralized system diagram of a desalination process.

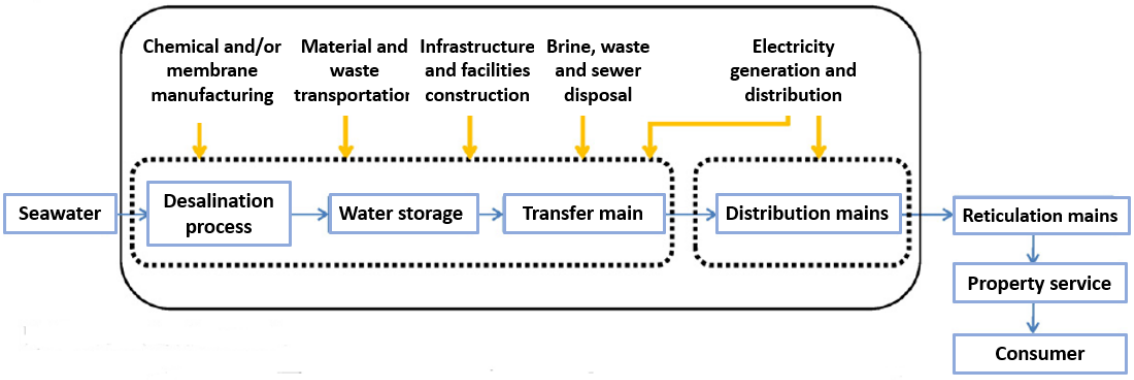

Source: (Shahabi et al., 2015)

Boundary conditions.

In the next step, the boundaries for the cost calculation must be defined in order to not underestimate the total costs. Depending on the purpose of the calculation and the specific conditions in every site, it might make sense to consider the auxiliary equipment and materials under the capital cost and their running requirements under operating costs. Items that can be either included or excluded are: water storage, desalinated water distribution, laboratory for quality control, electricity grid extension, access roads opening and desalination plant decommissioning at the end-of-life (Papapetrou et al., 2017).

For example, in one of the bibliography references checked (Shahabi et al., 2015), when comparing alternative desalination options for the water supply in terms of RO plants alternative sizes and siting options, included in the calculation the investment and running costs of the infrastructure for the water distribution to the end-users, concluding that one of the decentralised scenarios provided water that costs 18% less than in the centralised scenario. If the distribution costs were ignored, the centralised scenario would appear to cost 40% less than the selected decentralised scenario, leading to a totally different conclusion. This example reflects the importance of defining properly the boundary conditions. In this project, the cost per m^3 of freshwater will also include the water distribution network costs, making the difference between the short and long-distance scenarios. More details are given in the tables of the different scenarios below.

Calculation methodology.

Once the components and the system definition diagram are clear and the boundary conditions defined, the final step is to choose a calculation methodology. Among the existent methodologies there is the amortization factor method. This method aims to use the following equation (Eq. 29) for the simplified cost of water:

$$\text{Simplified Cost of Water} = \text{SCOW} = \frac{I_o * \alpha + C}{M_w} \qquad \text{(Eq. 29)}$$

where: I_o is the capital cost (in euros), α is the amortization factor, C is the operating cost (in euros) and M_w is the water production (in cubic meters).

Because each of the three desalination scenarios of the project are hypothetical and general designs (not real plant design and calculations), accurate calculation of the SCOW for each of them would be difficult. Due to that, the procedure to perform the SCOW for each of the three scenarios is based on the average values of I_o, α and C found in the assessed bibliography (Papapetrou et al., 2017; Shahabi et al., 2015).

In more detail, the capital costs (CAPEX, I_o) and the operating costs (OPEX, C) include the following measurements:

- Capital costs:

  - Hardware costs (equipment and material for the desalination technology, the pre-treatments and the post-treatments).
  - Engineering, construction and project management.
  - Cost of land.
  - Transfer main pipeline construction.
- Operating costs:
  - Energy (electricity and heat) for the desalination process.
  - Water distribution network electricity use.
  - Chemicals and other consumables.
  - Operation and maintenance (O&M) labors.
  - Brine disposal and other externalities.

In the following parts, a cost breakdown will be done for each of the three different scenarios.

8.2.1. Eastern Desert: MSF plant + short-distance pipeline.

Table 35 presents the desalination cost breakdown for the Eastern Desert. In this specific scenario, some comments are necessary to understand the final values of the MSF desalination plant costs and the short distance pipeline.

In the case of the MSF desalination plant costs, the measurements are being divided into CAPEX and OPEX as explained before. The reported values of the cost per m^3 of freshwater with MSF technology (only process, not water distribution) are normally ranged between 0.56-1.75 $/m^3$ (Wakil et al., 2017) (which is approximately 0.52-1.61 euros/m^3). The average chosen for the project is 1.07 euros/m^3.

Regarding the water distribution network, in the case of the short-distance pipeline, a similar procedure has been followed as the described in the bibliography (Shahabi et al., 2015), where there is a study of a centralised scenario with single SWRO desalination plant (320.000 m^3/day capacity) and 75 km of trunk of pipeline for the water distribution network. Also the percentages are been designed thanks to the same mentioned paper. The result is that around a 38% of the total cost per m^3 of freshwater comes from its distribution. Then, the final levelized cost for the Eastern Desert scenario is 1,71 euros/m^3.

Table 39: Levelized cost breakdown for functional m3 of desalinated water by an MSF plant (with short distance pipeline).

Levelized cost breakdown for functional m^3 of desalinated water by an MSF plant (with short distance pipeline)			
Desalination process costs			
Type of expenditure	Measurement	%	euros/m^3
Capex	Building and facilities construction (equipment & material, engineering, construction & project management)	33	0,564
	Cost of land	2	0,034
Opex	Energy	20	0,342
	Chemicals & other consumables	2,5	0,043
	O&M (fixed costs)	2,5	0,043
	O&M (variable costs)	1,5	0,026
	Brine disposal & other externalities (brine, waste &sewer disposal, waste transport)	1	0,017
Water distribution network costs (short distance pipeline)			
Type of expenditure	Measurement	%	euros/m^3
Capex	Transfer main pipeline construction	37	0,633
Opex	Distribution network electricity use	0,5	0,009
Total costs			
Type of expenditure	Measurement	%	euros/m^3
Capex (total)	Levelized Capital Cost (LCC)	72	1,231
Opex (total)	Levelized Operational Cost (LOC)	28	0,479
Final cost	Levelized Cost (LC = LCC + LOC)	100	1,71

8.2.2. Ténéré Desert: MSF plant + long-distance pipeline.

Table 36 presents the desalination cost breakdown for the Ténéré Desert. The same procedure as the previous scenario has been used to estimate the desalination process costs. However, in this case there is the need of a long-distance pipeline. Since the detailed cost breakdown of a long-distance pipeline scenario is beyond the scope of the project, as a first approach, the cost estimation of the water distribution network has been considered 20 times bigger than the short-distance pipeline because the length is also 20 times bigger. With all, a more expensive levelized cost is obtained for the Ténéré Desert scenario of 13,789 euros/m^3.

Table 40: Levelized cost breakdown for functional m3 of desalinated water by an MSF plant (with long distance pipeline).

Levelized cost breakdown for functional m^3 of desalinated water by an MSF plant (with long distance pipeline)		
Desalination process costs		
Type of expenditure	Measurement	euros/m^3
Capex	Building and facilities construction (equipment & material, engineering, construction & project management)	0,564
	Cost of land	0,034
Opex	Energy	0,342
	Chemicals & other consumables	0,043
	O&M (fixed costs)	0,043
	O&M (variable costs)	0,026
	Brine disposal & other externalities (brine, waste &sewer disposal, waste transport)	0,017
Water distribution network costs (long distance pipeline)		
Type of expenditure	Measurement	euros/m^3
Capex	Transfer main pipeline construction	12,654
Opex	Distribution network electricity use	0,066
Total costs		
Type of expenditure	Measurement	euros/m^3
Capex (total)	Levelized Capital Cost (LCC)	13,253
Opex (total)	Levelized Operational Cost (LOC)	0,536
Final cost	Levelized Cost (LC = LCC + LOC)	13,789

8.2.3. Sylvo-Pastorale des Six Forages Reserve: BWRO + short-distance pipeline.

Finally, Table 37 refers to the levelized cost breakdown of a BWRO with short-distance pipeline scenario. Here some of the reported values for the RO desalination process range between 0.26-0.54 \$/m^3 (Wakil et al., 2017) (which is approximately 0.24-0.50 euros/m^3). The average chosen for the project is 0.55 euros/m^3. Comparing this case with the first one (Eastern Desert scenario), the same cost is produced for the water distribution network, since there is also a short-distance pipeline. However, there are some basic cost division differences in the desalination process costs with respect to the MSF technology. In the end, the MSF and RO desalination plant investment cost are similar. This is because, in the chemicals and other consumables consumption is higher for RO plants than for MSF. However, it is compensated with the energy consumption, which is higher for the MSF. The percentages of the table are based on the previous arguments. At last, levelized cost obtained for the Sylvo-Pastorale des Six Forages Reserve scenario is 1,19 euros/m^3.

Table 41: Levelized cost breakdown for functional m3 of desalinated water by an BWRO plant (with short distance pipeline).

Levelized cost breakdown for functional m^3 of desalinated water by a BWRO plant (with short distance pipeline)			
Desalination process costs			
Type of expenditure	Measurement	%	euros/m^3
Capex	Building and facilities construction (equipment & material, engineering, construction & project management)	23	0,2737
	Cost of land	2	0,0238
Opex	Energy	10	0,119
	Chemicals & other consumables	6	0,0714
	O&M (fixed costs)	2	0,0238
	O&M (variable costs)	2	0,0238
	Brine disposal & other externalities (brine, waste &sewer disposal, waste transport)	1	0,0119
Water distribution network costs (short distance pipeline)			
Type of expenditure	Measurement	%	euros/m^3
Capex	Transfer main pipeline construction	53	0,6307
Opex	Distribution network electricity use	1	0,0119
Total costs			
Type of expenditure	Measurement	%	euros/m^3
Capex (total)	Levelized Capital Cost (LCC)	85	1,0115
Opex (total)	Levelized Operational Cost (LOC)	15	0,1785
Final cost	Levelized Cost (LC = LCC + LOC)	100	1,19

8.2.4. Desalination market references: the Mediterranean case.

In order to give magnitude perspective of the desalination costs, it is possible to check the average prices of the desalination market of the Mediterranean and compare it with the cost of the study scenarios. Must be highlighted that the following prices include the desalination process only, while the previous study scenarios cost analysis also includes the cost of the water distribution network.

The assessed reference (Cosín, 2018) shows the development of the cost of freshwater by desalination of countries in the Mediterranean Sea like Cyprus, Spain, Israel, Argelia, Tunisia, Egypt and Morocco. For example:

- In Cyprus, the most famous desalination projects are Larnaca with a rate in 2001 of 0,74 US$/$m^3$ and Limassol in 2012 with 0,87 US$/$m^3$, reaching the lowest price in the country in October 2018, when the Paphos desalination plant of 20.000 m^3/day was awarded to local contractor Caramondani for 0,51 US$/$m^3$.
- In Israel, the current reference projects both for their size and technological advances are Askhelon (396.000 m^3/day) at a rate of 0,52 US$/$m^3$; Hadera (525.000 m^3/day) at 0,58 US$/$m^3$ and Sorek (624.000 m^3/day) at 0,58 US$/$m^3$. The reality is that they were disruptive tariffs, but today it is known that they were conditional on inflated parameters and that, updated as of today, they represent tariffs of around 0,95 – 0,89 – 0,7 US$/$m^3$ respectively.
- In Argelia, the first plants were Hamma (200.000 m^3/day) with a rate of 0,78 US$/$m^3$ and Skikda (100.000 m^3/day) with a rate of 0,739 US$/$m^3$. Later, Beni Saf (200.000 m^3/day) reached 0,78 US$/$m^3$ and Honaine (200.000 m^3/day) reached 0,69 US$/$m^3$; to finish with Magtaa (500.000 m^3/day) and Ténès (200.000 m^3/day), which were contracted with practically the same costs of debt and energy below 0,57 US$/$m^3$.

After comparing the prices of different countries in the Mediterranean Sea, it is possible to verify the cost of functional 1 m^3 of freshwater for each of the three study scenarios.

8.2.5. Investment cost of a desalination plant: the Eastern Desert case.

Some assumptions are made in order to estimate the investment cost of an MSF desalination plant of the Eastern Desert study case, since this case seems by far the most suitable scenario. Again, the reader should notice that it is a preliminary estimation, so the calculations are made only using the data provided before in Table 35. For a complete and rigorous investment cost calculation, an economic analysis should be performed using economic parameters such as inflation rates, return on Debt and Equity, Tax Discount, etc for the projected Book Life of the desalination plant.

First of all, in order to estimate capital cost, CAPEX from the previous Table 35 is considered:

Total CAPEX = Desalination plant CAPEX (0,564 euros/m^3) + Water distribution pipeline CAPEX (0,633 euros/m^3) = 1,197 euros/m^3.

For 308.000.000 m3/year of freshwater production, it results in around 369.000.000 euros/year.

Assuming that the ratio between Levelized Carrying Charge and Investment is 0,14, which is a reasonable number for the mix of average-life desalination plant and long-life pipeline (National Renewable Energy Laboratory, 2020), investment cost for 1 plant and its pipeline turns out to be:

(369 M€/year)/(0,14/year) = 2636 M€ = 2,6 billion Euro.

Finally, the cost attributable to the desalination plant will be:

2,6 billion Euro * (0,564/1,197) = 1,225 billion Euro for a 1 GW plant (which is about 1000 €/kW).

8.3. Total cost per kilogram of CO_2 sequestered.

The final part of the chapter is dedicated to sum up all the costs described before: forestry running cost, desalination costs and water distribution network to obtain the final cost per ton of CO_2 sequestered (Tables 38, 39 and 40). As it was predictable, the most economic ton of CO_2 sequestered is for the case of Eastern Desert (10.000 km^2 of reforestation, 3 MSF plants and short-distance pipeline), then is followed by the Ténéré Desert (10.000 km^2 of reforestation, 3 MSF plants and long-distance pipeline) which has a price 20 times higher because of the long-distance pipeline costs. Finally, the Sylvo-Pastoral des Six Forages Reserve (10.000 km^2 of reforestation, 8 BWRO desalination plants and short-distance pipeline) which has been added in order to complete the information about the RO general desalination costs, but has a huge price for ton of CO_2 sequestered because of its huge number of desalination plants needed, as well as the low ability of the reforestation to capture CO_2.

8.3.1. Eastern Desert.

Table 42: Total cost per kilogram of CO2 sequestered: Eastern Desert reforestation + MSF desalination plants.

Eastern Desert reforestation + MSF desalination plants		
Measurement	Value	Unit
Freshwater production	924.000.000	m^3/year
Cost for functional 1 m^3 of desalinated water	1,71	euros/m^3
Total water production costs	1.580.040.000	euros/year
Total forestry running costs	240.000.000	euros/year
Net CO_2 sequestration	68,567	$MtCO_{2eq}$/year
Final cost per ton of CO_2 sequestered	**26,544**	**euros/tCO_{2eq}**

8.3.2. Ténéré Desert.

Table 43: Total cost per kilogram of CO2 sequestered: Ténéré Desert reforestation + MSF desalination plants.

Ténéré Desert reforestation + MSF desalination plants		
Measurement	Value	Unit
Freshwater production	924.000.000	m^3/year
Cost for functional 1 m^3 of desalinated water	13,789	euros/m^3
Total water production costs	12.740.805.000	euros/year
Total forestry running costs	240.000.000	euros/year
Net CO_2 sequestration	70,131	$MtCO_{2eq}$/year
Final cost per ton of CO_2 sequestered	**185,093**	**euros/tCO_{2eq}**

8.3.3. Sylvo-Pastorale des Six Forages Reserve.

Table 44: Total cost per kilogram of CO2 sequestered: Silvo-pastoral Reserve reforestation + BWRO desalination plants.

Silvo-pastoral reserve reforestation + BWRO desalination plants		
Measurement	Value	Unit
Freshwater production	2.958.000.000	m^3/year
Cost for functional 1 m^3 of desalinated water	1,19	euros/m^3
Total water production costs	3.520.020.000	euros/year
Total forestry running costs	240.000.000	euros/year
Net CO_2 sequestration	5,737	$MtCO_{2eq}$/year
Final cost per ton of CO_2 sequestered	**655,375**	**euros/tCO_{2eq}**

Conclusion

The goal of this project has been, since the beginning, to understand whether a reforestation in Sahara Desert has any chance of success, meaning if the final net CO_2 sequestration balance results in positive or negative values. For that, three different areas have been selected and studied. Reforestation and the necessary infrastructures deriving from it have been designed and calculated for each of the three regions. The main conclusion of this project is that there are some regions where reforestation is feasible and economically competitive.

The reforestation approach of this project consists of the monoculture of two endemic acacia species: *Acacia Tortilis* in the Eastern Desert (Egypt) and the Ténére Desert (Niger) and *Acacia Senegal* in the Sylvo-Pastorale des Six Forages Reserve (Sahel region, in the border between Mauritania and Senegal). These specific regions have been selected because they represent three totally different ecosystems: desert coastal, desert interior and cropland currently suffering deforestation due to climate change. On the other hand, the estimation of the carbon capture ability by the tree communities is based on the use of allometric equations, reported in several scientific papers. The allometric equations calculate the growth ratio and the biomass of the selected tree species with input parameters such as: trunk height (H), diameter at breast height (DBH) and wood density (ρ). Thanks to them is easy to obtain the carbon content of the trees, and so, the CO_2 sequestration. It should be mentioned that several other ways can be used to simulate a reforestation scenario: mixed species communities instead of monoculture, software to calculate biomass instead of specific allometric equations or equations relating growth rate-water availability instead of H-DHB-ρ. Because of that, the scope of the project is only to create an example of a possible simulation.

The hydrological resources' analysis made of the Sahara Desert shows that most of the surface water bodies are protected (Ramsar sites) and most of the underground water bodies, like basins, are overstressed. The need to desalinate water for irrigation has been demonstrated. Due to that, the state-of-art of the commercial desalination processes has been studied, concluding that nowadays Multistage Flash (MSF) and Reverse Osmosis (RO) desalination are the most used between the thermally driven and membrane separation technologies, respectively. RO has greater advantages over MSF, such as reduced energy consumption and, therefore, reduced GHG emissions and reduced costs (Wakil et al., 2017). However, MSF desalination is still needed for high salinity and/or high total dissolved solids (TDS) intake waters (Saeed et al., 2019; Wali, 2014). As a result, this project assess the use of Brackish Water RO (BWRO) desalination for the plants along the Sahel region that are fed with groundwater and MSF desalination for the plants along the coast, specifically Red Sea coast, because of its high salinity and TDS (well above average).

Nevertheless, conventional desalination technologies are not efficient enough solutions for sustainable future water supplies, as they are operating at lower efficiency then their thermodynamic limit. Research is being carried out on membranes to increase flux, selectivity, fouling resistance and stability with minimum cost and manufacturing defects and also on improved processes (hybridization) of thermally driven technologies for high efficiency (Wakil et al., 2017). Moreover, the future trends indicate the integration of desalination technologies with renewable energy sources (RES), which leads to a progressive decrease in the CO_2 emissions. However, desalination processes are best suited to continuous operation, whereas the principal RES, such as wind and solar, are non-continuous. Thus, the matching requires special design and operation which increases complexity and cost. At present, technological and economic constraints difficult large-scale applications (Bundschuh et al., 2017).

A final project evaluation has been done, where the following data and conclusions can be considered:

- Total surface where the reforestation has been simulated: 10.000 km^2 in the Eastern Desert (Egypt), 10.000 km^2 in the Ténéré Desert (Niger) and 10.000 km^2 in the Sylvo-Pastorale des Six Forages Reserve (Mauritania-Senegal).
- Best practices for sand dunes planting techniques assess 5x5m spacing blocks. So, the total number of trees that can be grown per region are 400.000.000. In other words, the trees density for the three regions is around 40.000 trees/km^2.
- Estimated CO_2 sequestration per tree species is: 6,822 $kgCO_{2eq}$/year for *A. tortilis* and 3,174 $kgCO_{2eq}$/year for *A. senegal*. The sequestration per tree is more than double for *A.tTortilis* than *A.*

senegal, which makes it more suitable for a reforestation. With all, the total CO_2 sequestration by region is: 68,627 $MtCO_{2eq}$/year in Eastern Desert and Ténéré Desert, then, 6,825 $MtCO_{2eq}$/year in the Sylvo-Pastorale des Six Forages Reserve.

- Estimated water needs are 2,31 m^3 of water/year for *A. Tortilis* and 7,395 m^3 of water/year for a *A. Senegal*. The water needs are more than double for *A. Senegal* than *A. Tortilis*, which again demonstrates the suitability of *A. Tortilis* for the reforestation. Total water needs for irrigation per area are: 924.000.000 m^3/year in Eastern Desert and the same amount for Ténéré Desert, then, 2.958.000.000 m^3/year in the Sylvo-Pastorale des Six Forages Reserve.
- According to the reviewed state-of-art in Chapter 5 of the specific energy consumption values for MSF and RO desalination, RO technology is the most suitable for desalination, due to its reduced energy consumption. However, MSF desalination will be needed for high salinity and/or high total dissolved solids (TDS) seawaters of the project, while underground waters will be treated with BWRO plants.
- Considering medium-large size desalination plants for the project, such as 1 GW_{elec} of power for MSF plants and around 20 MW_{elec} for the BWRO plants, the number of plants needed is: 3 MSF plants in Easter Desert (Red Sea Coast), 3 MSF plants for Ténéré Desert (located along the Libya Coast) and 8 BWRO plants for the Sylvo-Pastorale des Six Forages Reserve. It is easy to understand that Eastern Desert and Ténéré Desert reforestations are convenient, while the Sylvo-Pastorale des Six Forages Reserve reforestation is not, because of the large number of desalination plants needed.
- Regarding the CO_2 equivalent emissions, there will be two main sources causing them: the electricity production for the desalination energy needs and the pumping of the water distribution networks. Total CO_2 equivalent emissions by electricity production are: 9,24 $MtCO_{2eq}$/year in Easter Desert and in Ténéré Desert, then, 4,437 $MtCO_{2eq}$/year in the Sylvo-Pastorale des Six Forages Reserve. On the other hand, through the average CO_2 equivalent emissions per kWh produced in each of the countries, it is possible to obtain the total CO_2 equivalent emissions by pumping. They are: 0,065 $MtCO_{2eq}$/year in Easter Desert, 1,749 $MtCO_{2eq}$/year in Ténéré Desert and 0,280 $MtCO_{2eq}$/year in the Sylvo-Pastorale des Six Forages Reserve.
- The overall CO_2 balance is composed by subtracting CO_2 emissions (desalination and pumping) to CO_2 sequestrations (reforestation and avoided/displaced emissions), giving a final number of 'Net CO_2 sequestration'. Moreover, the sequestration/emissions (S/E) ratio has been performed for each region, being equal to: 8.4 for Eastern Desert, 7,4 for Ténéré Desert and 6,27 for the Sylvo-Pastorale des Six Forages Reserve. While the Net CO_2 sequestration is: 68,567 $MtCO_{2eq}$/year in Easter Desert, 70,131 $MtCO_{2eq}$/year in Ténéré Desert and 5,737 $MtCO_{2eq}$/year in the Sylvo-Pastorale des Six Forages Reserve. Again, the reforestation seems suitable for the Eastern Desert and for the Ténéré Desert, but not for the Reserve. In this case, while the S/E ratio is higher, the Net CO_2 sequestration is markedly less than the other two and does not give enough worth to that large number of desalination plants construction.
- Finally, the cost evaluation includes forestry running costs, desalination plants and operation costs and water distribution networks (short and long-distance pipeline scenarios). Total cost per kilogram of CO_2 sequestered for each study scenario is: 26,544 euros/tCO_{2eq} for Eastern Desert, 185,093 euros/tCO_{2eq} for Ténéré Desert and 655,375 euros/tCO_{2eq} for the Sylvo-Pastorale des Six Forages Reserve. The difference between the costs of Eastern and Ténéré Desert is due to the water distribution network: the first one needs short-distance pipeline (around 50 km long) while the second one needs long-distance pipeline (around 1000 km long), which it increases highly the costs.

It has been demonstrated that the most suitable scenario is the one proposed for the Eastern Desert, which includes 10.000 km^2 of *A. tortilis* reforestation, 3 MSF desalination plants along the Red Sea Coast and a water distribution network with short-distance pipeline. This project shows that there are favorable locations where reforestation is feasible.

To understand if reforestation can be also economically competitive, it needs to be compared with other current technologies. The state-of-art of the CO_2 Capture and Storage (CCS) (Dadhich et al., 2005) shows that the major cost components of these technologies include capture (separation plus compression), transport, and storage (including measurement, monitoring and verification).

Cost of capturing CO_2 is the largest component of overall CCS costs. Capture costs include the cost of compressing the CO_2 to a pressure suitable for pipeline transport (typically about 14 MPa). For this reason, the reported costs of CO_2 capture vary widely, even for similar applications. The CO_2 capture costs reported in the literature for baseload operations of new fossil fuel power plants (in the size range of 300–800 MW) employing current commercial technology is: between 33-57 US$/t$CO_2$ captured for new Natural Gas Combined Cycle (NGCC) plants, 23-35 US$/t$CO_2$ captured for new Pulverized Coal (PC) plants, 11-32 US$/t$CO_2$ captured for new Integrated Gasification Combined Cycle (IGCC) plants and 2-39 US$/t$CO_2$ captured for new Hydrogen plants. (See the full Performance and Cost Measures for all the previous technologies in the *Annex C. Cost of CCS technologies.*)

Regarding transport costs, the most common and usually most economical method to transport large amounts of CO_2 is through pipelines. While a cost competitive transport option for longer distances at sea might be the use of large tankers. The *Annex C. Cost of CCS technologies* includes a figure that shows the CO_2 transport costs range for onshore and offshore pipelines per 250 km, 'normal' terrain conditions. Note that economies of scale may dramatically reduce the cost, but that transportation in mountainous or densely populated areas could increase cost.

At last, storage costs estimates widely range for individual options. Representative estimates of the cost for storage in saline formations and disused oil and gas fields (geological storage) are typically between 0.5–8.0 US$/t$CO_2$ stored (see the related table in the *Annex C. Cost of CCS technologies*). Also ocean storage and storage via mineral carbonation are possible. In addition, monitoring is estimated to add 0.1–0.3 US$/t$CO_2$ stored.

Finally, it has been demonstrated by all the research and work developed in this project that reforestation is economically competitive with other CCS technologies, since the final cost per ton of CO_2 captured in the Eastern Desert is comprised between the ranged costs of other CCS technologies, so **reforestation is economically competitive and it is a potential CO_2 capture method for some favorable locations**.

Perspective

The hey take-home messages of this project are:

- The project demonstrates that reforestation should be considered as a future potential tool for CO_2 capturing because of its feasibility and because it is economically competitive.
- Here, the reforestation has been simulated in specific areas of Sahara Desert, where there are several constrictions (such as severe climate conditions and water scarcity), however, it is easy to understand that the same process can be replicated in other different regions and ecosystems in a relatively easy way.
- Reforestation in the next decades may have a strong potential to mitigate climate change and meet the requirements of the current climate policies.

Finally, some future work and research can be derived from the project:

- It would be interesting to investigate how to expand the reforestation both in Sahara Desert and in other types of ecosystems, by studying the favorability and the feasibility of other large areas of the Sahara and around the world.
- New results could be obtained if other ways are used to simulate a reforestation scenario such as considering mixed species communities instead of monoculture
- Also, new results can be derived by using software to calculate forest biomass instead of specific allometric equations or equations relating growth rate-water availability instead of H-DHB-ρ.
- Geographic Information Systems (GIS) Software encompasses a broad range of applications which involve the use of a combination of digital maps and georeferenced data. It can be used to create more accurate descriptions about several environmental factors involved in this project, such as: hydrological resources, land cover and uses, soil types, solar radiation, air and soil humidity, precipitations, temperatures and biomass.

Annexes

A. Global Land Cover by country.

A.1. Algeria.

Total surface: 2.312.167 km^2.

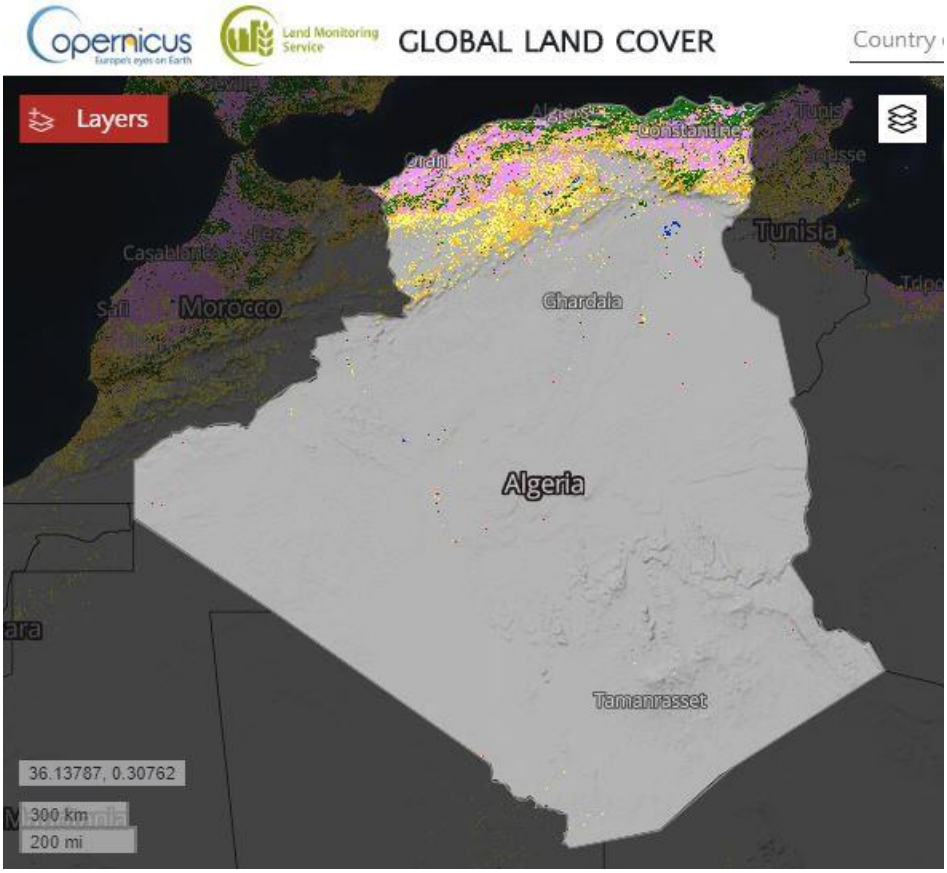

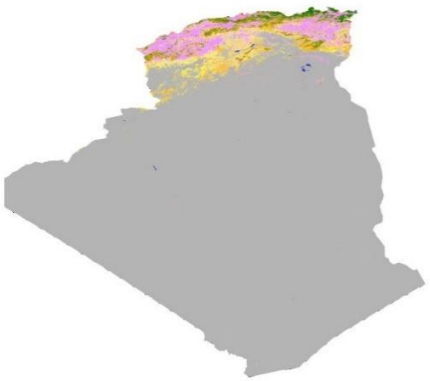

	LAND COVER TYPE	SURFACE (km^2)	%
	Forest	36.301,10	1,57
	Shrubland	45.780,91	1,98
	Herbaceous vegetation	47.168,21	2,04
	Herbaceous wetland	0,00	0,00
	Bare / sparse vegetation	2.109.158,74	91,22
	Cropland	68.902,58	2,98
	Built-up	3.005,82	0,13
	Permanent water bodies	1.387,30	0,06

A.2. Chad.

Total surface: 1.269.214 km^2.

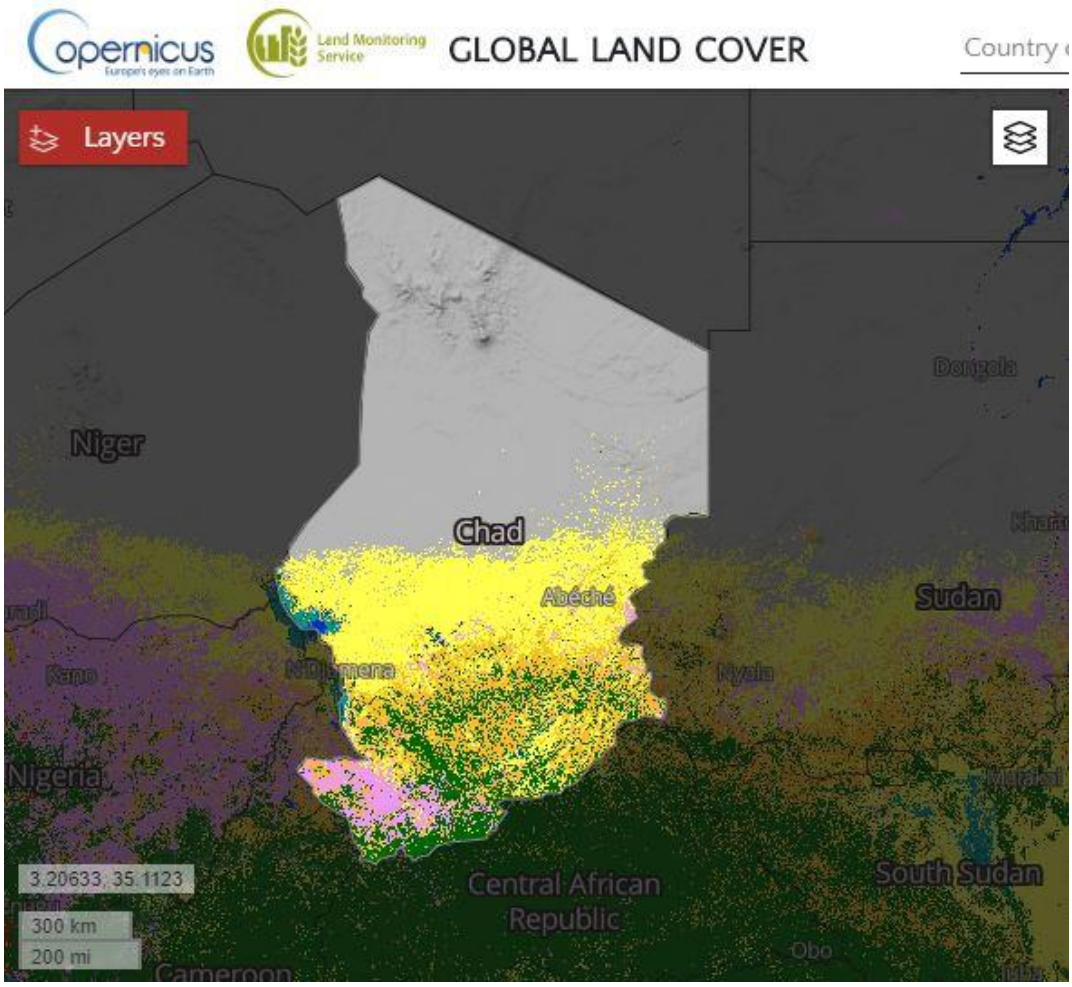

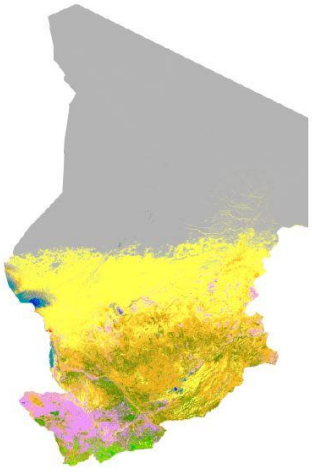

	LAND COVER TYPE	SURFACE (km^2)	%
	Forest	119.179,19	9,39
	Shrubland	147.863,43	11,65
	Herbaceous vegetation	267.169,55	21,05
	Herbaceous wetland	8.122,97	0,64
	Bare / sparse vegetation	675.221,85	53,20
	Cropland	49.499,35	3,90
	Built-up	380,76	0,03
	Permanent water bodies	1.523,60	0,12

A.3. Egypt.
Total surface: 984.275 km^2.

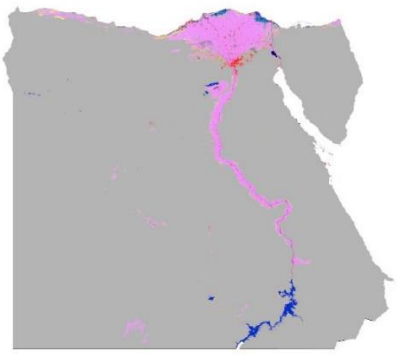

	LAND COVER TYPE	SURFACE (km^2)	%
	Forest	3.051,25	0,31
	Shrubland	1.968,55	0,20
	Herbaceous vegetation	2.755,97	0,28
	Herbaceous wetland	885,85	0,09
	Bare / sparse vegetation	925.612,21	94,04
	Cropland	39.075,72	3,97
	Built-up	4.133,96	0,42
	Permanent water bodies	6.299,36	0,64

A.4. Eritrea.
Total surface: 121.191 km^2.

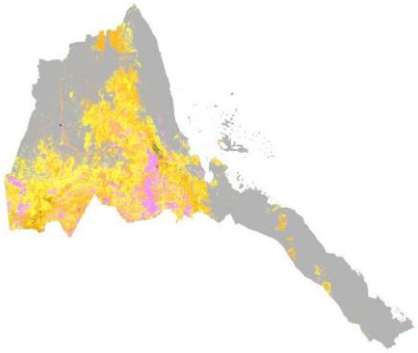

	LAND COVER TYPE	SURFACE (km^2)	%
	Forest	811,98	0,67
	Shrubland	25.244,9	20,83
	Herbaceous vegetation	21.935,57	18,1
	Herbaceous wetland	12,12	0,01
	Bare / sparse vegetation	65.697,64	54,21
	Cropland	7.319,94	6,04
	Built-up	60,60	0,05
	Permanent water bodies	48,48	0,04

A.5. Libya.
Total surface: 1.623.525 km^2.

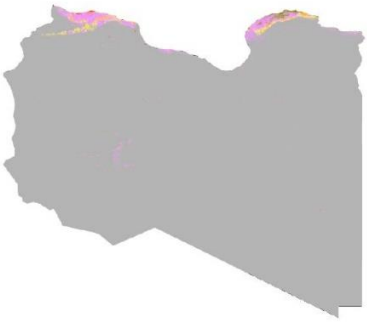

	LAND COVER TYPE	SURFACE (km^2)	%
	Forest	2.272,94	0,14
	Shrubland	4.221,17	0,26
	Herbaceous vegetation	5.682,34	0,35
	Herbaceous wetland	0,00	0,00
	Bare / sparse vegetation	1.589.918,30	97,93
	Cropland	20.131,71	1,24
	Built-up	974,12	0,06
	Permanent water bodies	162,35	0,01

A.6. Mali.
Total surface: 1.255.508 km^2.

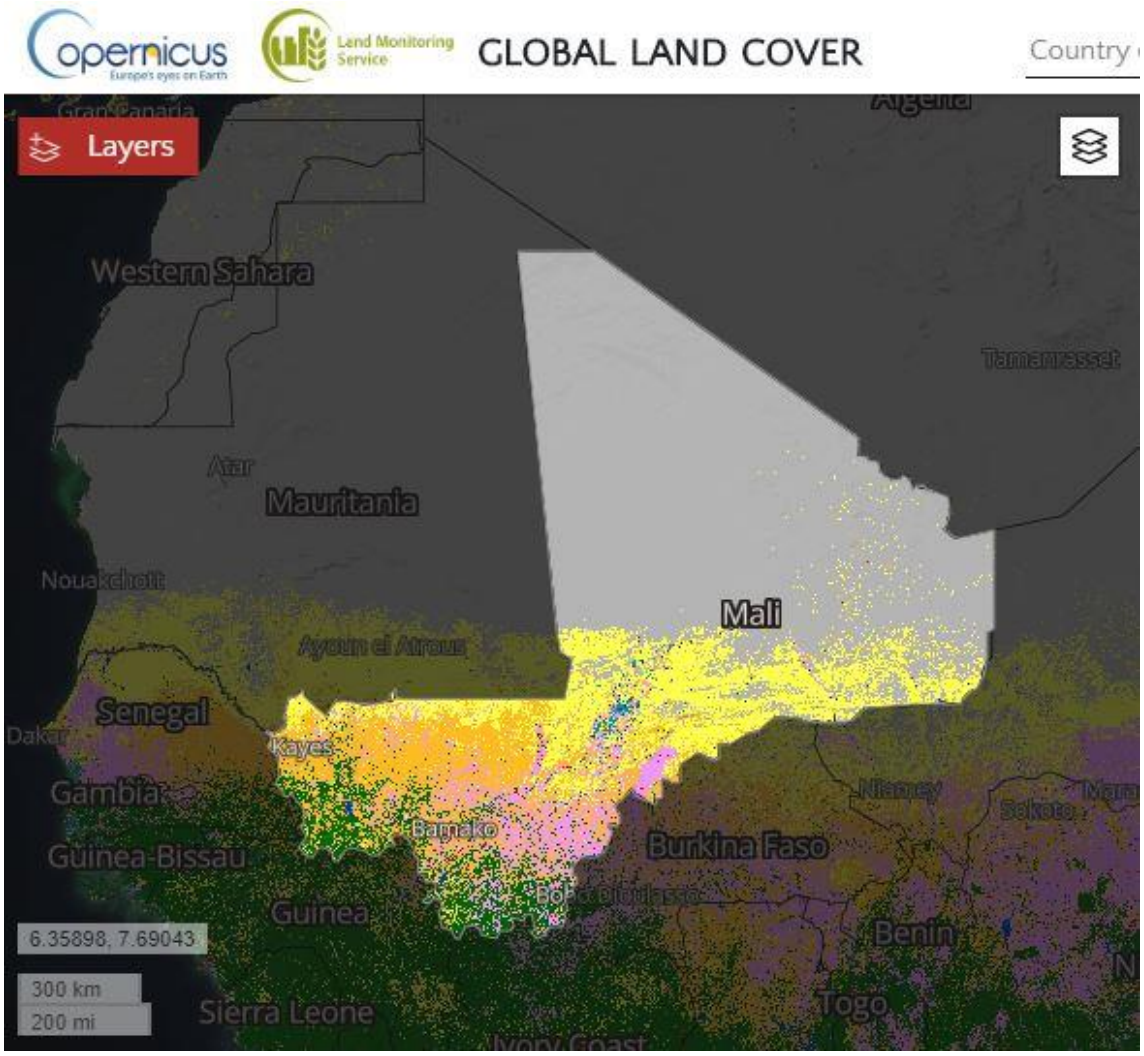

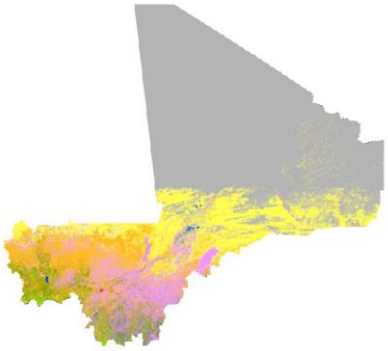

	LAND COVER TYPE	SURFACE (km^2)	%
	Forest	76.083,78	6,06
	Shrubland	170.874,64	13,61
	Herbaceous vegetation	192.846,64	15,36
	Herbaceous wetland	5.022,30	0,40
	Bare / sparse vegetation	723.298,16	57,61
	Cropland	83.993,49	6,69
	Built-up	2.134,36	0,17
	Permanent water bodies	1.381,60	0,11

A.7. Mauritania.
Total surface: 1.041.500 km^2.

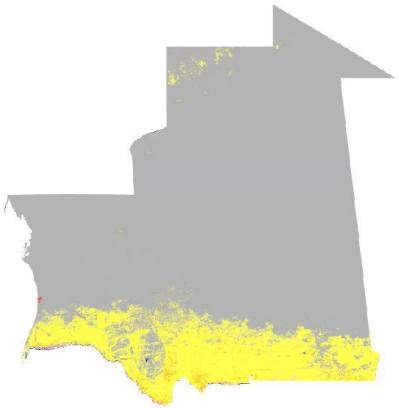

	LAND COVER TYPE	SURFACE (km^2)	%
	Forest	833,20	0,08
	Shrubland	9.373,50	0,90
	Herbaceous vegetation	168.723,00	16,20
	Herbaceous wetland	520,75	0,05
	Bare / sparse vegetation	859.341,65	82,51
	Cropland	2.187,15	0,21
	Built-up	208,30	0,02
	Permanent water bodies	104,15	0,01

A.8. Morocco.
Total surface: 414.346 km^2.

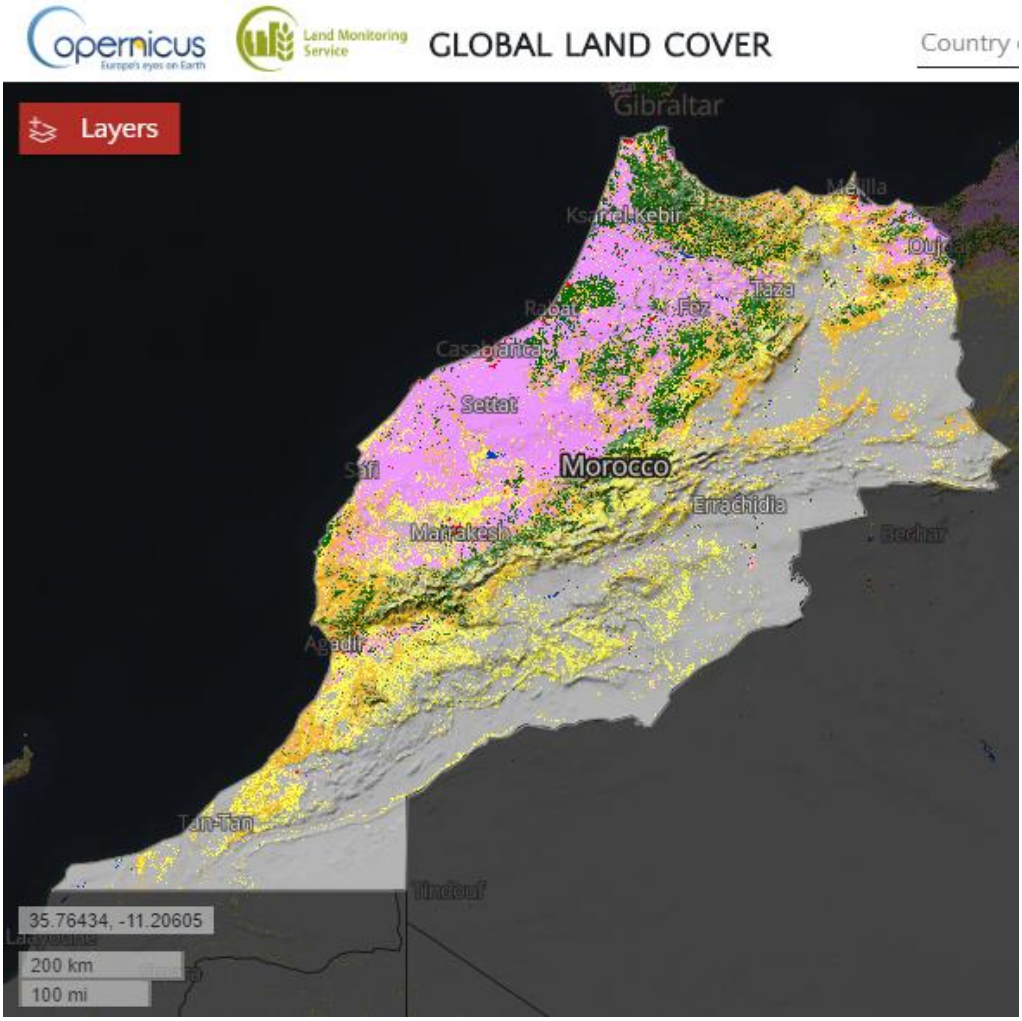

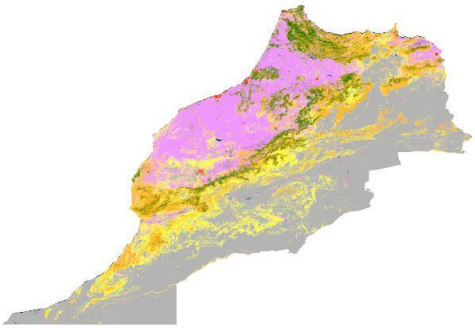

	LAND COVER TYPE	SURFACE (km^2)	%
	Forest	36.089,54	8,71
	Shrubland	59.672,58	13,75
	Herbaceous vegetation	59.168,61	14,28
	Herbaceous wetland	41,43	0,01
	Bare / sparse vegetation	185.585,57	44,79
	Cropland	74.250,80	17,92
	Built-up	1.574,51	0,38
	Permanent water bodies	621,52	0,15

A.9. Niger.
Total surface: 1.186.423 km^2.

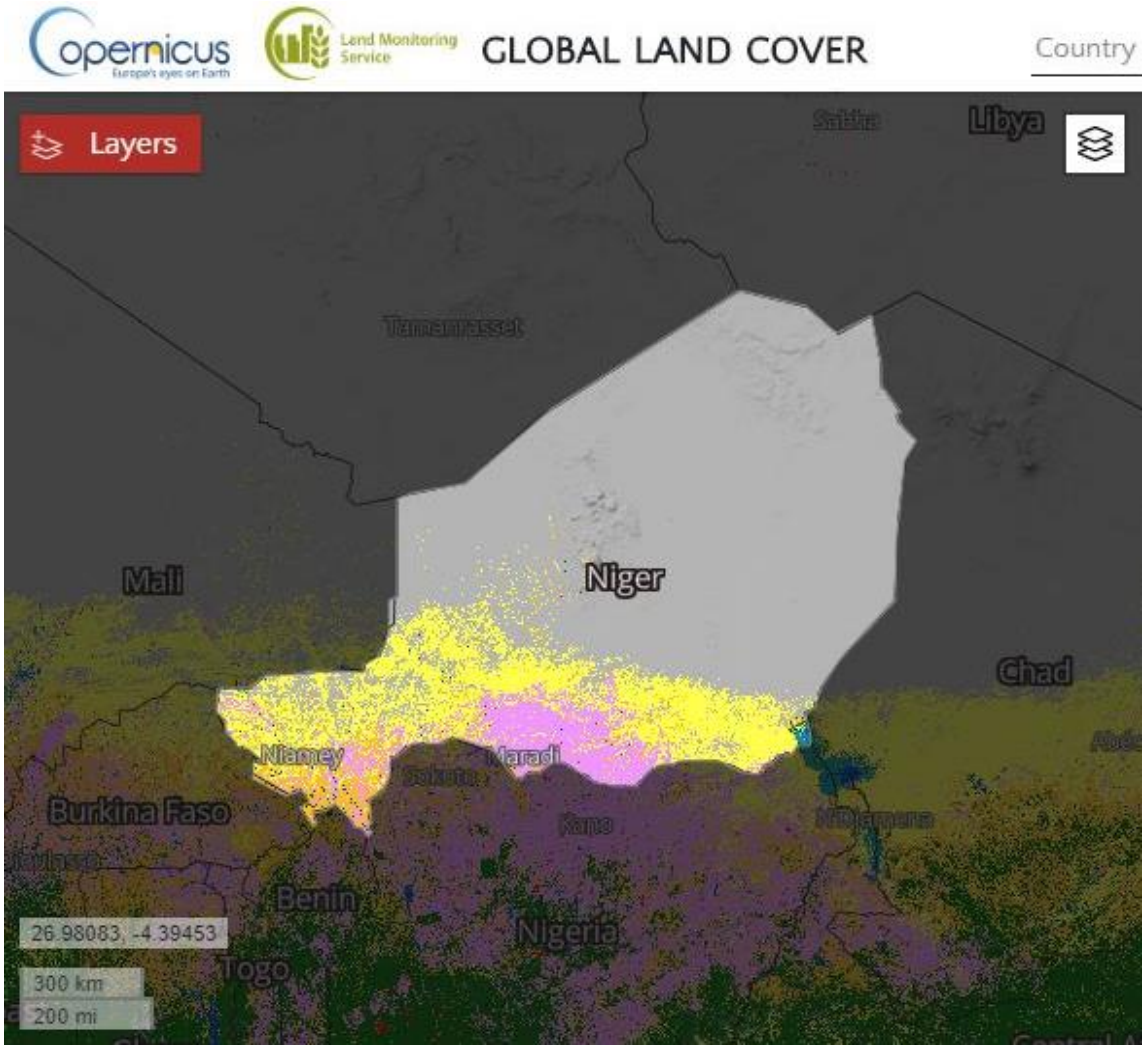

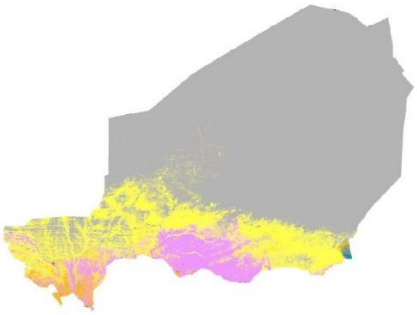

	LAND COVER TYPE	SURFACE (km^2)	%
	Forest	2.372,85	0,20
	Shrubland	32.745,27	2,76
	Herbaceous vegetation	200.742,77	16,92
	Herbaceous wetland	1.423,71	0,12
	Bare / sparse vegetation	860.275,32	72,51
	Cropland	88.151,23	7,43
	Built-up	355,93	0,03
	Permanent water bodies	237,28	0,02

A.10. Nigeria.
Total surface: 912.704 km^2.

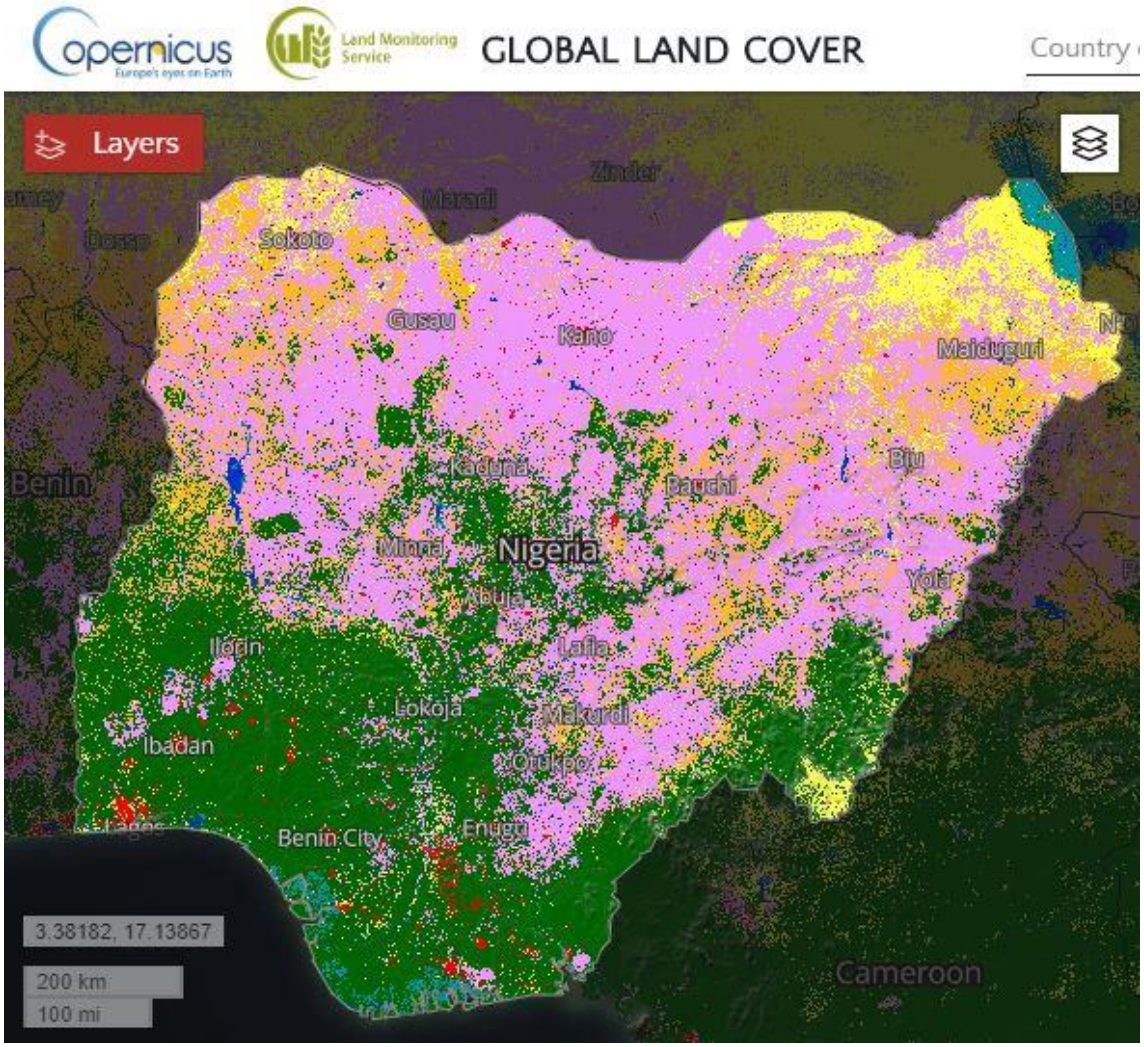

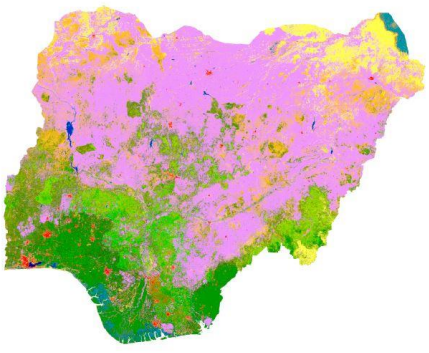

	LAND COVER TYPE	SURFACE (km^2)	%
	Forest	314.335,26	34,44
	Shrubland	120.111,85	13,16
	Herbaceous vegetation	65.988,50	7,23
	Herbaceous wetland	10.769,91	1,18
	Bare / sparse vegetation	456,35	0,05
	Cropland	382.422,98	41,9
	Built-up	14.238,18	1,56
	Permanent water bodies	3,377	0,37

A.11. Senegal.
Total surface: 196.920 km^2.

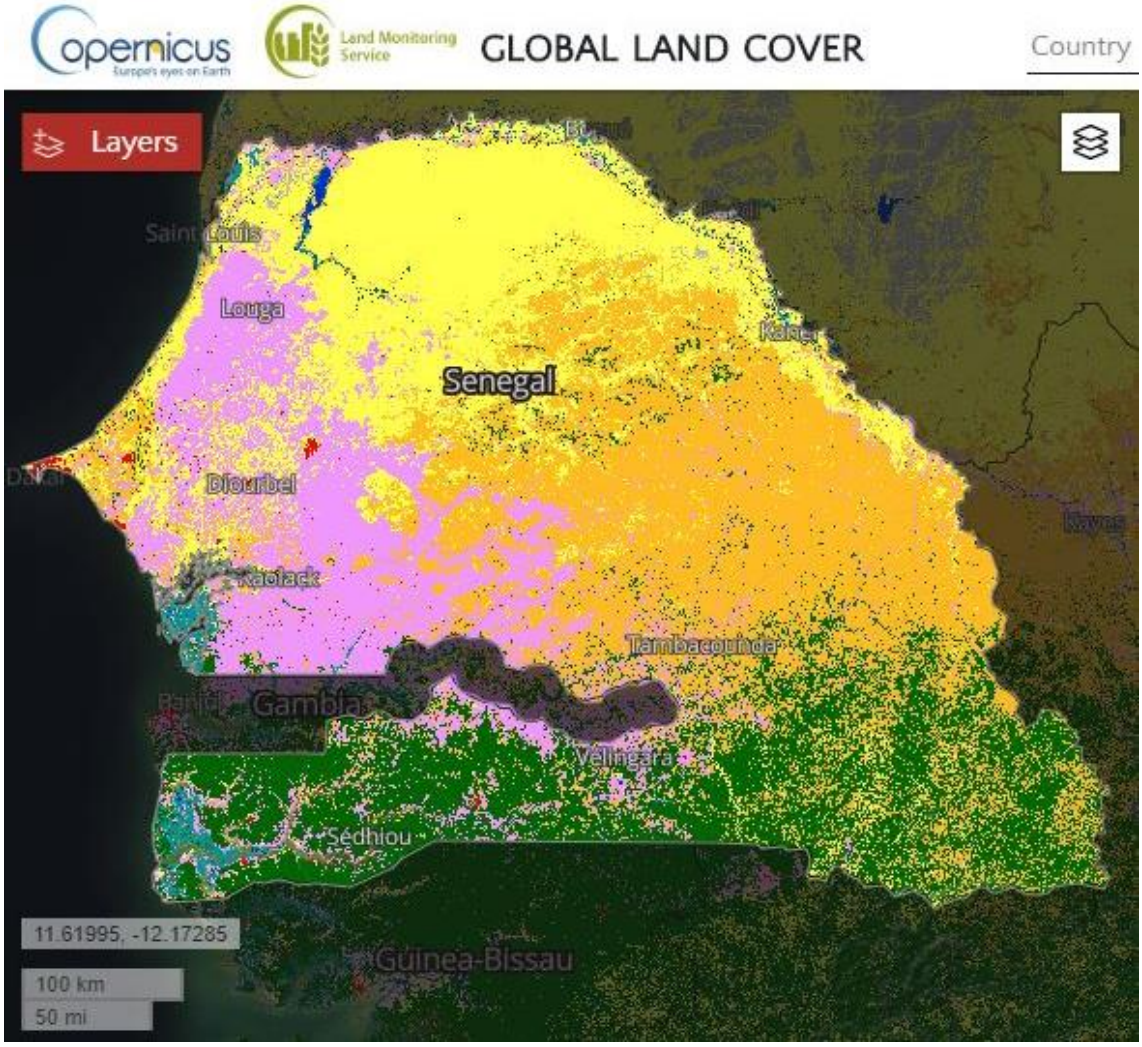

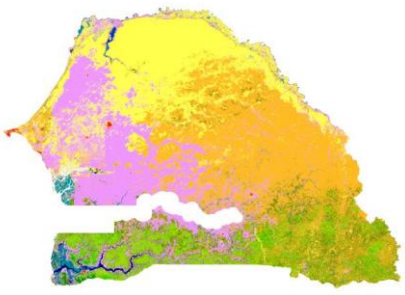

	LAND COVER TYPE	SURFACE (km^2)	%
	Forest	41.628,89	21,14
	Shrubland	65.357,75	33,19
	Herbaceous vegetation	45.980,82	23,35
	Herbaceous wetland	2.678,11	1,36
	Bare / sparse vegetation	610,45	0,31
	Cropland	38.005,56	19,3
	Built-up	728,60	0,37
	Permanent water bodies	354,46	0,18

A.12. Sudan.
Total surface: 1.849.510 km^2.

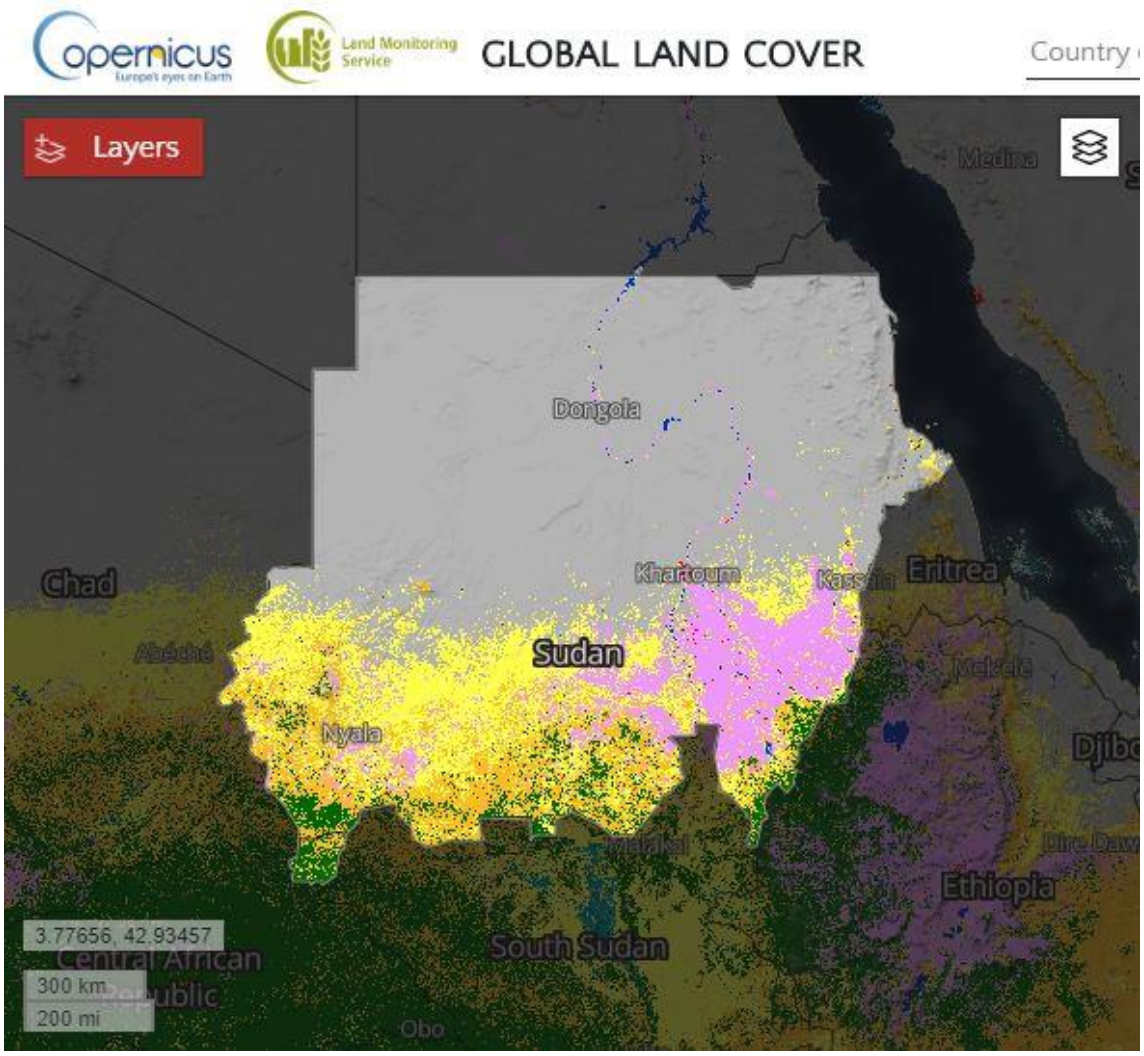

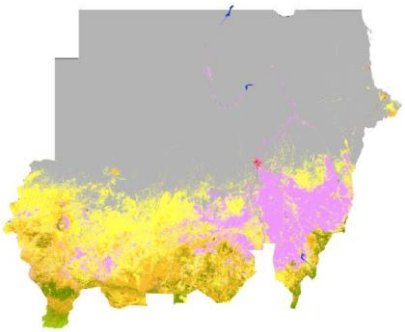

	LAND COVER TYPE	SURFACE (km^2)	%
	Forest	71.576,30	3,87
	Shrubland	171.819,48	9,29
	Herbaceous vegetation	295.366,75	15,97
	Herbaceous wetland	554,85	0,03
	Bare / sparse vegetation	1.121.912,77	60,66
	Cropland	183.656,34	9,93
	Built-up	1.664,56	0,09
	Permanent water bodies	2.589,31	0,14

A.13. Tunisia.
Total surface: 155.211 km^2.

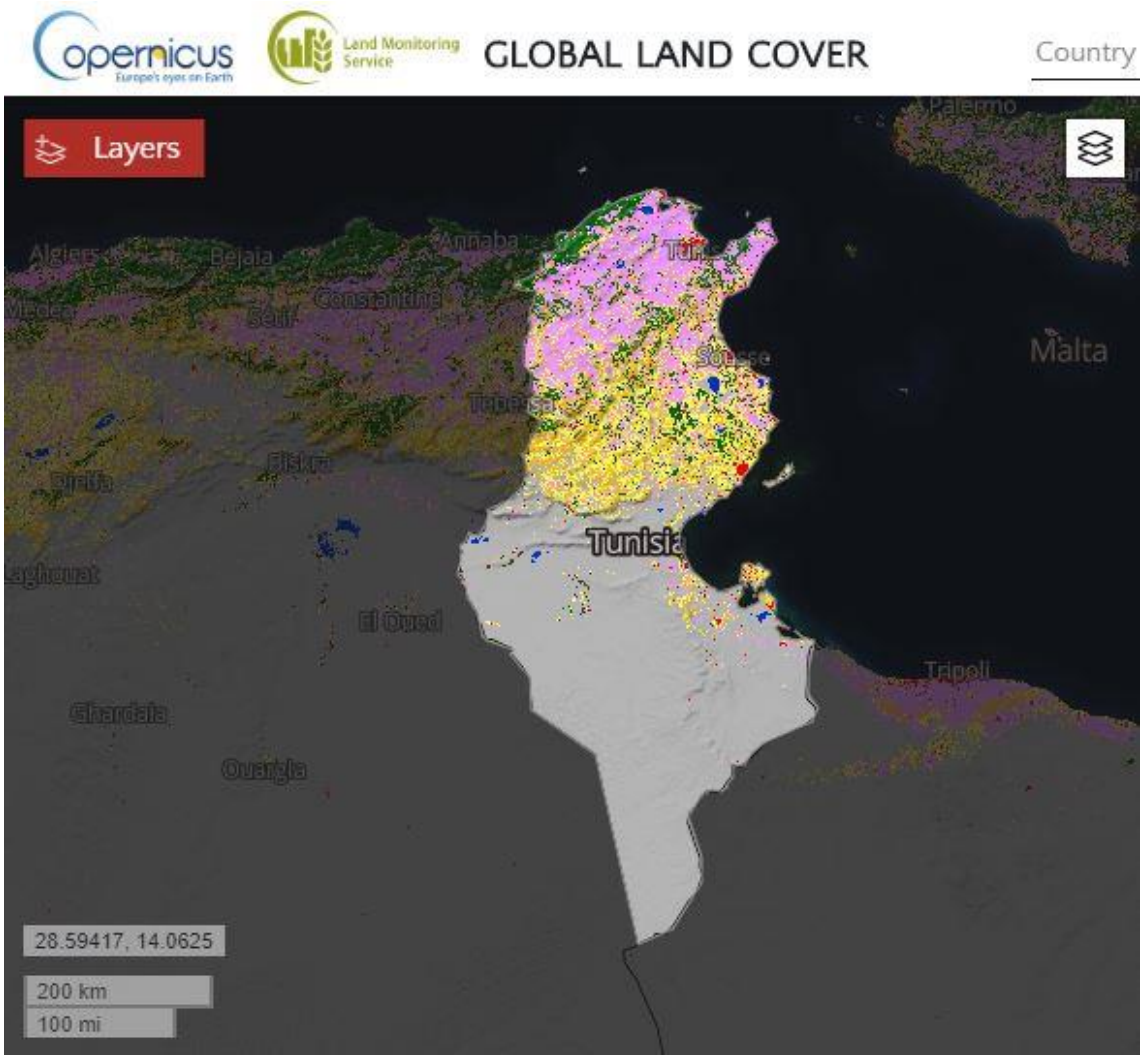

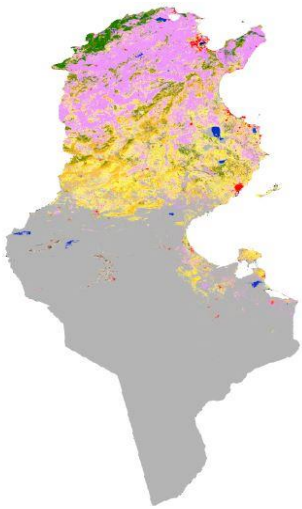

	LAND COVER TYPE	SURFACE (km^2)	%
	Forest	9.374,74	6,04
	Shrubland	11.211,76	7,23
	Herbaceous vegetation	16.685,18	10,75
	Herbaceous wetland	31,40	0,02
	Bare / sparse vegetation	90.612,18	58,38
	Cropland	24.538,86	15,81
	Built-up	1.909,10	1,23
	Permanent water bodies	729,49	0,47

A.14. Western Sahara.
Total surface: 269.196 km^2.

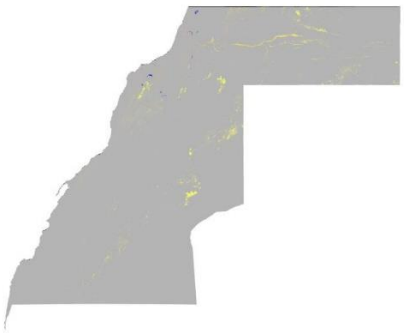

	LAND COVER TYPE	SURFACE (km^2)	%
	Forest	0,00	0,00
	Shrubland	619,15	0,23
	Herbaceous vegetation	2.449,67	0,91
	Herbaceous wetland	0,00	0,00
	Bare / sparse vegetation	265.992,57	98,81
	Cropland	0,00	0,00
	Built-up	0,00	0,00
	Permanent water bodies	107,68	0,04

B. Minimum, maximum and average temperatures and precipitations by country.

B.1. Algeria.

Tindouf

	January	February	March	April	May	June	July	August	September	October	November	December
Avg. Temperature (°C)	13.4	16.2	20	22.6	25.1	27.9	35.2	34.9	30.3	22.9	18.6	13.8
Min. Temperature (°C)	5.2	6.9	11.8	13	15.8	17.5	25.2	25.7	22.3	14.6	11.2	5.8
Max. Temperature (°C)	21.7	25.6	28.3	32.2	34.4	38.3	45.2	44.1	38.4	31.2	26.1	21.8
Precipitation (mm)	4	4	3	1	0	0	0	2	6	3	4	3

Adrar

	January	February	March	April	May	June	July	August	September	October	November	December
Avg. Temperature (°C)	12.3	15	19.1	24.5	28.4	34.3	36.9	35.6	32.2	25.2	18	10.6
Min. Temperature (°C)	4.1	6.9	10.7	15.9	19.8	25.6	27.9	27	24.1	17.4	10.7	5.6
Max. Temperature (°C)	20.5	23.1	27.6	33.1	37	43.1	45.9	44.2	40.4	33.1	25.4	15.7
Precipitation (mm)	1	1	2	1	1	0	0	1	1	3	3	2

Tamanrasset

	January	February	March	April	May	June	July	August	September	October	November	December
Avg. Temperature (°C)	11.7	13.7	17.2	21.8	25.4	28.2	28.5	27.9	26	22.3	18	13.6
Min. Temperature (°C)	4	5.7	9	13.6	17.6	21.3	21.9	21.3	19.1	15.1	10.6	6.1
Max. Temperature (°C)	19.4	21.7	25.5	30	33.2	35.1	35.1	34.5	32.9	29.5	25.5	21.1
Precipitation (mm)	2	1	2	2	5	5	4	8	7	3	2	2

Illizi

	January	February	March	April	May	June	July	August	September	October	November	December
Avg. Temperature (°C)	13.4	16.6	20.8	25.8	30.4	34.6	34.5	33.6	31.8	27	20.8	15.4
Min. Temperature (°C)	5.4	8.3	12.6	17.7	22.6	26.6	26.5	25.9	23.9	18.8	13.1	7.7
Max. Temperature (°C)	21.5	24.9	29.1	33.9	38.3	42.6	42.6	41.4	39.8	35.2	28.6	23.1
Precipitation (mm)	2	0	5	0	2	2	0	1	1	2	0	2

Ouargla

	January	February	March	April	May	June	July	August	September	October	November	December
Avg. Temperature (°C)	10.7	13.4	16.5	21.5	25.4	31.5	34.3	33.4	29.7	23.2	16.4	12.1
Min. Temperature (°C)	4.3	6.7	9.5	13.9	18	23.5	25.7	25.1	22.2	16	9.8	5.9
Max. Temperature (°C)	17.2	20.1	23.5	29.1	32.9	39.5	42.9	41.8	37.2	30.4	23.1	18.3
Precipitation (mm)	6	4	6	4	2	0	0	0	2	4	8	9

Ghardaïa

	January	February	March	April	May	June	July	August	September	October	November	December
Avg. Temperature (°C)	10.1	12.3	15.3	20	24.5	29.7	33.4	32.7	27.8	20.7	14.4	10.7

Min. Temperature (°C)	4.1	5.7	8.5	12.2	16.5	21.5	24.6	24.1	20.8	14.1	8.4	4.7
Max. Temperature (°C)	16.2	18.9	22.2	27.8	32.5	38	42.3	41.3	34.8	27.4	20.5	16.7
Precipitation (mm)	8	5	10	6	4	3	1	3	6	7	8	7

Bechar

	January	February	March	April	May	June	July	August	September	October	November	December
Avg. Temperature (°C)	8.7	11.6	15.2	19.5	23.6	28.5	32.6	31.8	27.1	20.5	13.9	9.7
Min. Temperature (°C)	1.8	4.4	8.2	12.4	16.5	21.4	25.3	24.8	20.3	13.8	7.7	2.8
Max. Temperature (°C)	15.6	18.9	22.2	26.7	30.8	35.6	40	38.9	33.9	27.2	20.1	16.6
Precipitation (mm)	9	7	8	7	5	3	1	3	7	13	14	10

El Oued

	January	February	March	April	May	June	July	August	September	October	November	December
Avg. Temperature (°C)	10.8	13	16.5	20.7	25.5	30.2	33.4	32.6	29	22.6	15.9	11.2
Min. Temperature (°C)	4.5	6.5	9.6	13.4	18	22.9	25.3	24.8	22	16	9.7	5.3
Max. Temperature (°C)	17.1	19.6	23.5	28.1	33	37.5	41.5	40.4	36	29.2	22.2	17.2
Precipitation (mm)	8	8	11	7	5	2	0	1	5	8	11	8

B.2. Burkina Faso.

Ouahigouya

	January	February	March	April	May	June	July	August	September	October	November	December
Avg. Temperature (°C)	24.2	27.2	30.2	32.9	33.2	30.8	28.3	27.4	28	29.9	27.5	24.8
Min. Temperature (°C)	16	18.6	22.2	25.6	26.6	24.8	23.1	22.5	22.6	22.7	19	16.5
Max. Temperature (°C)	32.5	35.8	38.3	40.2	39.9	36.9	33.5	32.3	33.4	37.1	36	33.1
Precipitation (mm)	0	0	1	8	30	80	157	188	109	25	1	0

B.3. Chad.

Tibesti (Bouro)

	January	February	March	April	May	June	July	August	September	October	November	December
Avg. Temperature (°C)	10.1	13	16.7	21.5	25.4	27.3	26.9	26.4	25.1	21.2	15.7	11.3
Min. Temperature (°C)	3.4	5.2	8.6	13.1	16.8	18.8	19	19	17.3	13.4	8.4	4.7
Max. Temperature (°C)	16.9	20.9	24.9	30	34	35.8	34.8	33.9	33	29	23	18
Precipitation (mm)	2	0	2	0	2	2	5	9	1	0	0	1

Borkou (Faya-Largeau)

	January	February	March	April	May	June	July	August	September	October	November	December
Avg. Temperature (°C)	19.5	22.5	26	30.1	32.5	34	33.1	33.1	32	29.9	25.6	21.3
Min. Temperature (°C)	13.7	15.1	18.1	21.6	24.3	26.1	25.3	26.1	25.2	22.8	18.8	14.8
Max. Temperature (°C)	25.4	30	33.9	38.6	40.8	42	40.9	40.1	38.9	37	32.4	27.8

Precipitation (mm)	0	0	0	0	1	1	3	11	1	0	0	0

Ennedi (Fada)

	January	February	March	April	May	June	July	August	September	October	November	December
Avg. Temperature (°C)	21.9	23.3	27.2	29.7	31.4	32.1	30.4	29.8	29.7	29.2	25.9	22.6
Min. Temperature (°C)	14.3	14.8	18.7	21.1	23	24.2	23.3	23.4	22.7	21.5	18.4	14.9
Max. Temperature (°C)	29.6	31.8	35.8	38.4	39.9	40.1	37.5	36.2	36.8	36.9	33.4	30.4
Precipitation (mm)	0	0	0	0	3	3	17	44	5	0	0	0

B.4. Egypt.

	January	February	March	April	May	June	July	August	September	October	November	December
Avg. Temperature (°C)	13.1	13.6	15.4	17.9	20	23.1	24.8	25.3	24.8	22.5	19.2	15.4
Min. Temperature (°C)	8.4	8.9	10.6	13.3	16	19.4	21.8	22.3	21.1	18.2	14.4	10.6
Max. Temperature (°C)	17.9	18.4	20.2	22.5	24.1	26.9	27.9	28.4	28.5	26.9	24	20.2
Precipitation (mm)	36	23	12	2	2	1	0	1	2	14	23	34

Giza

	January	February	March	April	May	June	July	August	September	October	November	December
Avg. Temperature (°C)	13	14	17.2	20.5	24	27.1	27.5	27.5	25.6	23.5	19.2	15
Min. Temperature (°C)	6.8	7.2	10.3	12.7	16.1	19.3	20.6	20.7	18.9	16.8	13	8.9
Max. Temperature (°C)	19.3	20.9	24.2	28.4	32	34.9	34.5	34.4	32.4	30.2	25.4	21.1
Precipitation (mm)	4	3	2	1	0	0	0	0	0	0	3	4

New Valley (Al Ghirizat)

	January	February	March	April	May	June	July	August	September	October	November	December
Avg. Temperature (°C)	13.6	15.2	18.6	23.3	27.1	29.2	29.2	29.4	27.2	24.7	20.2	15.3
Min. Temperature (°C)	5.4	6.5	9.4	13.9	18.2	20.7	21.1	21.6	20.4	17.9	12.4	7.4
Max. Temperature (°C)	21.9	23.9	27.8	32.8	36.1	37.7	37.3	37.3	34.1	31.6	28.1	23.3
Precipitation (mm)	0	0	0	0	0	0	0	0	0	0	0	0

Red Sea (Hurghada)

	January	February	March	April	May	June	July	August	September	October	November	December
Avg. Temperature (°C)	15.5	16.1	20.4	21.7	25.5	28	28.7	29.2	26.9	24.6	20.7	17.2
Min. Temperature (°C)	9.7	10	14.5	15.9	19.8	22.7	23.6	24.2	22.2	19.5	15.1	11.5
Max. Temperature (°C)	21.3	22.2	26.3	27.6	31.3	33.4	33.8	34.2	31.7	29.8	26.4	22.9
Precipitation (mm)	0	0	0	0	0	0	0	0	0	1	1	1

Minya (Al-Minya)

	January	February	March	April	May	June	July	August	September	October	November	December
Avg. Temperature (°C)	12.2	13.6	16.7	21.1	25.5	27.5	28.2	28.1	25.8	23.2	19	14.3
Min. Temperature (°C)	3.8	4.9	7.7	11.7	16.3	18.9	20	20.1	18.3	15.3	11.2	6.6
Max. Temperature (°C)	20.7	22.4	25.8	30.6	34.7	36.2	36.5	36.2	33.3	31.2	26.8	22

Precipitation (mm)	0	1	0	0	0	0	0	0	0	0	0	0

Cairo

	January	February	March	April	May	June	July	August	September	October	November	December
Avg. Temperature (°C)	13.1	14.1	17.4	20.7	24.1	27	27.6	27.6	25.8	23.5	19.2	15.1
Min. Temperature (°C)	7	7.4	10.5	12.9	16.2	19.3	20.7	20.8	19.1	16.8	13.1	9.1
Max. Temperature (°C)	19.3	20.9	24.3	28.5	32.1	34.8	34.6	34.5	32.5	30.2	25.4	21.1
Precipitation (mm)	5	3	2	1	0	0	0	0	0	0	3	4

Suez

	January	February	March	April	May	June	July	August	September	October	November	December
Avg. Temperature (°C)	14.8	15.5	18.1	21.7	25.7	28.1	29.7	29.8	27.5	25	20.3	16.5
Min. Temperature (°C)	9.3	9.8	11.9	14.8	18.3	20.9	22.7	23.1	21.4	19	14.7	11
Max. Temperature (°C)	20.3	21.2	24.3	28.6	33.1	35.3	36.7	36.5	33.7	31.1	26	22
Precipitation (mm)	3	3	3	1	0	0	0	0	0	2	5	3

North Sinai (Al Arish)

	January	February	March	April	May	June	July	August	September	October	November	December
Avg. Temperature (°C)	12.1	13.1	15.2	17.9	21	23.5	25.4	26.2	24.8	22.7	18.4	14
Min. Temperature (°C)	7.7	8.6	10.4	13.1	16	18.8	20.9	21.6	20.4	17.9	13.6	9.5
Max. Temperature (°C)	16.5	17.6	20	22.8	26	28.2	29.9	30.8	29.3	27.6	23.3	18.5
Precipitation (mm)	22	20	15	6	3	0	0	0	0	6	19	23

South Sinai (Nueiba)

	January	February	March	April	May	June	July	August	September	October	November	December
Avg. Temperature (°C)	15.6	16.9	19.7	23.2	26.3	29.5	30.7	30.9	29	25.8	21.3	16.8
Min. Temperature (°C)	10.4	11.3	14	17.3	19.8	23.4	25	25.1	23.7	20.3	16	11.6
Max. Temperature (°C)	20.8	22.5	25.4	29.2	32.9	35.7	36.5	36.8	34.4	31.3	26.6	22.1
Precipitation (mm)	1	3	3	1	0	0	0	0	0	1	2	2

B.5. Eritrea.

Keren

	January	February	March	April	May	June	July	August	September	October	November	December
Avg. Temperature (°C)	20.5	21.3	23.2	25.1	26.2	25.4	23.2	22.3	23.2	23.6	22.4	21.2
Min. Temperature (°C)	12.6	13.1	15.1	16.8	17.9	17.8	17.6	17.1	16.1	15.9	15	13.6
Max. Temperature (°C)	28.4	29.5	31.3	33.5	34.6	33.1	28.9	27.6	30.4	31.4	29.8	28.8
Precipitation (mm)	1	1	3	14	27	44	119	142	42	11	6	1

B.6. Ethiopia.

Mekele

	January	February	March	April	May	June	July	August	September	October	November	December
Avg. Temperature (°C)	17.3	18.1	19.9	21	20.9	21.3	19.3	19	19.2	19	17.9	16.5
Min. Temperature (°C)	8.7	9.2	11.6	13.5	13.3	13.4	13.4	13.4	12	11.4	9.8	8.2
Max. Temperature (°C)	25.9	27.1	28.3	28.5	28.5	29.2	25.3	24.6	26.5	26.7	26	24.9
Precipitation (mm)	5	7	25	30	32	41	185	202	35	8	6	5

B.7. Djibouti.

Djibouti

	January	February	March	April	May	June	July	August	September	October	November	December
Avg. Temperature (°C)	25.8	26.2	27.7	29.1	31	33.8	36	34.6	32.7	30	27.9	26
Min. Temperature (°C)	22.7	23.6	24.8	26	27.8	30.1	30.7	29.6	29.5	26.6	24.8	22.7
Max. Temperature (°C)	28.9	28.9	30.6	32.3	34.2	37.5	41.3	39.6	35.9	33.4	31.1	29.4
Precipitation (mm)	10	9	15	13	9	0	6	7	4	14	22	12

B.8. Libya.

Al Wahat (Awjilah)

	January	February	March	April	May	June	July	August	September	October	November	December
Avg. Temperature (°C)	12.7	14.4	17.2	21.4	26.5	28.5	28.8	28.9	27.8	24.3	19.5	14.5
Min. Temperature (°C)	5.6	7	9.2	13.1	18.3	19.9	21	21	19.9	16.3	12	7.7
Max. Temperature (°C)	19.9	21.9	25.3	29.7	34.7	37.2	36.7	36.9	35.8	32.4	27	21.4
Precipitation (mm)	3	3	3	2	0	0	0	0	0	3	2	3

Jabal al Gharbi

	January	February	March	April	May	June	July	August	September	October	November	December
Avg. Temperature (°C)	13.1	13.9	15.5	18.7	21	23.5	25.2	25.5	24.7	22.6	19.2	15.3
Min. Temperature (°C)	9	9.4	11	13.8	16.7	19.6	22.2	22.8	21.6	18.5	15.1	10.9
Max. Temperature (°C)	17.2	18.4	20.1	23.6	25.3	27.5	28.3	28.3	27.9	26.7	23.4	19.8
Precipitation (mm)	22	14	11	4	3	0	0	0	2	11	9	18

Kufra

	January	February	March	April	May	June	July	August	September	October	November	December
Avg. Temperature (°C)	13.3	15.5	19	24.3	29	30.8	30.8	30.8	28.5	24.5	19.9	14.9
Min. Temperature (°C)	6	8.2	11.4	16.4	20.3	21.9	23.5	23.5	21.7	17.2	12.8	7.8
Max. Temperature (°C)	20.6	22.9	26.7	32.2	37.8	39.8	38.1	38.1	35.3	31.8	27	22
Precipitation (mm)	0	0	0	0	0	0	0	0	0	0	0	0

Nalut

	January	February	March	April	May	June	July	August	September	October	November	December
Avg. Temperature (°C)	8	9.3	13.5	17.2	21.3	25.5	27.6	27.1	24.9	20.4	15.1	9.5

Min. Temperature (°C)	2.8	3.9	7.6	10.7	14.4	18.1	20.3	19.9	18.2	14.3	9.3	4.5
Max. Temperature (°C)	13.3	14.7	19.5	23.8	28.2	33	35	34.3	31.6	26.6	21	14.5
Precipitation (mm)	16	15	31	17	5	2	0	0	6	13	18	16

Jabal al Gharbi (Gharyan)

	January	February	March	April	May	June	July	August	September	October	November	December
Avg. Temperature (°C)	8.8	10.7	13.2	16.7	20.9	25.3	26.8	27.1	24.1	20.2	15.4	10.4
Min. Temperature (°C)	3.2	4.8	6.8	9.8	13.8	17.8	18.8	19.3	17.1	13.7	9.5	5
Max. Temperature (°C)	14.5	16.6	19.6	23.7	28	32.8	34.8	34.9	31.2	26.7	21.4	15.9
Precipitation (mm)	65	52	54	33	6	3	0	0	18	39	33	43

Misrata

	January	February	March	April	May	June	July	August	September	October	November	December
Avg. Temperature (°C)	12.4	13.6	15.8	18.1	20.6	24.3	26	26.8	25.8	23.1	18.8	14.1
Min. Temperature (°C)	7.5	8.1	10	12.3	15.2	18.5	20.5	21.6	20.6	17.6	13.8	9.2
Max. Temperature (°C)	17.4	19.1	21.6	23.9	26.1	30.1	31.6	32.1	31.1	28.7	23.8	19.1
Precipitation (mm)	55	26	20	9	4	1	0	0	10	38	38	60

Sirte (Ras Lanuf)

	January	February	March	April	May	June	July	August	September	October	November	December
Avg. Temperature (°C)	11.8	14.3	16.1	19.6	21.9	24.9	24.9	26.3	25.1	23.1	18.7	14.2
Min. Temperature (°C)	5.8	8.1	9.4	12.5	15.1	17.9	18.5	19.8	18.5	16.5	12.4	8.5
Max. Temperature (°C)	17.8	20.5	22.8	26.7	28.7	31.9	31.3	32.8	31.8	29.7	25	19.9
Precipitation (mm)	25	16	6	3	2	1	0	0	3	11	16	25

Jufra (Waddan)

	January	February	March	April	May	June	July	August	September	October	November	December
Avg. Temperature (°C)	11.3	13.4	16.4	20.2	23.8	27.7	28.2	28.3	27.1	23	17.7	13.3
Min. Temperature (°C)	3	5.3	7.4	10.8	15.2	18.7	19.2	19.4	18.3	14.5	9.7	5.9
Max. Temperature (°C)	19.6	21.6	25.4	29.7	32.4	36.8	37.3	37.3	35.9	31.6	25.7	20.7
Precipitation (mm)	3	3	4	3	2	0	0	0	3	6	3	3

Wadi al Shatii (Addisah)

	January	February	March	April	May	June	July	August	September	October	November	December
Avg. Temperature (°C)	11.8	15	18.7	23.8	27.7	31.4	31.2	30.9	28.7	25.1	19.5	12.5
Min. Temperature (°C)	5.1	7.6	10.7	15.5	19.3	22.9	23.1	23.2	21	17.4	12.4	7.2
Max. Temperature (°C)	18.5	22.4	26.7	32.2	36.1	40	39.4	38.6	36.5	32.8	26.7	17.9
Precipitation (mm)	1	1	1	1	1	0	0	0	0	1	1	1

Wadi al Hayaa (Awbari)

	January	February	March	April	May	June	July	August	September	October	November	December
Avg. Temperature (°C)	12	15	19.2	24.4	28.6	32.1	31.8	31.2	29.2	25.2	19.4	12.8
Min. Temperature (°C)	5.3	7.6	11.4	16.3	20.4	23.9	23.9	23.8	21.6	17.6	12.3	7.2
Max. Temperature (°C)	18.7	22.5	27	32.5	36.8	40.4	39.7	38.7	36.8	32.8	26.6	18.5

Precipitation (mm)	1	1	1	1	1	0	0	0	0	1	1	1

Murzuq (Waw al Kabir)

	January	February	March	April	May	June	July	August	September	October	November	December
Avg. Temperature (°C)	12	15.2	18.6	23.4	27.4	30.5	30	29.8	28.2	24.2	18.8	13.2
Min. Temperature (°C)	4.8	7.2	10.2	14.9	18.8	21.8	21.9	22	20.3	16.4	11.3	6.8
Max. Temperature (°C)	19.3	23.2	27	32	36	39.2	38.2	37.6	36.2	32.1	26.4	19.6
Precipitation (mm)	0	0	0	0	1	0	0	0	0	0	0	0

Sabha

	January	February	March	April	May	June	July	August	September	October	November	December
Avg. Temperature (°C)	11.4	14.9	18.2	23.5	27.6	31.6	31	30.4	28.5	25.1	19.6	11.9
Min. Temperature (°C)	5	7.6	10.4	15.3	19.2	23.1	23.1	23.1	20.9	17.6	12.6	7.1
Max. Temperature (°C)	17.8	22.2	26.1	31.8	36.1	40.1	38.9	37.8	36.1	32.7	26.7	16.8
Precipitation (mm)	2	1	1	1	1	0	0	0	0	1	1	1

B.9. Mali.

Tombouctou (Timbuktu)

	January	February	March	April	May	June	July	August	September	October	November	December
Avg. Temperature (°C)	20.6	23.5	26.8	30.4	33.2	33.9	31.8	30.4	30.9	30.1	25.4	21.6
Min. Temperature (°C)	12.2	14.4	18	22	25.3	26.6	25.4	24.4	24.2	22.1	17	13.5
Max. Temperature (°C)	29.1	32.6	35.7	38.8	41.1	41.3	38.2	36.4	37.6	38.1	33.8	29.8
Precipitation (mm)	0	0	0	1	4	16	50	72	30	3	0	0

Kidal

January	January	February	March	April	May	June	July	August	September	October	November	December
Avg. Temperature (°C)	20.2	23.1	26.7	30.7	34	35.3	33.5	32.5	32.6	30.4	25.1	21.8
Min. Temperature (°C)	12.5	14.9	18.6	23	26.8	28.5	27.1	26.1	25.9	23.1	17.6	14.3
Max. Temperature (°C)	27.9	31.4	34.9	38.5	41.3	42.1	39.9	39	39.3	37.7	32.7	29.4
Precipitation (mm)	0	0	0	1	5	12	31	46	21	3	0	0

Gao

January	January	February	March	April	May	June	July	August	September	October	November	December
Avg. Temperature (°C)	22.6	25.5	29.1	32.5	35.1	35.3	32.5	31.4	32.3	32	27.4	24.1
Min. Temperature (°C)	14.7	17	20.8	24.9	28.1	29	26.6	25.6	26	24.8	19.6	16.3
Max. Temperature (°C)	30.6	34.1	37.4	40.1	42.1	41.6	38.5	37.2	38.6	39.2	35.3	31.9
Precipitation (mm)	0	0	0	1	6	20	59	76	31	5	0	0

Mopti

	January	February	March	April	May	June	July	August	September	October	November	December
Avg. Temperature (°C)	23	25.7	29	31.6	32.9	31.5	28.9	27.4	27.8	28.6	26.6	23.4
Min. Temperature (°C)	14.4	16.7	20.2	23.5	25.5	24.9	23.4	22.8	23.1	22.8	19.1	15.6

Max. Temperature (°C)	31.6	34.8	37.8	39.8	40.4	38.1	34.4	32	32.6	34.5	34.2	31.2
Precipitation (mm)	0	0	0	4	23	58	141	166	85	18	0	0

B.10. Mauritania.

Tiris Zemmur (Bir Moghrein)

	January	February	March	April	May	June	July	August	September	October	November	December
Avg. Temperature (°C)	16.3	18.1	19.4	20.6	23.1	25.7	31.5	31.8	29.2	25.5	21	15.8
Min. Temperature (°C)	10	11.5	12.3	13.4	15.2	17.3	22.6	23.1	21.6	18.7	15	9.9
Max. Temperature (°C)	22.6	24.8	26.5	27.9	31	34.2	40.4	40.5	36.8	32.3	27	21.8
Precipitation (mm)	2	3	1	1	0	1	1	2	10	8	4	6

Adrar (Ouadane)

	January	February	March	April	May	June	July	August	September	October	November	December
Avg. Temperature (°C)	18.7	20.9	23.5	25.9	29.5	32.9	34.4	33.8	32.5	28.9	24	19.1
Min. Temperature (°C)	11.5	13.1	15.7	17.9	21.4	24.7	26.2	25.9	25	21.6	16.9	12.1
Max. Temperature (°C)	26	28.7	31.3	34	37.6	41.1	42.6	41.7	40	36.3	31.2	26.1
Precipitation (mm)	3	2	2	0	1	2	5	14	15	4	4	2

Tagant (Tidjikja)

	January	February	March	April	May	June	July	August	September	October	November	December
Avg. Temperature (°C)	20.3	22.6	25.3	28.2	31.6	34.1	32.9	31.9	31.8	30	25.3	21.1
Min. Temperature (°C)	13.1	15	17.7	20.7	24.3	27.4	26.7	26	25.6	23.2	18.2	14.3
Max. Temperature (°C)	27.5	30.3	32.9	35.7	39	40.9	39.1	37.9	38.1	36.8	32.4	28
Precipitation (mm)	2	2	0	1	3	9	21	48	31	8	2	1

Dakhlet Nouadhibou

	January	February	March	April	May	June	July	August	September	October	November	December
Avg. Temperature (°C)	18.9	19.4	20.2	20.3	21	22.4	22.8	23.9	25.3	24.5	22	19.4
Min. Temperature (°C)	13.3	13.7	14.3	14.7	15.8	17	18.6	19.6	20.1	18.7	16.5	14.3
Max. Temperature (°C)	24.5	25.1	26.1	25.9	26.3	27.9	27.1	28.2	30.6	30.3	27.5	24.6
Precipitation (mm)	1	2	1	0	0	0	1	3	5	3	2	0

Hodh el Charqui (Nema)

	January	February	March	April	May	June	July	August	September	October	November	December
Avg. Temperature (°C)	23.9	26.8	29.7	32.5	35.3	35.6	32.6	30.9	31.9	32.5	28.6	24.7
Min. Temperature (°C)	17.1	19.5	22.5	25.4	28.4	29.2	26.4	25	25.5	26.1	22.1	18.2
Max. Temperature (°C)	30.8	34.1	37	39.7	42.3	42.1	38.8	36.9	38.3	39	35.2	31.2
Precipitation (mm)	1	0	0	3	4	19	59	84	49	10	1	1

B.11. Morocco.

Guelmim

	January	February	March	April	May	June	July	August	September	October	November	December
Avg. Temperature (°C)	13.8	14.7	16.7	18	20	21.6	23.2	23.6	22.5	20.7	17.5	14.5
Min. Temperature (°C)	8.8	9.4	11.7	13.2	15.7	17.3	18.9	19.2	18.1	15.9	12.6	9.6
Max. Temperature (°C)	18.9	20.1	21.7	22.9	24.4	25.9	27.6	28	26.9	25.6	22.5	19.5
Precipitation (mm)	18	16	11	9	2	1	1	1	5	10	19	26

Bouarfa

	January	February	March	April	May	June	July	August	September	October	November	December
Avg. Temperature (°C)	7.8	10	12.4	15.4	23.1	25	29.4	29.1	23.9	18.3	12.6	7.7
Min. Temperature (°C)	1.8	3.2	5.8	8.1	16	17.6	21.4	21.6	16.5	12.1	6.4	1.7
Max. Temperature (°C)	13.9	16.8	19.1	22.8	30.3	32.5	37.5	36.6	31.3	24.5	18.9	13.7
Precipitation (mm)	14	15	22	20	13	6	2	7	18	24	25	22

Taourirte

	January	February	March	April	May	June	July	August	September	October	November	December
Avg. Temperature (°C)	11.2	12.5	14.3	16.1	17.7	20	21.4	21.9	21.1	18.4	15.6	12.5
Min. Temperature (°C)	6.2	7.2	9.1	10.3	12	14	14.7	15.5	14.9	12.8	10.5	7.7
Max. Temperature (°C)	16.3	17.8	19.6	21.9	23.5	26.1	28.2	28.3	27.3	24	20.7	17.3
Precipitation (mm)	20	24	23	31	27	11	2	3	16	21	19	21

Er Rachidia

	January	February	March	April	May	June	July	August	September	October	November	December
Avg. Temperature (°C)	9.1	11.2	14.4	18.5	22.1	27.2	31.6	30.7	21.8	19.3	13.8	10.3
Min. Temperature (°C)	2.5	4.4	7.3	10.9	14.1	19	22.6	22.1	14.1	12.4	7.4	3.9
Max. Temperature (°C)	15.7	18	21.6	26.1	30.2	35.5	40.6	39.4	29.5	26.3	20.3	16.7
Precipitation (mm)	8	6	8	10	8	4	3	6	17	20	18	19

B.12. Niger.

Agadez

	January	February	March	April	May	June	July	August	September	October	November	December
Avg. Temperature (°C)	19.7	22.6	26.8	30.9	33.4	33.6	31.8	30.6	31.2	29.4	24.1	21
Min. Temperature (°C)	11.5	13.9	18.2	22.9	25.7	26.2	24.9	24	24	21.6	15.9	13
Max. Temperature (°C)	28	31.4	35.4	39	41.2	41	38.8	37.3	38.5	37.2	32.3	29.1
Precipitation (mm)	0	0	0	1	6	9	38	56	11	0	0	0

Zinder

	January	February	March	April	May	June	July	August	September	October	November	December
Avg. Temperature (°C)	21.8	24.9	28.9	32.2	33	31.6	28.7	27.5	29	29.6	26	22.9
Min. Temperature (°C)	14.2	16.8	21	24.4	25.9	25.2	23.3	22.4	22.9	22.2	18.1	15

Max. Temperature (°C)	29.5	33.1	36.8	40	40.1	38	34.2	32.7	35.1	37.1	34	30.8
Precipitation (mm)	0	0	1	0	17	34	115	156	53	4	0	0

Diffa

	January	February	March	April	May	June	July	August	September	October	November	December
Avg. Temperature (°C)	21.1	23.8	27.8	30.9	32.2	31	28.7	27.3	28.5	28.5	24.9	21.6
Min. Temperature (°C)	12.5	14.8	19.3	22.6	24.6	24.4	23.3	22.3	22.3	20.7	16.3	12.8
Max. Temperature (°C)	29.8	32.8	36.4	39.2	39.8	37.7	34.1	32.4	34.7	36.4	33.6	30.4
Precipitation (mm)	0	0	0	1	7	23	82	147	39	7	0	0

Tounga Aoudou

	January	February	March	April	May	June	July	August	September	October	November	December
Avg. Temperature (°C)	25.8	29.3	32.1	33.4	32.1	29.3	27.4	26.6	27.2	28.9	27.9	25.8
Min. Temperature (°C)	17.8	21.7	24.8	26.9	26.7	24.1	22.9	22.4	22.3	22.4	19.6	17.7
Max. Temperature (°C)	33.8	36.9	39.4	39.9	37.5	34.6	31.9	30.9	32.1	35.4	36.2	34
Precipitation (mm)	0	1	2	21	76	130	188	245	166	27	1	0

Dolé

	January	February	March	April	May	June	July	August	September	October	November	December
Avg. Temperature (°C)	25.8	29.1	32.1	33.4	32	29.3	27.4	26.6	27.2	28.8	27.8	25.8
Min. Temperature (°C)	17.8	21.5	24.8	26.9	26.6	24.1	22.9	22.4	22.3	22.4	19.5	17.7
Max. Temperature (°C)	33.8	36.8	39.4	39.9	37.4	34.6	31.9	30.9	32.1	35.3	36.1	34
Precipitation (mm)	0	1	3	22	77	131	188	247	167	27	1	0

B.13. Nigeria.

Sokoto

	January	February	March	April	May	June	July	August	September	October	November	December
Avg. Temperature (°C)	24.5	26.6	30.4	33.2	32.5	30.2	28.1	26.5	27.5	29.3	27.5	24.6
Min. Temperature (°C)	16	17.3	22	25.7	26.1	24.3	23.1	22	22.1	21.8	18.9	16.1
Max. Temperature (°C)	33	35.9	38.8	40.8	39	36.2	33.1	31.1	33	36.9	36.1	33.1
Precipitation (mm)	0	0	1	6	38	86	164	211	108	15	0	0

Katsina

	January	February	March	April	May	June	July	August	September	October	November	December
Avg. Temperature (°C)	21.2	23.8	28.2	30.8	30.7	28.8	25.8	24.8	25.8	26.7	24.3	21.2
Min. Temperature (°C)	12.3	14.7	19.5	23.1	24.2	23	21.1	20.7	20.7	19.4	15.3	12.3
Max. Temperature (°C)	30.1	32.9	36.9	38.5	37.2	34.7	30.6	28.9	30.9	34.1	33.4	30.2
Precipitation (mm)	0	0	0	4	31	74	171	217	93	10	0	0

B.14. Senegal.

Kébémer

	January	February	March	April	May	June	July	August	September	October	November	December
Avg. Temperature (°C)	22.5	22.8	24	24.4	25.3	27.3	27.4	27.1	27.3	27.5	25.9	23.2
Min. Temperature (°C)	14.6	14.9	16	16.9	18.6	21.9	23	23	23	21.9	18.7	15.8
Max. Temperature (°C)	30.5	30.8	32.1	31.9	32	32.7	31.8	31.3	31.6	33.1	33.1	30.7
Precipitation (mm)	1	0	0	0	0	11	66	137	120	28	2	1

B.15. Sudan.

North Darfur (Kutum)

	January	February	March	April	May	June	July	August	September	October	November	December
Avg. Temperature (°C)	17.9	18.5	22.5	26.1	27.7	28.5	26.7	24.7	25.6	24.7	20.9	18.4
Min. Temperature (°C)	7.1	7.6	11.9	16.4	18.8	20.7	20.2	19.2	18.2	16	11.3	7.9
Max. Temperature (°C)	28.7	29.4	33.2	35.8	36.6	36.3	33.2	30.3	33.1	33.4	30.5	28.9
Precipitation (mm)	0	0	0	1	5	15	77	127	30	4	0	0

Ash-Shamaliyah (Northern State)

	January	February	March	April	May	June	July	August	September	October	November	December
Avg. Temperature (°C)	17.2	18.6	22.7	27.4	31.5	33.1	33.2	33.3	32	29	22.9	18.5
Min. Temperature (°C)	9	9.9	13.8	18.4	22.8	24.6	25.1	25.8	24.4	21.1	15.3	10.6
Max. Temperature (°C)	25.4	27.4	31.7	36.5	40.2	41.7	41.4	40.9	39.6	37	30.6	26.5
Precipitation (mm)	0	0	0	0	0	0	1	1	0	0	0	0

Shamal Kurdufan

	January	February	March	April	May	June	July	August	September	October	November	December
Avg. Temperature (°C)	22.5	23.9	27	30.2	30.8	30.1	28.1	27	27.8	28.8	26.4	23.4
Min. Temperature (°C)	14.7	15.9	19	22.2	23.6	23.8	22.9	22.1	22	22	19.1	15.9
Max. Temperature (°C)	30.3	31.9	35	38.2	38.1	36.4	33.3	31.9	33.6	35.6	33.7	31
Precipitation (mm)	0	0	0	2	15	44	128	134	67	20	0	0

Khartoum

	January	February	March	April	May	June	July	August	September	October	November	December
Avg. Temperature (°C)	23.3	24.8	28.3	31.5	34.1	34.1	32	30.7	32	32.1	28	24.2
Min. Temperature (°C)	15.4	16.4	19.7	22.8	26.2	26.9	25.9	25	25.6	25	20.8	16.6
Max. Temperature (°C)	31.2	33.2	37	40.3	42.1	41.3	38.1	36.5	38.5	39.3	35.3	31.9
Precipitation (mm)	0	0	0	0	3	5	41	62	20	4	0	0

Nahr an Nil (Nile River state)

	January	February	March	April	May	June	July	August	September	October	November	December
Avg. Temperature (°C)	22.4	23.5	27	30.3	33.7	35.3	33.5	32.3	33.8	32.2	27.7	23.6
Min. Temperature (°C)	14.5	15.1	18.2	21.6	25.5	27.7	26.9	25.6	26.8	25.3	20.4	16

Max. Temperature (°C)	30.4	32	35.8	39.1	42	42.9	40.2	39.1	40.9	39.1	35	31.3
Precipitation (mm)	0	0	0	0	3	1	19	26	7	3	0	0

Al-Bahr Al-Ahmar (Red Sea State)

	January	February	March	April	May	June	July	August	September	October	November	December
Avg. Temperature (°C)	23.1	23	24.2	26.4	29.2	32.1	34	34.5	32	29.1	27.2	24.7
Min. Temperature (°C)	19.4	18.8	19.5	21.2	23.3	25.5	27.9	28.8	26.6	24.7	23.5	21.1
Max. Temperature (°C)	26.9	27.2	28.9	31.6	35.1	38.8	40.2	40.3	37.5	33.6	30.9	28.3
Precipitation (mm)	1	0	1	2	1	0	4	2	0	10	31	13

B.16. Tunisia.

Tataouine

	January	February	March	April	May	June	July	August	September	October	November	December
Avg. Temperature (°C)	10.2	11.9	15	18.9	22.2	26.5	29.2	28.8	27.5	22.1	16.4	11.7
Min. Temperature (°C)	5.6	6.8	9.3	12.9	15.7	19.9	21.6	21.7	20.9	16.5	11.1	6.7
Max. Temperature (°C)	14.8	17.1	20.8	24.9	28.7	33.1	36.8	36	34.2	27.8	21.8	16.8
Precipitation (mm)	21	14	25	11	7	1	0	2	8	15	16	14

Kebili

	January	February	March	April	May	June	July	August	September	October	November	December
Avg. Temperature (°C)	9.4	12	15.8	20.1	24.1	28.6	31.8	31.8	28.5	22.5	15.8	10.2
Min. Temperature (°C)	4	5.9	9.4	13.4	17.3	21.8	24.3	24.5	22	16.4	10	4.9
Max. Temperature (°C)	14.8	18.1	22.3	26.8	30.9	35.4	39.4	39.1	35.1	28.7	21.6	15.6
Precipitation (mm)	12	9	16	9	6	1	1	2	6	10	15	11

Medenine

January	January	February	March	April	May	June	July	August	September	October	November	December
Avg. Temperature (°C)	11.3	12.7	15.6	19.1	22.5	26.2	29	29	27.2	22.6	17.1	12.7
Min. Temperature (°C)	6.6	7.6	10	13.3	16.2	19.9	21.7	22.1	20.8	17.1	11.9	7.8
Max. Temperature (°C)	16	17.9	21.2	24.9	28.9	32.6	36.4	36	33.6	28.2	22.3	17.6
Precipitation (mm)	17	14	21	16	7	2	0	1	13	29	19	17

Gabes

	January	February	March	April	May	June	July	August	September	October	November	December
Avg. Temperature (°C)	11	12.3	15.1	17.8	21.1	23.9	26.9	27.6	25.5	22	16.8	12.1
Min. Temperature (°C)	6.1	6.8	9.6	12.4	16	19.1	21.8	22.2	20.5	16.7	11.4	7.2
Max. Temperature (°C)	16	17.9	20.6	23.3	26.3	28.7	32	33	30.6	27.3	22.2	17.1
Precipitation (mm)	19	18	19	15	7	2	0	1	18	33	21	24

Tozeur

	January	February	March	April	May	June	July	August	September	October	November	December
Avg. Temperature (°C)	11	13.4	16	19.6	24.6	29.1	31.9	31.7	27.6	21.8	15.7	11.4

Min. Temperature (°C)	5.4	7.3	9.6	12.9	17.6	22.4	24.4	24.7	21.5	15.8	10	6.1
Max. Temperature (°C)	16.7	19.5	22.5	26.3	31.6	35.8	39.4	38.7	33.8	27.9	21.4	16.7
Precipitation (mm)	10	8	13	10	6	3	0	3	8	10	12	10

B.17. Western Sahara.

Dakhla

	January	February	March	April	May	June	July	August	September	October	November	December
Avg. Temperature (°C)	17.4	18.4	19.2	19.5	20	21	22	22.8	23	22.5	21	18.2
Min. Temperature (°C)	13.2	13.9	15	15.6	16.1	17.1	18.4	18.9	19.4	18.3	17.1	14.3
Max. Temperature (°C)	21.7	22.9	23.4	23.4	23.9	25	25.6	26.7	26.7	26.7	25	22.2
Precipitation (mm)	2	1	1	0	1	0	2	4	14	3	4	13

Guelmim

	January	February	March	April	May	June	July	August	September	October	November	December
Avg. Temperature (°C)	13.8	14.7	16.7	18	20	21.6	23.2	23.6	22.5	20.7	17.5	14.5
Min. Temperature (°C)	8.8	9.4	11.7	13.2	15.7	17.3	18.9	19.2	18.1	15.9	12.6	9.6
Max. Temperature (°C)	18.9	20.1	21.7	22.9	24.4	25.9	27.6	28	26.9	25.6	22.5	19.5
Precipitation (mm)	18	16	11	9	2	1	1	1	5	10	19	26

Laayoune

	January	February	March	April	May	June	July	August	September	October	November	December
Avg. Temperature (°C)	16	16.7	17.9	18.6	20.3	21.4	23.3	23.9	23.3	22.3	20.1	15.4
Min. Temperature (°C)	10	10.8	12.2	13.4	15.2	16.5	17.9	18.3	17.4	16.6	15.3	10.3
Max. Temperature (°C)	22	22.6	23.7	23.9	25.4	26.4	28.8	29.6	29.2	28.1	25	20.5
Precipitation (mm)	3	2	1	1	0	1	0	0	0	4	7	8

C. Cost of CCS technologies.

Table of the Summary of new plant performance and CO_2 capture cost based on current technology:

Performance and Cost Measures	New NGCC Plant				New PC Plant				New IGCC Plant				New Hydrogen Plant				(Units for H_2 Plant)
	Range			Rep. Value	Range			Rep. Value	Range			Rep. Value	Range			Rep. Value	
	low		high		low		high		low		high		low		high		
Emission rate without capture (kg CO_2 MWh^{-1})	344	-	379	367	736	-	811	762	682	-	846	773	78	-	174	137	kg CO_2 GJ^{-1} (without capture)
Emission rate with capture (kg CO_2 MWh^{-1})	40	-	66	52	92	-	145	112	65	-	152	108	7	-	28	17	kg CO_2 GJ^{-1} (with capture)
Percent CO_2 reduction per kWh (%)	83	-	88	86	81	-	88	85	81	-	91	86	72	-	96	86	% reduction/unit of product
Plant efficiency with capture, LHV basis (%)	47	-	50	48	30	-	35	33	31	-	40	35	52	-	68	60	Capture plant efficiency (% LHV)
Capture energy requirement (% more input MWh^{-1})	11	-	22	16	24	-	40	31	14	-	25	19	4	-	22	8	% more energy input per GJ product
Total capital requirement without capture (US$ kW^{-1})	515	-	724	568	1161	-	1486	1286	1169	-	1565	1326	[No unique normalization for multi-product plants]				Capital requirement without capture
Total capital requirement with capture (US$ kW^{-1})	909	-	1261	998	1894	-	2578	2096	1414	-	2270	1825					Capital requirement with capture
Percent increase in capital cost with capture (%)	64	-	100	76	44	-	74	63	19	-	66	37	-2	-	54	18	% increase in capital cost
COE without capture (US$ MWh^{-1})	31	-	50	37	43	-	52	46	41	-	61	47	6.5	-	10.0	7.8	H_2 cost without capture (US$ GJ^{-1})
COE with capture only (US$ MWh^{-1})	43	-	72	54	62	-	86	73	54	-	79	62	7.5	-	13.3	9.1	H_2 cost with capture (US$ GJ^{-1})
Increase in COE with capture (US$ MWh^{-1})	12	-	24	17	18	-	34	27	9	-	22	16	0.3	-	3.3	1.3	Increase in H_2 cost (US$ GJ^{-1})
Percent increase in COE with capture (%)	37	-	69	46	42	-	66	57	20	-	55	33	5	-	33	15	% increase in H_2 cost
Cost of CO_2 captured (US$/$tCO_2$)	33	-	57	44	23	-	35	29	11	-	32	20	2	-	39	12	US$/$tCO_2$ captured
Cost of CO_2 avoided (US$/$tCO_2$)	37	-	74	53	29	-	51	41	13	-	37	23	2	-	56	15	US$/$tCO_2$ avoided

Figure of the CO_2 transport costs range for onshore and offshore pipelines per 250 km, 'normal' terrain conditions:

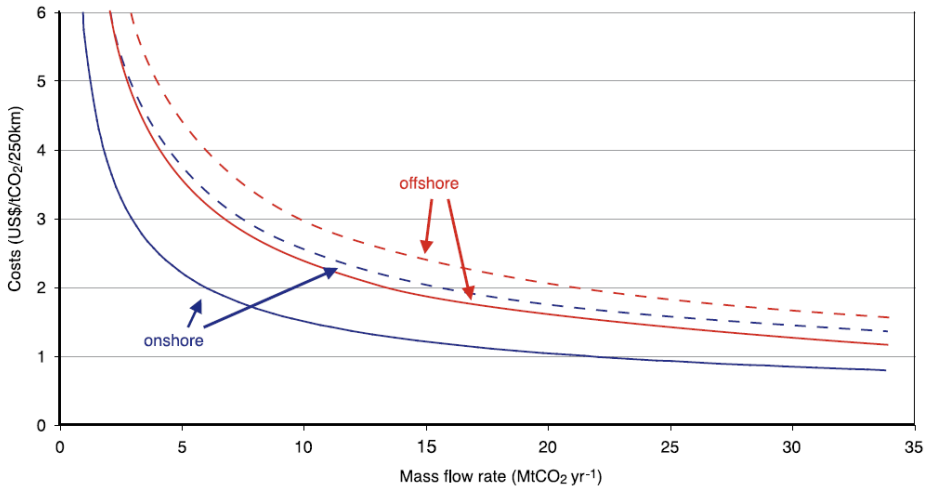

Table of Estimates of CO2 storage costs and monitoring:

Option	Representative Cost Range (US$/tonne CO_2 stored)
Geological - Storage[a]	0.5-8.0
Geological - Monitoring	0.1-0.3
Ocean[b]	
Pipeline	6-31
Ship (Platform or Moving Ship Injection)	12-16
Mineral Carbonation[c]	50-100

Bibliography.

Ahuchaogu, A., Chukwu, J., Obike, A., & Nnorom, I. C. (2018). *Reverse Osmosis Technology , its Applications and Nano-Enabled Membrane*. *March*. https://doi.org/10.20431/2349-0403.0502005

Alcamo, J., Kaspar, F., & Siebert, S. (1997). *Global Change and Global Scenarios of Water Use and Availability: An Application of water*. file:///home/sasha/Documents/Research/papers/alcamo_etal_1997.pdf

Andersen, G. L., & Krzywinski, K. (2007). *Longevity and growth of Acacia tortilis ; insights from 14 C content and anatomy of wood*. *14*, 1–14. https://doi.org/10.1186/1472-6785-7-4

Awouda, E. H. M. (1990). *Indicators for present and future supply of gum Arabic*.

Bellion, Y. C. (1897). *Histoire géodynamique post-paléozoïque de l'Afrique de l'Ouest d'après l'étude de quelques bassins sédimentaires (Sénégal, Taoudenni, Iullemmeden, Tchad)*.

Bennett, A. (2016). *Desalination technology in power generation*. *December*, 30–35. https://doi.org/10.1016/S0015-1882(16)30255-5

Borsani, R., & Rebagliati, S. (2005). *Fundamentals and costing of MSF desalination plants and comparison with other technologies*. *182*(May), 29–37. https://doi.org/10.1016/j.desal.2005.03.007

Bundschuh, J., Tomaszewska, B., Ghaffour, N., & Reardon-smith, K. (2017). *Solar , wind and geothermal energy applications in agriculture : back to the future ? Solar , wind and geothermal energy applications in agriculture : July*.

Cairns, M. A., Brown, S., Helmer, E. H., & Baumgardner, G. A. (1997). Root biomass allocation in the world's upland forests. *Oecologia*, *111*(1), 1–11. https://doi.org/10.1007/s004420050201

Climate-Data.org. (2020). *Climate-Data.org*. https://en.climate-data.org/

Cloudsley-Thompson, J. L. (1984). *Sahara Desert (Key Environment)*.

Copernicus. (2020). *The Global Land Cover Viewer*. https://lcviewer.vito.be/

Cornejo, P. K., Hokanson, D. R., Technologies, T., & Zhang, Q. (2014). *Carbon footprint of water reuse and desalination : A review of greenhouse gas emissions and estimation tools*. *December*. https://doi.org/10.2166/wrd.2014.058

Cosín, C. (2018). *La evolución de las tarifas en desalación (Parte I)*. https://www.iagua.es/blogs/carlos-cosin/evolucion-tarifas-desalacion-parte-i

D'Hoore, J. L. (1964). Soil Map of Africa, scale 1 : 5 000 000 - explanatory monograph. *Publication N°93*, *11*, 205 (Publication N°93).

Dadhich, P., Dooley, J., Fujii, Y., Hohmeyer, O., & Riahi, K. (2005). Cost and economic potential. *IPCC Special Report on Carbon Dioxide Capture and Storage*, 341–362. http://scholar.google.com/scholar?hl=en&btnG=Search&q=intitle:Cost+and+economic+potential#8

De Vries, S. (2002). *Groundwater recharge: An overview of process and challenges.*

Diagrams, P. F. (2017). *Process Flow Diagrams 1*. *April*.

Digital Journey. (2018). *Sahara Desert*. http://www.digitaljournal.com/topic/Sahara+desert

Djomo, A. N., Picard, N., Fayolle, A., & Henry, M. (2016). *Tree allometry for estimation of carbon stocks in African tropical forests*. *July*, 446–455. https://doi.org/10.1093/forestry/cpw025

EIA. (2020). *How much carbon dioxide is produced per kilowatthour of U.S. electricity generation?* https://www.eia.gov/tools/faqs/faq.php?id=74&t=11

El-Ghonemy, A. M. K. (2018). Performance test of a sea water multi-stage flash distillation plant : Case study. *Alexandria Engineering Journal*, *57*(4), 2401–2413. https://doi.org/10.1016/j.aej.2017.08.019

Encyclopedia Britannica. (2020). *Encyclopedia Britannica*. https://www.britannica.com/

Esfahani, I. J., Rashidi, J., Ifaei, P., & Yoo, C. (2016). *Efficient thermal desalination technologies with renewable energy systems : A state-of-the-art review*. *33*(2), 351–387. https://doi.org/10.1007/s11814-015-0296-3

FAO. (1986). *Groundwater resources development for rangelands*. http://www.fao.org/3/r7488e/r7488e07.htm#6. groundwater resources development for rangelands

FAO. (1997). *Classification of surface and groundwater resources in North Africa in billions of cubic meters*.

FAO. (2014). *Presupuesto para plantaciones de madera como combustible*.

FAO, EU, & Mechanism, T. G. (2012). *Sahara and Sahel Observatory OSS 2020 Strategy. Harmonised regional strategy for implementation of the "Great Green Wall Initiative of the Sahara and the Sahel."*

Fath, H., Abbas, Z., & Khaled, A. (2011). *Techno-economic assessment and environmental impacts of desalination technologies*. *266*, 263–273. https://doi.org/10.1016/j.desal.2010.08.035

GGW. (2020). *GGW: Great Green Wall Project*. https://www.greatgreenwall.org/about-great-green-wall

Ghamdi, A. Al, & Mustafa, I. (2016). Exergy analysis of a MSF desalination plant in Yanbu , Saudi Arabia. *DES*, *399*, 148–158. https://doi.org/10.1016/j.desal.2016.08.020

Goffner, D., Sinare, H., & Gordon, L. J. (2019). *The Great Green Wall for the Sahara and the Sahel Initiative as an opportunity to enhance resilience in Sahelian landscapes and livelihoods*.

Google Maps. (2020). *No Title*.

Green, S., Dixon, S., Al-yamani, W., Green, S., Pangilinan, R., Dixon, S., & Shahid, S. A. (2019). Water use of Al Samr (Acacia tortilis) forests irrigated with saline groundwater and treated sewage effluent in the hyper-arid deserts of Abu Dhabi Water use of Al Samr (Acacia tortilis) forests irrigated with saline groundwater and treated sewage e f. *Agricultural Water Management*, *216*(February), 361–364. https://doi.org/10.1016/j.agwat.2019.01.024

IAEA. (2017). *Integrated and Sustainable Management of Shared Aquifer Systems and Basins of the Sahel Region*.

IEA. (2020). *International Energy Agency (IEA)*. https://www.iea.org/

Iglesias Martín, J. A. (2016). *Captaciones subterráneas. Perforación y equipamiento de sondeos para captación de aguas subterráneas*.

Indian Council of Forestry Research and Education, D. (1958). *Acacia tortilis*.

Jia, X. (2019). *Analyzing the Energy Consumption, GHG Emission, and Cost of Seawater Desalination in China*. 1–16. https://doi.org/10.3390/en12030463

Kamal, I. (2008). *Myth and reality of the hybrid desalination process *. 230*(October 2007), 269–280. https://doi.org/10.1016/j.desal.2007.11.030

Kaukora, N. (2020). *Image of Acacia Tortilis species*. shuttrestock.com

Khouri, H. (1989). *Development in hydrological mapping of the Arab region: a contribution to hydrogeological mapping in arid zones. Memoirs of the Int. Symp. On Hydrogeological Maps as Tools for Economic and Social Development*.

Kim, J., Park, K., Ryook, D., & Hong, S. (2019). A comprehensive review of energy consumption of seawater reverse osmosis desalination plants. *Applied Energy*, *254*(August), 113652. https://doi.org/10.1016/j.apenergy.2019.113652

Koirala, S., Yeh, P. J., Hirabayashi, Y., Kanae, S., & Oki, T. (2014). *Global-scale land surface hydrologic modeling with the representation of water table dynamics.*

Kotb, O. A. (2015). *Optimum numerical approach of a MSF desalination plant to be supplied by a new specific 650 MW power plant located on the Red Sea in Egypt*. 257–265. https://doi.org/10.1016/j.asej.2014.09.001

Le Houérou, H. N. (1990). *Agroforestry and sylvopastoralism to combat land degradation in the Mediterranean Basin: old approaches to new problems.*

Lianying, W., Yangdong, H., & Congjie, G. (2013). Optimum design of cogeneration for power and desalination to satisfy the demand of water and power. *DES*, *324*, 111–117. https://doi.org/10.1016/j.desal.2013.06.006

Lo, M., Yeh, P., & Famiglietti, J. (2008). *Constraining water table depth simulations in a land surface model using estimated baseflow*.

Macedonio, F., & Drioli, E. (2017). Membrane Engineering for Green Process Engineering. *Engineering*, *3*(3), 290–298. https://doi.org/10.1016/J.ENG.2017.03.026

Mehdizadeh, H. (2006). *Membrane desalination plants from an energy – exergy viewpoint*. *191*(March 2005), 200–209. https://doi.org/10.1016/j.desal.2005.06.037

Migliorini, G., & Luzzo, E. (2004). *Seawater reverse osmosis plant using the pressure exchanger for energy recovery : a calculation model*. *165*, 289–298.

Miladi, R., Frikha, N., Kheiri, A., & Gabsi, S. (2019). Energetic performance analysis of seawater desalination with a solar membrane distillation. *Energy Conversion and Management*, *185*(October 2018), 143–154. https://doi.org/10.1016/j.enconman.2019.02.011

Najafi, B., Shirazi, A., Aminyavari, M., Rinaldi, F., & Taylor, R. A. (2014). Exergetic, economic and environmental analyses and multi-objective optimization of an SOFC-gas turbine hybrid cycle coupled with an MSF desalination system. *Desalination*, *334*(1), 46–59. https://doi.org/10.1016/j.desal.2013.11.039

National Renewable Energy Laboratory. (2020). *LCOE Calculator*.

Papapetrou, M., Cipollina, A., La, U., Micale, G., & Zaragoza, G. (2017). *Assessment of methodologies and data used to calculate desalination costs*. *419*, 8–19. https://doi.org/10.1016/j.desal.2017.05.038

Postel, S. L., Daily, G. C., & Ehrlich, P. R. (1996). *Human appropriation of renewable fresh water*.

Quézel, P. (1965). *La végétation du Sahara, du Tchad à la Mauritanie*.

Ramsar Convention. (2020). *List of Ramsar wetlands of international importante*. https://rsis.ramsar.org/

Romero, F. T. (2016). *Estudio de Costos de las Especies Forestales beneficiarias Informe Final*. *March*.

Saeed, M. O., Al-nomazi, M. A., & Al-amoudi, A. S. (2019). Evaluating suitability of source water for a proposed SWRO plant location. *Heliyon*, *October 2018*, e01119. https://doi.org/10.1016/j.heliyon.2019.e01119

Shahabi, M. P., Mchugh, A., Anda, M., & Ho, G. (2015). Comparative economic and environmental assessments of centralised and decentralised seawater desalination options. *DES*, *376*, 25–34. https://doi.org/10.1016/j.desal.2015.08.012

Shiklomanov, I. (2000). *Appraisal and assessment of world water resources*.

Thorweihe, H. (2002). *Groundwater resources of the Nubian aquifer system. Major basins – non-renewable Water Resources, Modified synthesis.*

Toochi, E. C. (2018). Carbon sequestration: how much can forestry sequester CO2? *Forestry Research and Engineering: International Journal*, *2*(3), 148–150. https://doi.org/10.15406/freij.2018.02.00040

UN;, Development, C. on S., & Organisation, W. M. (1997). *Comprehensive assessment of the freshwater resources of the world*.

United Nations. (2003). *Water for People—Water for Life*.

United Nations. (2020). *United Nations Geospatial Information Section*. https://www.un.org/Depts/Cartographic/english/htmain.htm

Vorosmarty, C. J., Green, P., Salisbury, J., & Lammers, R. B. (2000). *Global water resources: Vulnerability from climate change and population growth*.

Voss, K., Swenson, S., Rodell, M., Richey, A. S., Thomas, B. F., Lo, M.-H., Reager, J. T., & Famiglietti, J. S. (2015). Quantifying renewable groundwater stress with GRACE. *Water Resources Research*, *51*(7), 1–22. https://doi.org/10.1002/2015WR017349.Received

Voutchkov, N. (2017). Energy use for membrane seawater desalination – current status and trends Energy use for membrane seawater desalination – current status and trends. *Desalination*, *October*, 0–1. https://doi.org/10.1016/j.desal.2017.10.033

Wakil, M., Burhan, M., Ang, L., & Choon, K. (2017). Energy-water-environment nexus underpinning future desalination sustainability. *Desalination*, *413*, 52–64. https://doi.org/10.1016/j.desal.2017.03.009

Wali, F. (2014). *The future of desalination research in the Middle East.*

Walvoord, S. (2004). *"Hydrologic processes in deep vadose zones in interdrainage arid environments, in Groundwater Recharge in a Desert Environment: THe Southwestern United States*.

White, F. (1983). *The Vegetation of Africa*.

WHYMAP. (2020). *WHYMAP (World-wide Hydrogeological Mapping and Assessment Program)*. https://www.whymap.org/whymap/EN/Home/whymap_node.html

Wikipedia. (2008a). *AT1317 map: Red Sea coastal desert ecoregion - of the Deserts and xeric scrublands biome, on the Red Sea in northeastern*. https://es.wikipedia.org/wiki/Archivo:AT1317_map.png

Wikipedia. (2008b). *Map of Africa, with Sahel highligthed in orange*.

Wikipedia. (2008c). *Sahara Desert ecoregion map*.

Wikipedia. (2008d). *Saharan topographic elements map*.

Wikipedia. (2013). *Ecoregion PA1321: North Saharan steppe and woodlands*. https://es.wikipedia.org/wiki/Estepas_y_bosques_nord-saharianos#/media/Archivo:Ecoregion_PA1321.svg

Williams, M. A. J., & Faure, H. (1980). *Sahara Prehistory - The Sahara and the Nile: Quaternary environments and prehistoric occupation in northern Africa*.

WWWF Panda. (2020). *Biomes - World Wide Fund for Nature*. https://www.worldwildlife.org/biomes

Yeh. (2005). *Representation of water table dynamics in a land surface scheme. Part I: Model development.*

Yinyangperu. (2020). *Image of Acacia Senegal species*. http://www.yinyangperu.com/acacia.html

Zektser, E. (2004). *Resources of the World and Their Use*.